Impacto del cambio climático sobre la ecofisiología y capacidad fitorremediadora de halófitas

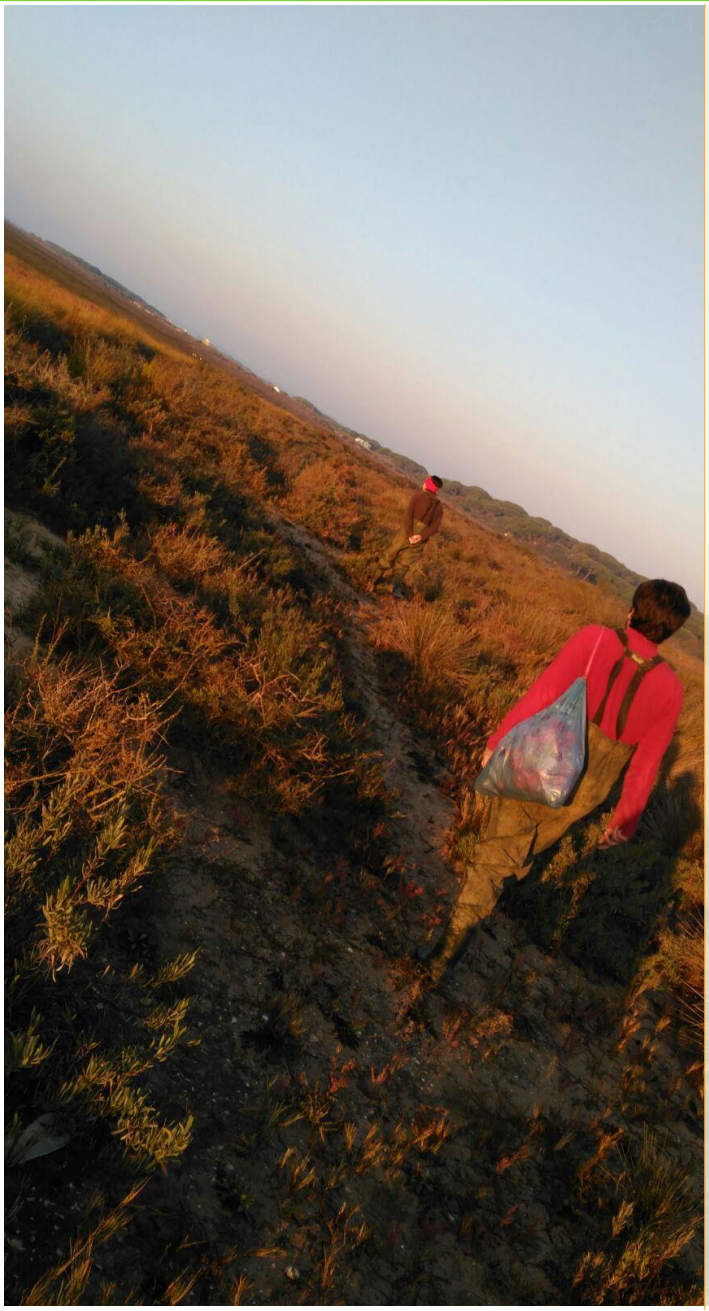

Jesús Alberto Pérez Romero

Facultad de Biología

Dpto. Biología Vegetal y Ecología

ÍNDICE

ABSTRACT

Climate Change is considered one of the main global changes facing by humanity, and is the result of the exacerbated increase in the emission of carbon dioxide (CO_2) into the atmosphere from the pre-industrial stage. The vegetation is one of the components of the ecosystem with greater vulnerability to this phenomenon, having described possible alterations on its distribution, phenology, productivity, etc. In this context, it is very important to study how the interactions of different factors associated with climate change (high CO_2, rising temperatures and sea level, extreme climatic events, etc.) affect the ecophysiology of plants.

Halophytes are plant species that have developed a series of mechanisms that allow them to complete their life cycle in highly stressful environments. In addition, many halophytes have demonstrated an enormous technological potential for their use as resources of different nature or in phytoremediation of pollutants. However, little is known about the response of these species to the interaction of factors associated with Climate Change or how these interactions affect their phytoremediation capacity; and this is the knowledge gap that tries to fill this Doctoral Thesis.

Our results shown how the increase in CO_2 (700 ppm) improved the tolerance of a halophyte model, *Salicornia ramosissima*, against salinity (510 mM NaCl). The improvement in tolerance was reflected in the maintenance of the CO_2 assimilation rate and the functionality of the photosystems. This positive effect became apparent even under conditions of permanent soil flooding. Regarding the impact of extreme thermal events of short duration (40-28ºC and 12-5ºC during three days), a thermo-dependent response was observed, so that *S. ramosissima* was more sensitive to low temperatures for the two levels of salinity studied (171 and 1040 mM).

On the other hand, the results of this Thesis showed a specific effect on the phytoremediation capacity of the halophytes *Spartina densiflora* and *Juncus acutus*. Thus, in the case of *S. densiflora*, high CO_2 (700 ppm) increased its tolerance to Cu excess, maintaining the ability to phytostabilize Cu in its roots. For *J. acutus*, its greater tolerance to Zn was largely mediated by the reduction of the concentration of Zn in its tissues in the presence of salt (85 mM NaCl).

In conclusion, halophytes grown in an atmosphere enriched in CO_2 in combination with other environmental factors of stress shown a better physiological response than

those subjected only to high salinity, flood or the toxic effect of a heavy metal. The interaction of factors generates synergistic effects that differ from the responses that are recorded when the factors are analyzed separately. Therefore, in order to predict the response of plants to climate change it is necessary to address the trials considering the interaction of factors.

RESUMEN

El Cambio Climático está considerado como uno de los principales cambios globales a los que se enfrenta la humanidad, y es consecuencia del incremento exacerbado de la emisión de dióxido de carbono (CO_2) a la atmósfera desde la etapa preindustrial. La vegetación es uno de los componentes del ecosistema con mayor vulnerabilidad frente a este fenómeno, habiéndose descrito posibles alteraciones sobre su distribución, fenología, productividad, etc. En este contexto, es de gran importancia estudiar cómo afectan a la ecofisiología de las plantas las interacciones de distintos factores asociados al Cambio Climático (elevado CO_2, aumento de las temperaturas y nivel del mar, eventos climáticos extremos, etc.).

Las halófitas son especies vegetales que han desarrollado una serie de mecanismos que les permiten completar su ciclo vital en ambientes altamente estresantes. Además, muchas halófitas han demostrado un enorme potencial tecnológico para su empleo como recursos de diferente naturaleza (alimentación, fármacos, etc.) o en fitorremediación de contaminantes. Sin embargo, poco se sabe sobre la respuesta de estas especies frente a la interacción de factores asociados con el Cambio Climático o cómo estas interacciones afectan a su capacidad fitorremediadora; y este es el vacío de conocimiento que trata de llenar esta Tesis Doctoral.

Nuestros resultados mostraron cómo el aumento del CO_2 (700 ppm) mejoró la tolerancia de una halófita modelo, *Salicornia ramosissima*, frente a la salinidad (510 mM NaCl). La mejora de la tolerancia se reflejó en el mantenimiento de la tasa de asimilación de CO_2 y la funcionalidad de los fotosistemas. Este efecto positivo se hizo patente incluso bajo condiciones de inundación permanente del suelo. Respecto al impacto de eventos térmicos extremos de corta duración (40-28 ºC y 12-5ºC durante tres días), se observó una respuesta termo-dependiente, de forma que *S. ramosissima* fue más sensible a las bajas temperaturas que a las altas para los dos niveles de salinidad estudiados (171 y 1040 mM).

Por otro lado, los resultados de esta Tesis mostraron un efecto específico en la capacidad fitorremediadora de las halófitas *Spartina densiflora* y *Juncus acutus*. Así, en el caso de *S. densiflora*, el elevado CO_2 (700 ppm) aumentó su tolerancia frente al exceso de Cu, manteniendo la capacidad para fitoestabilizar Cu en sus raíces. Para *J. acutus* su

mayor tolerancia frente al Zn estuvo en gran parte mediada por la reducción de la concentración de Zn en sus tejidos en presencia de sal (85 mM NaCl).

En conclusión, las halófitas crecidas en una atmósfera enriquecida en CO2 en combinación con otros factores ambientales de estrés mostraron mejor respuesta fisiológica que aquellas sometidas solamente a alta salinidad, inundación o al efecto tóxico de un metal pesado. La interacción de factores genera efectos sinérgicos que difieren de las respuestas que se registran cuando se analizan los factores por separado. Por tanto, para poder predecir la respuesta de las plantas frente al Cambio Climático es necesario abordar los ensayos considerando la interacción de factores.

Capítulo 1: INTRODUCCIÓN

1.1 Las marismas, su relevancia ecológica y socio-económica

Las marismas mareales son ecosistemas, que se localizan en los estuarios de los ríos, con unas características muy especiales debido a su posicionamiento entre el medio terrestre y el marino. El efecto de la marea crea en estos ecosistemas un fuerte gradiente de diferentes factores ambientales, como las horas de inundación o la salinidad. Así, se conforman los diferentes hábitats, generalmente paralelos al límite de la marea (Figura 1), que son dominados por diferentes especies vegetales con características especiales de gran interés (Adams, 1963; Chapman, 1974).

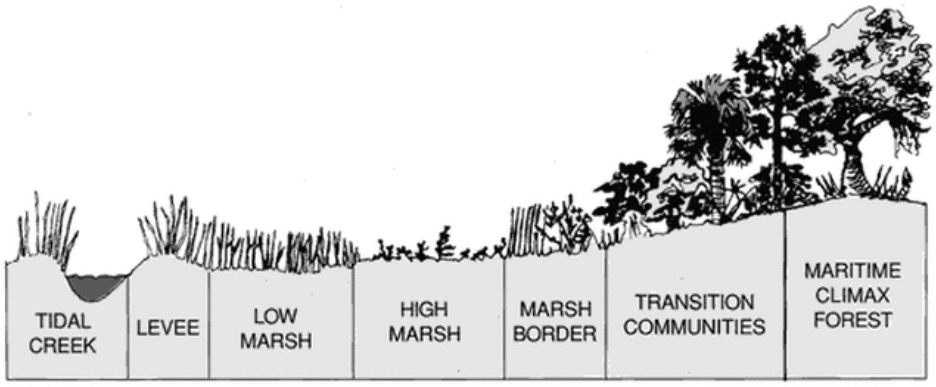

Figura 1. Esquema de los diferentes hábitats paralelos al límite de la marea (visto en: https://saltmarshesofsouthjersey.weebly.com/what-is-a-salt-marsh.html ©Rolling College)

Además, las marismas sirven como zona de cría para numerosas especies de animales (Castillo, 2001; Castellanos et al., 2004; Sánchez et al., 2006) lo cual aumenta su valor ecológico. También poseen una gran importancia medioambiental y socio-económica (Zharikow et al., 2005). Son uno de los ecosistemas con mayores niveles de producción en el mundo, siendo base de las redes tróficas de los sistemas fluviales y marinos cercanos (Delaune y Gambell, 1996). Su valor económico y social reside en los núcleos familiares de ámbito costero, que desarrollan actividades de explotación tradicionales en las marismas, y su puesta en valor como zonas ideales para realizar turismo natural, especialmente en el sur de España donde son zonas de avistamiento de aves (Farhad et al., 2015). Además, muchas especies con gran interés comercial tienen en ellas sus lugares de cría y refugio (Zharikow et al., 2005; Morzaria-Luna et al., 2014), es el caso de los peneídos (Hart et al., 2018), entre los que se encuentran los langostinos, gambas o camarones. También brindan una función de protección frente a temporales y

crecidas fluviales (DeLaune y Gambell 1996; Luque et al., 1999; Fagherazzi et al., 2013; Bonemetto et al., 2019).

A pesar de los servicios que brindan estos ecosistemas, la actividad humana ha generado grandes presiones sobre las marismas, tanta que aproximadamente el 50% de las marismas existentes sufren un deterioro grave derivado de acciones humanas (Barbier et al., 2011), y esto ha provocado una situación en la que su conservación se ha visto comprometida.

1.2 Principales amenazas para la conservación: Cambio Global y Cambio Climático

Cambio Global y Cambio Climático son dos conceptos que, a menudo, se usan de forma errónea como sinónimos. Sin embargo, mientras que el Cambio Climático hace referencia a las variaciones atmosféricas que suponen una modificación en el clima de la tierra, el Cambio Global es un concepto más amplio que incluye además las modificiaciones que ocurren a nivel de usos de suelo, pérdida de biodiversidad y de recursos en general (IPCC, 2007). Por lo tanto, el Cambio Climático es uno de los diferentes tipos de Cambio Global que están ocurriendo en la actualidad (Rockström et al., 2009).

El Cambio Climático se debe, principalmente, a un rápido aumento de la concentración de gases de efecto invernadero en la atmósfera en los últimos años debido; como el dióxido de carbono (CO_2), cuya concentración ha ido aumentado exponencialmente desde la etapa preindustrial y se estima que pueda llegar a duplicarse con respecto a la actual (apróx. 760 ppm) a finales de este siglo (Figura 2; IPCC, 2007).

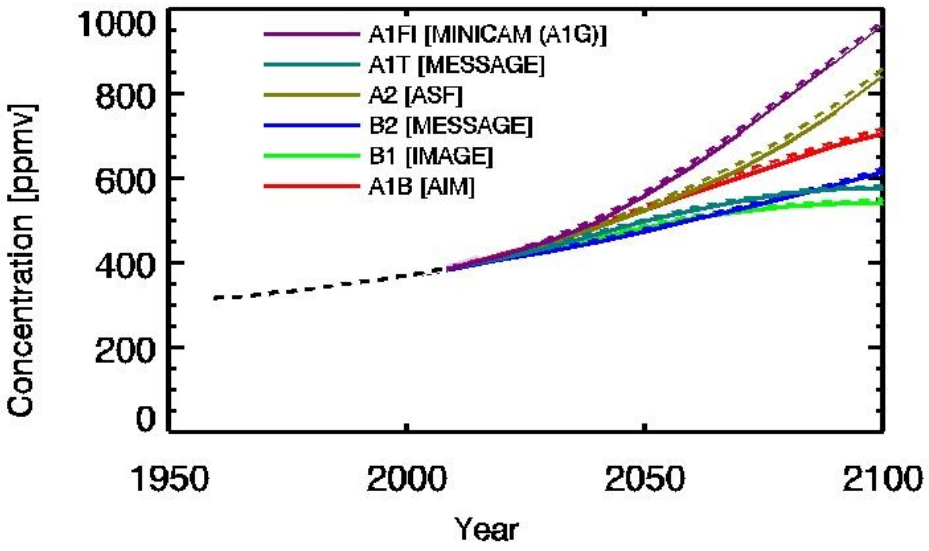

Figura 2. Concentración atmosférica de CO_2 (ppmv) predicha desde el año 2007 hasta el 2100 por seis modelos de Cambio Climático diferentes, representados cada uno con un color distinto (IPCC, 2007).

Los gases de efecto invernadero permiten que parte de la radiación del sol que penetra la atmósfera hasta la superficie terrestre no pueda volver a salir hacia el exterior, reflejándose de nuevo hacia la superficie de la tierra, aumentando la temperatura de la misma. Este efecto invernadero permite que la temperatura media del planeta sea de unos 15ºC y no de -18ºC, posibilitando la vida en su superficie (Popescu y Luca, 2017). El problema radica en la emisión descontrolada de este tipo de gases debido a la acción del hombre, así las predicciones de Cambio Climático pronostican un aumento de la temperatura media del planeta entre 2.4-6.4ºC para el año 2100 (Figura 3).

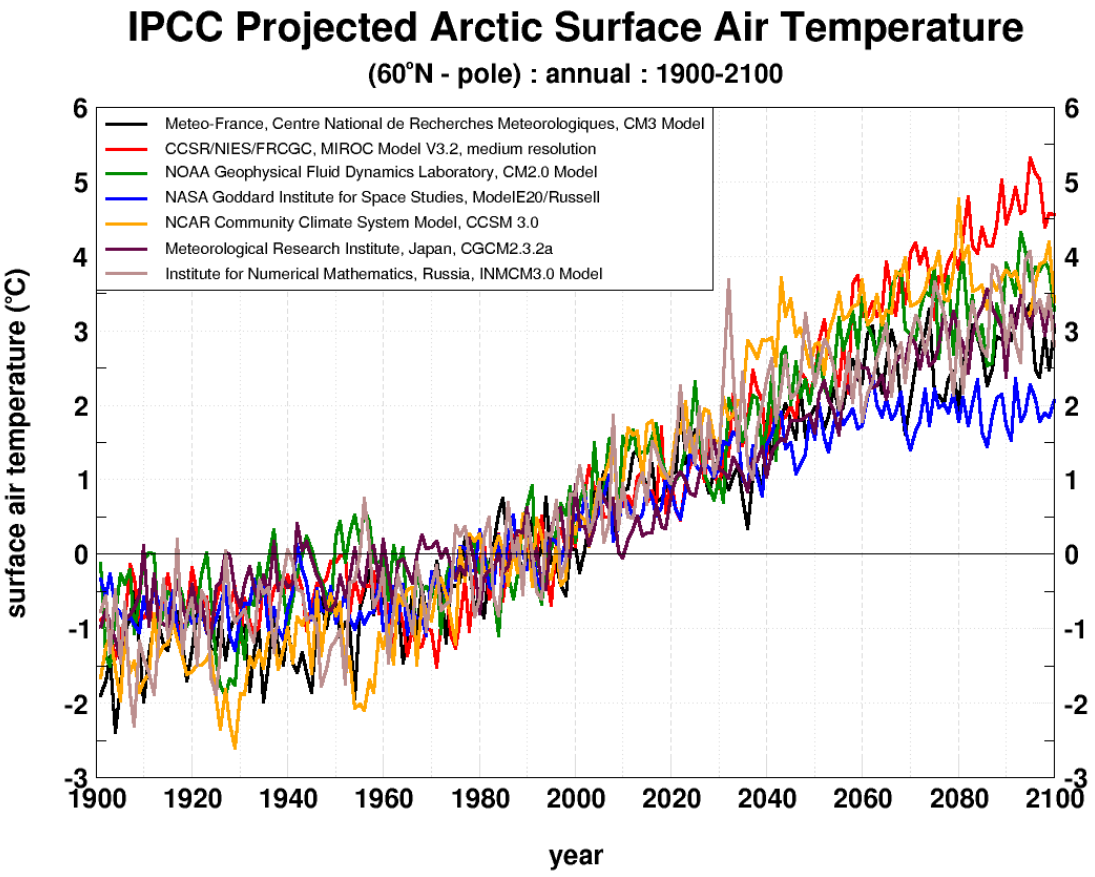

Figura 3. Tendencia de la temperatura del aire en el Ártico del año 1900 al 2100 realizada por 7 modelos de Cambio Climático diferentes diferentes (IPCC, 2007).

El aumento de la temperatura tendrá una serie de consecuencias de difícil predicción a nivel global. Una de las más consensuadas sería la del aumento del nivel del mar debido al deshielo de los polos y a la expansión térmica de los océanos por un aumento en su temperatura, lo que supondría una pérdida de recursos del litoral, pondría en peligro las playas y las marismas y podría contribuir a la salinización de los suelos (IPPC, 2007; Lu et al., 2018). También se prevé un aumento de la duración e intensidad de las sequías, inundaciones, largos periodos estivales con veranos tórridos y disminución del caudal de los ríos, lo que aumentaría la presión sobre los acuíferos (IPCC, 2007). En definitiva, una mayor frecuencia de eventos climáticos extremos que contribuirán a la degeneración de los suelos, mediante la salinización o la pérdida de nutrientes (IPCC, 2007). No obstante, sucesos meteorológicos extremos, como las olas de calor o de frío también tienen efectos directos sobre las especies vegetales. Entre estos efectos podemos observar limitaciones en su desarrollo y distribución, debido a alteraciones en la fenología, reproducción o fisiología de las plantas (Orsenigo et al., 2014). Además, las

modificaciones climáticas globales afectarán a las respuestas fisiológicas basales de las especies vegetales, a corto y largo plazo, pudiendo generar cambios en la estructura y funcionamiento de los ecosistemas (Curtis et al., 1995), afectando a la productividad de las comunidades vegetales (Naudts et al., 2014). En este futuro escenario, no solo las comunidades naturales como las de marismas se verán afectadas, también los cultivos estarán bajo la influencia de complejas interacciones: incremento de la concentración atmosférica de CO_2, aumento de la temperatura, sequías y salinización de los suelos (Peng et al., 2004). Los eventos de salinización derivados del Cambio Climático suponen una de las mayores amenazas para la conservación de los ecosistemas pero también para la seguridad alimentaria, ya que conlleva la degradación de los suelos y la pérdida de terrenos cultivables (IPCC, 2007). El Panel Interguvernamental sobre Cambio Climático (IPCC) establece que los efectos del Cambio Climático sobre los cultivos pueden ser mayores en España y la zona Mediterránea que en otros países de la Unión Europea por su localización geográfica (IPCC 2007, 2014; Figura 4).

En consecuencia, el Cambio Climático aparece como uno de los grandes desafíos que debe afrontar la humanidad para sostener la producción agrícola en niveles adecuados a la creciente demanda de alimentos, la cual debe aumentar en un 70% para mitades de siglo (Tester y Langridge, 2010). Esto hace que sea fundamental buscar soluciones, como el uso de cultivos alternativos. Estos cultivos deberían ser capaces de crecer y producir recursos en ambientes hostiles. Por ello, numerosas halófitas han sido propuestas como cultivos alternativos, por su gran capacidad de tolerar diversas condiciones adversas, gracias a sus mecanismos de protección frente al estrés, así como por su alta producitividad y sus valores nutricionales excepcionales (Ventura y Sagi, 2013; Ventura et al., 2015).

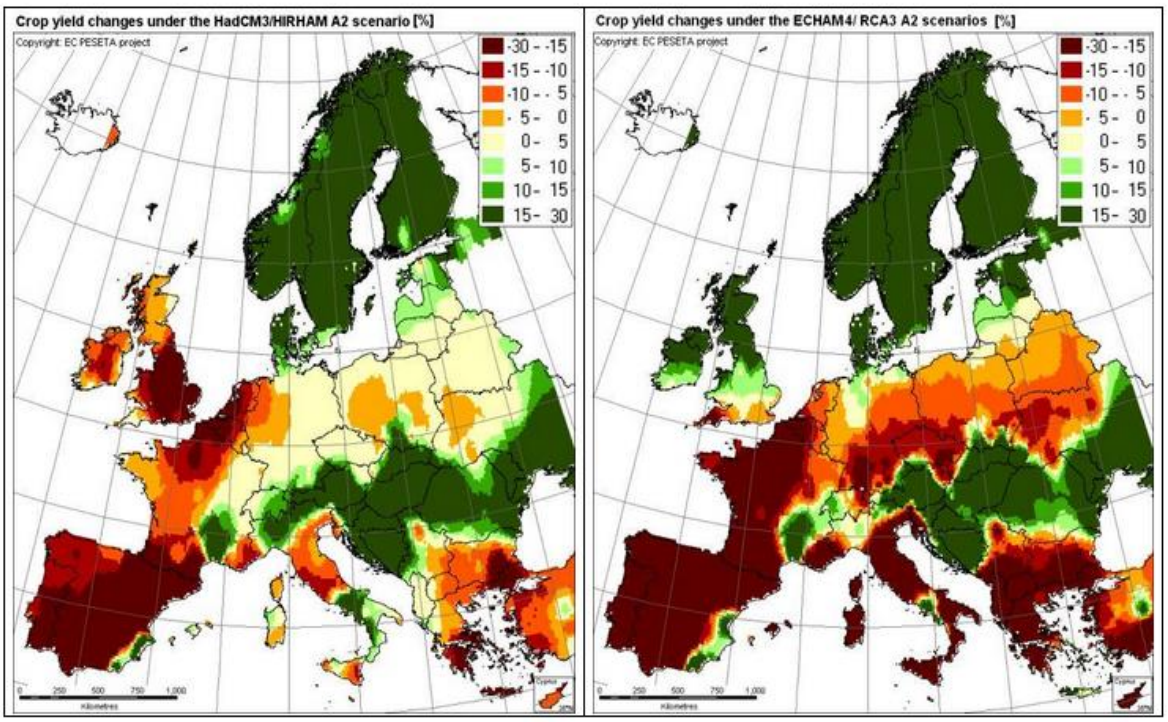

Figura 4. Impacto del Cambio Climático sobre el porcentaje de producción de los cultivos en dos predicciones diferentes de Cambio Climático (PESETA I, 2016).

Por otro lado, este cambio en las condiciones climáticas del planeta no es el único reto para la conservación de los ecosistemas pues, como anteriormente se ha comentado, se encuentra dentro de un marco de Cambio Global. Dentro de este marco el cambio en el uso del suelo es uno de los principiales problemas para la conservación. Además de la pérdida de hábitats y biodiversidad, el uso de suelos para la agricultura, la industria y la urbanización generan una serie de residuos que, al no ser tratados correctamente, se distribuyen por los diferentes ecosistemas (Lu et al. 2018). Se prevé que la generación de residuos por persona sigan aumentando durante este siglo (Figura 5; Hoornweg et al. 2013).

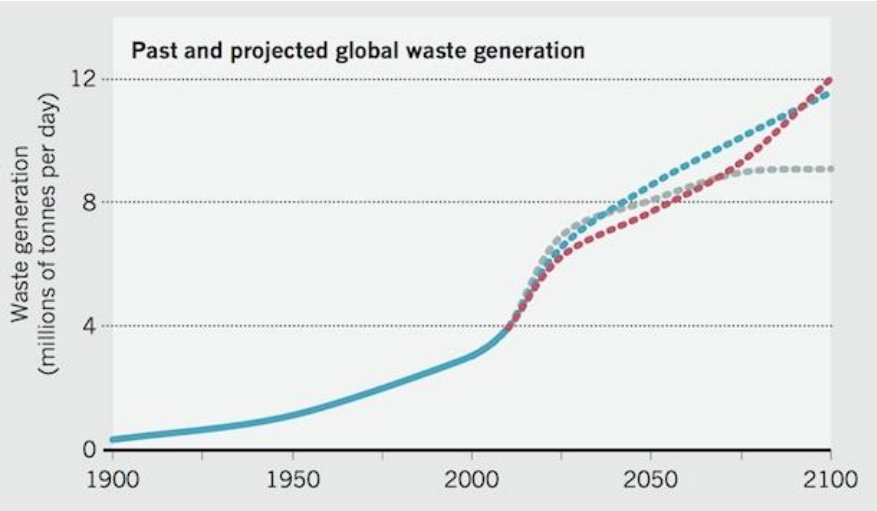

Figura 5. Evolución predicha de la producción de residuos por tres modelos diferentes (Hoornweg et al., 2013)

Entre estos residuos se pueden encontrar metales pesados como cobre, zinc, plomo o cadmio (Lu et al. 2018; Tabla 1), aunque la tendencia general de la contaminación por metales es difícil de predecir. Hay estudios que aseguran un incremento de algunos metales y otros que se mantendrán estables (Lu et al., 2018). La contaminación de los suelos por metales pesados derivados de la actividad humana es otra de las amenazas principales que afecta a la conservación de los ecosistemas (Occhipinti-Ambrogi, 2007). Especialmente en ecosistemas marinos como estuarios y marismas, que sirven como barrera de los contaminantes antes de que lleguen a los oceános desde los continentes (Lu et at., 2018). Además, estas zonas suelen estar más pobladas debido a la cantidad de recursos que generan, por lo que son más vulnerables a los contaminantes antropogénicos, así como a ciertos factores de Cambio Climático anteriormente comentados (IPCC, 2007; Lu et al., 2018).

Tabla 1. Principales fuentes de contaminación por metales pesados de los ecosistemas (Lu et al. 2018)

Metal	Fuente	Referencias
Cu	Minería, manufacturas de pinturas, siderurgia, pinturas de barcos, aguas residuales industriales o urbanas, maderas, vertidos de petróleo	Osher et al., 2006; Nieto et al., 2007; Moreno et al., 2011; Popadic et al., 2013; Brady et al. 2014
Zn	Minería, manufactura de pinturas, siderurgia, pinturas de barcos, aguas residuales industriales o urbanas, vertidos de petróleo	Osher et al., 2006; Nieto et al., 2007; Moreno et al., 2011; Popadic et al., 2013; Brady et al., 2014
Pb	Refinerías, producción de metales, quema de carbón, producción de cemento, astilleros, vertidos de petróleo	Moreno et al., 2011; Popadic et al., 2013; Chae et al., 2014
Cd	Minería, coque, litogénico, fertilizantes de fosfato	Osher et al., 2006; Nieto et al., 2007; Dou et al., 2013; Brady et al., 2014
Cr	Manufactura de pinturas, quema de combustibles fósiles, fuentes geogénicas, navegación, vertidos de petróleo	Osher et al., 2006; Moreno et al., 2011; Popadic et al., 2013; Brady et al., 2014; Keshavarzi et al., 2015
Ni	Quema de combustibles fósiles, fuentes geogénicas	Brady et al., 2014; Keshavarzi et al., 2015
As	Manufactura de pinturas, refinería de metales, quema de carbón, industria química	Popadic et al., 2013; Brady et al., 2014; Chae et al., 2014
Hg	Minería, coque, manufactura de pintura, residuos de materiales calcinados, industria del papel, pesticidas y erupciones volcánicas	Osher et al., 2006; Choi et al., 2007; Nieto et al.,2007; Popadic et al., 2013; Brady et al., 2014; Looi et al., 2015

1.3 La vegetación de marisma: Las halófitas

En las marismas encontramos vegetación adaptada a condiciones de alta salinidad en el suelo, debido a la influencia mareal (Flowers et al., 2008; 2015). Las plantas con capacidad de crecer y completar su ciclo vital en estos suelos, con una concentración de al menos 200 mM NaCl, son conocidas como halófitas (Flowers et at., 1986). Dentro de las especies halófitas podemos encontrar diferentes efectos de la sal sobre el creimiento (Flowers et al., 2008), desde las que simplemente toleran crecer en estos ambientes, aunque también pueden crecer en suelos con concentraciones más bajas de sal o en ausencia de la misma, hasta las que aumentan la producción de biomasa cuando son expuestas a concentraciones de sal elevadas (Flowers et al., 2008). Además de su potencial para vivir en ambientes salinos, estas plantas son interesantes por su alta producción, equiparable a la de algunos cultivos (Flowers et al., 2008). Para poder crecer con éxito en estas condiciones han desarrollado una serie de adaptaciones, muchas de ellas todavía por conocer en profundidad (Flowers et al., 2008). Entre estas adaptaciones tenemos: glándulas que exudan la sal, tejidos suculentos o la compartimentación de los iones Na^+ y Cl^- (Munns and Tester, 2008; Flowers et al., 2008; 2015). Saslis-Lagoudakis et al. (2015) sugirieron que la adaptación a altas salinidades de las halófitas puede haber dado lugar a mecanismos que les permiten tolerar otros tipos de estrés abiótico. Esto podría explicar la resistencia a la presencia de metales pesados en el medio de estas plantas (Lutts y Lefèvre, 2015). Ventura et al. (2015) discutieron ampliamente la posibilidad de aprovechar estas plantas como recursos alimentarios o como fuentes de metabolitos con interés farmacológico, incluso su aplicación como plantas ornamentales. Aún así, todavía falta mucho para tener una idea completa sobre el funcionamiento de estas especies (Flowers et al., 2015) y, sobre todo, acerca de su respuesta ante las posibles condiciones climáticas del futuro próximo.

Muchos estudios han demostrado el efecto beneficioso que puede tener el aumento del CO_2 atmosférico en halófitas C_3 (Ghannoum et al., 2000) y C_4 (Mateos-Naranjo et al., 2010a; b). Pero este efecto está altamente influenciado por otros factores abióticos como la salinidad. Lenssen et al. (1993) encontraron en la especie con metabolismo C_3 *Elymus athericus* que una atmósfera enriquecida en CO_2 aumentaba la biomasa seca y que este aumento era mayor en condiciones de alta salinidad. También encontraron para la especie *Spartina anglica* que concentraciones altas de CO_2 atmosférico reducían la biomasa, aunque en condiciones de alta salinidad no se producía ese decrecimiento. Lenssen et al.

(1995) observaron un efecto positivo de las altas concentraciones de CO_2 en *Aster tripolium* y *Puccinellia maritima*, que en las raíces era solo evidente cuando las plantas estaban anegadas, y estos efectos eran incluso mayores en presencia de sal. Duarte et al. (2014) comprobaron que la inundación completa de las hojas no afectaba el efecto positivo del CO_2 sobre la fotosíntesis, que incrementaba la actividad de la Rubisco en *Halimium portulacoides* y *Spartina maritima*. Sin embargo, también se comprobó que *A. tripolium* en condiciones de alto CO_2 y presencia de sal invertía el excedente fotosintético en generar más defensas de estrés oxidativo y no en acumular más biomasa (Geissler et al., 2009; Geissler et al., 2010). Rozema (1993) estudió el efecto de la salinidad en combinación con una atmósfera de elevado CO_2 en la fotosíntesis y el uso del agua en diferentes especies, entre ellas *Spartina patens*. Observó que la alta salinidad mejoraba aún más el uso del agua que ocurría a concentraciones de CO_2 elevadas, algo que también demostraron otros estudios posteriores (Geissler et al., 2009; 2010). También se ha comprobado que la concentración de CO_2 alta paliaba los efectos perjudiciales de la salinidad elevada en *Spartina maritima*, *Spartina densiflora* (Mateos-Naranjo et al., 2010a; b) y *Aster tripolium* (Geissler et al., 2009; 2010). No obstante, todavía quedan muchas incógnitas sobre cómo afectará el Cambio Climático a la fisiología y el crecimiento de las halófitas.

Para responder a todas las cuestiones que todavía quedan por resolver (por qué disminuye el crecimiento de las halófitas a altas salinidades, cómo funcionan sus mecanismos, cómo se verán afectados estos mecanismos por las futuras condiciones del planeta) lo idóneo sería trabajar con plantas modelo. Flower et al. (2008) sugieren estudiar plantas que tengan una amplia tolerancia a la sal y que sean un grupo taxonómico con una buena representación entre las halófitas. Una familia que cumple estas condiciones sería Chenopodiaceae, dentro de la cual se encuentra el género *Salicornia*. La especie *Salicornia ramosissima* J. Woods ha sido propuesta como un cultivo alternativo en regiones áridas o semi-áridas (Lu et al., 2010) y actualmente está siendo utilizada en países como España o Francia, junto con otras halófitas, como un ingrediente de la cocina gourmet (Barrerira et al., 2017). Además, varias especies del género *Salicornia* han demostrado la capacidad de poder acumular compuestos de interés económico (Singh et al., 2014). Por ello, *S. ramosissima* es una especie interesante como modelo de las halófitas, para estudiar cómo respondería frente a las condiciones climáticas predichas para los próximos años.

Como ya se ha comentado, la respuesta de las plantas a condiciones de alto CO_2 están influidas por otros factores abióticos. Así, por ejemplo, la presencia de metales pesados derivados de la actividad humana junto con el aumento del CO_2 atmosférico debido al Cambio Climático pueden tener importantes consecuencias sobre las especies vegetales. Tian et al. (2014) encontraron que en condiciones de alto CO_2 atmosférico las plantas que no toleraban la presencia de metales pesados veían disminuido los efectos negativos de estos. Li et al. (2012) describieron mayores tolerancia y capacidad de fitoremediación en plantas tolerantes a metales pesados cuando eran crecidas a altas concentraciones de CO_2.

Entre las halófitas originarias de ecosistemas costeros encontramos también varias especies con capacidad de tolerar y acumular metales pesados (van Oesten et al., 2015; Pérez-Romero et al., 2016; Liang et al., 2017; Feng et al.; 2018). La especie C_4 *Spartina densiflora*, por ejemplo, demuestra gran tolerancia al cobre (Mateos-Naranjo et al., 2008). La contaminación por Cu es una de las más comunes y preocupantes en ecosistemas costeros debido a que está presente en los residuos de aguas agrícolas y urbanas (Kessel et al., 2008; Lu et al., 2018). También encontramos especies C_3 como *Juncus acutus* con capacidad de tolerancia a diferentes metales pesados como el zinc (Mateos-Naranjo et al., 2014; Santos et al., 2014; Christofilopoulos et al., 2016). No obstante, se desconoce cómo se verían afectadas la tolerancia y la capacidad de fitorremediación de estas halófitas frente a factores derivados del Cambio Climático.

En definitiva, hay un gran vacío de conocimiento respecto a la respuesta de las halófitas frente a las interacciones de factores de estrés abiótico, relacionados con los cambios globales que experimenta el planeta. Los estudios en los que interaccionan más de dos factores son muy limitados (Lenssen et al., 1995). El escenario previsto de Cambio Climático y la propuesta de halófitas como cultivos alternativos, para responder a la demanda de alimentos de la creciente población, hacen aún más necesarios estudios que cubran ese vacío de conocimiento. En esa línea es en la que se ha desarrollado la presente Tesis Doctoral.

OBJETIVOS

En esta Tesis Doctoral se pretende mejorar el conocimiento sobre la respuesta fisiológica de las halófitas frente a las condiciones climáticas previstas en el escenario de Cambio Climático. Con tal fin se establecieron dos objetivos principales:

1) Comprobar los efectos que diferentes factores derivados del Cambio Climático podrían tener sobre la fisiología de una halófita modelo. Para ello, se realizó un análisis fisiológico profundo sobre el efecto de las interacciones de factores abióticos relacionados con el Cambio Climático en la especie *Salicornia ramosissima* (familia Chenopodiaceae); debido al interés, anteriormente mencionado, que presenta esta especie como cultivo alternativo y a su potencial como planta modelo. Para la consecución de este primer objetivo se estudió:

1. La respuesta fisiológica de *S. ramossisima* frente a un incremento de CO_2 en interacción con diferentes salinidades en el medio de crecimiento.
2. La respuesta fisiológica de *S. ramossisima* frente a un incremento de CO_2 en interacción con un aumento de la salinidad y una situación de inundación.
3. El efecto de eventos extremos cortos de alta y baja temperatura, en presencia de distintas concentraciones de sal, sobre la fisiología de *S. ramossisima.*

2) Analizar el efecto de la interacción de factores derivados del Cambio Climático y factores relacionados con otro tipo de Cambio Global, la contaminación, en halófitas. Para ello, se estudió la respuesta fisiológica de dos halófitas de probada capacidad fitorremediadora, *Spartina densiflora* y *Juncus acutus* (Mateos-Naranjo et al., 2008; 2014; Santos et al., 2014; Christofilopoulos et al., 2016), frente a la interacción de factores abióticos relacionados con el Cambio Climático. Para la consecución de este segundo objetivo se realizaron dos ensayos diferentes:

1. Estudio del efecto de distintas concentraciones de CO_2 atmosférico sobre la capacidad fitorremediadora de cobre de *Spartina densiflora*.
2. Estudio del efecto de diferentes concentraciones de sal sobre la capacidad fitorremediadora de zinc de *Juncus acutus*.

La consecución de estos dos objetivos principales ha posibilitado profundizar en el conocimiento general de las halófitas, incorporando medidas de parámetros

fisiológicos pocas veces usados en este tipo de plantas. Además, los estudios realizados contribuyen a establecer a *S. ramossisima* como halófita modelo de estudio.

PUBLICACIONES

CAPÍTULO 2:

Disentangling the effect of atmospheric CO_2 enrichment on the halophyte *Salicornia ramosissima* J. Woods physiological performance under optimal and suboptimal saline conditions

Pérez-Romero et al., 2018, Plant Physiology and Biochemistry

Plant Physiology and Biochemistry 127 (2018) 617–629

Contents lists available at ScienceDirect

Plant Physiology and Biochemistry

journal homepage: www.elsevier.com/locate/plaphy

Research article

Disentangling the effect of atmospheric CO_2 enrichment on the halophyte *Salicornia ramosissima* J. Woods physiological performance under optimal and suboptimal saline conditions

Jesús Alberto Pérez-Romero[a,*], Yanina Lorena Idaszkin[b,c], Jose-Maria Barcia-Piedras[d], Bernardo Duarte[e], Susana Redondo-Gómez[a], Isabel Caçador[e], Enrique Mateos-Naranjo[a]

[a] Departamento de Biología Vegetal y Ecología, Facultad de Biología, Universidad de Sevilla, 1095, 41080, Sevilla, Spain
[b] Instituto Patagónico para el Estudio de los Ecosistemas Continentales (IPEEC-CONICET), Boulevard Brown, 2915, U9120ACD, Puerto Madryn, Chubut, Argentina
[c] Universidad Nacional de la Patagonia San Juan Bosco, Boulevard Brown, 3051, U9120ACD, Puerto Madryn, Chubut, Argentina
[d] Department of Ecological Production and Natural Resources Center IFAPA Las Torres, Tomejil Road Sevilla, Cazalla Km 12'2, 41200, Alcalá del Río, Seville, Spain
[e] MARE - Marine and Environmental Sciences Centre, Faculty of Sciences of the University of Lisbon, Campo Grande, 1749-016, Lisbon, Portugal

ARTICLE INFO

Keywords:
Atmospheric CO_2 enrichment
Climate change
Halophyte
Gas exchange
Chlorophyll fluorescence
Salinity

ABSTRACT

A mesocosm experiment was designed to assess the effect of atmospheric CO_2 increment on the salinity tolerance of the C_3 halophyte *Salicornia ramosissima*. Thus, the combined effect of 400 ppm and 700 ppm CO_2 at 0, 171 and 510 mM NaCl on plants growth, gas exchange, chlorophyll fluorescence parameters, pigments profiles, anti-oxidative enzyme activities and water relations was studied. Our results highlighted a positive effect of atmospheric CO_2 increment on plant physiological performance under suboptimal salinity concentration (510 mM NaCl). Thus, we recorded higher net photosynthetic rate (A_N) values under saline conditions and 700 ppm CO_2, being this effect mainly mediated by a reduction of mesophyll (g_m) and biochemical limitation imposed to salt excess. In addition, rising atmospheric CO_2 led to a better plant water balance, linked with a reduction of stomatal conductante (g_s) and an overall increment of osmotic potential (Ψ_o) with NaCl concentration increment. In spite of these positive effects, there were no significant biomass variations between any treatments. Being this fact ascribed by the investment of the higher energy fixed for salinity stress defence mechanisms, which allowed plants to maintain more active the photochemical machinery even at high salinities, reducing the risk of ROS production, as indicated an improvement of the electron flux and a rise of the energy dissipation. Finally, the positive effect of the CO_2 was also supported by the modulation of pigments profiles (mainly zeaxhantin and violaxhantin) concentrations and anti-oxidative stress enzymes, such as superoxide dismutase (SOD) and ascorbate peroxidase (APx).

1. Introduction

Climatic change and salinization of soil are two of the greatest problems that will threat the conservation of the ecosystems worldwide (Occhipinti-Ambrogi, 2007), being soil degradation one of its main consequences (IPCC, 2007). In addition together with this conservation problem, it is expect that these environmental changes could alter the economy and health of the people (Peng et al., 2004; Naudts et al., 2013). Among the main economy activities, it seems that the productivity of agricultural systems will be severely affect by these changes (Yadav et al., 2011). Thus, climate change emerges as one of the biggest challenges for sustaining global agriculture production, being therefore crucial to find options to mitigate its effects on agricultural production. One of such options is the use of alternative crops, species capable of growing in hostile environments (salinity and water deficit). In this regard, halophyte species have been proposed, since these plants species present tolerance mechanisms against environmental stress, high productivity and exceptional nutritional values (Ventura et al., 2015; Ventura and Sagi, 2013). Some studies have assessed the response of halophytes to NaCl salinity conditions and atmospheric CO_2 enrichment (Geissler et al. 2009a, 2009b, 2015; Hussin et al., 2017) indicating an overall improvement of photosynthetic rate and water use efficiency. However, this information is limited for a small number of species. Being necessary to increase this knowledge for a great number of species and especially for those, which are valuable resources for human activities.

* Corresponding author. Dpto. Biología Vegetal y Ecología, Facultad de Biología, Universidad de Sevilla, Av Reina Mercedes s/n, 41012, Sevilla, Spain.
E-mail address: jperez77@us.es (J.A. Pérez-Romero).

https://doi.org/10.1016/j.plaphy.2018.04.041
Received 4 October 2017; Accepted 30 April 2018
Available online 01 May 2018
0981-9428/

Abbreviations

RGR	Relative growth rate
RWC	Relative water content
Ψ_o	Osmotic potential
A_N	Net photosynthetic rate
g_s	Stomatal conductance
C_i	Intercellular CO2 concentration
iWUE	Intrinsic water use efficiency
ETR_{max}	Maximum electron transport rate
g_m	Mesophyll conductance
RuBP	Ribulose-1,5-biphospate carboxylase/oxygenase
$V_{c,max}$	Maximum carboxylation rate allowed by ribulose-1,5-biphospate carboxylase/oxygenase
PSII	Photosystem II
F_v/F_m	Maximum quantum efficiency of PSII photochemistry
Φ_{PSII}	PS II Operational and Maximum Quantum Yield
CAT	Catalase enzymatic activity
APX	Ascorbate peroxidase enzymatic activity
SOD	Superoxide dismutase enzymatic activity
ROS	Reactive oxygen species

Salicornia ramosissima J. Woods is a C_3 halophyte species which has been proposed as an alternative crop especially in arid and semiarid regions of the world (Lu et al., 2010). Nowadays this species is recognized as a multifunctional cash crop, since it is being used as gourmet ingredient in many countries like Spain or France along with others halophytes (Barreira et al., 2017). In addition, it possible use for feed the cattle due its edible characteristic (Isca et al., 2014) and as phytoremediation tool; (Sharma et al., 2010; Zhang et al., 2013; Pedro et al., 2013; Nunes da Silva et al., 2014; Perez-Romero et al., 2016). In addition, few species of *Salicornia* genus have demonstrated the ability to accumulate a broad variety of compounds (metabolites) with economic interest (Singh et al., 2014). However, for its efficient exploitation it is necessary to assess the evolution of this species of special interest in the near future climatic conditions. Up-to-day, the effect of the incipient rising CO_2 atmospheric concentration in this specie has not been study. Being a C_3 specie our hypothesis is that atmospheric CO_2 enrichment could lead to an increase in the photosynthetic efficiency and a better capacity to use the water with a consequent increment in biomass, as has been described for other plants species (Ghannoum et al., 2000). Despite the positives evidences, there is not a consensus about this. Since this response is specie dependent and highly influenced by others abiotic factors, such as salinity (Lenssen et al., 1993; Lenssen et al., 1995; Rozema, 1993; Geissler et al., 2009b; Geissler et al., 2010; Mateos-Naranjo et al., 2010a; b) or drought (Calvo et al., 2017). Therefore, this study was designed and conduced to: (1) determine the growth *S. ramosissima* plants in salinity treatments ranging from 0 to 510 Mm NaCl at two CO_2 concentrations (400 and 700 ppm CO_2); (2) assess the relation between the growth and photosynthetic apparatus responses, in terms of CO_2 fixation, isotopes signature PSII efficiency, photosynthetic pigments, electron transport rate energy fluxes; and (3) in the modulation of its antioxidant defence abilities.

2. Material and methods

2.1. Plant material

Seeds of *S. ramosissima*, which were collected in September 2014 from Odiel marshes (37º15′N, 6º58′O; SW Spain), were moved into a germinator (ASL Aparatos Científicos M-92004, Madrid, Spain). There, the seeds were subjected to a day-night regime of 16 h of light (photon flux rate, 400–700 nm, 35 μmol m^{-2} s^{-1}) at 25 °C and 8 h of darkness at 12 °C, for 15 days. Then, seedlings were planted in individual plastic plots (9 cm high x 11 cm diameter) using perlite as substrate, and placed in a greenhouse with controlled conditions (temperature between 21 and 25 °C, relative humidity 40–60% and natural daylight of 250 μmol m^{-2} s^{-1} as minimum and 1000 μmol m^{-2} s^{-1} as maximum light flux). The pots were allocated in shallow trays watering with 20% Hoagland's solution (Hoagland and Arnon, 1938) and 171 mM NaCl. Plants were kept under the previously described conditions until the experimental setup.

2.2. Experimental treatments

In October of 2015, after 3 months of seedling culture, plants with an initial height of 17 cm were randomly divided in six blocks of 10 plants. Then, they were subjected to three NaCl concentrations (0, 171 and 513 mM NaCl) in shallow trays. These salt treatments were chosen based on the concentrations that can be found in the natural distribution of the specie (Redondo-Gómez et al., 2006), being 171 mM the optimal concentration for the growth of this specie (Perez-Romero et al., 2016). The three salinities were combined with two atmospheric CO_2 concentrations (400 ppm and 700 ppm) in controlled-environment chambers (Aralab/Fitoclima 18.000 EH, Lisbon, Portugal) for 30 days. Being an annual specie, this period of time was used to avoid a decreased in the physiology variables due to age. The high level of CO_2 concentration was selected following the data from the IPCC (2014) for the next century. Chamber environmental conditions were: alternating diurnal regime of 14 h of light and 10 h of darkness, light intensity of 300 μmol m^{-2} s^{-1}, temperature between 21 and 25 °C and 40–60% relative humidity. Atmospheric CO_2 concentrations in chambers were continuously recorded by CO_2 sensors (Aralab, Lisbon, Portugal) and maintained by supplying pure CO_2 from a compressed gas cylinder (Air liquide, B50 35K).

2.3. Growth analysis

At the beginning and at the end of the experiment belowground and aboveground fractions of 10 plants for each time were separated, dried at 80 °C for 48 h and weighed. The relative growth rate (RGR) was calculated using the formula:

$$RGR = (\ln (Bf) - \ln (Bi))\ D^{-1}\ (g\ g^{-1}\ day^{-1})$$

Where Bf = final dry mass (an average ten plants per treatment), Bi = initial dry mass (an average of the plants dried at the beginning of the experiment) and D = duration of experiment (days).

In addition, before and after the treatments, the height of the main branches and the number of branches longer than 1 cm were measured.

2.4. Water content

Relative water content (RWC) of primary branches (n = 10 per treatment) were calculated after 30 days of treatment as follow:

$$RWC = ((FW - DW) / (FW - TW))\ 100$$

Where FW = fresh weight of the branches, DW = dry weight after oven-drying at 80 °C for 48 h and TW = turgid weight after being in water at 4 °C for 24 h.

2.5. Osmotic potential

The osmotic potential (Ψ_o) of primary branches (n = 6) was determined after the 30 days of the treatments, using psychrometric technique with a Vapor Pressure Osmometer (5600 Vapro, Wescor,

Logan, USA).

2.6. Measurement of gas exchange

Gas exchange measurements were taken on random primary branches using an infrared gas analyser in an open system (LI-6400, LI-COR Inc., Neb., USA) after 30 days of treatment (n = 7). Net photosynthetic rate (A_N), stomatal conductance (g_s) and intercellular CO_2 concentration (C_i) were determined. With following conditions: a photosynthetic photon flux density (PPFD) 1000 μmol m^{-2} s^{-1} (with 15% blue light to maximize stomatal aperture), vapour pressure deficit of 2.0–3.0 kPa and air temperature of 25 ± 2 °C. The ambient CO_2 concentration (C_a) was of 400 ppm air or 700 ppm air depending on the concentration that plants were exposed to during the experiment.

Photosynthetic area was approximated as half the area of the cylindrical branches, as only the upper half received the unilateral illumination in the leaf chamber (Redondo-Gómez et al., 2010). Intrinsic water use efficiency ($_i$WUE) was also calculated as the ratio between A_N and g_s. In addition, ETR_{max}/A_N ratio was calculated with the values obtained from fluorescence rapid light curves (see below) and gas exchange measurements.

Furthermore, mesophyll conductance (g_m) and maximum carboxylation rate allowed by ribulose-1,5-biphospate (RuBP) carboxylase/oxygenase ($V_{c,max}$) were obtained by the curve-fitting method (Ethier and Livingston, 2004) using the software package developed by Sharkey et al. (2007). To attain this approach, we performed four A_N/C_i curves on random primary branches at the same environmental conditions used previously for instantaneous gas exchange measurements. An infrared gas analyser in an open system (LI-6400, LI-COR Inc., Neb., USA) equipped with a light leaf chamber (Li-6400-02B, Li-Cor Inc.) was used. When the steady-state was reached the curves were performed by decreasing C_a stepwise until 50 μmol mol^{-1}. Therefore, to complete the curve the chamber conditions were restored to the initial C_a and increased stepwise until 2000 ppm (Flexas et al., 2009; Pons et al., 2009). For each curves, 12 different C_a values were used. At each step, gas exchange was allowed to equilibrate for less than 120 s to reduce changes in Rubisco activity (Long and Bernacchi, 2003).

On the same branches dark respiration rate (R_d, μmol CO_2 m^{-2} s^{-1}) measurements were performed after curves assessment as CO_2 efflux. Branches chamber was darkened for 30 min to avoid transient post-illumination bursts of CO_2 releasing (Flexas et al., 2013). Leakage of CO_2 in and out of the leaf chamber was determined with photosynthetically inactive primary branches and corrected in all curves (Flexas et al., 2013).

2.7. Carbon and nitrogen content and stable isotope analysis

At the end of the experiment, carbon isotopic composition of the pulverized dry branches samples randomly collected (n = 5) was determined according to Duarte et al. (2014), using a Flash EA 1112 Series elemental analyser coupled on line via Finningan conflo III interface to a Thermo delta V S mass spectrometer. Using the formula: $\delta^{13}C$ or $\delta^{15}N = [(R_{sample}/R_{standard})^{-1}] - 10^3$, where R is $^{13}C/^{12}C$ or $^{15}N/^{14}N$, the carbon and nitrogen isotope ratio were calculated. They were expressed in delta (δ) notation, explained as the parts per thousand (‰) deviation from a standard material (PDB limestone for $\delta^{13}C$ in air for $\delta^{15}N$). The analytical precision for the measurement was 0.2‰. Carbon and nitrogen contents (%) were assessed simultaneously using the same method.

2.8. Measurement of chlorophyll fluorescence

Chlorophyll fluorescence measurements were performed using a FluorPen FP100 (Photo System Instruments, Czech Republic) in the same branches of gas exchange analysis at the end of the experiment (n = 7). Branches were dark-adapted for 30 min with special pliers designed for that purpose before the measurement. All the parameters were measured again in light adapted branches. As Schreiber et al. (1986) described, light energy yields of Photosystem II (PSII) reaction centers were determined with a saturation pulse method. To estimate the maximum fluorescence signal across time, a saturating light pulse of 0.8 s with an intensity of 8000 μmol m^{-2} s^{-1} was used. A comparison of the minimum fluorescence (F'0), the maximum fluorescence (F'm) and the operational photochemical efficiency values were made with the values of light and dark adapted branches. Quantum yield of PS II (QY) and relative Quantum yield of PS II (Q'Y) were calculated as F_v/F_m and Φ_{PSII} respectively. Following (Duarte et al., 2015a), maximum electron transport rate (ETR_{max}) and the chlorophyll a fast kinetics, or JIP-test (or Kautsky curves), which depicts the rate of reduction kinetics of various components of PSII, were also measured in dark-adapted leaves (n = 5 for each one) according to Duarte et al. (2015a), using the pre-programmed OJIP protocols of the FluorPen. All derived parameters for both RLC and OJIP were calculated according to Marshall et al. (2000) and Strasser et al. (2004) respectively (Table 1).

Table 1
Summary of fluorometric analysis parameters and their description.

Photosystem II Efficiency	
Fv/Fm	Maximum quantum efficiency of PSII photochemistry
PS II Operational and Maximum Quantum Yield (ΦPSII)	Light and dark-adapted quantum yield of primary photochemistry, equal to the efficiency by which a PS II trapped photon will reduce Q_A to Q_A^-
Rapid Light Curves (RLCs)	
ETR_{max}	Maximum ETR after which photo-inhibition can be observed
Energy Fluxes (Kautsky curves)	
Area	Corresponds to the oxidized quinone pool size available for reduction and is a function of the area above the Kautsky plot
W_K	Amplitude of the K-step.
φ_{E0}	Probability that an absorbed photon will move an electron into the electronic transport chain
φR_0	Electron movement efficiency from the reduced intersystem electron acceptors to the PSI and electron acceptors.
N	Reaction centre turnover rate
Sm	Relative pool size of PQ.
M_0	Net rate of PS II RC closure.
ABS/CS	Absorbed energy flux per leaf cross-section.
TR/CS	Trapped energy flux per leaf cross-section
ET/CS	Electron transport energy flux per leaf cross-section
DI/CS	Dissipated energy flux per leaf cross-section.
RC/CS	Number of available reaction centres per leaf cross section
Grouping Probability (P_G)	The grouping probability is a direct measure of the connectivity between the two PS II units (Strasser and Stribet, 2001)

2.9. Gauss peak-spectra pigment analysis

At the end of the experimental period, branches samples were randomly collected (n = 5), flash-frozen in liquid N_2 and freeze-dried for 48 h in the dark to avoid photodegratation processes (Duarte et al., 2015a). Then, samples were subsequently grinded in pure acetone and pigments extracted at −20 °C during 24 h in the dark to prevent its degradation, centrifuged at 4000 rpm during 15 min at 4 °C and the resulting supernatant scanned in a dual beam spectrophotometer (Hitachi Ltd., Japan) from 350 to 750 nm at 1 nm step. The resulting absorbance spectrum was use for pigment quantification by introducing the absorbance spectrum in a Gauss-Peak Spectra (GPS) fitting library, using SigmaPlot Software (Küpper et al., 2007).

2.10. Anti-oxidant enzymatic activity

Enzyme extraction was done following the methodology used by Duarte et al. (2015a). At the end of experiment, 500 mg of fresh branches samples were grounded in 8 ml of 50 mM sodium phosphate buffer (pH 7.6) with 0.1 mM Na-EDTA and were centrifuged at 10,000 × g for 20 min at 4 °C to obtained the soluble proteins. Three samples per treatment were used and three measurements per sample were registered. Protein content in the extracts was obtained according to Bradford (1976) protocol, using bovine serum albumin as a standard.

To quantify catalase (CAT) activity, the decrease in absorbance at 240 nm due to the consumption of H_2O_2 was measured according to Teranishi et al. (1974). The reaction mixture contained 50 mM of sodium phosphate buffer (pH 7.6), 0.1 mM of Na-EDTA, and 100 mM of

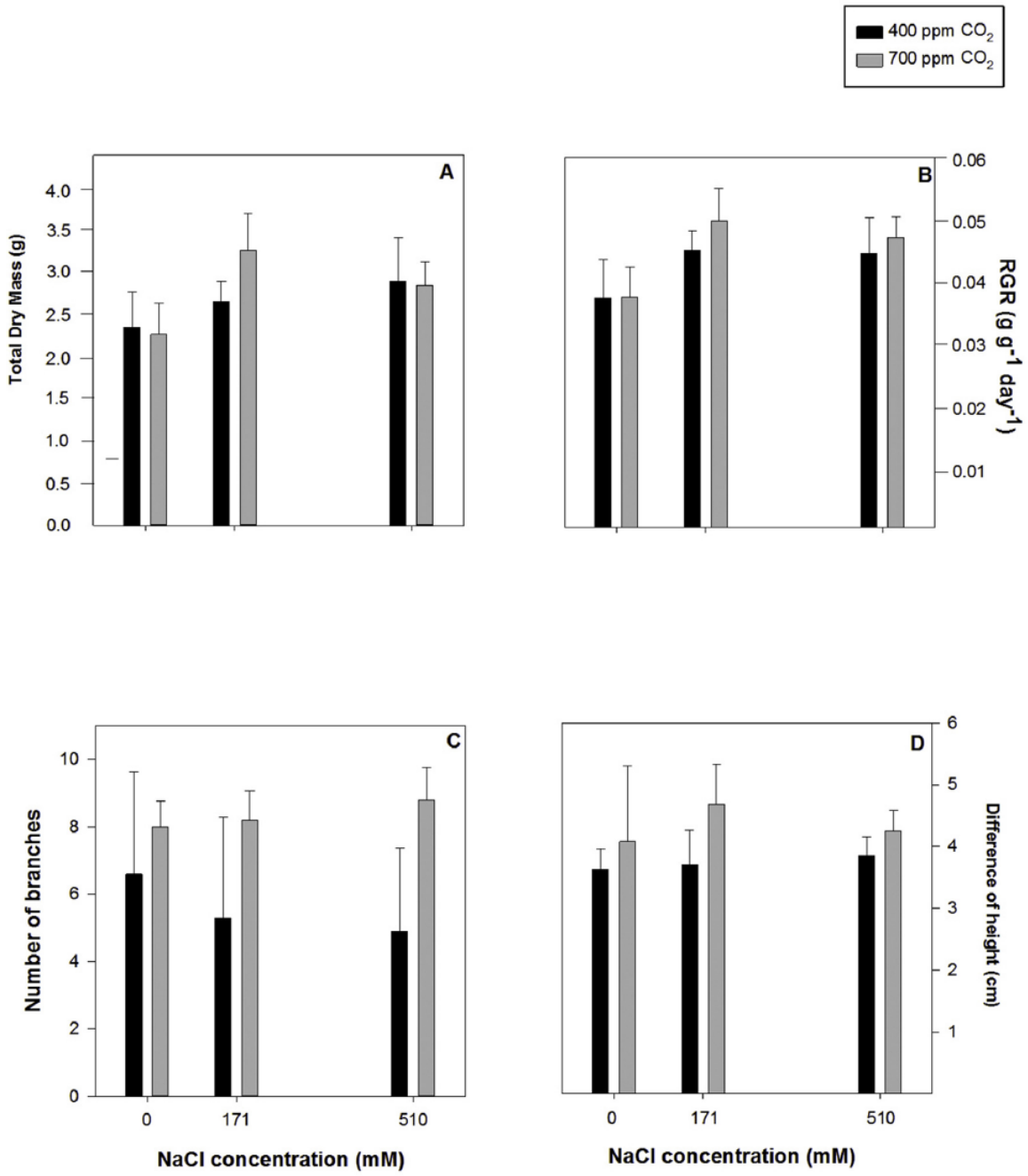

Fig. 1. Growth of *Salicornia ramosissima* in response to treatment with a range of NaCl concentrations at 400 and 700 ppm CO_2 for 30d. Relative growth rate (RGR) (A), height differences (B), ramification difference (C) and total dry mass (D). Values represent mean ± SE, n = 10. Different letters indicate means that are significantly different from each other (LSD test, $P < 0.05$).

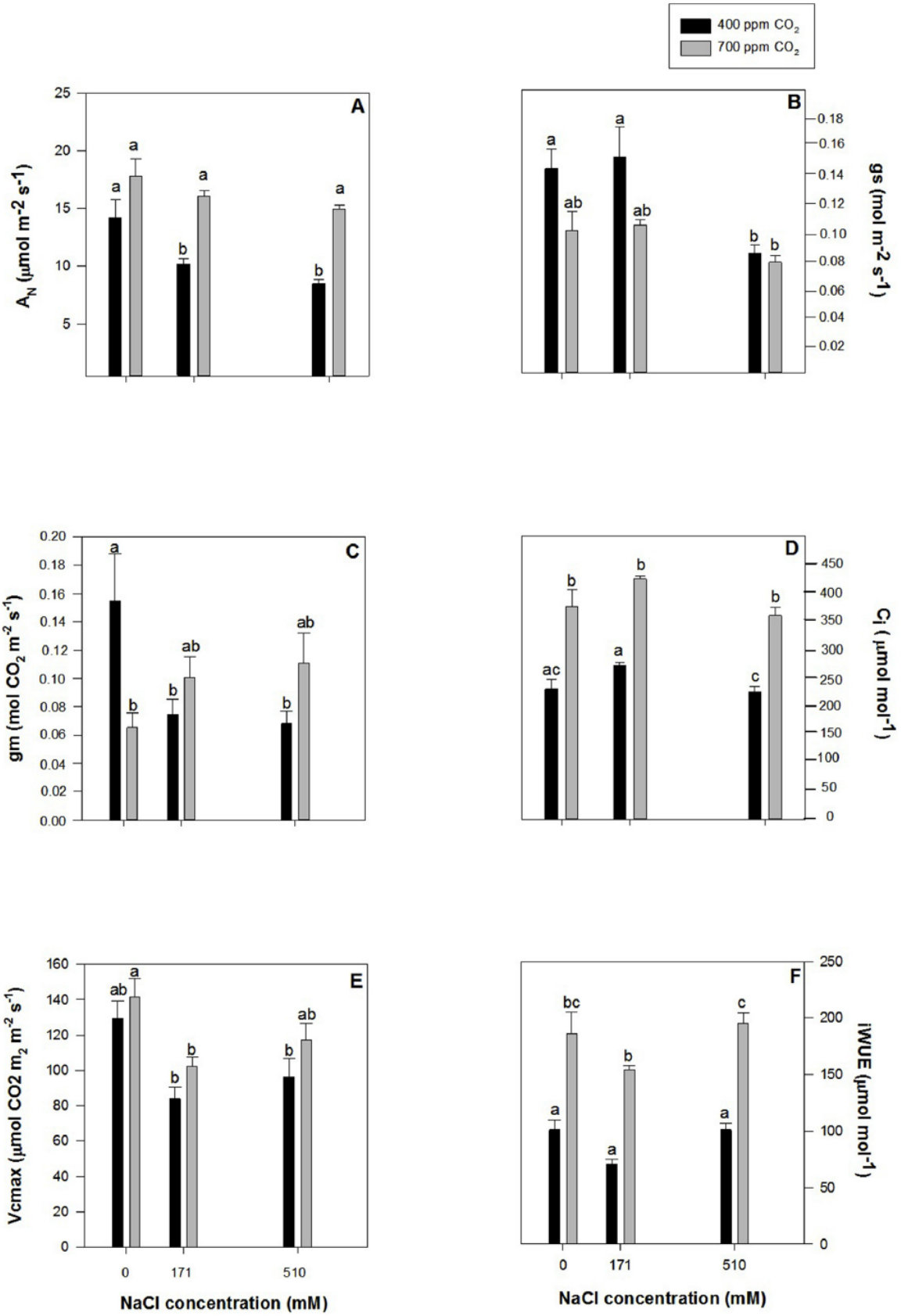

Fig. 2. Net photosynthetic rate, A_N (A), stomatal conductance, g_s (B) mesophyll conductance, gm (C), intercellular CO_2 concentration, Ci (D), maximum carboxylation rate, Vc_{max} (E) and intrinsic water use efficiency (iWUE) (F) in randomly selected, primary branches of *Salicornia ramosissima* in response to treatment with a range of NaCl concentrations at 400 and 700 ppm CO_2 after 30d of treatment. Values represent mean ± SE, n = 4. Different letters indicate means that are significantly different from each other (LSD, $P < 0.05$).

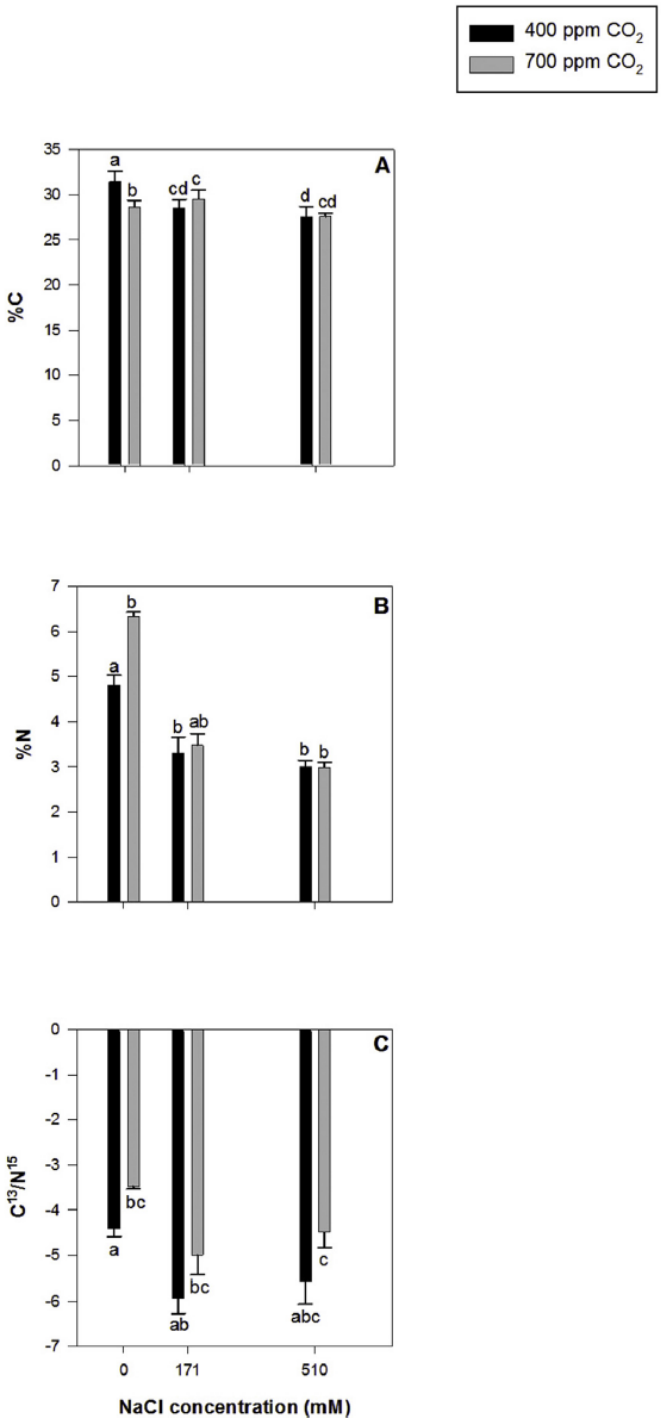

Fig. 3. Carbon percentage in leaves, %C (A), nitrogen percentage in leaves, %N (B) and carbon an nitrogen concentrations ratio, C/N (C) in randomly selected, primary branches of *Salicornia ramosissima* in response to treatment with a range of NaCl concentrations at 400 and 700 ppm CO_2 after 30d of treatment. Values represent mean ± SE, n = 5. Different letters indicate means that are significantly different from each other (LSD, $P < 0.05$).

H_2O_2. Ascorbate peroxidase (APX) activity was measured by monitoring the decrease in the absorbance at 290 nm. The reaction mixture contained 50 mM of sodium phosphate buffer (pH 7.0), 12 mM of H_2O_2, 0.25 mM l-ascorbate (Tiryakioglu et al., 2006). Molar coefficient of 2.8 mM^{-1} cm^{-1} was used to calculated the amount of ascorbate oxidized. For all this enzymatic enzymes 100 µL of vegetal extract was added at the reaction mixture to begin with the reaction. Superoxide dismutase (SOD) activity was assayed according to Marklund and Marklund (1974) by monitoring the reduction of pyrogallol at 325 nm. The reaction mixture was 50 mM of sodium phosphate buffer (pH 7.6), 0.1 mM of Na-EDTA, 3 mM of pyrogallol, Mili-Q water. The reaction was started with the addition of 10 µL of enzyme extract. The auto-oxidation of the substrates was evaluated by control samples without the enzyme extract.

2.11. Statistical analysis

All the statistic tests were performed by a statistical software package R. The differential effect of NaCl and atmospheric CO_2 concentrations treatments were determined by Two-way analysis of variance. Multiple comparisons were analyzed by a Tukey test. Before statistical analysis, Kolmogorov-Smirnov and Levene tests were used to verify the assumptions of normality and homogeneity of variances, respectively.

3. Results

3.1. Growth analysis

Salinity and atmospheric CO_2 concentration had not any significant effect on the growth of *S. ramosissima* after 30 day of treatments (Two-way ANOVA, $p > 0.05$). Thus total dry mass and RGR values did not significantly vary between each specific treatment, although overall plants grown at 700 ppm of CO_2 showed higher values than their non-CO_2 supplied counteracts (Fig. 1A and B). In addition, there were no statistical differences in the height and the number of branches (Fig. 1C and D).

3.2. Plant water state

The RWC values did not show any significant differences between salinity or CO_2 treatments (Two-way ANOVA, $p > 0.05$), ranging between 83 and 89% for all treatments. Contrary, in Ψ_0 we found an increased with the raise of NaCl concentration in similar degree for both CO_2 levels (Two-way ANOVA: salinity, $p > 0.05$), with values c. −2.4, −2.7 and −4.2 MPa for 0, 171 and 510 mM NaCl, respectively (data non-presented).

3.3. Gas exchange measurements

There was a significant effect of salinity and atmospheric CO_2 concentration on the gas exchange parameters of *S. ramosissima* after 30 day of treatments (Two-way ANOVA: salinity x CO_2, $p > 0.05$). Thus, A_N values decreased considerably in presence of NaCl in plants grown at ambient atmospheric CO_2 concentration, while it did not vary with salinity increment at elevated level of CO_2 (Fig. 2A). g_s values decreased considerably in plants grown at the highest salinity concentration compared with those exposed to low and middle NaCl concentrations and at ambient atmospheric CO_2. The values from gs were a 31% lower in plants grown at 700 ppm compared with those expose to 400 ppm at 0 and 171 mM NaCl, while it did not vary between both CO_2 levels at the highest NaCl concentration (Fig. 2B).

On the other hand, g_m values decreased considerably in presence of NaCl in plants grown at 400 ppm CO_2. In addition, g_m values were lower at elevated CO_2 and absence of NaCl addition, while it increased under saline conditions (Fig. 2C). $V_{c,max}$ decreased c. 22.5% for all treatments in presence of NaCl in the solution compared with those without NaCl supplementation (Fig. 2E). However, it was higher in plants grown at 700 ppm CO_2. Furthermore, C_i values were significantly greater in plants grown at 700 ppm for all salinity concentrations (Fig. 2D). Finally, overall ¡WUE did not vary between NaCl treatments, although it was considerably greater under elevated atmospheric CO_2 concentration (Fig. 2F).

3.4. Carbon and nitrogen content and stable isotope analysis

Carbon content did not highly vary between salinity and CO_2 treatments, showing in all cases values c. 29% (Fig. 3A). While N content decreased significantly with the presence of NaCl in the grown medium in similar degree for both atmospheric CO_2 levels, and it was higher in plants grown at 700 ppm in absence of NaCl addiction (Two-way ANOVA: salinity x CO_2, $p > 0.05$; Fig. 3B). On the other hand, C^{13}/N^{15} ratio increased with the presence of NaCl in the solution and were higher for the treatments grown at 400 ppm CO_2 (Two-way ANOVA: salinity x CO_2, $p > 0.05$; Fig. 3C).

3.5. Fluorescence measurements

F_v/F_m and Φ_{PSII} did not show a clear pattern of variation concerning to CO_2 and salinity treatments at the end of the experiment, showing closely similar values in all experimental treatments (Two-way ANOVA: salinity x CO_2, $p > 0.05$; Fig. 4A and B). Similarly, ETR_{max} values did not vary between treatments, showing mean values c. 40. However, the ETR_{max}/A_N remained constant for plants grown at 700 ppm CO_2. While it increased with NaCl concentration augmentation in those grown at 400 ppm CO_2 concentration (Fig. 4C).

Focusing on derived-parameters from the Kautsky curves, there is to notice that overall there was certain significant effect of CO_2 and NaCl concentrations in several variables (Two-way ANOVA: salinity x CO_2, $p > 0.05$). Thus, Wk, M_0, N, Sm, P_G, and φR_0 values were lower and EOCs higher in presence of NaCl in the grown medium, and overall these values did not differ between both atmospheric CO_2 concentration treatments (Fig. 5A and B,C,E,F). Contrary Area was not significant influenced by NaCl concentration, but was 35% greater in plants grown at 700 ppm and 510 mM NaCl compared those expose to 400 ppm CO_2 (Two-way ANOVA: CO_2, $p < 0.05$; Fig. 5D). On the other hand, the energetic fluxes on a leaf cross-section basis (phenomological fluxes) showed that ABS/CS, TR/CS, ET/CS and DI/CS did not present any statistical relationship with NaCl concentration, but these values were significantly higher in plants grown at 700 ppm CO_2 at the highest salinity concentration treatment (Two-way ANOVA: CO_2, $p < 0.05$; Fig. 6A–D).

3.6. Pigment concentration

Pigments concentration analysis showed that chlorophyll *a* and *b* concentrations did not vary between the different NaCl treatments, but overall these values were significantly higher at 700 ppm than at 400 ppm CO_2 (Two-way ANOVA: CO_2 $p < 0.05$; Table 2). Being the differences more accused at 0 and 171 mM NaCl. A similar trend could be seen in neoxanthin values, while violaxanthin and zeaxanthin concentration only varied between CO_2 levels at 0 mM NaCl.

3.7. Anti-oxidant enzymatic activity

CAT enzyme activity did not show a clear trend regarding salinity and CO_2 increment (Fig. 7A). While we found that APx and SOD enzymes activities were higher in plants grown at 700 ppm at 171 and 510 mM NaCl, and decreased in plant exposed to 0 mM NaCl compared with those plants grown at 400 ppm CO_2 (Two-way ANOVA: salinity x CO_2, $p > 0.05$; Fig. 7B and C).

4. Discussion

This study indicated that atmospheric CO_2 enrichment improved the physiological performance of *S. ramosissima* under suboptimal salinity concentration (NaCl excess), which becomes relevant for the future development of this interesting multifunctional cash crop in a context of future global climate change scenario. According to these results, Geissler et al. (2009a,b; 2015) found that the rising atmospheric CO_2 concentration had an ameliorative effect on salinity stress experienced by the halophytes C_3 *Aster trifolium* and C_4 *Atriplex numularia*, but without a positive effect on the biomass production. Accordingly, we found that *S. ramosissima* biomass did not highly vary with the atmospheric CO_2 increment, which could be linked with the investment of certain amount of the energy fixed during the photosynthetic process in several mechanisms for defense against salinity excess, as was

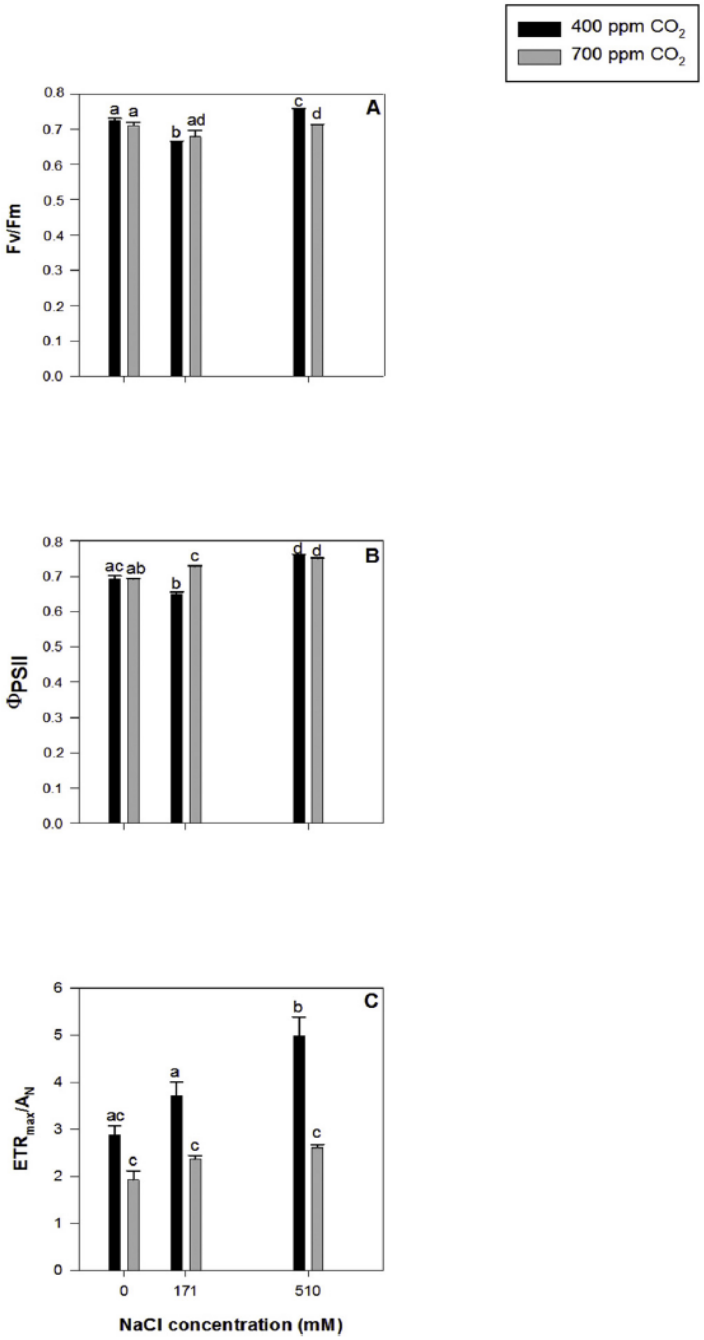

Fig. 4. Maximum quantum efficiency of PSII photochemistry, F_v/F_m (A), Light and dark-adapted quantum yield of primary photochemistry, equal to the efficiency by which a PS II trapped photon will reduce Q_A to Q_A^-, Φ_{PSII} (B) and Maximum ETR after which photo-inhibition can be observed net photosynthetic rate ratio, ETR_{max}/A_N (C) in dark adapted randomly selected, primary branches of *Salicornia ramosissima* in response to treatment with a range of NaCl concentrations at 400 and 700 ppm CO_2 after 30d of treatment. Values represent mean ± SE, n = 5. Different letters indicate means that are significantly different from each other (LSD, $P < 0.05$).

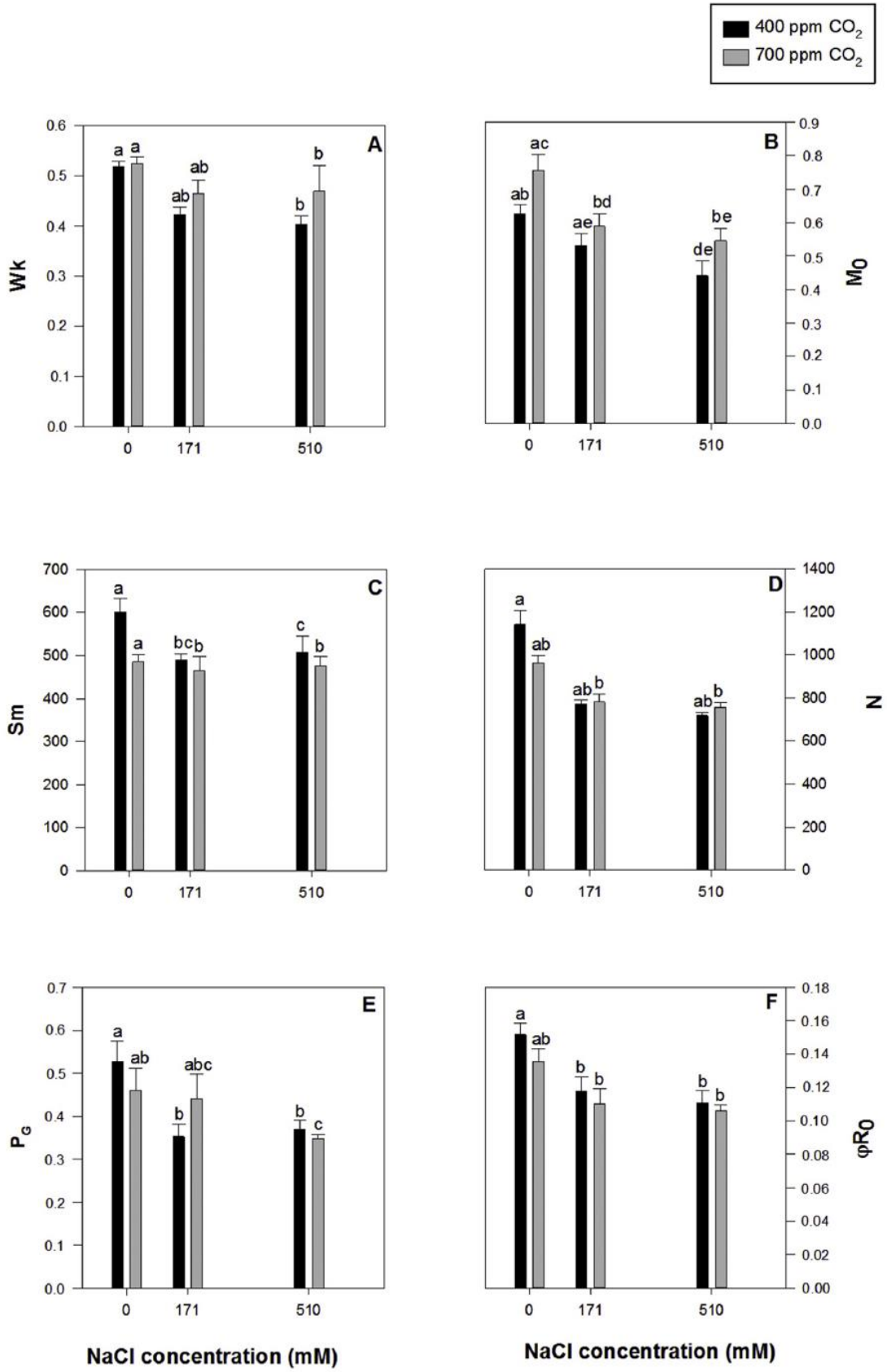

Fig. 5. Amplitude of the K-step, Wk (A), net rate of PS II RC closure, M_0 (B), relative PQ pool size, Sm (C), reaction centre turnover rate, N (D), grouping probability, PG (E) and maximum yield of primary photochemistry, φ_{R0}, (F) in dark adapted randomly selected, primary branches of *Salicornia ramosissima* in response to treatment with a range of NaCl concentrations at 400 and 700 ppm CO_2 after 30d of treatment. Values represent mean ± SE, n = 5. Different letters indicate means that are significantly different from each other (LSD, $P < 0.05$).

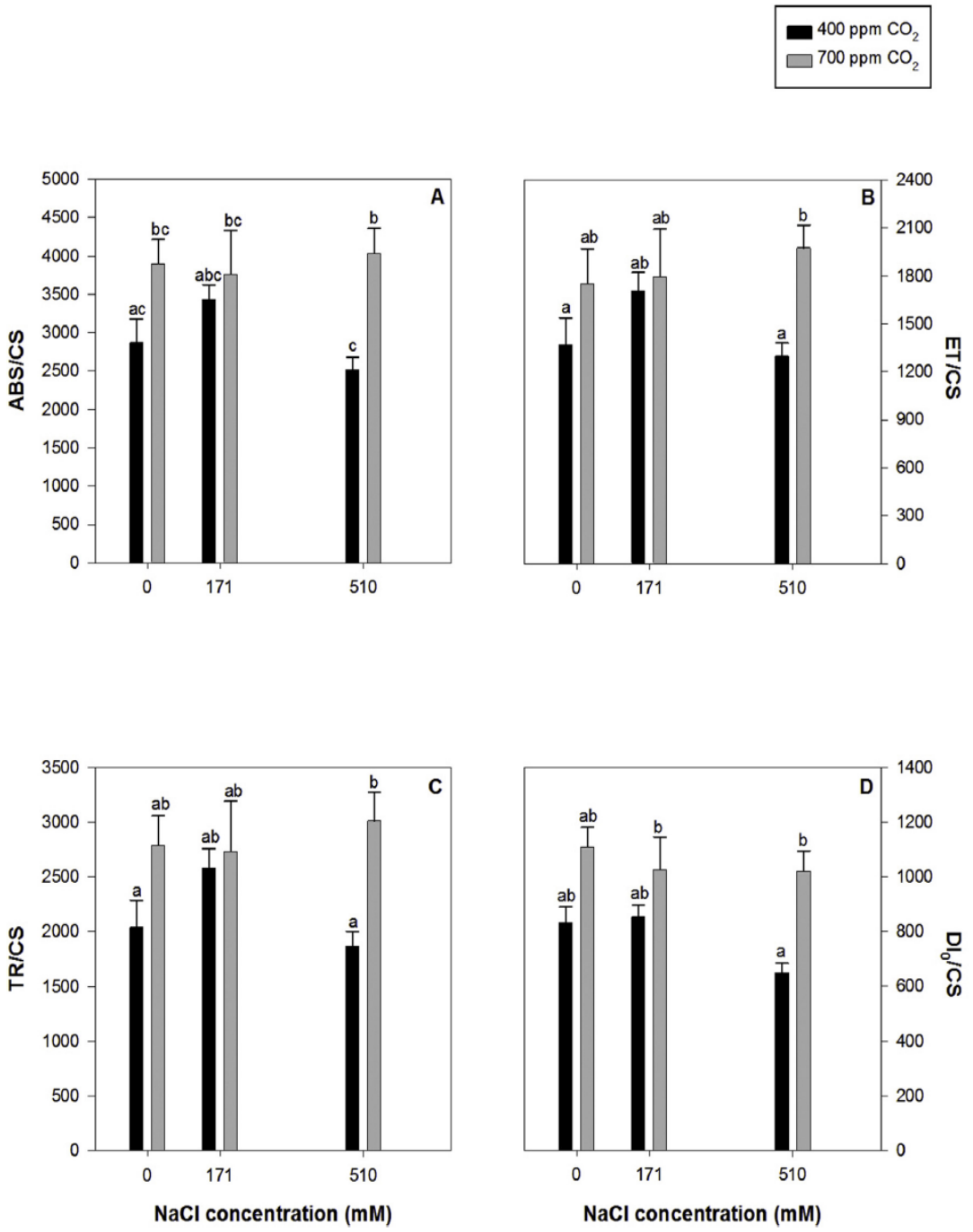

Fig. 6. Number of available reaction centres, ABS/CS (A), trapped energy flux, ET_0/CS (B) electron transport energy flux TR_0/CS (C) and dissipated energy fluxes, DI_0/CS (D) per leaf cross section and the performance index on absorption basis, PI (F) in dark adapted randomly selected, primary branches of *Salicornia ramosissima* in response to treatment with a range of NaCl concentrations at 400 and 700 ppm CO_2 after 30d of treatment. Values represent mean ± SE, n = 5. Different letters indicate means that are significantly different from each other (LSD, $P < 0.05$).

Table 2
Photosynthetic pigments concentrations (μg/g) and DES state in randomly selected branch of *Salicornia ramosissima* in response to treatment with a range of NaCl concentrations at 400 and 700 ppm CO_2 after 30d of treatment. Values represent mean ± SE, n = 5. Different letters indicate means that are significantly different from each other (LSD, $P < 0.05$).

[NaCl] (mM)	[CO_2] (ppm)	Chl *a*	Chl *b*	Phe *a*	b-carotene	Lutein	Neoxanthin	Violaxanthin	Zeaxanthin	DES
0	700	247.2 ± 15.2^{ab}	91.5 ± 6.7^{ab}	13.4 ± 2.3^{a}	7.5 ± 0.4^{a}	22.4 ± 2.3^{a}	8.9 ± 0.6^{a}	8.6 ± 1.1^{a}	8.7 ± 1.6^{a}	0.50 ± 0.03^{a}
	400	205.9 ± 16.7^{a}	82.6 ± 5.1^{a}	16.0 ± 2.5^{a}	6.2 ± 0.3^{a}	17.2 ± 2.4^{b}	4.8 ± 1.2^{b}	7.1 ± 1.6^{a}	7.9 ± 1.6^{ab}	0.45 ± 0.11^{b}
171	700	161.8 ± 6.5^{c}	51.4 ± 1.9^{c}	5.3 ± 0.2^{b}	5.1 ± 0.3^{a}	13.6 ± 0.8^{b}	5.6 ± 0.4^{b}	5.7 ± 0.3^{a}	4.8 ± 0.3^{b}	0.54 ± 0.01^{ab}
	400	121.8 ± 16.2^{bc}	44.4 ± 1.6^{c}	8.7 ± 2.5^{ab}	7.3 ± 1.2^{a}	13.1 ± 2.6^{b}	4.0 ± 0.8^{b}	7.9 ± 1.8^{a}	5.9 ± 1.2^{ab}	0.54 ± 0.02^{ab}
510	700	166.6 ± 8.8^{bc}	54.0 ± 3.1^{bc}	4.4 ± 0.5^{b}	5.3 ± 0.3^{a}	13.4 ± 0.8^{b}	5.8 ± 0.4^{b}	5.7 ± 0.7^{a}	5.1 ± 0.3^{b}	0.52 ± 0.02^{ab}
	400	166.1 ± 7.5^{bc}	58.3 ± 4.5^{bc}	7.0 ± 1.5^{ab}	5.5 ± 0.3^{a}	14.2 ± 0.9^{b}	4.9 ± 0.4^{b}	6.8 ± 0.8^{a}	5.5 ± 0.4^{b}	0.56 ± 0.02^{ab}

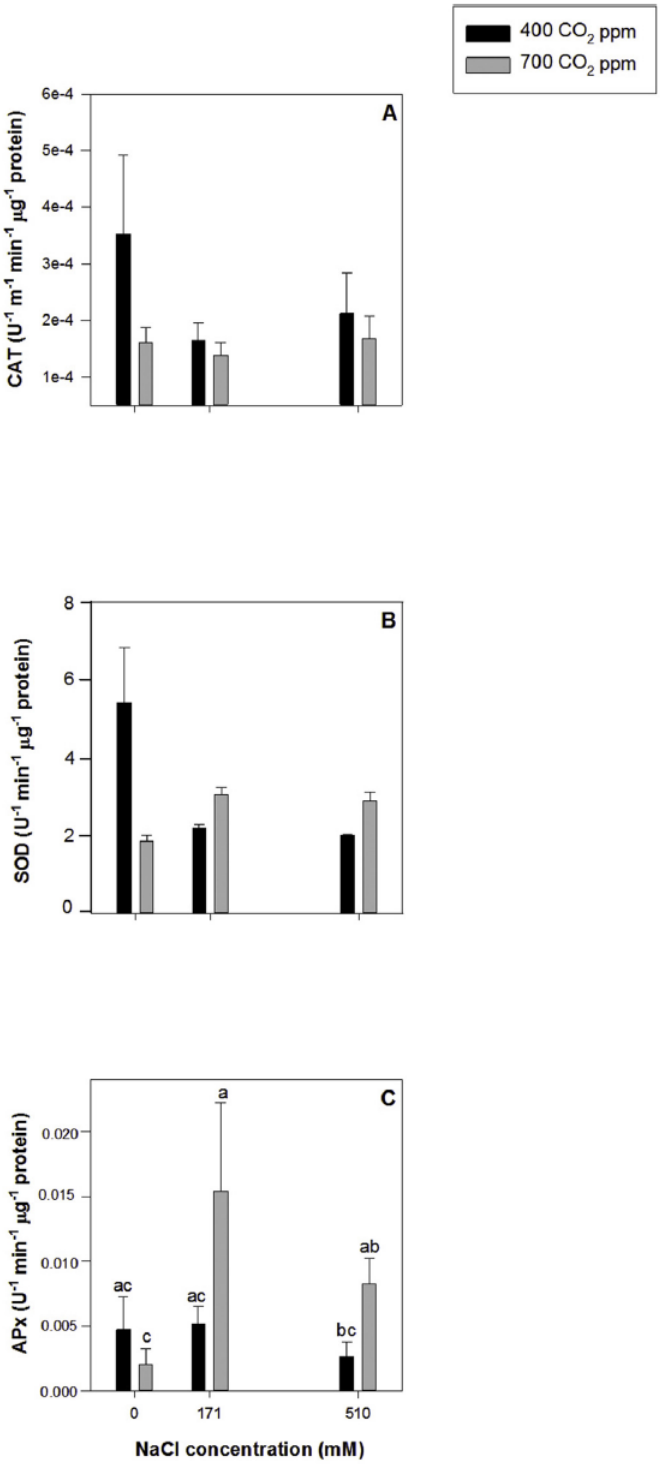

Fig. 7. Catalase (CAT) (A), and superoxide dismutase (SOD) (B), ascorbate peroxidase (APx) (C) enzymatic activities in randomly selected, primary branches of *Salicornia ramosissima* in response to treatment with a range of NaCl concentrations at 400 and 700 ppm CO_2 after 30d of treatment. Values represent mean ± SE, n = 3. Different letters indicate means that are significantly different from each other (LSD, $P < 0.05$).

previously suggested for other halophytes (Geissler et al., 2015).

Among physiological processes, photosynthetic metabolism has demonstrated to be especially sensible to salt excess (Flexas et al., 2004). Thus, it has been described that salinity affects photosynthetic metabolism mainly in terms of diffusion of CO_2 in leaves through a decrease in stomatal and mesophyll conductance (Flexas et al., 2004; Fanourakis et al., 2015). This could lead to a reduction in C_i with the consequence decrease in A_N (Verena et al., 2016). In this regard, our study indicated that at elevated salinity and ambient atmospheric CO_2 level photosynthetic responses of *S. ramosissima* were clearly impaired, as indicated the reduction of several parameters. Thus, A_N values decreased with NaCl supplementation, together with a sharply decrease in g_m for both salinity treatments and reduction in g_s only in the highest salinity concentration. However, although overall salinity involved a simultaneous reduction in A_N, g_m and g_s, there would not have a clear direct relation between them, since contrary to be expected C_i values did not change with increasing NaCl concentration. A decline in both CO_2 assimilation (A_N) and diffusion through leaf (i.e g_s and g_m) without a corresponding reduction in C_i may be interpreted as a direct effect of NaCl on the carbon fixation apparatus (Brugnoli and Lauteri, 1991). Thereby, salinity effects are related to alterations in metabolic functions such as protein synthesis, which determine photoinhibition levels (Ohad et al., 1984), and they may lead to biochemical limitations that affect carboxylase activity of RuBisCO (Antolín and Sánchez-Díaz, 1993). Therefore, the decrease of A_N could be linked by alteration of Rubisco activity, as it has been previously described for other halophytes, such as *S. densiflora* in response to NaCl stress (Mateos-Naranjo et al., 2015). Hence, we found that $V_{c,max}$ values decreased in plants grown in presence of NaCl addition compared with those without NaCl supplementation.

Despite the evident impact of salinity excess on some of the essential steps of *S. ramosissima* photosynthetic pathway, we found that rising atmospheric CO_2 had a positive effect on its photosynthetic apparatus performance. A stimulation of photosynthesis in C_3 species is a general response to CO_2 atmospheric concentration enrichment (Duarte et al., 2014, Geissler et al., 2015), varying between species and environmental conditions (Hussin et al., 2017). The results of this experiment were in concordance with that trend, since at 700 ppm CO_2 A_N values remained at the same level as the non-salinized plants. Furthermore, g_s values were considerably lower at the higher atmospheric CO_2 concentration and it was not affected by salinity increment; being this reduction explained by the increase of C_i originated by the elevated CO_2 concentration, which could promote partial stomatal closure, although the mechanism whereby stomata respond to the CO_2 signal remains unknown (Robredo et al., 2007). However, there is to notice that g_s reduction would contribute to preserve the trade-off between CO_2 acquisition for photosynthetic process and water losses in *S. ramosissima* plants. Hormaetxe et al. (2006) indicated that an increment in Ψ_o together with a decrease in g_s, as was also reported in our study, would contribute to a better water balance under stress, idea that was supported by the overall higher $_i$WUE values under rising atmospheric CO_2 conditions. According to our study, several authors have reported an increment of $_i$WUE in enrichment CO_2 atmosphere combined with NaCl salinity in the grown medium (Geissler et al., 2009a; b; Mateos-Naranjo et al., 2010b; Reef et al., 2015). Furthermore, the beneficial effect of CO_2 enrichment in A_N could be ascribed to the reduction on mesophyll CO_2 diffusion and biochemical limitations imposed by salinity stress aforementioned. So we found that overall maximum $V_{c,max}$ and g_m values of *S. ramosissima* tended to increase with atmospheric CO_2 concentration under saline conditions; so we could hypothesized that the resistance to CO_2 diffusion imposed by the stomatal resistance under saline conditions (as indicated the lower g_s values), could be in certain degree counterbalance through reducing mesophyll and biochemical limitations, as indicated the maintenance of RuBisCO carboxylation and g_m in values close to control plants. In fact, Centritto et al. (2003) indicated that the main limitation to CO_2 diffusion in presence of salt NaCl stress was caused by a reduction in the mesophyll conductance, rather than stomatal effects. Furthermore, the lower C/N and C^{13}/N^{15} ratios recorded in *S. ramosissima* under elevated CO_2 supported our hypothesis. These lower values were related with an increment in N acquisition and could be linked with the maintenance of RuBisCO functions. Since the activity of the Rubisco enzyme is in

relation with the photosynthetic capacity along with N content, as great amounts of N are supplied in Rubisco protein (Evans, 1989; Makino et al., 1992).

On the other hand, the ameliorative effect of rising atmospheric CO_2 concentration on the deleterious impacts of NaCl excess on the photosynthetic apparatus of *S. ramosissima* was ascribed by variations of PSII photochemistry, which would improve its functionality in terms of energy harvesting, transport and dissipation. It has been stated that salinity excess could impaired PSII photochemistry in different ways; thus several studies have indicated that the electron transport chain efficiency decrease along with the ability to use the incident photons (Panda et al., 2006; Mateos-Naranjo et al., 2007; Duarte et al., 2015b). Causing a decrease in the maximum yield for primary photochemistry (Kalaji et al., 2011). Also, Duarte et al. (2015b) indicated that salinity excess contributed to decline the reaction centers available for photon harvesting in the halophyte *Spartina patens*. However, our fluorescence data showed that the reduction of N and the φ_{R0} in presence of salt was in certain degree attenuated by the high CO_2 concentration. In addition, M_0, ABS/CS, TR_0/CS and ET_0/CS values were higher for those plants, indicating that energy harvesting and the electron flux were more efficient and active in presence of salt when *S. ramosissima* plants were exposed to 700 ppm CO_2, despite of the higher P_G values showed at ambient CO_2 concentration. Moreover, we found that the DI_0/CS increased at the highest salinity concentration, this trend similar to TR_0/CS and ET_0/CS could be explained by the higher values for ABS/CS. Being this parameter related with the activation of some defense mechanism to protect the photochemical apparatus through the dissipation of energy excess as heat (including NPQ that is correlated with the xanthophyll cycle) along with the photorespiration (Duarte et al., 2017). Thus we found several signs of the activation of this cycle, such as the greater concentration of zeaxhantin and violaxhantin at higher atmospheric CO_2 concentration and the rise observed at DES with NaCl supplementation (Duarte et al., 2015b). This cycle is activated as a consequence of an excess of light energy that decrease the lumen pH dissipating excessive energy and reducing the PSII and associated proteins excessive protonation (Duarte et al., 2015b). Therefore the positive impact of atmospheric CO_2 enrichment on photochemical apparatus of *S. ramosissima* was also linked with the enhanced of the efficiency for energy excess dissipation, which could contribute to reduce the accumulation of reactive oxygen species (ROS). Being the lower risk of ROS production supported by the decrease in ETR_{max}/A_N ratio recorded in *S. ramosissima* plants grown at elevated NaCl and CO_2 concentrations, since this ration has been considered an indicator of ROS production in plants in response to several stress (Salazar-Parra. 2012; Hussin et al., 2017). Finally another mechanism to reduce the accumulation of ROS is the modulation of the anti-oxidative stress enzymes machinery (Geissler et al., 2009a). Our results indicated that SOD enzyme activities tended to be higher in plants grown under elevated NaCl and atmospheric CO_2 concentration compared with their non-CO_2 supplied counterparts. The H_2O_2 created in presence of many types of stress due to photorespiration or the SOD activity had two ways to be reduced, through the catalase and the ascorbate peroxidase activities (Pérez-López et al., 2009). Our data showed that APx enzyme activities followed the SOD activity trend in plants grown at 700 ppm CO_2, which indicated the CO_2 increment would modulated APx enzyme activity in order to cope with salinity stress.

5. Conclusion

This study indicates that atmospheric CO_2 enrichment would increase the tolerance of the halophyte *S. ramosisima* to suboptimal salinity concentration (NaCl excess). Thus, we found that plants grown under elevated CO_2 and salt were able to maintain greater values of A_N than their non-CO2 supplied counterparts. This positive effect was in certain degree linked with a reduction on g_m and $V_{c,max}$ limitations imposed by salinity excess. Also, these plants showed a better water balance, as indicated the greater $_i$WUE values, due to its lower values of g_s together with an overall enhance on Ψ_o with NaCl concentration increment. However the positive effect on the carbon assimilation capacity did not results to a significant biomass variation, being this lack of correlation ascribed by the investment of part of the energy fixed for salinity stress defense mechanisms, such as pigments productions or anti-oxidative stress enzymes modulation. This fact was supported by the greater values obtained of zeaxhantin and violaxhantin concentrations and SOD and APx enzymes activities, which could have led to the capacity of maintaining active the photochemical machinery even at high salinities, in terms of light energy harvesting, transport and dissipation, reducing in this way the risk of ROS production, as indicated the lower values ETR_{max}/A_N ratio values. For all these reasons, we can conclude that this multifunctional cash crop specie could be an interesting suitable natural resource to be cultivated in a future climate change scenario, where an increment of soil salinity concentration it is expected together with the atmospheric CO_2 enrichment.

Contributions

SRG, EMN and YI conceived and designed research. JAPR, YI and JMBP conducted experiments. BD and IC contributed with new analytical tools. JAPR, EMN and BD analyzed data. JAPR wrote the manuscript. All authors read and approved the manuscript.

Acknowledgements

This work has been co-funded by Oficina de Cooperación Universidad de Sevilla (Conv. Ay. Act. y Proy. Coop. Des. Mod. 2, 2014/15-2015/2016) and Ministerio de Economía y Competitividad (MINECO Project CGL2016-75550-R cofunded by FEDER). J.A Pérez-Romero thanks Ministerio de Educación, Cultura y Deporte for its personal financial support (FPU014/03987). We are grateful University of Seville Greenhouse General Services (CITIUS) for its collaboration. The authors would also like to thank to the "Fundação para a Ciência e a Tecnologia" for funding the research in the Marine and Environmental Sciences Centre (MARE) throughout the project UID/MAR/04292/2013. B. Duarte investigation was supported by FCT throughout a Posdoctoral grant (SFRH/BPD/115162/2016).

References

Antolín, M.C., Sánchez-Díaz, M., 1993. Effects of temporary droughts on photosynthesis of alfalfa plants. J. Exp. Bot. 44 (8), 1341–1349.

Barreira, L., Resek, E., Rodrigues, M.J., Rocha, M.I., Pereira, H., Bandarra, N., da Silva, M.M., Varela, J., Custódio, L., 2017. Halophytes: gourmet food with nutritional health benefits? J. Food Compos. Anal. 59, 35–42. https://doi.org/10.1016/j.jfca.2017.02.003.

Bradford, M.M., 1976. A rapid and sensitive method for the quantitation of microgram quantities of protein utilizing the principle of protein-dye binding. Anal. Biochem. 72, 248–254.

Brugnoli, Enrico, Lauteri, Marco, 1991. Effects of salinity on stomatal conductance, photosynthetic capacity, and carbon isotope discrimination of salt- tolerant (Gossypium Hirsutum L.) and salt-sensitive (Phaseolus Vulgaris L.) C3 non-halophytes. Plant Physiol. 95, 628–635.

Calvo, Olga C., Franzaring, J., Schmid, I., Müller, M., Brohon, N., Fangmeier, A., 2017. Atmospheric CO2 enrichment and drought stress modify root exudation of barley. Global Change Biol. 23 (3), 1292–1304.

Centritto, M., Loreto, F., Chartzoulakis, K., 2003. The use of low [CO2] to estimate diffusional and non-diffusional limitations of photosynthetic capacity of salt-stressed olive saplings. Plant Cell Environ. 26 (4), 585–594.

Duarte, B., Cabrita, M.T., Gameiro, C., Matos, A.R., Godinho, R., Marques, Joao Carlos, Cacador, Isabel, 2017. Disentangling the photochemical salinity tolerance in aster tripolium L.: connecting biophysical traits with changes in fatty acid composition. Plant Biol. 19 (2), 239–248.

Duarte, B., Goessling, J.W., Marques, J.C., Caçador, I., 2015a. Ecophysiological constraints of aster tripolium under extreme thermal events impacts: merging biophysical, biochemical and Genetic insights. Plant Physiol. Biochem. 97, 217–228. https://doi.org/10.1016/j.plaphy.2015.10.015.

Duarte, B., Santos, D., Marques, J.C., Caçador, I., 2015b. Ecophysiological constraints of two invasive plant species under a saline Gradient: halophytes versus Glycophytes. Estuar. Coast Shelf Sci. 167, 154–165. https://doi.org/10.1016/j.ecss.2015.04.007.

Duarte, B., Santos, D., Silva, H., Marques, J.C., Cacador, Isabel, 2014. Photochemical and

biophysical feedbacks of C3 and C4 mediterranean halophytes to atmospheric CO2 enrichment confirmed by their stable isotope signatures. Plant Physiol. Biochem. 80, 10–22. https://doi.org/10.1016/j.plaphy.2014.03.016.
Ethier, G.J., Livingston, N.J., 2004. On the need to incorporate sensitivity to CO2 transfer conductance into the Farquharevon CaemmerereBerry leaf photosynthesis model. Plant Cell Environ. 27, 137–153.
Evans, J.R., 1989. Photosynthesis and nitrogen relationship in leaves of C3 plants. Oecologia 78 (1), 9–19.
Fanourakis, Dimitrios, Giday, H., Milla, R., Pieruschka, R., Kjaer, K.H., Bolger, M., 2015. Pore size regulates operating stomatal conductance, while stomatal densities drive the partitioning of conductance between leaf sides. Ann. Bot. 115 (4), 555–565.
Flexas, J., Bota, J., Loreto, F., Cornic, G., Sharkey, T.D., 2004. Diffusive and metabolic limitations to photosynthesis under drought and salinity in C3 plants. Plant Biol. 6 (3), 269–279.
Flexas, Jaume, Barón, M., Bota, J., Ducruet, J.M., Gallé, A., Galmés, J., Jiménez, M., Pou, A., Ribas-Carbó, M., Sajnani, C., Tomàs, M., Medrano, H., 2009. Photosynthesis limitations during water stress acclimation and recovery in the drought-adapted vitis hybrid Richter-110 (V. berlandieri × V. Rupestris). J. Exp. Bot. 60 (8), 2361–2377.
Flexas, Jaume, Niinemets, Ü., Gallé, A., Barbour, M.M., Centritto, M., Diaz-Espejo, A., Douthe, C., Galmés, J., Ribas-Carbo, M., Rodriguez, P.L., Rosselló, F., Soolanayakanahally, R., Tomas, M., Wright, I.J., Farquhar, G.D., Medrano, H., 2013. Diffusional conductances to CO2 as a target for increasing photosynthesis and photosynthetic water-use efficiency. Photosynth. Res. 117 (1–3), 45–59.
Geissler, N., Hussin, S., El-Far, M.M.M., Koyro, H.W., 2015. Elevated atmospheric CO2 concentration leads to different salt resistance mechanisms in a C3 (Chenopodium quinoa) and a C4 (Atriplex Nummularia) halophyte. Environ. Exp. Bot. 118, 67–77. http://linkinghub.elsevier.com/retrieve/pii/S0098847215001124.
Geissler, N., Hussin, S., Koyro, H.W., 2010. Elevated atmospheric CO2 concentration enhances salinity tolerance in aster tripolium L. Planta 231 (3), 583–594.
Geissler, N., Hussin, S., Koyro, H.W., 2009a. Elevated atmospheric CO2 concentration enhances salinity tolerance in aster tripolium L. Planta 231 (3), 583–594. http://www.scopus.com/inward/record.url?eid=2-s2.0-76049115940&partnerID=tZOtx3y1 (October 19, 2015).
Geissler, N., Hussin, S., Koyro, H.W., 2009b. Elevated atmospheric CO2 concentration ameliorates effects of NaCl salinity on photosynthesis and leaf structure of aster tripolium L. J. Exp. Bot. 60 (1), 137–151.
Ghannoum, O., Von Caemmerer, S., Ziska, L.H., Conroy, J.P., 2000. The growth response of C4 plants to rising atmospheric CO2 partial pressure: a reassessment. Plant Cell Environ. 23 (9), 931–942. http://onlinelibrary.wiley.com/doi/10.1046/j.1365-3040.2000.00609.x/full%5Cnhttp://onlinelibrary.wiley.com/store/10.1046/j.1365-3040.2000.00609.x/asset/j.1365-3040.2000.00609.
Hoagland, D.R., Arnon, D.I., 1938. The water culture method for growing plants without soil. California Agricultural Experiment Station Circulation 347. pp. 32.
Hormaetxe, K., Becerril, J.M., Hernández, A., Esteban, R., García-Plazaola, J.I., 2006. Plasticity of photoprotective mechanisms of buxus sempervirens L. Leaves in response to extreme temperatures. Plant Biol. 9 (1), 59–68.
Hussin, S., Geissler, N., El-Far, M.M.M., Koyro, H.W., 2017. Effects of salinity and short-term elevated atmospheric CO 2 on the chemical equilibrium between CO 2 fixation and photosynthetic electron transport of Stevia Rebaudiana bertoni. Plant Physiol. Biochem. 118, 178–186. http://linkinghub.elsevier.com/retrieve/pii/S0981942817302085.
IPCC, 2007. In: Core Writing Team, Pachauri, R.K., Reisinger, A. (Eds.), Climate Change 2007: Synthesis Report. Contribution of Working Groups I, II and III to the Fourth Assessment Report of the Intergovernmental Panel on Climate Change. IPCC, Geneva, Switzerland, pp. 104.
Isca, Vera M.S., Seca, A.M.L., Pinto, D.C.G.A., Silva, H., Silva, Artur M.S., 2014. Lipophilic profile of the edible halophyte Salicornia ramosissima. Food Chem. 165, 330–336. https://doi.org/10.1016/j.foodchem.2014.05.117.
Kalaji, Hazem M., Govindjee, B.K., Koscielniak, J., Zuk-Golaszewska, K., 2011. Effects of salt stress on Photosystem II efficiency and CO2 assimilation of two syrian barley Landraces. Environ. Exp. Bot. 73 (1), 64–72.
Küpper, Hendrik, Seibert, Sven, Parameswaran, Aravind, 2007. Fast, sensitive, and inexpensive alternative to analytical pigment HPLC: quantification of chlorophylls and carotenoids in crude extracts by fitting with Gauss peak Spectra. Anal. Chem. 79 (20), 7611–7627.
Lenssen, G.M., van Duin, W.E., Jak, P., Rozema, J., 1995. The response of aster tripolium and puccinellia maritima to atmospheric carbon dioxide enrichment and their interactions with flooding and salinity. Aquat. Bot. 50 (2), 181–192.
Lenssen, Gm, Lamers, J., Stroetenga, M., Rozema, J., 1993. Interactive effects of atmospheric CO 2 enrichment, salinity and flooding on Growth of C 3 (elymus Athericus) and C 4 (Spartina anglica) salt marsh species. Vegetatio 104/105 (0), 379–388. http://www.springerlink.com/index/K850461766217437.pdf.
Long, S.P., Bernacchi, C.J., 2003. Gas exchange measurements, what can they tell us about the underlying limitations to Photosynthesis? Procedures and sources of error. J. Exp. Bot. 54 (392), 2393–2401.
Lu, D., Zhang, M., Wang, S., Cai, J., Zhou, X., Zhu, C., 2010. Nutritional characterization and changes in quality of Salicornia bigelovii torr. During storage. LWT - Food Sci. Technol. (Lebensmittel-Wissenschaft -Technol.) 43 (3), 519–524. https://doi.org/10.1016/j.lwt.2009.09.021.
Makino, A., Sakashita, H., Hidema, J., Mae, T., Ojima, K., Osmond, B., 1992. Distinctive responses of ribulose-1,5-bisphosphate carboxylase and carbonic anhydrase in Wheat leaves to nitrogen nutrition and their possible relationships to CO2-transfer resistance. Plant Physiol. 100 (4), 1737–1743. http://www.plantphysiol.org/cgi/doi/10.1104/pp.100.4.1737.
Marklund, S., Marklund, G., 1974. "Involvement of the superoxide anion radical in the autoxidation of pyrogallol and a conveniente assay for superoxide dismutase. Eur. J. Biochem. 47, 469–474.
Marshall, H.L., Geider, R.J., Flynn, K.J., 2000. A mechanistic model of photoinhibition. New Phytol. 145 (2), 347–359.
Mateos-Naranjo, E., Mesa, J., Pajuelo, E., Perez-Martin, A., Caviedes, M., Rodríguez-Llorente, A.I.D., 2015. Deciphering the role of plant growth-promoting rhizobacteria in the tolerance of the invasive cordgrass Spartina densiflora to physicochemical properties of salt-marsh soils. Plant Soil 394 (1–2), 45–55.
Mateos-Naranjo, E., Redondo-Gomez, S., Alvarez, R., Cambrolle, J., Gandullo, J., Figueroa, M.E., 2010a. Synergic effect of salinity and CO2 enrichment on growth and photosynthetic responses of the invasive cordgrass Spartina densiflora. J. Exp. Bot. 61 (6), 1643–1654. http://www.scopus.com/inward/record.url?eid=2-s2.0-77951122141&partnerID=tZOtx3y1 (October 19, 2015).
Mateos-Naranjo, E., Redondo-Gómez, S., Andrades-Moreno, L., Davy, A.J., 2010b. Growth and photosynthetic responses of the cordgrass Spartina maritima to CO2 enrichment and salinity. Chemosphere 81 (6), 725–731. http://www.scopus.com/inward/record.url?eid=2-s2.0-77957234390&partnerID=tZOtx3y1 (October 19, 2015).
Mateos-Naranjo, E., Redondo-Gómez, S., Silva, J., Santos, R., Figueroa, M.E., 2007. Effect of prolonged flooding on the invader Spartina densiflora brong. J. Aquat. Plant Manag. 45 (2), 121–123. https://www.scopus.com/inward/record.uri?eid=2-s2.0-36649032871&partnerID=40&md5=d43570803eedbcd28dd2b512c5117a7f.
Meyer, Leo, Brinkman, Sander, van Kesteren, Line, Leprince-Ringuet, Noëmie, van Boxmeer, Fijke, 2014. In: Pachauri, R.K., Meyer, L.A. (Eds.), Climate Change 2014: Synthesis Report. Contribution of Working Groups I, II and III to the Fifth Assessment Report of the Intergovernmental Panel on Climate Change, pp. 3–87.
Naudts, K., van den Berge, J., Farfan, E., Rose, P., AbdElgawad, H., Ceulemans, R., Janssens, I.A., Asard, H., Nijs, I., 2013. Future climate alleviates stress impact on Grassland productivity through altered antioxidant capacity. Environ. Exp. Bot. 99, 150–158. https://doi.org/10.1016/j.envexpbot.2013.11.003.
Nunes da Silva, M., Nunes da Silva, M., Mucha, A.P., Rocha, A.C., Silva, C., Carli, C., Gomes, C.R., Almeida, C.M., 2014. Evaluation of the ability of two plants for the phytoremediation of Cd in salt marshes. Estuar. Coast Shelf Sci. 141, 78–84. https://doi.org/10.1016/j.ecss.2014.03.004.
Occhipinti-Ambrogi, A., 2007. Global change and marine communities: alien species and climate change. Mar. Pollut. Bull. 55 (7–9), 342–352.
Ohad, I., Kyle, D.J., Arntzen, C.J., 1984. Membrane protein damage and repair: removal and replacement of inactivated 32-kilodalton polypeptides in chloroplast membranes. JCB (J. Cell Biol.) 99 (2), 481–485.
Panda, D., Rao, D.N., Sharma, S.G., Strasser, R.J., Sarkar, R.K., 2006. Submergence effects on rice Genotypes during seedling stage: probing of submergence driven changes of Photosystem 2 by chlorophyll a fluorescence induction O-J-I-P transients. Photosynthetica 44 (1), 69–75.
Pedro, Carmen A., Santos, M.S.S., Ferreira, S.M.F., Gonçalves, S.C., 2013. The influence of cadmium contamination and salinity on the survival, growth and phytoremediation capacity of the saltmarsh plant Salicornia ramosissima. Mar. Environ. Res. 92, 197–205. https://doi.org/10.1016/j.marenvres.2013.09.018.
Peng, S., Huang, J., Sheehy, J.E., Laza, R.C., Visperas, R.M., Zhong, X., Centeno, G.S., Khush, G.S., Cassman, K.G., 2004. Rice yields decline with higher night temperature from global Warming. Proc. Natl. Acad. Sci. U.S.A. 101 (27), 9971–9975. http://www.ncbi.nlm.nih.gov/pubmed/15226500 (July 3, 2017).
Pérez-López, U., Robredo, A., Lacuesta, M., Sgherri, C., Muñoz-Rueda, A., Navari-Izzo, F., Mena-Petite, A., 2009. The oxidative stress caused by salinity in two barley cultivars is mitigated by elevated CO2. Physiol. Plantarum 135 (1), 29–42.
Perez-Romero, Jesus Alberto, Redondo-Gomez, Susana, Mateos-Naranjo, Enrique, 2016. Growth and photosynthetic limitation analysis of the Cd-Accumulator Salicornia ramosissima under excessive cadmium concentrations and optimum salinity conditions. Plant Physiol. Biochem. 109, 103–113.
Pons, T.L., Flexas, J., Von Caemmerer, S., Evans, J.R., Genty, B., Ribas-Carbo, M., Brugnoli, E., 2009. Estimating mesophyll conductance to CO2: methodology, potential errors, and recommendations. J. Exp. Bot. 60 (8), 2217–2234.
Redondo-Gómez, S., Mateos-Naranjo, E., Figueroa, M.E., Davy, A.J., 2010. Salt stimulation of growth and photosynthesis in an extreme halophyte, arthrocnemum macrostachyum. Plant Biol. 12 (1), 79–87. http://www.scopus.com/inward/record.url?eid=2-s2.0-77951104035&partnerID=tZOtx3y1 (October 19, 2015).
Redondo-Gómez, S., Wharmby, C., Castillo, J., Mateos-Naranjo, E., Luque, C.J., De Cires, A., Luque, T., Davy, A.J., Figueroa, M.E., 2006. Growth and photosynthetic responses to salinity in an extreme halophyte, Sarcocornia fruticosa. Physiol. Plantarum 128 (1), 116–124.
Reef, R., Winter, K., Morales, J., Adame, M.F., Reef, D.L., Lovelock, C.E., 2015. The effect of atmospheric carbon dioxide concentrations on the performance of the mangrove Avicennia Germinans over a range of salinities. Physiol. Plantarum 154 (3), 358–368.
Robredo, A., Pérez-López, U., de la Maza, H.S., González-Moro, B., Lacuesta, M., Mena-Petite, A., Muñoz-Rueda, A., 2007. Elevated CO2 alleviates the impact of drought on barley improving water status by lowering stomatal conductance and delaying its effects on photosynthesis. Environ. Exp. Bot. 59 (3), 252–263.
Rozema, J., 1993. Plant-responses to atmospheric carbon-dioxide enrichment - interactions with some soil and atmospheric conditions. Vegetatio 104, 173–190.
Salazar-Parra, C., 2012. Climate change (elevated CO 2, elevated temperature and moderate drought) triggers the antioxidant enzymes' response of Grapevine cv. Tempranillo, avoiding oxidative damage. Physiol. Plantarum 144 (2), 99–110.
Schreiber, U., Schliwa, U., Bilger, W., 1986. Continuous recording of photochemical and non-photochemical chlorophyll fluorescence quenching with a new type of modulation fluorometer. Photosynth. Res. 10 (1–2), 51–62.
Sharma, A., Gontia, I., Agarwal, P.K., Jha, B., 2010. An extreme halophyte. Mar. Biol. Res. 6 (5), 511–518.
Sharkey, T.D., Bernacchi, C.J., Farquhar, G.D., Singsaas, E.L., 2007. Fitting

photosynthetic carbon dioxide response curves for C3 leaves. Plant Cell Environ. 30, 1035–1040.
Singh, D., Buhmann, A.K., Flowers, T.J., Seal, C.E., Papenbrock, J., 2014. Salicornia as a crop plant in temperate regions: selection of Genetically characterized ecotypes and optimization of their cultivation conditions. AoB PLANTS 6.
Strasser, R.J., Tsimilli-Michael, M., Srivastava, A., 2004. Analysis of the chlorophyll a fluorescence transient. In: Christos Papageorgiou, George, Govindjee (Eds.), Chlorophyll a Fluorescence: a Signature of Photosynthesis. Springer, Dordrecht, pp. 321–362. Netherlands. https://doi.org/10.1007/978-1-4020-3218-9_12.
Strasser, R.J., Stribet, A.D., 2001. Connectivity of PS II centres in plants using the fluorescence rise O-J-I-P - Fitting of experimental data to three different PS II models. Math. Comput. Simulat. 56 (4-5), 451–461.
Teranishi, Y., Tanaka, A., Osumi, M., Fukui, S., 1974. Catalase activities of hydrocarbon-utilizing Candida yeasts. Agric. Biol. Chem. 38 (6), 1213–1220.
Tiryakioglu, M., Eker, S., Ozkutlu, F., Husted, S., Cakmak, I., 2006. Antioxidant defense system and cadmium uptake in barley Genotypes differing in cadmium tolerance. J. Trace Elem. Med. Biol. 20 (3), 181–189.
Ventura, Y., Eshel, A., Pasternak, D., Sagi, M., 2015. The development of halophyte-based agriculture: past and present. Ann. Bot. 115 (3), 529–540.
Ventura, Y., Sagi, M., 2013. Halophyte crop cultivation: the case for Salicornia and sarcocornia. Environ. Exp. Bot. 92, 144–153. https://doi.org/10.1016/j.envexpbot.2012.07.010.
Verena, I., Becker, A., Johannes, A., Goessling, J.W., Duarte, B., Caçador, I., 2016. Combined Effects of Soil Salinity and High Temperature on Photosynthesis and Growth of Quinoa Plants (Chenopodium Quinoa).
Yadav, A.K., Singh, S., Dhyani, D., Ahuja, P.S., 2011. A review on the improvement of stevia [Stevia Rebaudiana (bertoni)]. Can. J. Plant Sci. 91 (1), 1–27. (2011). http://pubs.aic.ca/doi/abs/10.4141/cjps10086.
Zhang, Heerink, L.N., Dries, L., Shi, X., Kadirbeyo, Z., Vlotman, W.F., Agrawal, A., 2013. Integration of drainage, water quality and flood management in rural, urban and lowland areas. Agric. Water Manag. 56 (1), 161–177.

CAPÍTULO 3:

Investigating the physiological mechanisms underlying *Salicornia ramosissima* response to atmospheric CO_2 enrichment under coexistence of prolonged soil flooding and saline excess

Pérez-Romero et al., 2019, Plant Physiology and Biochemistry

Plant Physiology and Biochemistry 135 (2019) 149–159

Contents lists available at ScienceDirect

Plant Physiology and Biochemistry

journal homepage: www.elsevier.com/locate/plaphy

Research article

Investigating the physiological mechanisms underlying *Salicornia ramosissima* response to atmospheric CO_2 enrichment under coexistence of prolonged soil flooding and saline excess

Jesús Alberto Pérez-Romero[a,*], Bernardo Duarte[b], Jose-Maria Barcia-Piedras[c], Ana Rita Matos[d], Susana Redondo-Gómez[a], Isabel Caçador[c], Enrique Mateos-Naranjo[a]

[a] Departamento de Biología Vegetal y Ecología, Facultad de Biología, Universidad de Sevilla, 1095, 41080, Sevilla, Spain
[b] MARE - Marine and Environmental Sciences Centre, Faculty of Sciences of the University of Lisbon, Campo Grande, 1749-016, Lisbon, Portugal
[c] Department of Ecological Production and Natural Resources Center IFAPA Las Torres-Tomejil Road Sevilla - Cazalla Km 12'2, 41200, Alcalá del Río, Seville, Spain
[d] BioISI—Biosystems and Integrative Sciences Institute, Plant Functional Genomics Group, Departamento de Biologia Vegetal, Faculdade de Ciências da Universidade de Lisboa, Campo Grande, 1749-016, Lisboa, Portugal

ARTICLE INFO

Keywords:
Climate change
Fluorescence
Gas exchange
Halophyte
Salinity
Water logging

ABSTRACT

A 45-days long climatic chamber experiment was design to evaluate the effect of 400 and 700 ppm atmospheric CO_2 treatments with and without soil water logging in combination with 171 and 510 mM NaCl in the halophyte *Salicornia ramosissima*. In order to ascertain the possible synergetic impact of these factors associate to climatic change in this plant species physiological and growth responses. Our results indicated that elevated atmospheric CO_2 concentration improved plant physiological performance under suboptimal root-flooding and saline conditions plants. Thus, this positive impact was mainly ascribed to an enhancement of energy transport efficiency, as indicated the greater P_G, N and Sm values, and the maintaining of carbon assimilation capacity due to the higher net photosynthetic rate (A_N) and water use efficiency ($_i$WUE). This could contribute to reduce the risk of oxidative stress owing to the accumulation of reactive oxygen species (ROS). Moreover, plants grown at 700 ppm had a greater capacity to cope with flooding and salinity synergistic impact by a greater efficiency in the modulation in enzyme antioxidant machinery and by the accumulation of osmoprotective compounds and saturated fatty acids in its tissues. These responses indicate that atmospheric CO_2 enrichment would contribute to preserve the development of *Salicornia ramosissima* against the ongoing process of increment of soil stressful conditions linked with climatic change.

1. Introduction

The most recent climate change predictions indicate that it will impose significant increases in the global average air and sea surface temperatures by about 2.5 °C (IPCC, 2001) together with an increase of atmospheric CO_2 concentration to value of c. 760 ppm by 2100. Due to this global warming, sea level rise (SLR) and soil salinization will be some of the major side-effects, as a result of polar ice meltdown and the increment of surface water evaporation, respectively (IPCC, 2001). There is a consensus on the direct physiological impact of increasing CO_2 concentration on plant photosynthesis and metabolism, stimulating growth and development in hundreds of plants species (Ghannoum et al., 2000). However, the information is very scarce in relation with the effect of atmospheric CO_2 enrichment on photosynthesis in plants subjected to a complex environmental matrix. Therefore, the majority of studies that have tried to address this concern were designed to explore as much two environmental factor interactions; i.e. the effect of rising CO_2 along with salinity (Lenssen et al., 1993; Rozema, 1993; Geissler et al., 2009a, 2015, 2009b; Mateos-Naranjo et al., 2010a, 2010b; Pérez-Romero et al., 2018), drought (Yang et al., 2014; Slama et al., 2015; Calvo et al., 2017), temperature (Bernacchi et al., 2006) or flooding (Duarte et al., 2014), etc. Only few studies have addressed the impact of more than two coexisting factors (Lenssen et al., 1995). Although the majority of them only performed shallow physiological evaluations being difficult to find a complete analysis of photosynthetic responses taking into account carbon assimilation capacity and energy use efficiency together with other metabolism processes, such as antioxidant enzyme modulation, involved in the plants responses to environmental stress.

Salicornia ramosissima J. Woods (Chenopodiaceae), represent a

* Corresponding author. Dpto. Biología Vegetal y Ecología, Facultad de Biología, Universidad de Sevilla, Av Reina Mercedes s/n, 41012, Sevilla, Spain.
E-mail address: jperez77@us.es (J.A. Pérez-Romero).

https://doi.org/10.1016/j.plaphy.2018.12.003
Received 14 August 2018; Received in revised form 13 November 2018; Accepted 3 December 2018
Available online 06 December 2018

Abbreviations

WL	Water logging
RGR	Relative growth rate
WC	Water content
Ψ_o	Osmotic potential
A_N	Net photosynthetic rate
g_s	Stomatal conductance
C_i	Intercellular CO_2 concentration
iWUE	Intrinsic water use efficiency
ETR_{max}	Maximum electron transport rate
PSII	Photosystem II
F_v/F_m	Maximum quantum efficiency of PSII photochemistry
Φ_{PSII}	PS II Operational and Maximum Quantum Yield
GPX	Guaiacol peroxidase enzymatic activity
SOD	Superoxide dismutase enzymatic activity
ROS	Reactive oxygen species
SFA	Saturated fatty acids
UFA	Unsaturated fatty acids
MUFA	Monounsaturated fatty acids
PUFA	Poliunsaturated fatty acids
DBI	Double bond index

suitable model plant to study in detail the effect of atmospheric CO_2 enrichment on the physiological responses of a plant species under co-existing suboptimal environmental conditions, such as soil flooding and salinity conditions. Since this species is a C_3 halophyte which inhabits salt marshes and inland salty habitats like shores of salt lakes being able to tolerate a wide range of salinity and a certain degree of immersion (Davy et al., 2001). However, these estuarine areas will be particularly vulnerable to SLR (Reed, 2002; Duarte et al., 2014) and salinization events (IPCC, 2007). Our recent study showed that CO_2 enrichment improves *S. ramosissima* response to suboptimal salinity conditions through an overall protection of its photosynthetic pathway (Pérez-Romero et al., 2018), but non-attention have been paid in SLR risk.

Therefore, this study was designed and conducted to fill this gap of knowledge. In particular, we asked the following questions: (i) Would atmospheric CO_2 enrichment have a positive impact on *S. ramosissima* physiological performance under co-occurrence of different stress factors, such as prolonged soil flooding and salinity? (ii) Would this effect be different to previous described only in presence of salinity, especially at the level of specific steps of photosynthetic pathway? (iii) Would other metabolism processes, such as antioxidant enzyme machinery or fatty acids profiles modulation, be involved in these differential responses?

2. Material and methods

2.1. Plant material

Seeds of *S. ramosissima* were collected in September 2016 from a well stablished population located in Odiel marshes (37°15'N, 6°58'O; SW Spain). Then, collected seed were placed into a germinator (ASL Aparatos Científicos M-92004, Madrid, Spain) and subjected to a day-night regime of 16 h of light (photon flux rate, 400–700 nm, 35 μmol m^{-2} s^{-1}) at 25 °C and 8 h of darkness at 12 °C, for 15 days. After germination, seedlings were planted in individual plastic plots (9 cm high x 11 cm diameter) filled with pearlite as substrate, and moved to a greenhouse with controlled conditions (temperature between 21 and 25 °C, 40–60% relative humidity and natural daylight 250–1000 μmol m^{-2} s^{-1} light flux). The pots were placed in shallow trays watering with 20% Hoagland's solution (Hoagland and Arnon, 1938) and 171 mM NaCl (Pérez-Romero et al., 2016). Plants were kept under the previously described conditions until the beginning of the experiment.

2.2. Experimental treatments

After 3 months of seedlings culture, when plants had a mean height c. 13 cm, pearlite was washed off and plants were transferred to individual plastic pots of 0.25 l containing an organic commercial substrate (Gramoflor GmbH und Co. KG.) and sand mixture (2:1) in order to facilitate water level treatment. Pots were randomly divided in eight experimental blocks with eleven plants in each one, as follow: two atmospheric CO_2 concentrations (400 ppm and 700 ppm) in combination with two water levels (water logging, WL and no water logging, noWL) and two salinity concentrations (171 and 510 mM NaCl). These conditions were kept for 45 days in order to obtain a more realistic approximation about the maximum permanent inundation period that we have observed during field surveys in natural populations of *S. ramosissima* which inhabits inland salty habitats (data not published). In addition, being an annual specie, this period was used to avoid a decreased in the physiology variables due to age because after the 3 months of seedlings culture the plants where around 135 days old.

Salinity treatments, 171 and 510 mM NaCl, were established by using tap water and NaCl of the appropriate concentration. In addition, these solutions were added to each tray to get water treatments. Thus, for the WL treatment, water level was continuous maintained at soil surface level, and for no WL treatment water level was continuous covering 2 cm from the bottom of the tray. Finally, for the atmospheric CO_2 concentration treatments pots were placed in controlled-environment chambers (Aralab/Fitoclima 18.000 EH, Lisbon, Portugal) with alternating diurnal regime of 14 h of light and 25 °C and 10 h of darkness and 18 °C and relative humidity between 40 and 60% and atmospheric CO_2 control. Atmospheric CO_2 concentrations in chambers were continuously recorded by CO_2 sensors (Aralab, Lisbon, Portugal) and maintained by supplying pure CO_2 from a compressed gas cylinder (Air liquide, B50 35 K). As well as the salinity and water levels to avoid changes due to evaporation.

2.3. Growth analysis

At the beginning of the experiment just before treatments imposition belowground and aboveground fractions of 10 randomly selected plants were separated, dried at 80 °C for 48 h and weighed. At the end of the essay, 8 plants per treatment were processed in the same way. The relative growth rate (RGR) was calculated using the formula:

$$RGR = (\ln Bf - \ln B_i)\, D^{-1} \ (g\ g^{-1}\ day^{-1})$$

Where Bf = final dry mass (an average eight plants per treatment), B_i = initial dry mass (an average of the ten plants dried at the beginning of the experiment) and D = duration of experiment (days).

2.4. Plant water status

Water content (WC) of primary branches (n = 8, per treatment) were calculated after 45 days of treatment as follow:

$$WC = ((FW - DW) / FW)\ 100$$

Where FW = fresh weight of the branches and DW = dry weight after oven-drying at 80 °C for 48 h.

On the other hand, the osmotic potential (Ψ_o) of primary branches (n = 5, per treatment) was determined 45 days after the onset of the treatments, using psychrometric technique with a Vapour Pressure Osmometer (5600 Vapro, Wescor, Logan, USA).

2.5. Measurement of gas exchange

Instantaneous gas exchange measurements were taken on randomly selected primary branches of individual plants (n = 7, per treatment) using an infrared gas analyser in an open system (LI-6400, LI-COR Inc., Neb., USA) equipped with a light leaf chamber (Li-6400-02B, Li-Cor Inc.) after 45 days of treatment. Net photosynthetic rate (A_N), stomatal conductance (g_s), intercellular CO_2 concentration (C_i) and intrinsic water use efficiency ($_i$WUE) were determined under the follow leaf cuvette conditions: a photosynthetic photon flux density (PPFD) 1000 µmol photon m^{-2} s^{-1} (with 15% blue light to maximize stomatal aperture), vapour pressure deficit of 2.0–3.0 kPa, air temperature of 25 ± 2 °C, relative humidity of 50 ± 2% and CO_2 concentration surrounding leaf (C_a) of 400 and 700 µmol mol^{-1} air for plants exposed to 400 and 700 ppm CO_2, respectively. Photosynthetic area was calculated as half the area of the cylindrical branches, as only the upper half received the unilateral illumination in the leaf chamber (Redondo-Gómez et al., 2010). Intrinsic water use efficiency ($_i$WUE) was calculated as the ratio between A_N and g_s.

2.6. Chlorophyll fluorescence

Modulated chlorophyll fluorescence measurements were performed at the same time as gas exchange measures on the same branches of gas exchange using a FluorPen FP100 (Photo System Instruments, Czech Republic) on light and 30 min dark-adapted primary branches after 45 days of treatment (n = 7, per treatment). Light energy yields of photosystem II (PS II) reaction centres were determined with a saturation pulse method as Schreiber et al. (1986) described. The maximum fluorescence signal across time was estimated by using a saturating light pulse of 0.8 s with an intensity of 8000 µmol m^{-2} s^{-1}. The minimum fluorescence (F'_0), the maximum fluorescence (F'_m) and the operational photochemical efficiency values of light and dark adapted branches were compared. Quantum yield of PS II (QY) and relative Quantum yield of PS II (Q'Y) were calculated as F_v/F_m and Φ_{PSII} respectively. Maximum electron transport rate (ETR_{max}) and the Kausky curves, or JIP-test, which depicts the rate of reduction kinetics of various components of PSII, were also measured in dark-adapted branches (n = 5, per treatment) according to Duarte et al. (2015). For this purpose, the pre-programmed RLC and OJIP protocols of the FluorPen were used. All derived parameters for both RLC and OJIP were calculated according to Marshall et al. (2000) and Strasser et al. (2004) respectively (Table 1). Finally, ETR_{max}/A_N ratio was calculated with the values obtained from fluorescence rapid light curves, RLC (see below) and instantaneous gas exchange measurements.

2.7. Anti-oxidant enzymatic activity

Enzyme extraction was done following the method used by Duarte et al. (2015). At the end of experiment, 500 mg of fresh branches samples were grounded in 8 ml of 50 mM sodium phosphate buffer (pH 7.6) with 0.1 mM Na-EDTA and were centrifuged at 10.000 rpm for 20 min at 4 °C to obtained the soluble proteins. Three samples per treatment were used and three measurements per sample were registered. Protein content in the extracts was obtained according to Bradford (1976), using bovine serum albumin as a standard.

Guaiacol peroxidase EC 1.11.1.7 (GPX) was calculated as Bergmeyer (1974) indicated. With a reaction mixture made of 50 mM of sodium phosphate buffer (pH 7.0), 2 mM of H_2O_2 and 20 mM of guaiacol. For all this enzymatic activities 100 µL of vegetal extract was added at the reaction mixture to start the reaction. Superoxide dismutase EC 1.15.1.1 (SOD) activity was assayed by monitoring the reduction of pyrogallol at 325 nm following Marklund and Marklund (1974) work. The reaction mixture was 50 mM of sodium phosphate buffer (pH 7.6), 0.1 mM of Na-EDTA, 3 mM of pyrogallol, Mili-Q water. The reaction was started with the addition of 10 µL of enzyme extract. Auto-oxidation of the substrates was evaluated by control samples with the reaction mixture but without the enzyme extract.

2.8. Betain concentration

Betain were determined as the main osmocompatible solute present in succulent halophytes (Duarte et al., 2013). To quantify the betain concentration 500 mg samples of fresh branches were collected at the end of the essay and freeze-dried for 48 h. Then, the samples were grinded and left in ultra-pure water for 24 h. After that, the sample extract was diluted 1:1 with 2 N H_2SO_4. Cold KI-I_2 reagent (0.20 ml) was mixed with 0.5 ml of the diluted sample. The tubes were stored at 4 °C for 16 h and then centrifuged at 10.000 rpm for 15 min at 0 °C. The supernatant was carefully aspirated with a fine tipped glass tube. The

Table 1
Summary of fluorometric analysis parameters and their description.

Photosystem II Efficiency	
Fv/Fm	Maximum quantum efficiency of PSII photochemistry
PS II Operational and Maximum Quantum Yield (ΦPSII)	Light and dark-adapted quantum yield of primary photochemistry, equal to the efficiency by which a PS II trapped photon will reduce Q_A to Q_A^-
Rapid Light Curves (RLCs)	
ETR_{max}	Maximum ETR after which photo-inhibition can be observed
Energy Fluxes (Kautsky curves)	
Area	Corresponds to the oxidized quinone pool size available for reduction and is a function of the area above the Kautsky plot
φ_{P0}	Maximum yield of primary photochemistry
φ_{E0}	Probability that an absorbed photon will move an electron into the electronic transport chain
φ_{D0}	Quantum yield of the non-photochemical reactions
Ψ_0	Probability of a PS II trapped electron to be transported from Q_A to Q_B
δR_0	Electron movement efficiency from the reduced intersystem electron acceptors to the PSI and electron acceptors.
N	Reaction centre turnover rate
Sm	Relative pool size of PQ.
M_0	Net rate of PS II RC closure.
ABS/CS	Absorbed energy flux per leaf cross-section.
TR/CS	Trapped energy flux per leaf cross-section
ET/CS	Electron transport energy flux per leaf cross-section
DI/CS	Dissipated energy flux per leaf cross-section.
RC/CS	Number of available reaction centres per leaf cross section
Grouping Probability (P_G)	The grouping probability is a direct measure of the connectivity between the two PS II units (Strasser and Stribet, 2001)

periodide crystals produced were dissolved in 9.0 ml of 1,2-dichloroethane (reagent grade). After 2–2.5 h, the absorbance was measured at 365 nm with a Hitachi Spectrometer model 100–20 (Grieve and Grattan, 1983).

2.9. Fatty acid profile

At the end of the experiment, 150 mg samples of fresh and green branches were taken to determine the fatty acids composition. The method used was the direct acidic trans-esterification previously described by Matos et al. (2007). A gas chromatograph (3900 Gas Chromatograph; Varian, Palo Alto, CA, USA) equipped with a hydrogen flame-ionisation detector was used to separate the fatty acid methyl esters (FAME) with a fused silica 0.25 mm i.d. x 50 m capillary column (WCOT Fused Silica, CP-Sil 88 for FAME; Varian). The internal standard was heptadecanoate (C17:0). Double-bond index (DBI) was calculated as:

DBI = ((16:1t% + 18:1%) + (2*18:2%) + (3*18:3%)) * 100

Where 16:1t% was the percentage of palmitoleic fatty acid, 18:1% the percentage of oleic fatty acid, 18:2% the percentage of linoleic fatty acid and 18:3% the percentage of omega-3 fatty acid.

2.10. Statistical analysis

Statistical software package R was used to perform the entire statistic. A multivariate statistical approach using a principal component analysis model was performed to get an overview of the plant development, physiological and biochemical status in response to the different experimental treatments. Then, a downscaling assess was carried out through to generalized linear models (GLM) to analyze the interactive effects of atmospheric CO_2 concentration, water level and NaCl concentrations (as categorical factors) on the growth, physiological and biochemical parameters (as dependent variables) of *S. ramosissima* plants. Multiple comparisons were analysed by a LSD (post hoc) test. Before statistical analysis, Kolmogorov-Smirnov and Levene tests were used to verify the assumptions of normality and homogeneity of variances, respectively.

3. Results

3.1. Multivariate approach: global overview of physiological and biochemical status

PCA ordination provided an overall picture of the physiological/biochemical condition of *S. ramosissima* during the experimental setup explaining 64% of the proportion of variation of the recorded data (i.e. Axis 1 and Axis 2 a 43% and a 21%, respectively; Fig. 1). Hence, the bidimensional plot revealed a certain divergence between both atmospheric CO_2 concentration treatments along axis 2, with most of non-CO_2 enrichment plants located in the upper part (Fig. 1A). This separation by CO_2 treatment was mainly explained by higher A_N, C_i, $_i$WUE, Ψ_o, SOD activity and SFA accumulation at 700 ppm CO_2 compared to 400 ppm CO_2 (Fig. 1B). In addition, PCA analysis reflected a clear divergence of plants grown at 700 ppm CO_2 + WL + 510 mM NaCl in the left part of the plot linked with the greater P_G, N, Sm, φ_{D0}, DI/CS and Betain concentration compared with the rest of treatments (Fig. 1A and B).

Table 2
Relative growth rate (RGR), water content (WC) and absolute value of osmotic potential (Ψ_o) (MPa) state in randomly selected branches of *Salicornia ramosissima* in response to treatment with two atmospheric CO_2 concentrations (400 ppm and 700 ppm) in combination with two water levels (water logging, WL and no water logging, noWL) and two salinity concentrations (171 and 510 mM NaCl) for 45 days. Values represent mean ± SE, n = 8 for RGR and WC and n = 5 for Ψ_o. (GLM, [CO_2] x WLx [NaCl]; LSD test, P < 0.05). [CO_2],WL, NaCl or [CO_2]xWLxNaCl indicate main or interaction significant effects (*P < 0.01,**P < 0.001,***P < 0.0001).

[CO_2]	Water level	[NaCl]	RGR^{WL*}	WC	$\Psi_o^{[CO2]*[NaCl]**}$
400	no WL	171	0.104 ± 0.01	87.1 ± 1.0	3.38 ± 0.06
		510	0.093 ± 0.01	85.8 ± 0.3	4.94 ± 0.09
	WL	171	0.095 ± 0.01	86.9 ± 0.8	4.14 ± 0.08
		510	0.096 ± 0.01	87.8 ± 0.3	4.24 ± 0.06
700	no WL	171	0.113 ± 0.01	86.0 ± 0.4	3.05 ± 0.18
		510	0.118 ± 0.00	84.9 ± 0.9	4.71 ± 0.11
	WL	171	0.098 ± 0.01	87.0 ± 0.8	2.99 ± 0.07
		510	0.100 ± 0.01	86.3 ± 0.3	4.14 ± 0.07

3.2. Growth analysis

RGR values were greater overall in plants exposed to 700 ppm CO_2 than their non-CO_2 enrichment counterpart, obtaining the highest values in plants grown at 700 ppm CO_2 + noWL at both NaCl concentrations; however this positive effect was in certain degree mitigated under WL conditions (GLM: $_{WL,}$ p < 0.05; Table 2).

3.3. Plant water status

Water content (WC) did not vary with atmospheric CO_2 concentration, water logging and salinity, showing in all cases values c. 86% (Table 2). Contrarily, there were significant effects of atmospheric CO_2 concentration and salinity on the osmotic potential (Ψ_o) but no

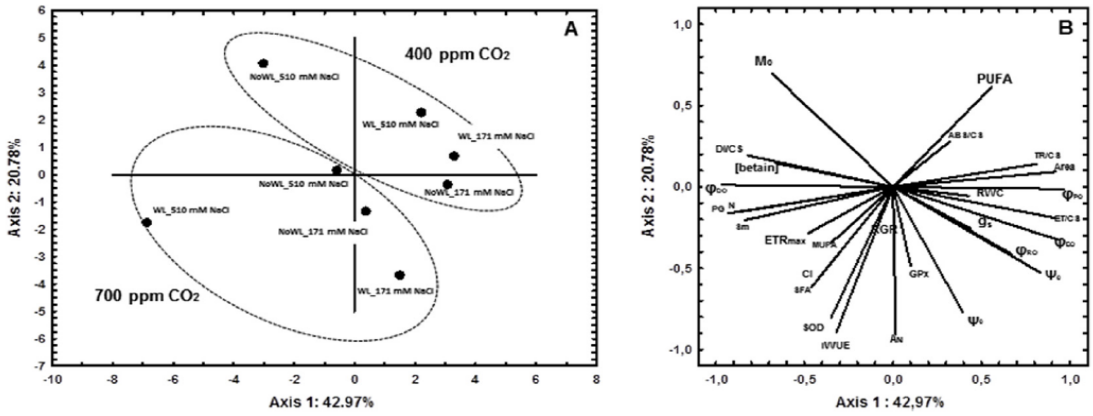

Fig. 1. PCA biplot of the physiological and biochemical data of *Salicornia ramosissima* plants in the experimental set-up. Loading plots for the first axis (explained variation is 42.97%) and second axis (explained variation is 20.78%).

significant interactions (GLM: $_{[CO2]}$, $p < 0.001$; $_{[NaCl]}$, $p < 0.05$; Table 2). Thus, Ψ_o increased at 510 mM NaCl being this increment overall reduced at elevated CO_2 concentration, independently of WL level (Table 2).

3.4. Gas exchange measurements

There were significant effects of atmospheric CO_2 concentration, WL and salinity on net photosynthetic rate (A_N) after 45 d of treatment, but no synergistic effect could be identified (GLM: $_{[CO2],\ WL,\ [NaCl]}$, $p < 0.05$). Thus, plants grown at higher CO_2 concentration showed slightly higher values of A_N than their 400-ppm CO_2 counterparts; being this augmentation more evident under water logging conditions compared with the remaining treatments. In addition, there was a decrease in A_N at 510 mM NaCl, but less pronounced at high CO_2 concentration and in presence of water logging (Fig. 2A). Furthermore, stomatal conductance (g_s) values were lower at elevated atmospheric CO_2 concentration and at 510 mM NaCl in noWL plants (GLM: $_{[CO2],\ WL,\ [NaCl]}$, $p < 0.05$; Fig. 2B). Overall, intercellular CO_2 concentration (C_i) values were greater in plants grown at 700 ppm CO_2 independently of saline and water logging conditions (GLM: $_{[CO2]}$, $p < 0.01$; Fig. 2C). Finally, $_i$WUE was only affected by CO_2 concentration with higher values for plants grown at 700 ppm CO_2 (GLM: $_{[CO2]}$, $p < 0.01$; Fig. 2D).

3.5. Fluorescence measurements

F_v/F_m and Φ_{PSII} values did not show any significant differences between atmospheric CO_2 concentration, WL or salinity treatments showing mean values of between 0.68–0.63 and between 0.64 and 0.65 for F_v/F_m and Φ_{PSII}, respectively (data not shown). However, there was a significant effect of atmospheric CO_2 concentration on ETR_{max} with higher values at 700 ppm CO_2 (GLM: $_{[CO2]}$, $p < 0.001$; Fig. 2E). Also, there was a synergistic effect of the three factors studied on ETR_{max}/A_N, thus this ratio increased in plants grown at 510 mM NaCl but this increment was mitigated at elevated atmospheric CO_2 concentration and plants exposed to WL conditions (GLM: $_{[CO2]\ x\ WL\ x\ [NaCl]}$, $p < 0.01$; Fig. 2F).

Focusing on the derived-parameters from the Kautsky curves, there was not a clear pattern of response to atmospheric CO_2 concentration, WL and salinity treatments. This lack of pattern was seeing at the oxidized quinone pool size available for reduction (Area), net rate of PS II RC closure (M_0), electron movement efficiency from the reduced intersystem electron acceptors to the PSI and electron acceptors (δR_0), maximum yield of primary photochemistry (φ_{P0}), probability of a PS II trapped electron to be transported from Q_A to Q_B (Ψ_0), probability that an absorbed photon will move an electron into the electronic transport chain (φ_{E0}), quantum yield of the non-photochemical reactions (φ_{D0}) (Fig. 3A, B, E, F and Fig. 4A–D). Nevertheless, grouping probability (P_G), reaction centre turnover rate (N) and relative pool size of PQ (Sm) values increased markedly in plants grown at 700 ppm CO_2 and elevated water and salinity levels compared with the rest of treatments (GLM: $_{[CO2]\ x\ WL\ x\ [NaCl]}$, $p < 0.05$; Fig. 3B, C, D). Finally, regarding the energetic fluxes on a leaf cross-section basis (phenomological fluxes) showed that absorbed (ABS/CS), trapped (TR/CS), dissipated (DI/CS)

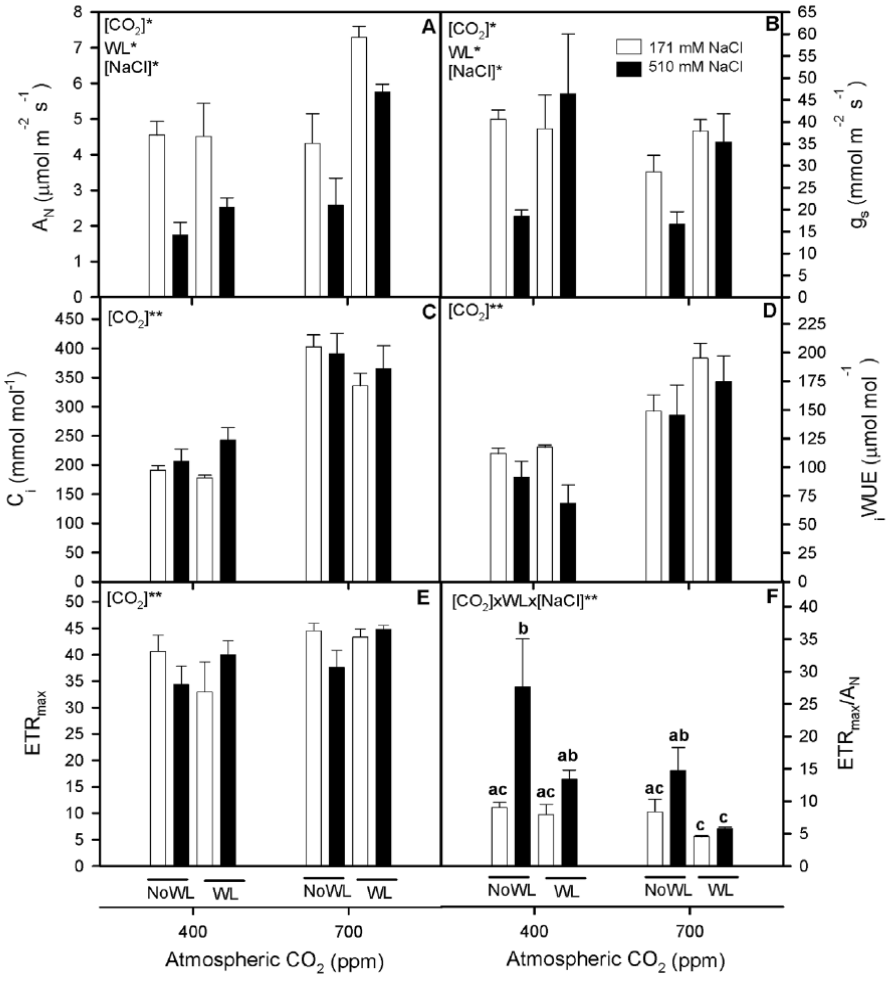

Fig. 2. Net photosynthetic rate, A_N (A), stomatal conductance, g_s (B), intercellular CO_2 concentration, C_i (C), intrinsic water use efficiency ($_i$WUE) (D), maximum ETR after which photo-inhibition can be observed (ETR_{max}) (E) and ETR_{max} net photosynthetic rate ratio, ETR_{max}/A_N (F) in randomly selected, primary branches of *Salicornia ramosissima* in response to treatment with two atmospheric CO_2 concentrations (400 ppm and 700 ppm) in combination with two water levels (water logging, WL and no water logging, noWL) and two salinity concentrations (171 and 510 mM NaCl) for 45 days. Values represent mean ± SE, n = 7. Different letters indicate means that are significantly different from each other (GLM, $[CO_2]$ x WLx [NaCl]; LSD test, $P < 0.05$). $[CO_2]$,WL, [NaCl] or $[CO_2]$ x WL x [NaCl] in the corner of the panels indicate main or interaction significant effects ($^*P < 0.01$, $^{**}P < 0.001$, $^{***}P < 0.0001$).

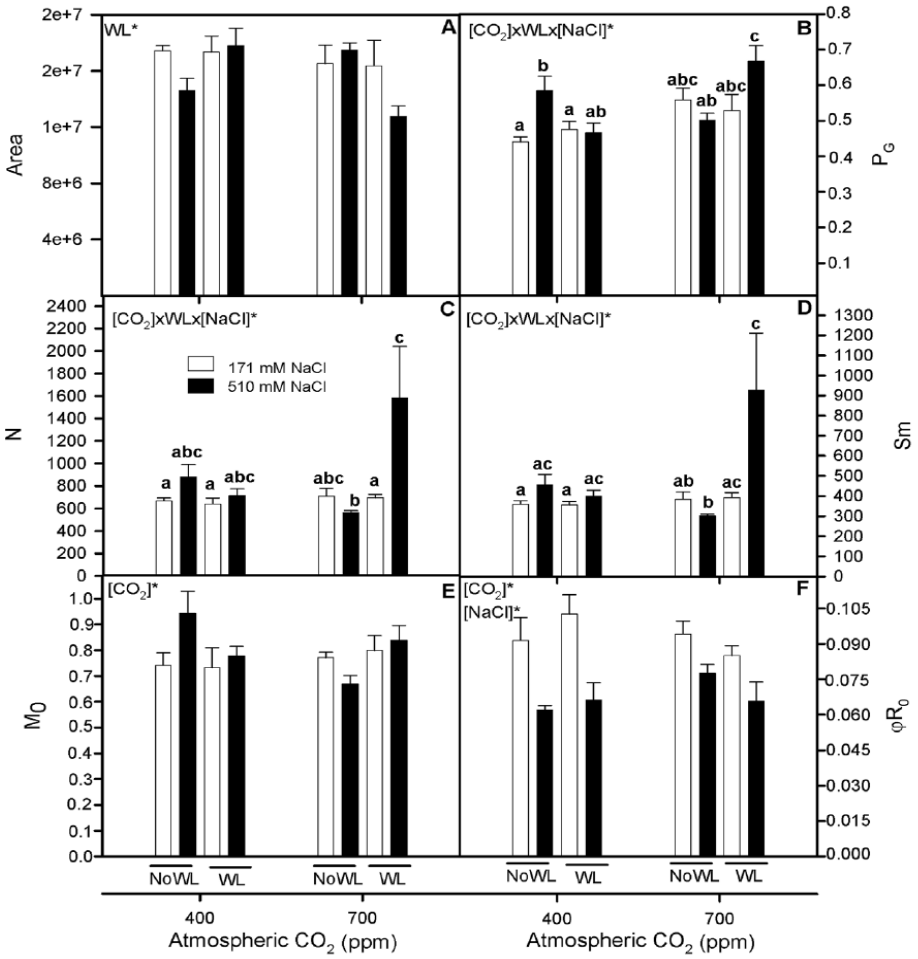

Fig. 3. Area (A), grouping probability (P_G) (B), reaction centre turnover rate (N) (C), relative PQ pool size (Sm) (D), net rate of PS II RC closure (M_0) (E) and maximum yield of primary photochemistry, (φ_{R0}) (F) in dark adapted randomly selected, primary branches of *Salicornia ramosissima* in response to treatment with two of NaCl concentrations (171 and 510 mM) and with water logging (WL) and with no water logging (noWL) at 400 and 700 ppm CO_2 after 45d of treatment. Values represent mean ± SE, n = 7. Different letters indicate means that are significantly different from each other (GLM, $[CO_2]$ x WLx [NaCl]; LSD test, $P < 0.05$). $[CO_2]$,WL, [NaCl] or $[CO_2]$ x WL x [NaCl] in the corner of the panels indicate main or interaction significant effects ($^{*}P < 0.01$, $^{**}P < 0.001$, $^{***}P < 0.0001$).

and electron transported (ET/CS) for cross section had very similar values in all treatments with no relevant differences between them (Fig. 5A–D).

3.6. Anti-oxidant enzymatic activity and osmocompatible solutes

GP_X enzyme activity did not vary between the plant exposed to the different experimental treatment (Fig. 6A), but SOD presented a clear tendency to be higher when *S. ramosissima* was grown at 700 ppm of CO_2 (GLM $_{[CO2]}$, $p < 0.001$; Fig. 6B): although without WL or salinity treatment variations.

On the other hand, there was a synergistic effect of the three experimental factors in betain concentration (GLM: $_{[CO2] \times WL \times [NaCl]}$, $p < 0.05$). Thus, betain concentration increased considerable at 700 ppm CO_2 in plants grown at 510 mM NaCl at both WL treatments (Fig. 6C).

3.7. Fatty acid composition

Percentage of palmitic acid (C16:0) and linolenic acid (C18:3) were significantly affected by CO_2 (GLM: $_{[CO2]}$, $p < 0.01$). Hence, overall 16:0 percentage was greater at elevated CO_2 concentration for all salinity and WL treatments; while the percentage of C18:3 decreased (Fig. 7A). In both cases, the differences were less evident for low salinity and water level being statistically significant the interactions for palmitic acid (GLM: $_{[CO2] \times WL \times [NaCl]}$, $p < 0.05$). For the remaining fatty acids analysed there were no significant differences between experimental treatments (Fig. 7A). The relative abundance of the saturation classes showed an increase in saturated fatty acid (SFA) and a decrease in the unsaturated classes (UFA, PUFA and MUFA) owing to the increment in atmospheric CO_2 (GLM: $_{[CO2]}$, $p < 0.01$) (Fig. 7B). Unsaturated/saturated ratio (UFA/SFA) (Fig. 7C) showed a significant slightly decrease at high CO_2 atmospheric concentration along with 510 mM NaCl at both WL treatments (GLM: $_{[CO2] \times WL \times [NaCl]}$, $p < 0.05$). Nevertheless, there were no significant effect in PUFA/SFA, 18:2/18:3 and DBI for any of the variables studied (Fig. 7C).

4. Discussion

Understanding the effects of possible interactions between atmospheric CO_2 enrichment and other ecosystems factors on plants species physiological performance is essential for designing more realistic models about the impact of climatic change on plant species development (Bernacchi et al., 2006). This information is particularly important in the most vulnerable ecosystems such as coastal areas and its vegetation, owing to its elevated risk of SLR (Reed, 2002; Duarte et al., 2014) and salinization events (IPCC, 2007).

This study showed that atmospheric CO_2 enrichment could ameliorate the deleterious impact of co-existed water logging and salinity suboptimal growth conditions on the physiological performance of *S. ramosissima*. Thus, plants grown at 700 ppm CO_2, WL and at both salinity levels surpassed the A_N values obtained by the plants grown in

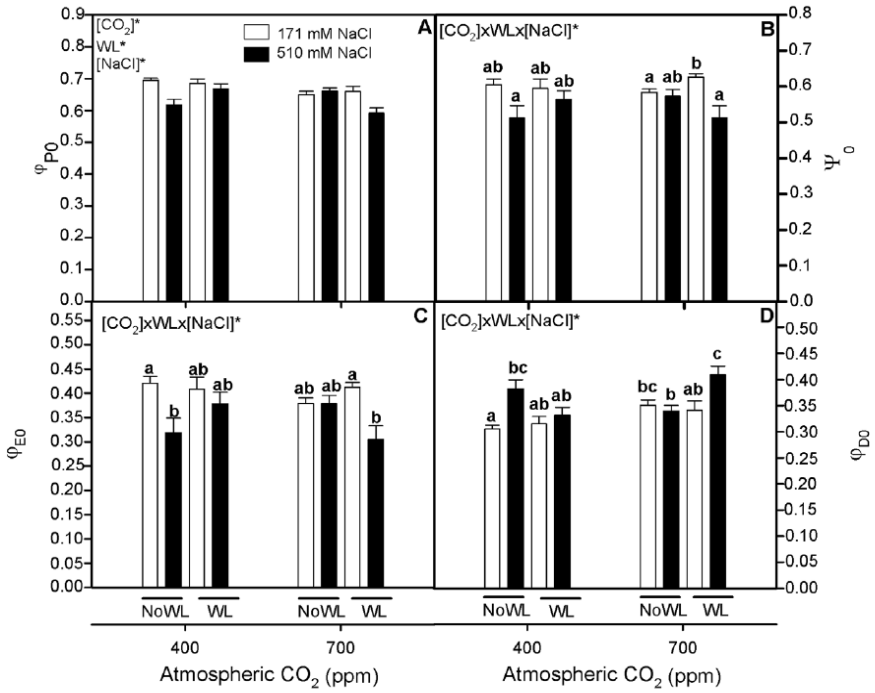

Fig. 4. φ_{P0} (A), Ψ_0 (B), φ_{E0} (C), and φ_{D0} (D) in dark adapted randomly selected, primary branches of *Salicornia ramosissima* in response to treatment with two of NaCl concentrations (171 and 510 mM) and with water logging (WL) and with no water logging (noWL) at 400 and 700 ppm CO_2 after 45d of treatment. Values represent mean ± SE, n = 7. Different letters indicate means that are significantly different from each other (GLM, [CO_2] x WLx [NaCl]; LSD test, $P < 0.05$). [CO_2],WL, [NaCl] or [CO_2] x WL x [NaCl] in the corner of the panels indicate main or interaction significant effects ($^{*}P < 0.01$, $^{**}P < 0.001$, $^{***}P < 0.0001$).

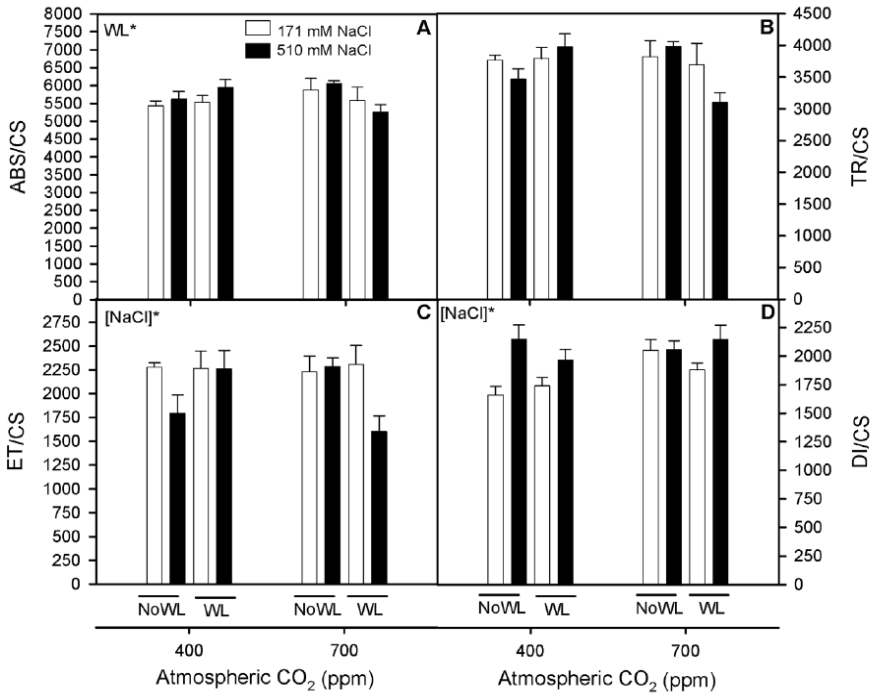

Fig. 5. Absorbed energy fluxtrapped energy flux, ABS/CS (A), trapped TR/CS (B) electron transport energy flux ET/CS (C) and dissipated energy fluxes, DI/CS (D) in dark adapted randomly selected, primary branches of *Salicornia ramosissima* in response to treatment with two of NaCl concentrations (171 and 510 mM) and with water logging (WL) and with no water logging (noWL) at 400 and 700 ppm CO_2 after 45d of treatment. Values represent mean ± SE, n = 7. Different letters indicate means that are significantly different from each other (GLM, [CO_2] x WLx [NaCl]; LSD test, $P < 0.05$). [CO_2],WL, [NaCl] or [CO_2] x WL x [NaCl] in the corner of the panels indicate main or interaction significant effects ($^{*}P < 0.01$, $^{**}P < 0.001$, $^{***}P < 0.0001$).

optimal conditions (i.e no WL and low salinity). Furthermore, g_s values decreased at 510 mM NaCl in no WL plants and overall were lower at elevated CO_2 atmospheric concentration. This reduction could be explained by the increase of C_i originated by the elevated CO_2 concentration; this could promote partial stomatal closure (Robredo et al., 2007). In addition, it is worth to mention that g_s values did not vary respect to values registered in plants grown at noWL+171 mM NaCl contrary to the drop recorded in A_N at high salinity and WL levels in not CO_2 enrichment plants. This mitigation effect fot g_s of water logging has been previously described by Ullah et al. (2017). Ullah et al. (2017) ascribed it to the water excess which would stimulates the stomatal aperture ameliorating the stomata closure effect of high salinity. This effect was also evident at 700 ppm CO_2 for our treated plants. The general g_s reduction at 700 ppm CO_2 would contribute to preserve the trade-off between CO_2 acquisition for photosynthetic process and water losses in *S. ramosissima* as indicated the higher ¡WUE values, being this impact especially important at 510 mM NaCl since these plants would be able to cope with the stress derived from salt excess. Robredo et al.

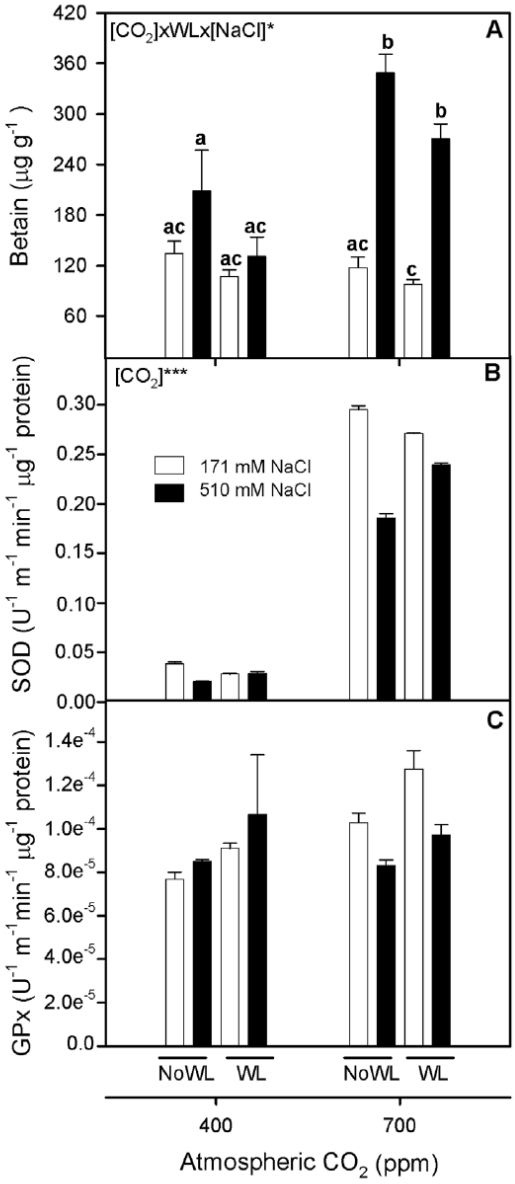

Fig. 6. Betain (A), superoxide dismutase (SOD) (B) and guaiacol peroxidase (GPx) (C) enzymatic activities in randomly selected, primary branches of *Salicornia ramosissima* in response to treatment with two of NaCl concentrations (171 and 510 mM) and with water logging (WL) and with no water logging (no WL) at 400 and 700 ppm CO_2 after 45d of treatment. Values represent mean ± SE, n = 3. Different letters indicate means that are significantly different from each other (GLM, [CO_2] x WLx [NaCl]; LSD test, $P < 0.05$). [CO_2],WL, [NaCl] or [CO_2] x WL x [NaCl] in the corner of the panels indicate main or interaction significant effects ($^{*}P < 0.01$, $^{**}P < 0.001$, $^{***}P < 0.0001$).

(2007) previously highlighted, the increment in CO_2 atmospheric concentration allow plants to acquire the carbon needed with less stoma aperture rising the efficiency in the use of water for them. A very similar trends have been previously reported in *S. ramosissima* and in other halophytes (Geissler et al., 2009a, 2009b; 2015; Mateos-Naranjo et al., 2010a, 2010b; Pérez-Romero et al., 2018) in response to NaCl excess and in combination with soil flooding conditions (Lenssen et al., 1995). Nevertheless, to our knowledge, this is the first study where CO_2 enrichment beneficial effects under coexisted root flooding conditions could be also ascribed to up-regulation of some component involved in PSII energy transport chain, accumulation of osmoprotective compounds and the modulation of fatty acids profiles, as indicated our multivariate statistical approach.

Despite the existence of widely documented deleterious effect of prolonged water logging (Mateos-Naranjo et al., 2007; Cao et al., 2017; Ullah et al., 2017) and NaCl concentration excess (Flexas et al., 2004; Mateos-Naranjo and Redondo-Gómez, 2016) on photochemical apparatus our results showed a different scenario. It could be seen that in general PS II and its antennae complex were not affected by any of the tested stressful treatments. As it was indicated by the similarities in F_v/F_m, Φ_{PSII}, Area, δR0, φ_{P0}, Ψ_0, φ_{E0}, ABS/CS, TR/CS and ET/CS values between all experimental treatments. Nevertheless, plants exposed to 700 ppm CO_2 + WL + 510 mM NaCl presented the higher P_G, N and Sm values, which indicate that their reaction centres had lower re-oxidation rates and thus were able to generate electrons from photons in higher amounts per unit of time (Duarte et al., 2017). Moreover, the lack of difference in electron transport flux (ET/CS) suggests that the electron transport chain can deal with this increased number of electrons, derived from higher P_G, N and Sm values, and therefore under normal conditions it would be working at sub-saturated conditions. Hence, the positive impact of atmospheric CO_2 enrichment on photochemical apparatus of *S. ramosissima* could be ascribed to the enhanced of the efficiency for energy transport, avoiding the accumulation of energy excess, which could contribute to reduce the risk of oxidative stress due to the accumulation of reactive oxygen species (ROS). In fact, the lower risk of ROS production was supported by the decrease in ETR_{max}/A_N ratio recorded in *S. ramosissima* plants grown at 700 ppm CO_2 + WL + 510 mM NaCl compared with their non-CO_2 supplied counterparts. This ratio could be considered as an indicator of the potential ROS stress that plants are subjected to and derived from a possible lack of carbon units correspondent to the number of electrons generated (Salazar-Parra et al., 2012; Hussin et al., 2017). Together with the maintenance of energy transport efficiency, the accumulation of different protection compounds as osmocompatible solutes or the modulation of the anti-oxidative stress enzymes machinery was also in the basis of the redox-balance maintenance. Therefore, compounds such as betain are known to be produced by plants to cope with salinity or drought stress (Moradi et al., 2017). In this study, betain concentration showed a clear pattern of increment in relation with the atmospheric CO_2 in plants grown under stressful conditions. In addition, there was modulation effect, driven from an atmospheric CO_2 enrichment, in certain anti-oxidant enzymes of *S. ramosissima* as SOD. This enzyme showed higher activity levels compared their 400-ppm CO_2 counterpart contributing to cope with oxidative stress in greater extent.

Finally, the ameliorative effect of atmospheric CO_2 fertilization on *S. ramosissima* physiological responses under coexistence of water logging and salt excess was also supported by fatty acids profiles. Fatty acids profile has been suggested as useful biomarker for abiotic stress in halophytes species, such as *Spartina maritima*, *Spartina patens*, *Halimione portulacoides* and *Sarcocornia fruticosa*, and its levels are highly related to the photosynthetic functioning of these species (Duarte et al., 2017, 2018a; 2018b). Our results revealed that generally at elevated CO_2 concentrations there was a decrease in unsaturated/saturated ratio for all WL and salinity treatments, due to a major decrease in C18:3. A direct action of ROS production during stress exposition with the augmentation of the membrane lipid peroxidation has been described, which could led to a decrease in the C18:2 and C18:3 relative contents (Ouariti et al., 1997; Upchurch, 2008). In addition, it is well known that in photosynthetic tissues the C18:3 fatty acid is mostly associated with the galactolipids monogalactosyldiacylglycerol (MGDG) and digalactosyldiacylglycerol (DGDG), which are fundamental for the correct function of photosynthesis (Mizusawa and Wada, 2012). Hence, tissues with low amount of these kind of lipids (and consequently low C18:3 content) have disrupted photosynthetic membranes and a complete impairment of photochemical processes (Kobayashi et al., 2007;

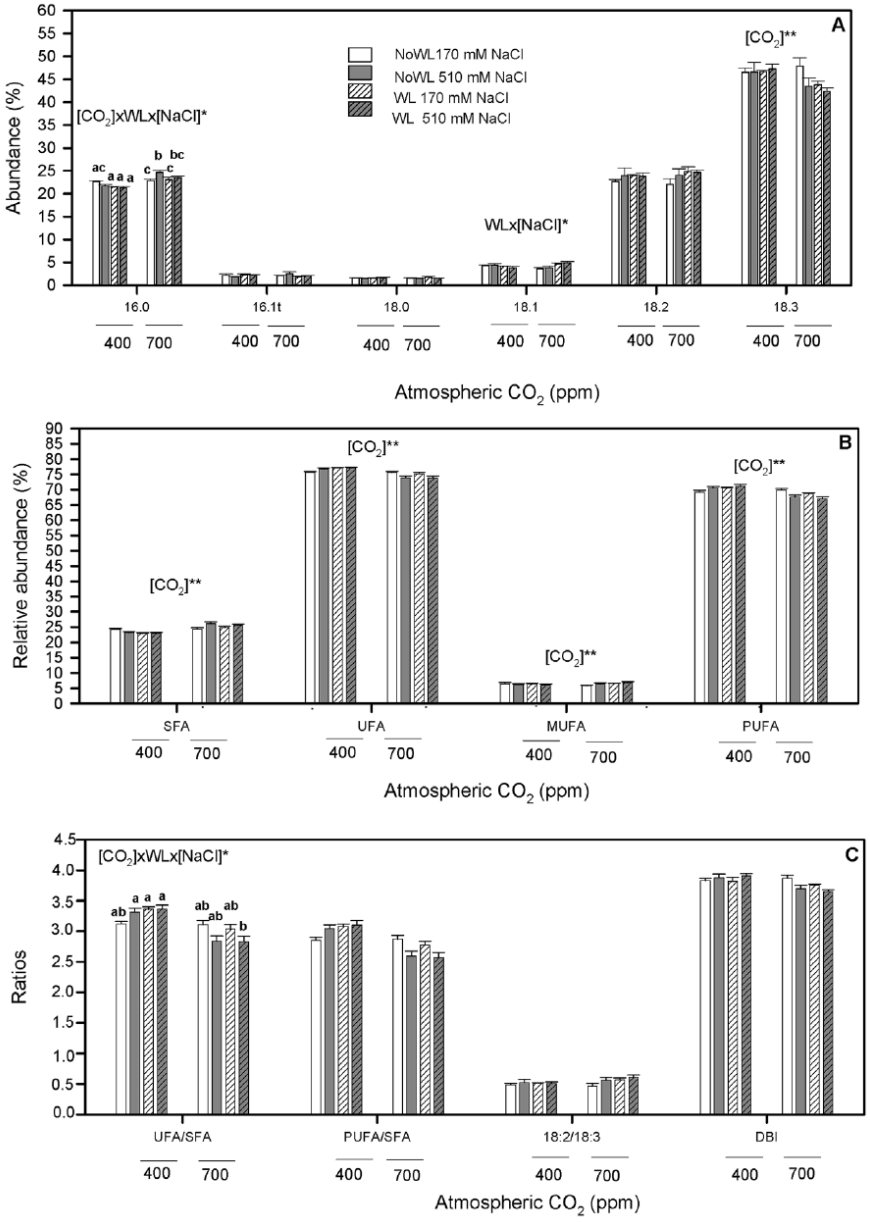

Fig. 7. Palmitic acid (16:0), palmitoleic acid (16:1t), stearic acid (18:0), oleic acid (18:1), linoleic acid (18:2) and omega-3 (18:3) abundance (A); saturated (SFA), unsaturated (UFA), monounsaturated (MUFA) and polyunsaturated (PUFA) relative abundance (B); unsaturated-saturated fatty acids (UFA/SFA), polyunsaturated-saturated fatty acids (PUFA/SFA), linoleic acid-omega-3 fatty acids (18:2/18:3) ratios and double-bond index (DBI) (C) calculated in randomly selected primary branches of *Salicornia ramosissima* in response to treatment with two of NaCl concentrations (171 and 510 mM) and with water logging (WL) and with no water logging (noWL) at 400 and 700 ppm CO_2 after 45d of treatment. Values represent mean ± SE, n = 5. Different letters indicate means that are significantly different from each other (GLM, [CO_2] x WLx [NaCl]; LSD test, $P < 0.05$). [CO_2],WL, [NaCl] or [CO_2] x WL x [NaCl] in the corner of the panels indicate main or interaction significant effects ($^{*}P < 0.01$, $^{**}P < 0.001$, $^{***}P < 0.0001$).

Aronsson et al., 2008). However, according to Duarte et al. (2017) in the halophyte *Aster tripolium* we found that there was not a correlation between the decrease in C18:3 and photosynthetic apparatus performance. The lack of relationship was ascribe to an adaptation in which the polyunsaturated fatty acids (more specific the C18:3) decrease to cope with salinity stress (Duarte et al., 2017). In addition, we found that plants grown at 700 ppm CO_2 showed higher values for the fatty acid C16:0. This increment would be associated to an improvement in the PS II function since this fatty acid presents an important role in this component of the photosynthetic pathway (Gounaris and Barber, 1985; Duarte et al., 2017).

5. Conclusion

This experiment confirmed previous work that had demonstrated atmospheric CO_2 enrichment ameliorative effect on salinity tolerance of *S. ramosissima* (Pérez-Romero et al., 2018). Nevertheless, we found that this positive effect under synergistic root-flooding was mainly owing to upregulation its energy sink capacity, as indicated the increment in the rate of reaction centre turnover, relative pool size of PQ and the connectivity beween PSII units, together with the already previously described increment in carbon assimilation and water balance capacity. In addition, our results indicated that the beneficial effect of CO_2 concentration was ascribed to a better modulation of the antioxidant enzyme machinery and of the betain accumulation on tissues to cope with oxidative stress, as well as to a great presence in saturated fatty acids, which would be associated with the aforementioned improvement in the PSII function.

CRediT authorship contribution statement

Jesús Alberto Pérez-Romero: Conceptualization, Investigation, Methodology, Formal analysis, Writing – original draft. **Bernardo Duarte:** Formal analysis, Supervision, Writing – review & editing. **Jose-Maria Barcia-Piedras:** Data curation, Methodology. **Ana Rita Matos:** Formal analysis, Resources. **Susana Redondo-Gómez:** Conceptualization, Project administration. **Isabel Caçador:** Formal analysis, Resources. **Enrique Mateos-Naranjo:** Formal analysis, Conceptualization, Supervision, Writing – review & editing.

Acknowledgements

This work has been funded by Ministerio de Economía y Competitividad (MINECO Project CGL2016-75550-R cofunded by FEDER). J.A Pérez-Romero thanks Ministerio de Educación, Cultura y Deporte for its personal financial support (FPU014/03987). We are grateful University of Seville Greenhouse General Services (CITIUS) for its collaboration. The authors would also like to thank to the "Fundação para a Ciência e a Tecnologia" for funding the research in the Marine and Environmental Sciences Centre (MARE) and the Intercollegiate Studies Institute throughout the projects UID/MAR/04292/2013 and UID/MULTI/04046/2013 respectively. B. Duarte investigation was supported by FCT throughout a Posdoctoral grant (SFRH/BPD/115162/2016). We are grateful to Pablo Robles Delgado for revision of the English text of this manuscript.

References

Aronsson, H., Schottler, M.A., Kelly, A.A., Sundqvist, C., Dormann, P., Karim, S., Jarvis, P., 2008. Monogalactosyldiacylglycerol deficiency in *Arabidopsis* affects pigment composition in the prolamellar body and impairs thylakoid membrane energization and photoprotection in leaves. Plant Physiol. 148 (1), 580–592.

Bergmeyer, H.U., 1974. Methods of enzymatic analysis, vol. 4 Academic Press. http://www.sciencedirect.com/science/book/9780120913046.

Bernacchi, C.J., Leakey, A.D., Heady, L.E., Morgan, P.B., Dohleman, F.G., McGrath, J.M., et al., 2006. Hourly and seasonal variation in photosynthesis and stomatal conductance of soybean grown at future CO2 and ozone concentrations for 3 years under fully open-air field conditions. Plant Cell Environ. 29 (11), 2077–2090.

Bradford, M.M., 1976. A rapid and sensitive method for the quantification of micro-gram quantities of protein utilizing the principle of protein–dye binding. Anal. Biochem. 72, 248–254.

Calvo, O.C., Franzaring, J., Schmid, I., Müller, M., Brohon, N., Fangmeier, A., 2017. Atmospheric CO2 enrichment and drought stress modify root exudation of barley. Global Change Biol. 23 (3), 1292–1304.

Cao, Y., Ma, C., Chen, G., Zhang, J., Xing, B., 2017. Physiological and biochemical responses of *Salix integra* Thunb. under copper stress as affected by soil flooding. Environ. Pollut. 225, 644–653.

Davy, A.J., Bishop, G.F., Costa, C.S.B., 2001. *Salicornia* L. (*Salicornia pusilla* J. Woods, *S. ramosissima* J. Woods, *S. europaea* l., *S. obscura* P. W. Ball & Tutin, *S. nitens* P. W. Ball & Tutin, *S. fragilis* P. W. Ball & Tutin, P. W. Ball & Tutin and *S. dolichostachya* Moss). J. Ecol. 89, 681–707.

Duarte, B., Santos, D., Marques, J.C., Caçador, I., 2013. Ecophysiological adaptations of two halophytes to salt stress: photosynthesis, PS II photochemistry and anti-oxidant feedback - Implications for resilience in climate change. Plant Physiol. Biochem. 67, 178–188.

Duarte, B., Santos, D., Silva, H., Marques, J.C., Caçador, I., Sleimi, N., 2014. Light–dark O_2 dynamics in submerged leaves of C_3 and C_4 halophytes under increased dissolved CO_2: clues for saltmarsh response to climate change. AoB Plants 6 plu067. http://doi.org/10.1093/aobpla/plu067.

Duarte, B., Goessling, J.W., Marques, J.C., Caçador, I., 2015. Ecophysiological constraints of *Aster tripolium* under extreme thermal events impacts: Merging biophysical, biochemical and genetic insights. Plant Physiol. Biochem. 97, 217–228.

Duarte, B., Cabrita, M.T., Gameiro, C., Matos, A.R., Godinho, R., Marques, J.C., Caçador, I., 2017. Disentangling the photochemical salinity tolerance in *Aster tripolium* L.: connecting biophysical traits with changes in fatty acid composition. Plant Biol. 19 (2), 239–248.

Duarte, B., Carreiras, J., Pérez-Romero, J.A., Mateos-Naranjo, E., Redondo-Gómez, S., Matos, A.R., Redondo-Gómez, S., Marques, J.C., Caçador, I., 2018a. Halophyte fatty acids as biomarkers of anthropogenic-driven contamination in Mediterranean marshes: Sentinel species survey and development of an integrated biomarker response (IBR) index. Ecol. Indicat. 87, 86–96.

Duarte, B., Matos, A.R., Marques, J.C., Caçador, I., 2018b. Leaf fatty acid remodeling in the salt-excreting halophytic grass *Spartina patens* along a salinity gradient. Plant Physiol. Biochem. 124, 112–116.

Flexas, J., Bota, J., Loreto, F., Cornic, G., Sharkey, T.D., 2004. Diffusive and metabolic limitations to photosynthesis under drought and salinity in C3 plants. Plant Biol. 6 (3), 269–279.

Ghannoum, O., Von Caemmerer, S., Ziska, L.H., Conroy, J.P., 2000. The growth response of C4 plants to rising atmospheric CO2 partial pressure: A reassessment. Plant Cell Environ. 23 (9), 931–942.

Geissler, N., Hussin, S., Koyro, H.W., 2009a. Elevated atmospheric CO2 concentration ameliorates effects of NaCl salinity on photosynthesis and leaf structure of *Aster tripolium* L. J. Exp. Bot. 60 (1), 137–151.

Geissler, N., Hussin, S., Koyro, H.W., 2009b. Interactive effects of NaCl salinity and elevated atmospheric CO2 concentration on growth, photosynthesis, water relations and chemical composition of the potential cash crop halophyte *Aster tripolium* L. Environ. Exp. Bot. 65 (2–3), 220–231.

Geissler, N., Hussin, S., El-Far, M.M.M., Koyro, H.W., 2015. Elevated atmospheric CO2 concentration leads to different salt resistance mechanisms in a C3 (*Chenopodium quinoa*) and a C4 (*Atriplex nummularia*) halophyte. Environ. Exp. Bot. 118, 67–77.

Gounaris, K., Barber, J., 1985. Isolation and characterisation of a photosystem II reaction centre lipoprotein complex. FEBS Lett. 188, 68–72.

Grieve, C.M., Grattan, S.R., 1983. Rapid assay for determination of water soluble quaternary ammonium compounds. Plant Soil 70, 303.

Hoagland, D.R., Arnon, D.I., 1938. The water culture method for growing plants without soil. Calif. Agric. Ext. Serv. Circ. 347, 32.

Hussin, S., Geissler, N., El-Far, M.M.M., Koyro, H.W., 2017. Effects of Salinity and Short-Term Elevated Atmospheric CO 2 on the Chemical Equilibrium between CO 2 Fixation and Photosynthetic Electron Transport of *Stevia rebaudiana* Bertoni. Plant Physiol. Biochem. 118, 178–186. http://linkinghub.elsevier.com/retrieve/pii/S0981942817302085.

IPCC, 2001. In: Watson, R.T., the Core Writing Team (Eds.), Climate Change 2001: Synthesis Report. A Contribution of Working Groups I, II, and III to the Third Assessment Report of the Integovernmental Panel on Climate Change. Cambridge University Press, Cambridge, United Kingdom, and New York, NY, USA 398 pp.

IPCC, 2007. In: Core Writing Team, Pachauri, R.K., Reisinger, A. (Eds.), Climate Change 2007: Synthesis Report. Contribution of Working Groups I, II and III to the Fourth Assessment Report of the Intergovernmental Panel on Climate Change. IPCC, Geneva, Switzerland 104 pp.

Kobayashi, K., Kondo, M., Fukuda, H., Nishimura, M., Ohta, H., 2007. Galactolipid synthesis in chloroplast inner envelope is essential for proper thylakoid biogenesis, photosynthesis, and embryogenesis. Proc. Natl. Acad. Sci. U. S. A 104 (43), 17216–17221.

Lenssen, G., Lamers, J., Stroetenga, M., Rozema, J., 1993. Interactive effects of atmospheric CO2 enrichment, salinity and flooding on growth of C 3 (*Elymus athericus*) and C 4 (*Spartina anglica*) salt marsh species. Vegetatio 104/105 (0), 379–388.

Lenssen, G.M., van Duin, W.E., Jak, P., Rozema, J., 1995. The response of *Aster tripolium* and *Puccinellia maritima* to atmospheric carbon dioxide enrichment and their interactions with flooding and salinity. Aquat. Bot. 50 (2), 181–192. http://doi.org/10.1016/0304-3770(95)00453-7.

Marklund, S., Marklund, G., 1974. Involvement of the superoxide anion radical in the autoxidation of pyrogallol and a conveniente assay for superoxide dismutase. Eur. J. Biochem. 47, 469–474.

Marshall, H.L., Geider, R.J., Flynn, K.J., 2000. A mechanistic model of photoinhibition. New Phytol. 145 (2), 347–359.

Mateos-Naranjo, E., Redondo-Gómez, S., Silva, J., Santos, R., Figueroa, M.E., 2007. Effect of Prolonged Flooding on the Invader *Spartina densiflora* Brong. J. Aquat. Plant Manag. 45 (2), 121–123.

Mateos-Naranjo, E., Redondo-Gomez, S., Alvarez, R., Cambrolle, J., Gandullo, J., Figueroa, M.E., 2010a. Synergic effect of salinity and CO2 enrichment on growth and photosynthetic responses of the invasive cordgrass Spartina densiflora. J. Exp. Bot. 61 (6), 1643–1654.

Mateos-Naranjo, E., Redondo-Gómez, S., Andrades-Moreno, L., Davy, A.J., 2010b. Growth and photosynthetic responses of the cordgrass *Spartina maritima* to CO_2 enrichment and salinity. Chemosphere 81, 725–731.

Mateos-Naranjo, E., Redondo-Gómez, S., 2016. Inter-population differences in salinity tolerance of the invasive cordgrass *Spartina densiflora*: Implications for invasion process. Estuar. Coast 39, 98–107.

Matos, A.R., Hourton-Cabassa, C., Çiçek, D., Rezé, N., Arrabaça, J.D., Zachowski, A., Moreau, F., 2007. Alternative oxidase involvement in cold stress response of *Arabidopsis thaliana fad2* and *FAD3+* cell suspensions altered in membrane lipid composition. Plant Cell Physiol. 48 (6), 856–865.

Mizusawa, N., Wada, H., 2012. The role of lipids in photosystem II. Biochim. Biophys. Acta Bioenerg. 1817 (1), 194–208.

Moradi, P., Ford-Lloyd, B., Pritchard, J., 2017. Metabolomic approach reveals the biochemical mechanisms underlying drought stress tolerance in thyme. Anal. Biochem. 527, 49–62.

Ouariti, O., Boussama, N., Zarrouk, M., Cherif, A., Ghorbal, M.H., 1997. Cadmium- and copper-induced changes in tomato membrane lipids. Phytochemistry 45 (7), 1343–1350.

Pérez-Romero, J.A., Redondo-Gomez, S., Mateos-Naranjo, E., 2016. Growth and photosynthetic limitation analysis of the Cd-accumulator *Salicornia ramosissima* under excessive cadmium concentrations and optimum salinity conditions. Plant Physiol. Biochem. 109, 103–113.

Pérez-Romero, J.A., Idaszkin, Y., Barcia-Piedras, J.M., Duarte, B., Redondo-Gomez, S., Caçador, I., Mateos-Naranjo, E., 2018. Disentangling the effect of atmospheric CO2 enrichment on the halophyte Salicornia ramosissima J. Woods physiological performance under optimal and suboptimal saline conditions. Plant Physiol. Biochem. 127, 617–629.

Redondo-Gómez, S., Mateos-Naranjo, E., Figueroa, M.E., Davy, A.J., 2010. Salt stimulation of growth and photosynthesis in an extreme halophyte, *Arthrocnemum macrostachyum*. Plant Biol. 12 (1), 79–87.

Reed, D.J., 2002. Sea-level rise and coastal marsh sustainability: geological and ecological factors in the Mississippi delta plain. Geomorphology 48 (1–3), 233–243.
Robredo, A., Pérez-López, U., de la Maza, H.S., González-Moro, B., Lacuesta, M., Mena-Petite, A., Muñoz-Rueda, A., 2007. Elevated CO2 alleviates the impact of drought on barley improving water status by lowering stomatal conductance and delaying its effects on photosynthesis. Environ. Exp. Bot. 59 (3), 252–263.
Rozema, J., 1993. Plant-responses to atmospheric carbon-dioxide enrichment - interactions with some soil and atmospheric conditions. Vegetatio 104, 173–190.
Salazar-Parra, C., Aquirreolea, J., Sánchez-Díaz, M., Irigoyen, J.J., Morales, F., 2012. Climate Change (elevated CO2, elevated temperature and moderate drought) triggers the antioxidant enzymes' response of grapevine cv. tempranillo, avoiding oxidative damage. Physiol. Plantarum 144 (2), 99–110.
Slama, I., M'Rabet, R., Ksouri, R., Talbi, O., Debez, A., Abdelly, C., 2015. Water deficit stress applied only or combined with salinity affects physiological parameters and antioxidant capacity in *Sesuvium portulacastrum*. Flora −Morphol. Distrib. Funct. Ecol. Plants 213, 69–76.
Schreiber, U., Schliwa, U., Bilger, W., 1986. Continuous recording of photochemical and non-photochemical chlorophyll fluorescence quenching with a new type of modulation fluorometer. Photosynth. Res. 10 (1–2), 51–62.
Strasser, R.J., Tsimilli-Michael, M., Srivastava, A., 2004. Analysis of the chlorophyll a fluorescence transient. In: Papageorgiou, G.C., Govindjee (Eds.), Chlorophyll a Fluorescence: A Signature of Photosynthesis. Springer Netherlands, Dordrecht, pp. 321–362.
Ullah, I., Waqas, M., Khan, M.A., Lee, I.J., Kim, W.C., 2017. Exogenous ascorbic acid mitigates flood stress damages of *Vigna angularis*. Applied Biological Chemistry 60 (6), 603–614.
Upchurch, R.G., 2008. Fatty acid unsaturation, mobilization, and regulation in the response of plants to stress. Biotechnol. Lett. 30 (6), 967–977.
Yang, Z., Xie, T., Liu, Q., 2014. Physiological responses of *Phragmites australis* to the combined effects of water and salinity stress. Ecohydrology 7, 420–426.

CAPÍTULO 4:

Impact of short-term extreme temperature events on physiological performance of *Salicornia ramosissima* J. Woods under optimal and sub-optimal saline conditions

Pérez-Romero et al., 2019, Scientific Reports

SCIENTIFIC REPORTS

OPEN

Impact of short-term extreme temperature events on physiological performance of *Salicornia ramosissima* J. Woods under optimal and sub-optimal saline conditions

Received: 27 July 2018
Accepted: 30 November 2018
Published online: 24 January 2019

Jesús Alberto Pérez-Romero[1], Jose-Maria Barcia-Piedras[2], Susana Redondo-Gómez[1] & Enrique Mateos-Naranjo[1]

Increasing extreme temperature climatic events could exert an important effect on plant photosynthetic performance, which could be modulated by the co-occurrence with other environmental factors, such as salinity, in estuarine ecosystems. Therefore, a mesocosm experiment was designed to assess the impact of temperature events for three days (13/5 °C, 25/13 °C and 40/28 °C) in combination with two NaCl concentrations (171 and 1050 mM NaCl) on the physiological performance of *Salicornia ramosissima*. Extreme temperature events had a negative impact on *S. ramosissima* photosynthetic efficiency, this effect being more marked with cold wave at both salinities, compared with heat wave, even in presence of NaCl excess. This differential thermotolerance in the photosynthetic apparatus was ascribed to the greater integrity and functioning of its photosynthetic pathway at high temperature, as indicated by constant g_s, $V_{c,max}$ values at optimal salinity and the higher values of those parameters and g_m recorded in combination with NaCl excess. Moreover, *S. ramosissima* was able to upregulate the energy sink capacity of its photochemical apparatus at elevated temperature and salinity by a greater energy excess dissipation capacity. This could have contributed to reducing the risk of oxidative stress, along with the recorded higher capacity for antioxidant enzyme activity modulation under these conditions.

Together with the recognized atmospheric CO_2 enrichment and temperature increment, climate change models indicate that extreme climatic events, such as salinization, floods, drought and cold and heat waves are likely to increase, not only in intensity but also in frequency, especially in the Mediterranean area[1]. To date, there have been increasing reports investigating the effect of the main slower environmental changes related to climate change, such as atmospheric CO_2 enrichment or temperature increment, on plants species composition, structure and distribution[2]. In spite of this increasing number of reports, not many studies have addressed the impact of short extreme climatic events, such as heat and cold waves on plant species, despite the fact that it has been stated that in many cases these phenomena might have an important selective effect on plant species, limiting its development and distribution by dysfunction of essential biological processes such a plant phenology, reproduction, physiology, etc.[3]. Furthermore, the few existing studies only assessed the impact of a single extreme climatic event, not taking into account the co-occurrence with other important environmental factors that are likely to limit species survival, development and distribution. This is the case of estuarine ecosystems, where plant species survival and distribution is highly modulated by stressful abiotic factors such salinity, flooding, redox potential, etc.[4].

[1]Departamento de Biología Vegetal y Ecología, Facultad de Biología, Universidad de Sevilla, 1095, 41080, Sevilla, Spain. [2]Department of Ecological Production and Natural Resources Center IFAPA Las Torres-Tomejil Road Sevilla - Cazalla Km 12'2, 41200 - Alcalá del Río, Seville, Spain. Correspondence and requests for materials should be addressed to J.A.P.-R. (email: jperez77@us.es)

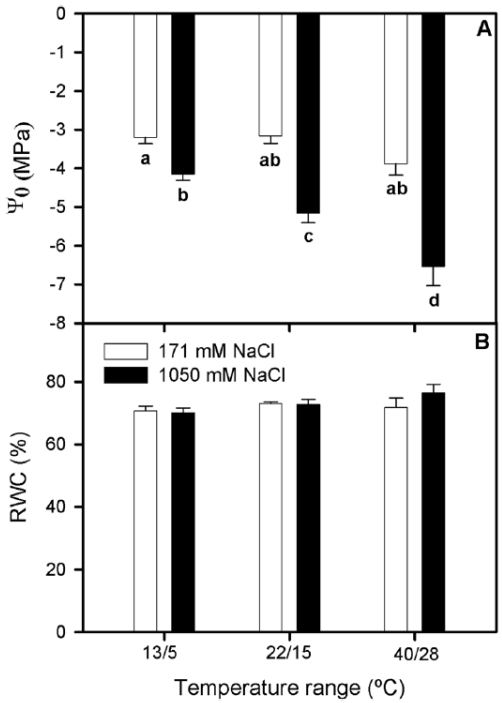

Figure 1. Osmotic potential, Ψ_o (**A**) and relative water content, RWC (**B**), in randomly selected, primary branches of *Salicornia ramosissima* in response to treatment with three temperature ranges (13/5 °C, 22/15 °C and 40/28 °C) and two NaCl concentrations (171 and 1050 mM) after 3 days. Values represent mean ± SE, n = 10. Different letters indicate means that are significantly different from each other.

Therefore, assessing the response of these plants species to extreme thermal climate events, in co-occurrence with medium salinity level variations, is of paramount importance for understanding the future fitness of these species. This experiment was thus designed and conducted to fill these gaps in knowledge.

Salicornia ramosissima J. Woods (Chenopodiaceae) is a C_3 species which has been considered an alternative multifunctional cash crop for many arid and semiarid regions of the world[5], due to its edibility[6] and its high physiological versatility, which allows it to tolerate a wide range of environmental factors, pollution[7], salinity[8], etc. Recently, like for other halophytes species[8–13], some authors have emphasized the positive impact of rising atmospheric CO_2 linked with climate change on *S. ramosissima* performance under sub-optimal salinity conditions[8]. Accordingly, we hypothesize that extreme short climatic events, such cold and heat waves, would lead to differential photochemical responses in *S. ramosissima* under optimal and suboptimal salinity conditions, with the consequent effect on the primary productivity and development of this important multifunctional cash crop species. Therefore, this study aimed to: (1) ascertain the extent to which photosynthetic apparatus (PSII chemistry), gas exchange characteristics (CO_2 diffusive and biochemical component) and photosynthetic pigments profiles determine plant tolerance to cold (13/5 °C) and heat (40/28 °C) waves under optimal (171 mM NaCl) and suboptimal saline conditions (1050 mM NaCl); and (2) examine possible role of antioxidant enzyme machinery in these responses.

Results

Osmotic potential and water content measurements. Overall, Ψ_o values increased in plants grown at 1050 mM NaCl compared with their non-high salinity treated counterparts, this increment being more marked in those exposed to 40–28 °C (Two-way $ANOVA_{NaCl}$, $F_{1,42} = 70.123$; Fig. 1A). Contrarily, there were not significant effects of salinity and temperature ranges treatments on RWC, in all cases the values being between 75–80% (Fig. 1B).

Gas exchange measurements and photosynthesis limitation analysis. There were significant effects of both salinity and temperature range treatments on the gas exchange characteristics of *S. ramosissima* after 3 d of treatment (Two-way $ANOVA_{NaCl}$, $F_{1,138} = 33.333$; Two-way $ANOVA_T$ $F_{1,132} = 21.578$; Fig. 2A–F). Thus, A_N values decreased considerably by NaCl excess in the grown medium and in plants grown at both extreme temperature ranges respect to the control, this temperature effect being more marked at low-temperature range and with salinity excess at both temperature range treatments. Hence, compared to the control (i.e medium temperature range and optimum salinity concentration) A_N decreased 31% and 71% in plants grown at 171 mM NaCl and temperature range of 40/28 °C and 13/5 °C, respectively; while at 1050 mM NaCl these reductions were

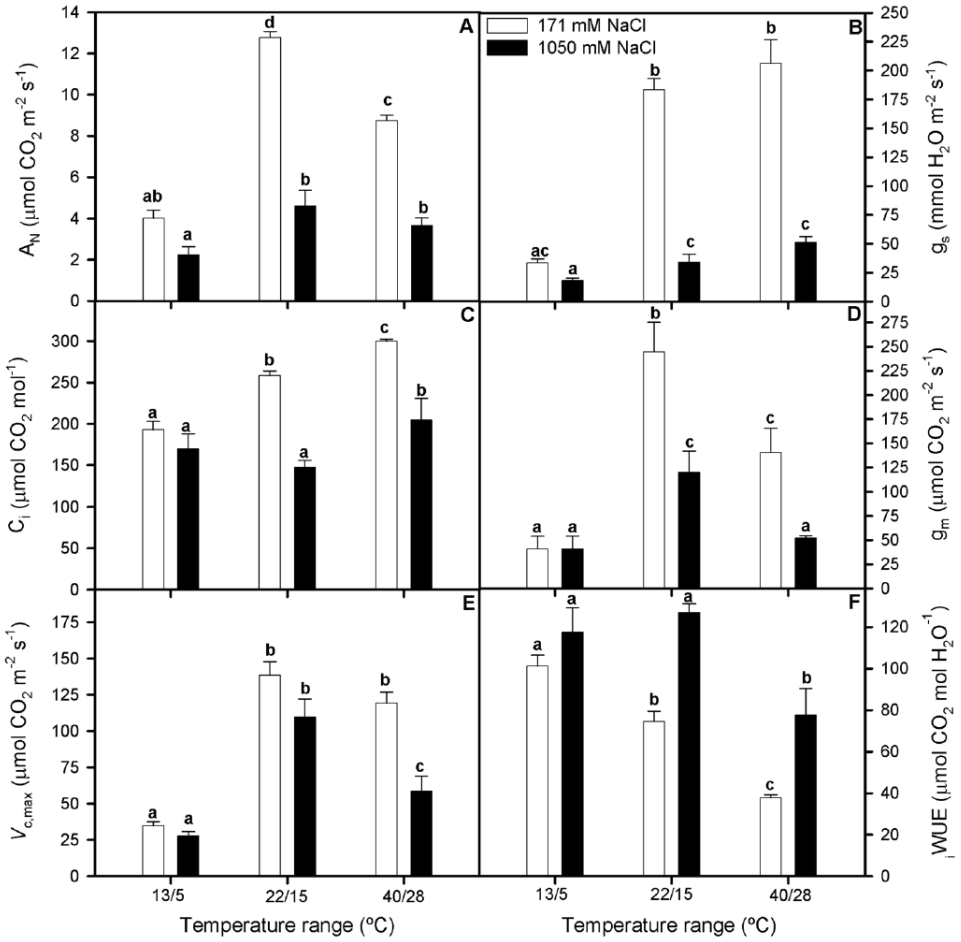

Figure 2. Net photosynthetic rate, A_N (**A**), stomatal conductance, g_s (**B**), intercellular CO_2 concentration, C_i (**C**), mesophyll conductance, g_m (**D**), maximum carboxylation rate, $V_{c,max}$ (**E**) and intrinsic water use efficiency ($_i$WUE) (**F**) in randomly selected, primary branches of *Salicornia ramosissima* in response to treatment with three temperature ranges (13/5 °C, 22/15 °C and 40/28 °C) and two NaCl concentrations (171 and 1050 mM) after 3 days. Values represent mean ± SE, n = 10 for A_N, g_s, C_i and $_i$WUE and n = 4 for g_m and $V_{c,max}$. Different letters indicate means that are significantly different from each other.

of 71% and 82% for those temperature ranges. Very similar trends were recorded for g_s, g_m, $V_{c,max}$ and C_i but high-temperature range treatment did not affect g_s, $V_{c,max}$ and C_i in plant grown at 171 mM NaCl. In addition, $V_{c,max}$ values were not affected by NaCl excess in plants grown at 25/13 °C and by high-temperature range in those grown at 171 mM NaCl compared with their non-high salinity and temperature treated counterparts (Fig. 2E). Contrarily, $_i$WUE values were higher in plant expose to 1050 mM NaCl and decreased with temperature range increment (Fig. 2F).

Regarding the photosynthesis quantitative limitation analysis (Fig. 3A,B), indicated that the observed decreases of A_N after 3 d of treatment, were mainly due to diffusional limitations, although the relative importance of stomatal (SL) and mesophyll conductance limitation (MCL) varied depending of medium salinity concentration and temperature range treatment. Thus, SL accounted for the highest percentage of photosynthetic limitation under sub-optimal salinity concentration (e.i. 1050 mM NaCl) in plants grown at low and medium temperature ranges, but the relative importance of MCL was higher in plants grown at 40/28 °C in both salinity concentrations and in those subjected to 13/5 °C and 171 mM NaCl. In addition, there is to notice that biochemical limitation (BL) augmented in both extreme temperature ranges, this increment being more marked at 13/5 °C, regardless of the medium NaCl concentration.

Fluorescence measurements. Chlorophyll fluorescence parameters were also affected by salinity and temperature ranges treatments after 3 d. F_v/F_m values decreased at both low and high temperatures ranges, this reduction being more marked at low-temperature range but without significant differences between salinity treatments (Two-way $ANOVA_T$, $F_{1,64} = 21.393$; Fig. 4A). Contrarily, ETR_{max} did not remarkably vary between salinity

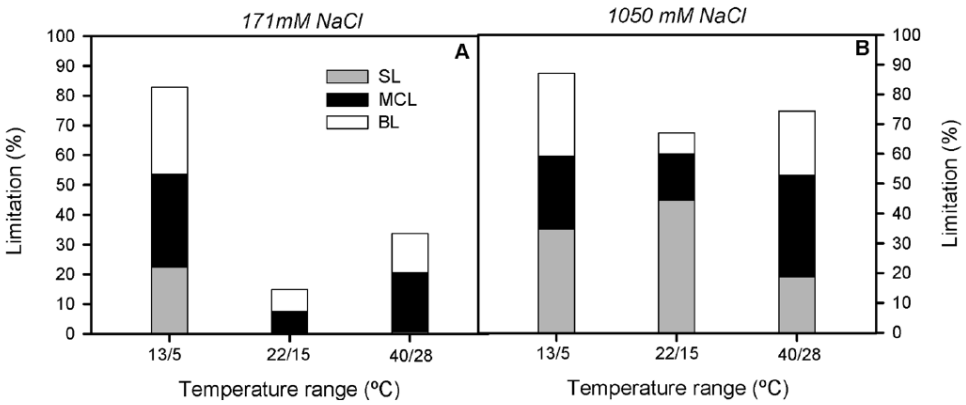

Figure 3. Quantitative limitation of photosynthesis in randomly selected, primary branches of *Salicornia ramosissima* in response to treatment with three temperature ranges (13/5 °C, 22/15 °C and 40/28 °C) and with 171 mM NaCl (**A**) and 1050 mM NaCl (**B**) after 3 days. SL, MCL and BL denote for stomatal, mesophyll and biochemical limitations, respectively. Values represent mean ± SE, n = 4.

and temperature ranges treatments, except in plants grown at 1050 mM NaCl and 13/5 °C, which showed the lowest values (Two-way $ANOVA_{NaClxT}$, F = 5.554; Fig. 4B). As a consequence, ETR_{max}/A_N values were higher in plants grown at 1050 mM NaCl compared with their non-NaCl supplied counterparts in all temperature ranges treatments, and tended to increase in plants grown at 13/5 °C in both salinity concentration treatments (Fig. 4C).

Focusing on the energetic fluxes on a leaf cross-section basis (phenomological fluxes), since reaction centres per cross section (RC/CS) varied between salinity and temperature range treatments (data not presented), our results showed that absorbed energy flux per leaf-cross section (ABS/CS) was significantly higher at high-temperature range, with no significant differences between NaCl treatments (Two-way $ANOVA_T$, $F_{1,54} = 37.892$; Fig. 5A). Moreover, trapped energy flux (TR/CS) values increased at high-temperature range and 171 mM NaCl, together with dissipated energy flux per cross section (DI/CS) values in plants grown at both salinity treatments. This effect, however, was more marked at 1050 mM NaCl (Two-way $ANOVA_{NaClxT}$, $F_{2,36} = 14.654$; Fig. 5B,D). Finally, electron transport energy per leaf cross section (ET/CS) did not vary with salinity and temperature treatments except in plants grown at 1050 mM NaCl and 40/28 °C, which showed the lowest values (Two-way $ANOVA_{NaClxT}$, $F_{2,54} = 3.243$; Fig. 5C).

Photosynthetic pigment concentration. Chlorophyll *a* and *b* concentrations did not vary between salinity and temperature ranges treatments, except in plants grown at 1050 mM and 40/28 °C, for which the lowest values were recorded, compared with the other treatments (Two-way $ANOVA_{NaClxT}$, $F_{2,24} = 24.573$, $F_{2,24} = 16.104$; Table 1). Very similar trends were recorded in pheophytine *a*, β-carotene, neoxanthin and zeaxanthin concentrations; while lutein concentration did not vary between experimental treatments and violaxanthin concentration was significantly lower in plants grown at 13/5 °C independently of salinity treatment (Table 1). Finally, the greatest DES values were recorded in plants grown at high-temperature range and 1050 mM (Table 1).

Anti-oxidant enzymatic activity measurements. CAT activity tended to increase in plants grown at high-temperature range but without significant differences between experimental treatments (Fig. 6A). While APx activity was overall higher in plants exposed to additional NaCl supplementation for all temperature range treatments, except at 40/28 °C, where this activity also increased in plants grown at 171 mM NaCl (Two-way $ANOVA_{NaClxT}$, $F_{2,14} = 12.675$; Fig. 6B). Finally, GPx enzyme activity was invariably high for all salinity and temperature treatments compared to the optimum grown conditions (i.e. medium temperature range and optimum salinity concentration; Fig. 6C).

Discussion

Increasing frequency and magnitude of short extreme thermal climatic events resulting from anthropogenic activities[1] will induce loss of carbon assimilation[14], with the consequent deleterious effect on the development and survival of many plant species. However, it has been described that plant species could present differential thermotolerance or sensitivity to cold or heat induced stress, these responses being species specific and dependent on the thermal characteristics of the niche they inhabit. The development of particular adaptation mechanisms could also allow them to cope with these extreme thermal conditions[15]. In this study we have explored the ways in which different short extreme thermal events could affect photosynthesis, the basis of plant bio-chemical system, in the halophytic species *S. ramosissima*. In addition, we have assessed if and how this impact could be modulated by the co-ocurrence of other stressful factors, such as the characteristic salt excess present in the original habitat of this species.

Our study showed that extreme temperature events had a negative impact on *S. ramosissima* photosynthetic performance after 3 days of exposition, the impairment degree temperature range treatment-dependent and modulated by the NaCl concentration in the growth medium only in plants grown at the heat-wave treatment.

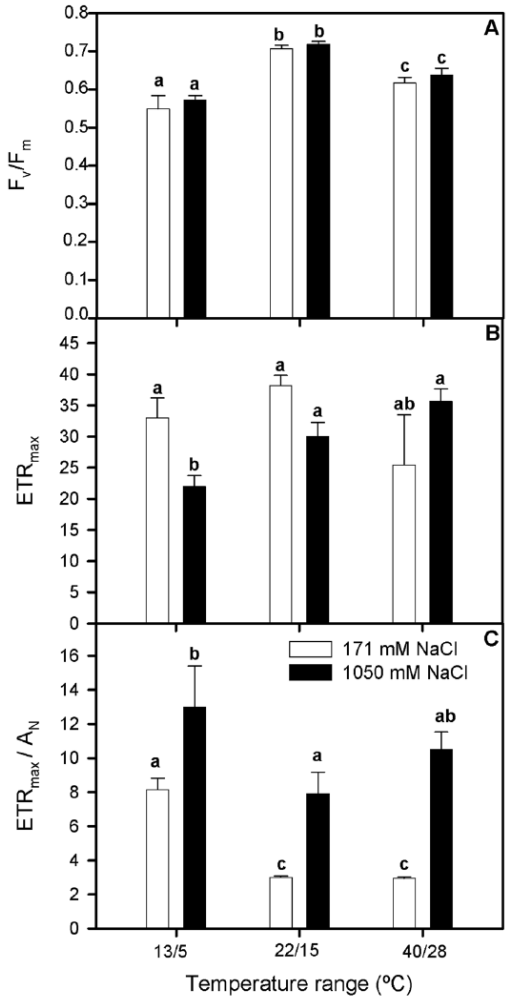

Figure 4. Maximum quantum efficiency of PSII photochemistry, F_v/F_m (**A**), maximum ETR after which photo-inhibition can be observed, ETR_{max} (**B**) and ETR_{max}/A_N (**C**) in randomly selected, primary branches of *Salicornia ramosissima* in response to treatment with three temperature ranges (13–5 °C, 22–15 °C and 40–28 °C) and two NaCl concentrations (171 and 1050 mM) after 3 days. Values represent mean ± SE, n = 7. Different letters indicate means that are significantly different from each other.

Thus, cold wave limited to a greater extent CO_2 assimilation capacity of *S. ramosissima* regardless of medium saline concentration compared with heat-wave treatment even in presence of NaCl excess. Moreover, the results showed that salinity excess exacerbated the negative impact of heat wave on the photosynthetic performance of *S. ramosissima*. However, this differential temperature and salinity deleterious effect were not reflected in *S. ramosissima* water imbalance, as indicated by the invariable RWC values due to changes in Ψ_0 and $_i$WUE in response to salinity and temperature excess.

One of the main reasons for this better photosynthetic efficiency of *S. ramosissima* under heat stress with both optimal and sub-optimal salinity was related to the greater integrity and functioning of some steps of its photosynthetic pathway, namely stomatal and mesophyll diffusion behavior, Rusbisco activity and light-harvesting antenna efficiency to temperature excess. Hence, although photosynthetic injury as a result of both tested extreme temperature ranges was mainly due to CO_2 diffusion limitation, the degree and the relative importance of the stomatal and mesophyll component differed in each specific temperature and salinity combination treatment, as our photosynthetic limitation analysis also indicated. Thus, cold wave imposed a sharply decrease in both g_s and g_m regardless of salinity treatment. This similar diffusion limitation when cold and salinity stress act individually or in combination suggests that the primary effects of low temperature and salinity excess are similar and not synergistic. Accordingly, similar g_s and g_m decreases have been observed in many sensitive species to low temperature and saline excess as a single factor, this response being linked with an ameliorated water stress induced by these stresses[16,17]. Contrarily, heat-wave treatment only increased stomatal limitation to CO_2 diffusion under hypersaline conditions, diffusional limitation to CO_2 appearing as a major result of g_m reduction

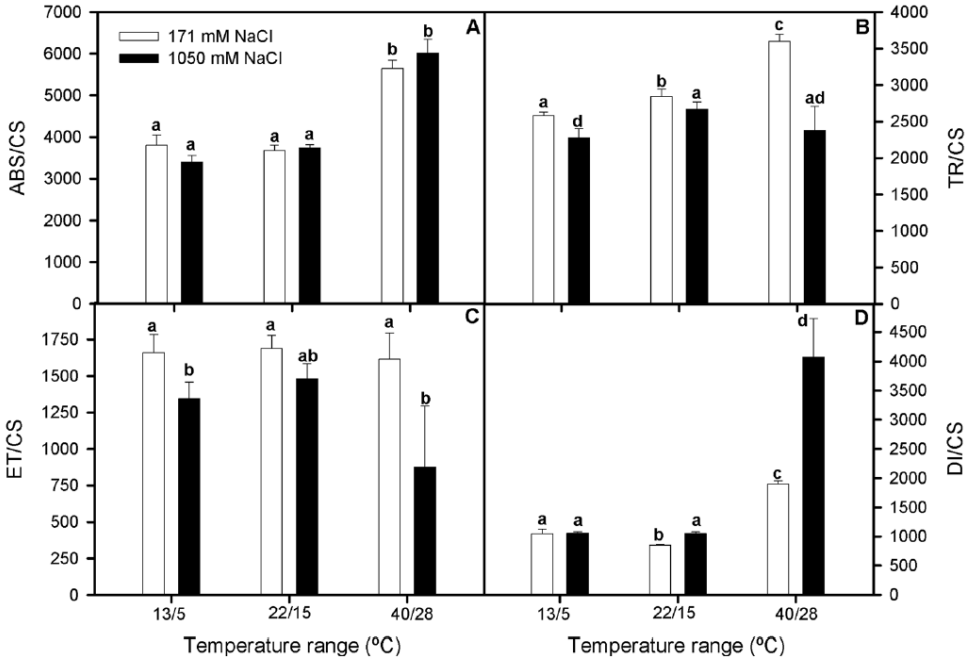

Figure 5. Absorbed energy flux, ABS/CS (**A**), trapped energy flux, TR/CS (**B**), transport energy flux ET/CS (**C**) and dissipated energy fluxes, DI/CS (**D**) per cross section in randomly selected, primary branches of *Salicornia ramosissima* in response to treatment with three temperature ranges (13/5 °C, 22/15 °C and 40/28 °C) and two NaCl concentrations (171 and 1050 mM) after 3 days. Values represent mean ± SE, n = 7. Different letters indicate means that are significantly different from each other.

under optimal saline. The absence of heat-wave effect on g_s could be associated with regulatory mechanisms to enhance leaf cooling through transpiration[18]. Regarding the effect of salinity excess, Redondo-Gómez *et al.*[19] also recorded a marked reduction in g_s of *Sarcocornia fruticosa* grown at 1030 mM NaCl. The observed trends in g_s and g_m resulted in an increase in C_i in plants grown at optimum salinity, where CO_2 was being transported to the intercellular space. However, it was not transferred to chloroplast due to a reduction in g_m with the consequent accumulation. Therefore, our results revealed a lack of relationship between g_s and g_m in *S. ramosissima* in response to heat wave and medium salinity concentration. Many studies suggest that g_s and g_m are co-regulated, since both variables respond in a similar way and magnitude to several environmental factors[20]. Nonetheless, like in our experiment, some authors have identified differential responses in both parameters under severe stress situations[21,22]. Moreover, although there is not a general consensus, it seems that the existence or not of a possible relationship between both parameters would be highly influenced by specific environmental variables as well as by the co-existence with other environmental factors[23]. This response would allow *S. ramosissima* to have a lower diffusional limitation when coping with heat waves. Furthermore, extreme temperature events could head to biochemical limitations of photosynthetic process due to inhibition or modifying carboxylase activity of Rubisco[24–26]. Hence, there are records of a reduction in Rubisco carboxylation rate at all temperatures below 25 °C and in particular at 5 °C, mainly on account of impairment in the activation state[24]. A very similar injury effect on Rubisco kinetics has also been reflected in plants when temperature exceeds the optimum values for the photosynthesis process[14,26]. Our results indicated that photosynthesis biochemical limitation in *S. ramosissima* augmented in both extreme temperature ranges but in greater proportion in cold-temperature range treatment at both salinity concentrations. Thus, it is noteworthy that $V_{c,max}$ values did not vary respect to the control (i.e medium temperature range and optimum salinity concentration) in plants exposed to 1050 mM NaCl and 22/15 °C, as well as in those subjected to heat wave and optimum salinity conditions. This result suggested that the high tolerance of *S. ramosissima* to heat waves even under salinity excess would be in part explained by the maintenance of a high Rubisco activation rate. Contrarily, Perdomo *et al.*[26]. found an increment of biochemical limitation at high temperature mainly attributed to a decrease in Rubisco activation state. However, Cen and Sage[27] indicated that, although temperature increment led to deactivating Rubisco activase, this deactivation was not sufficient to limit photosynthesis. In fact, it has been described that several iso-forms of Rubisco activase could play a role in the responses of plant tolerant to high temperature stress[14]. Accordingly, it is possible that the presence of Rubisco activase iso-forms that are highly tolerant to heat and salinity induced stress in *S. ramosissima*. This area is therefore worthy of further research.

On the other hand, the higher photosynthetic thermotolerance of *S. ramosissima* to elevated temperature range could be ascribed to the upregulation of the energy sink capacity of its photochemical apparatus, as well as to the impact on the photosynthetic pigments profile. In this regard, one of the best recognized effects of high

T (°C)	[NaCl]	Chl *a*	Chl *b*	Phe *a*	β-carotene	Lutein	Neoxanthin	Violaxanthin	Zeaxanthin	DES
13/5	171	111.1 ± 6.5^{a}	82.7 ± 6.0^{a}	156.6 ± 20.9^{ab}	8.6 ± 1.7^{ab}	17.1 ± 1.4	13.5 ± 1.7^{ab}	0.7 ± 0.6^{b}	9.1 ± 1.8^{ab}	0.04 ± 0.04^{c}
	1050	119.5 ± 9.7^{a}	84.0 ± 5.0^{a}	124.2 ± 8.6^{ab}	7.1 ± 0.6^{ab}	15.1 ± 1.5	9.6 ± 1.5^{b}	0.8 ± 0.5^{b}	7.5 ± 0.6^{ab}	0.21 ± 0.07^{a}
22/15	171	168.1 ± 31.7^{a}	92.7 ± 9.9^{a}	176.7 ± 20.9^{a}	11.6 ± 1.8^{a}	16.2 ± 4.0	13.9 ± 1.2^{ab}	3.4 ± 2.2^{a}	12.3 ± 1.9^{ab}	0.13 ± 0.09^{a}
	1050	125.4 ± 10.1^{a}	88.4 ± 9.3^{a}	156.9 ± 19.4^{ab}	10.9 ± 1.7^{a}	15.3 ± 1.5	15.1 ± 1.4^{ab}	2.1 ± 1.1^{a}	11.6 ± 1.8^{ab}	0.16 ± 0.05^{a}
40/28	171	166.9 ± 43.8^{a}	104.2 ± 19.7^{a}	137.1 ± 24.7^{b}	11.4 ± 2.9^{a}	21.7 ± 5.2	18.2 ± 7.0^{a}	2.6 ± 0.7^{a}	12.1 ± 3.1^{a}	0.19 ± 0.07^{a}
	1050	61.1 ± 4.4^{c}	51.1 ± 5.3^{b}	72.4 ± 11.5^{c}	5.5 ± 0.7^{b}	14.9 ± 2.4	8.5 ± 1.8^{b}	2.7 ± 0.9^{a}	5.9 ± 0.7^{b}	0.39 ± 0.00^{b}

Table 1. Photosynthetic pigments concentrations (μg /g) and deposidation state in randomly selected branches of *Salicornia ramosissima* in response to treatment with three ranges of temperatures and two NaCl concentrations (171 and 1050 mM) after 3 days. Values represent mean ± SE, n = 5. Different letters indicate means that are significantly different from each other.

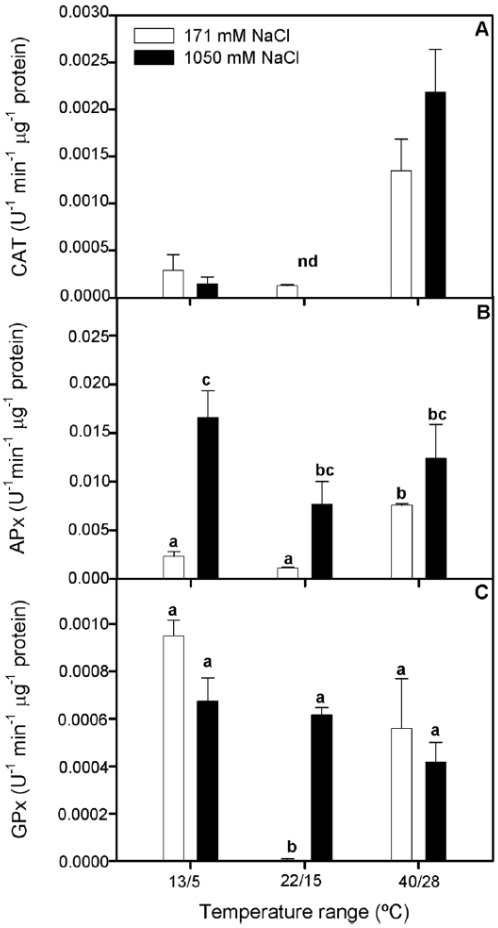

Figure 6. Catalase, CAT (**A**), ascorbate peroxidase, APx (**B**) and guaiacol peroxidase, GPx (**C**) activity in randomly selected, primary branches of *Salicornia ramosissima* in response to treatment with three temperature ranges (13/5 °C, 22/15 °C and 40/28 °C) and two NaCl concentrations (171 and 1050 mM) after 3 days. Values represent mean ± SE, n = 3. Different letters indicate means that are significantly different from each other.

temperature is the destruction of PSII components; however, PSII damage in well light-adapted systems, as could be the case of *S. ramosissima*, is supposed to occur only at very high temperatures (i.e. >45 °C[28]). Accordingly, our results indicated that, although photochemical efficiency (F_v/F_m) of *S. ramosissima* was significantly lower at both extreme temperature ranges, this effect was more drastic at the cold-temperature treatment. This trend was also confirmed by the lower ETR_{max} values recorded, especially in plants grown at 13/5 °C and 1050 mM NaCl. In addition, OJIP analysis provided a downscaling approach to this highlighted differences in the thermotolerance behavior of *S. ramosissima*. Thus, when energy fluxes were assessed, we found that plants treated under

high-temperature range showed greater values for ABS/CS and TR/CS compared with the other treatments. This fact was related to higher values obtained for these plants in the connectivity of their PSII units and the lower values of closure rate for its RC, respectively[29]. This could indicate that more energy was being absorbed and transformed in their photosystem. In addition, an increment of ABS/CS means a greater number of active reaction centers functioning as a heat radiator, protecting the plant against high temperature and light intensities[29]. This was also associated to an increase in DI/CS, especially at 1050 mM NaCl, which could explain the lower values for ET/CS obtained and indicates the activation of some defense mechanism such as the dissipation of energy as heat or photorespiration[30]. High salinity increased DI/CS, as Perez-Romero *et al.*[8] found, and this was shown at high and control temperature range. Nonetheless, plants at low temperature did not show a significant increment in this parameter. The DI/CS values include non-photochemical quenching (NPQ), which is correlated with the xantophyll cycle that is activated under an excess of light[31]. The results obtained for the de-epoxidation of the zeaxanthin, showed as DES, suggested that there was an activation of this cycle at high-temperature range and hypersalinity. This data could be an evidence of a response to reactive oxygen species (ROS) stress for plants under these treatments of high temperature and salinity. Hence, this mechanism could help plants subjected to heat waves to reduce its physiological stress as ROS accumulation by dissipation of energy excess. Consequently, plants subjected to low temperature range and 171 mM NaCl showed the lowest values of this parameter indicating that this mechanism could be triggered by heat and not by cold, although previous studies suggested that neither heat nor cold waves induced this cycle[32,33]. A good approximation to knowing the potential risk of stress due to ROS is the ratio ETR_{max}/A_N, which could indicate the number of electrons that are not being fixed, so that they are free to possibly create some ROS[34,35]. This parameter indicated that high salinity significantly increases the risk of ROS stress in *S. ramosissima*. In addition, plants subjected to cold waves presented the highest values at both salinities, this fact corroborating the idea that cold waves have a greater injury effect on *S. ramosissima* physiological performance. Since cold and heat stress events can lead to an increment in ROS production[36,37] there would be a need for antioxidative protection. One of the well-known mechanisms to reduce the accumulation of ROS is the modulation of the activity of antioxidative stress enzymes[9]. CAT and peroxidases as GPx and APx are enzymes that reduce the H_2O_2 produced[10]. Our experiment showed that antioxidant enzyme activity was modulated to a certain extent by temperature range characteristics and salinity excess, as indicated by the overall higher activation of GPx activity at both temperature range and salinity treatments compared with the control treatment. In addition, APx was also more activated for all temperature range treatments at 1050 mM NaCl than at 171 mM NaCl, as previously described for this species[38]. It is important to highlight that plants at both salinities subjected to heat wave showed higher activities for CAT and APx enzymes emphasizing the idea of higher capacity for antioxidant enzyme activity modulation of *S. ramosissima* in response to heat than to cold stress.

Thus, we can conclude that *S. ramosissima* photosynthetic metabolism would maintain its functionality better under heat waves than under cold waves, even in presence of hypersaline conditions during its vegetative natural cycle (i.e. from March to September[39]). This is mainly due to an improvement in its energy sink capacity while keeping its CO_2 assimilation capacity relatively constant by ameliorating the diffusion and biochemical photosynthesis limitations under those extreme conditions. This pattern of response fits well with its thermal niche characteristics in the southwest of Iberian Peninsula, where there is a prevalence of daily mean high temperatures and a higher occurrence of heat waves, even at the beginning of its growth period. With cold waves tending to decrease in the Iberian Peninsula[40], the higher photosynthetic efficiency of *S. ramosissima* against heat waves, even under hypersaline conditions could provide a great adaptation to these common conditions in its natural distribution area. However, the increase in frequency of extreme cold episodes due to climate change would compromise the primary productivity of this important multifunctional cash crop species.

Material and Methods

Plant Material. In September 2014 seeds of *S. ramosissima* were collected from Odiel marshes (37°15′N, 6°58′O; SW Spain) from a well-established population located in a well-drained intertidal lagoon (mean sea level +1.65 m relative to SHZ). Seeds were stripped for each plant and stored in the dark for 4 months at 4 °C until the beginning of the experiment.

In February of 2015 seeds were germinated on 9 cm Petri dishes filled with agar 10% into a germinator (ASL Aparatos Científicos M-92004, Madrid, Spain) with a day-night regime of 16 h of light (photon flux rate, 400–700 nm, 35 μmol m^{-2} s^{-1}) at 25 °C and 8 h of darkness at 12 °C, for 15 days. The seedlings obtained were carefully transferred with thin tweezers from the agar to individual plastic pots (9 cm high × 11 cm diameter) using perlite as substrate and making sure that the perlite was tight enough to conduct the nutrient solution until the roots. These pots were placed in a greenhouse with controlled conditions (temperature between 21–25 °C, 40–60% relative humidity and natural daylight of 250 μmol m^{-2} s^{-1} as minimum and 1000 μmol m^{-2} s^{-1} as maximum light flux). Pots were allocated in shallow trays watering with 20% Hoagland's solution[41] and 171 mM NaCl. Plants were kept under these conditions until the experimental setup.

Experimental treatments. In May of 2015, after 3 months of seedling culture, plants with an initial height of 17 cm were randomly divided in six blocks of 10 plants. They were then subjected to three different maximum and minimum temperature ranges (cold wave: 13/5 °C, control: 25/13 °C and heat wave: 40/28 °C) in combination with two NaCl concentrations (171 and 1050 mM NaCl) in controlled-environment chambers (Aralab/Fitoclima 18.000EH, Lisbon, Portugal) for 3 days after 2 days of salinity adaptation to emulate the effect of cold or heat waves. The salinity concentration of 171 mM NaCl was chosen as the optimum for *S. ramosissima* development, as we have stated previously[7], and the higher one (e.i. 1050 mM NaCl) was added to reproduce temporarily hypersaline conditions in the Gulf of Cadiz marshes, as occurs in saltpans[42]. Low and high temperature range treatments were based on extreme events recorder recently in the southwest of Iberian Peninsula in the seasons when *S. ramosissima* presents its vegetative phase (aemet.es). These extreme salinity and temperature situations

being likely to become more frequent in the future climatic reality[1]. Salinity treatments were established by using 20% Hoagland's solution[41] and NaCl of the appropriate concentration. Climatic chambers were programmed with alternating diurnal regime of 14 h of light and 10 h of darkness, light intensity of 1000 µmol m^{-2} s^{-1} and 40–60% relative humidity. During the experiment salinity concentrations were monitored and maintained at the same level.

Measurements of plant water status, gas exchange, chlorophyll fluorescence, photosynthetic pigments concentrations and anti-oxidant enzymatic activity were taken 3 days after the onset of temperature ranges treatments. All measurements, except for anti-oxidant enzymatic activity due to need for a greater amount of plant material, were made on fully developed internodes of similar size primary branches close to distal ends of principal stem, in order to facilitate the comparison between them and avoid the intra-plant modular variation in response to abiotic stress[43].

Measurement of osmotic potential and water content. At the end of the experiment, the osmotic potential (Ψ_o) of primary branches (n = 10) was determined, using psychrometric technique with a Vapor Pressure Osmometer (5600 Vapro, Wescor, Logan, USA).

In addition, the relative water content (RWC) of primary branches (n = 10) in each treatment was calculated as follow:

$$RWC = ((FW-DW)/(FW-TW))100$$

Where FW = fresh weight of the branches, DW = dry weight after oven-drying at 80 °C for 48 h and TW = turgid weight after being in water at 4 °C for 24 h.

Measurement of gas exchange and photosynthetic limitation analysis. Gas exchange measurements were taken on randomly selected primary branches using an infrared gas analyser in an open system (LI-6400XT, LI-COR Inc., Neb., USA) equipped with a light leaf chamber (Li-6400-02B, Li-Cor Inc.) after 3 days of treatment (n = 10). Net photosynthetic rate (A_N), stomatal conductance (g_s), intercellular CO_2 concentration (C_i) and intrinsic water use efficiency ($_iWUE$) were recorded under the following leaf chamber conditions: a photosynthetic photon flux density (PPFD) 1000 µmol photon m^{-2} s^{-1} (with 15% blue light to maximize stomatal aperture), vapour pressure deficit of 2.0–3.0 kPa and air, 50 ± 2% relative humidity, CO_2 concentration surrounding leaf (C_a) 400 and temperature of 13 ± 1 °C, 25 ± 1 °C and 40 ± 1 °C for plants grown at low, medium and high temperature ranges, respectively. Moreover, mesophyll conductance (g_m) and maximum carboxylation rate allowed by ribulose-1,5-biphospate (RuBP) carboxylase/oxygenase ($V_{c,max}$) were obtained by the curve-fitting method[44] using the software package developed by Sharkey *et al.*[45]. For this method, four A_N/C_i curves on randomly selected primary branches were performed. The curves were made under the same environmental conditions previously used for instantaneous gas exchange measurements. Once the steady-state was reached the curves were performed by decreasing C_a stepwise until 50 µmol mol^{-1}. Therefore, to complete the curve the chamber conditions were restored to the initial and C_a increased stepwise until 2000 µmol mol^{-1} [20,46]. For the curves, 12 different C_a values were used. At each step, gas exchange was allowed to equilibrate for less than 180 s to reduce changes in Rubisco activity[47]. On the same branches, dark respiration rate (R_d, µmol CO_2 m^{-2} s^{-1}) measurements were performed after curves assessment as CO_2 efflux. Branches chamber was darkened for 30 min to avoid transient post-illumination bursts of CO_2 releasing[48]. Leakage of CO_2 in and out of the leaf chamber was determined with photosynthetically inactive primary branches and corrected in all curves[48]. For all the measurements photosynthetic area was assimilated to the half the area of the cylindrical branches, since only the upper half received the unilateral illumination in the leaf chamber[49].

Finally, the effect of the different salinity and maximum and minimum temperature ranges treatments on the limitations to A_N was tested, through to quantification of the absolute limitations of the observed decrease of A_N at the end of experiment period (3 d) by stomatal conductance (SL), mesophyll conductance (MCL) and biochemistry (BL) following the approach of Grassi and Magnani[50].

Measurement of chlorophyll fluorescence. Chlorophyll fluorescence measurements were performed using a FluorPen FP100 (Photo System Instruments, Czech Republic) in the same branches of gas exchange analysis at the end of the experiment (n = 7). Branches were dark-adapted for 30 min with special pliers designed for that purpose before the measurement. As Schreiber *et al.*[51] described, light energy yields of Photosystem II (PSII) reaction centres were determined with a saturation pulse method. To estimate the maximum fluorescence signal across time, a saturating light pulse of 0.8 s with an intensity of 8000 µmol m^{-2} s^{-1} was used. A comparison of the minimum fluorescence (F'_0), the maximum fluorescence (F'_m) and the operational photochemical efficiency values were made with the values of dark adapted branches. Quantum yield of PS II (QY) were calculated as F_v/F_m.

Finally, the maximum electron transport rate (ETR_{max}) and the chlorophyll *a* fast kinetics, or JIP-test (or Kautsky curves), which depicts the rate of reduction kinetics of various components of PSII, were also measured in dark-adapted leaves (n = 5 for each treatment) according to Duarte *et al.*[33], using the pre-programmed RLC and OJIP protocols of the FluorPen. All derived parameters for both RLC and OJIP were calculated according to Marshall *et al.*[52] and Strasseret *et al.*[29] respectively. Furthermore, ETR_{max}/A_N ratio was calculated with the values obtained from fluorescence rapid light curves and gas exchange measurements.

Measurement of photosynthetic pigment concentration. At the end of the experimental period, branches samples were randomly collected (n = 5) and flash-frozen in liquid N_2 and freeze-dried for 48 h in the dark to avoid photodegratation processes for the concentration analysis of photosynthetic pigments[31]. Samples were subsequently ground in pure acetone and pigments extracted at −20 °C during 24 h in the dark to prevent its degradation, centrifuged at 4000 rpm during 15 min at 4 °C and the resulting supernatant scanned in a dual beam

spectrophotometer (Hitachi Ltd., Japan) from 350 to 750 nm at 1 nm step. The resulting absorbance spectrum was used for pigment quantification by introducing the absorbance spectrum in a Gauss-Peak Spectra (GPS) fitting library, using SigmaPlot Software[53]. De-epoxidation state index (DES) was calculated as:

$$([\text{Violaxanthin}] + [\text{Anteroxanthin}])/([\text{Violaxanthin}] + [\text{Anteroxanthin}] + [\text{Zeaxanthin}])$$

Measurement of anti-oxidant enzymatic activity. At the end of experiment, three replicates of 500 mg of fresh branches samples per treatment were ground in 8 ml of 50 mM sodium phosphate buffer (pH 7.6) with 0.1 mM Na-EDTA and were centrifuged at 10000 rpm for 20 min at 4 °C to obtaine the soluble proteins to determine anti-oxidant enzyme activities. Catalase (CAT) activity, was measured according to Teranishi *et al.*[54], by monitoring the consumption of H_2O_2 and consequent decrease in absorbance at 240 nm ($\varepsilon = 39.4\,mM^{-1}\,cm^{-1}$). The reaction mixture contained 50 mM of sodium phosphate buffer (pH 7.6), 0.1 mM of Na-EDTA, and 100 mM of H_2O_2. Ascorbate peroxidase (APx) activity was measured by monitoring the decrease in the absorbance at 290 nm. The reaction mixture contained 50 mM of sodium phosphate buffer (pH 7.0), 12 mM of H_2O_2, 0.25 mM L-ascorbate[55]. Molar coefficient of $2.8\,mM^{-1}\,cm^{-1}$ was used to calculate the amount of ascorbate oxidized. Guaiacol peroxidase (GPx) was calculated as Bergmeyer[56] (1974) indicated. With a reaction mixture made of 50 mM of sodium phosphate buffer (pH 7.0), 2 mM of H_2O_2 and 20 mM of guaiacol. For all these enzymes activities the reaction was initiated with the addition of 100 µl of enzyme extract. To calculate the enzyme activity per µg of protein, total protein content in the extracts was obtained following Bradford[57] (1976).

Statistical analysis. All the statistic tests were performed by a statistical software package R. Two-way analysis of variance were used to analyze the interactive effect of each temperature ranges and NaCl concentrations (as categorical factors) treatments on the main physiological parameters (as dependent variables) of *S. ramosissima*. Multiple comparisons were analyzed by a Tukey (post hoc) test. The significance level considered to assume means differences was of $P < 0.05$. Before statistical analysis, Kolmogorov-Smirnov and Levene tests were used to verify the assumptions of normality and homogeneity of variances, respectively.

References

1. IPCC. Climate Change 2014: Synthesis Report. Contribution of Working Groups I, II and III to the Fifth Assessment Report of the Intergovernmental Panel on Climate Change [Core Writing Team, R.K. Pachauri and L.A. Meyer (eds)]. IPCC, Geneva, Switzerland, 151 pp (2014).
2. Allen, D. J. & Ort, D. R. Impacts of chilling temperatures on photosynthesis in warm-climate plants. *Trends Plant Sci* **6**, 36–42 (2001).
3. Orsenigo, S., Mondoni, A., Rossi, G. & Abeli, T. Some like it hot and some like it cold, but not too much: plant responses to climate extremes. *Plant Ecology* **215**(7), 677–688 (2014).
4. Huckle, J. M., Potter, J. A. & Marrs, R. H. Influence of environmental factors on the growth and interactions between salt marsh plants: effects of salinity, sediment and waterlogging. *Journal of Ecology* **88**(3), 492–505 (2000).
5. Lu, D, *et al.* Nutritional Characterization and Changes in Quality of Salicornia Bigelovii Torr. during Storage. *LWT - Food Science and Technology*, https://doi.org/10.1016/j.lwt.2009.09.021 (2010).
6. Isca, V. M., Seca, A. M., Pinto, D. C., Silva, H. & Silva, A. M. Lipophilic Profile of the Edible Halophyte *Salicornia ramosissima*. *Food Chemistry* **165**, 330–36 (2014).
7. Pérez-Romero, J. A., Redondo-Gómez, S. & Mateos-Naranjo, E. Growth and Photosynthetic Limitation Analysis of the Cd-Accumulator *Salicornia ramosissima* under Excessive Cadmium Concentrations and Optimum Salinity Conditions. *Plant Physiology and Biochemistry* **109**, 103–13 (2016).
8. Pérez-Romero, J. A. *et al.* Disentangling the effect of atmospheric CO_2 enrichment on the halophyte *Salicornia ramosissima* J. Woods physiological performance under optimal and suboptimal saline conditions. *Plant Physiology and Biochemistry* **127**, 617–629 (2018a).
9. Geissler, N., Hussin, S. & Koyro, H. W. Elevated atmospheric CO_2 concentration enhances salinity tolerance in Aster tripolium L. *Planta* **231**(3), 583–594 (2009).
10. Pérez-López, U. *et al.* The oxidative stress caused by salinity in two barley cultivars is mitigated by elevated CO_2. *Physiol. Plantarum* **135**(1), 29–42 (2009).
11. Mateos-Naranjo, E. *et al.* Synergic effect of salinity and CO_2 enrichment on growth and photosynthetic responses of the invasive cordgrass *Spartina densiflora*. *Journal of experimental botany* **61**(6), 1643–1654 (2010a).
12. Mateos-Naranjo, E., Redondo-Gómez, S., Andrades-Moreno, L. & Davy, A. J. Growth and photosynthetic responses of the cordgrass *Spartina maritima* to CO_2 enrichment and salinity. *Chemosphere* **81**(6), 725–731 (2010b).
13. Reef, R. *et al.* The effect of atmospheric carbon dioxide concentrations on the performance of the mangrove Avicennia germinans over a range of salinities. *Physiologia plantarum* **154**(3), 358–368 (2015).
14. Sharkey, T. & Bernacchi, C. Photosynthetic responses to high temperature in *Terrestrial Photosyntesis in a Changing Environment* (ed. Flexas, J.), 290–298. (Cambridge University Press 2012).
15. Iba, K. Acclimative response to temperature stress in higher plants: Approaches of gene engineering for temperature tolerance. *Annu Rev Plant Biol.* **53**(1), 225–245, https://doi.org/10.1146/annurev.arplant.53.100201.160729 (2002).
16. Hendrikson, L. *et al*. Cold acclimation of the Arabidopsis*dgd1* mutant results in recovery from photosystem I-limited photosynthesis. *FEBS Letters*, https://doi.org/10.1016/j.febslet.2006.07.081 (2006).
17. Chaves, M. M., Flexas, J., Gulías, J., Loreto, F. & Medrano, H. Photosynthesis under water déficits, flooding and salinity in *Terrestrial Photosynhtesis in a Changing Environment* (ed. Flexas, J., Loreto, F., Medrano, H.), 299–311. (Cambridge University Press 2012).
18. Feller U. Stomatal opening at elevated temperature: an underestimated regulatory mechanism. *General and Applied Plant Physiology*, Special Issue: 19–31 (2006).
19. Redondo-Gómez, S. *et al*. *Physiologia Plantarum* **128**(1), 116–124 (2006).
20. Flexas, J. *et al.* Corrigendum to 'Mesophyll diffusion conductance to CO2: An unappreciated central player in photosynthesis'[Plant Sci. 193–194 (2012) 70–84]. *Plant Science*, (196), 31 (2012).
21. Flexas, J. *et al.* Photosynthesis limitations during water stress acclimation and recovery in the drought-adapted vitis hybrid Richter-110 (V. berlandieri×V. Rupestris). *J. Exp. Bot.* **60**(8), 2361–2377 (2009).
22. Galle, A. *et al.* The role of mesophyll conductance during water stress and recovery in tobacco (*Nicotiana sylvestris*): acclimation or limitation? *Journal of Experimental Botany* **60**(8), 2379–2390 (2009).
23. Perez-Martin, A. *et al.* Interactive effects of soil water deficit and air vapour pressure deficit on mesophyll conductance to CO_2 in *Vitis vinifera* and *Olea europaea*. *Journal of Experimental Botany* **60**(8), 2391–2405 (2009).

24. Hendrickson, L., Chow, W. S. & Furbank, R. T. Low temperature effects on grapevine photosynthesis: the role of inorganic phosphate. *Functional Plant Biology* **31**(8), 789–801 (2004).
25. Yamori, W., Noguchi, K., Kashino, Y. & Terashima, I. The role of electron transport in determining the temperature dependence of the photosynthetic rate in spinach leaves grown at contrasting temperatures. *Plant and Cell Physiology* **49**(4), 583–591 (2008).
26. Perdomo, J. A., Capó-Bauçà, S., Carmo-Silva, E. & Galmés, J. Rubisco and rubisco activase play an important role in the biochemical limitations of photosynthesis in rice, wheat, and maize under high temperature and water deficit. *Frontiers in plant science* **8**, 490 (2017).
27. Cen, Y. P. & Sage, R. F. The regulation of Rubisco activity in response to variation in temperature and atmospheric CO_2 partial pressure in sweet potato. *Plant physiology* **139**(2), 979–990 (2005).
28. Yamane, Y., Kashino, Y., Koike, H. & Satoh, K. Effects of high temperatures on the photosynthetic systems in spinach: oxygen-evolving activities, fluorescence characteristics and the denaturation process. *Photosynthesis Research* **57**(1), 51–59 (1998).
29. Strasser, R. J., Tsimilli-Michael, M. & Srivastava, A. Analysis of the chlorophyll a fluorescence transient. In: Christos Papageorgiou, George, Govindjee (Eds), Chlorophyll a Fluorescence: a Signature of Photosynthesis. Springer, Dordrecht, pp. 321–362. Netherlands https://doi.org/10.1007/978-1-4020-3218-9_12 (2004).
30. Duarte, B. *et al.* Disentangling the photochemical salinity tolerance in aster tripolium L.: connecting biophysical traits with changes in fatty acid composition. *Plant Biol.* **19**(2), 239–248 (2017).
31. Duarte, B., Santos, D., Marques, J. C. & Caçador, I. Ecophysiological constraints of two invasive plant species under a saline Gradient: halophytes versus Glycophytes. Estuar. *Coast Shelf Sci*. https://doi.org/10.1016/j.ecss.2015.04.007 (2015).
32. Saidi, Y., Finka, A. & Goloubinoff, P. Heat perception and signalling in plants: a tortuous path to thermotolerance. *New Phytol.* **190**, 556–565 (2010).
33. Duarte, B., Goessling, J. W., Marques, J. C. & Caçador, I. Ecophysiological constraints of aster tripolium under extreme thermal events impacts: merging biophysical, biochemical and Genetic insights. *Plant Physiol. Biochem*. https://doi.org/10.1016/j.plaphy.2015.10.015 (2015).
34. Salazar-Parra, C. Climate change (elevated CO_2, elevated temperature and moderate drought) triggers the antioxidant enzymes' response of Grapevine cv. Tempranillo, avoiding oxidative damage. *Physiol. Plantarum* **144**(2), 99–110 (2012).
35. Hussin, S., Geissler, N., El-Far, M. M. M. & Koyro, H. W. Effects of salinity and shortterm elevated atmospheric CO_2 on the chemical equilibrium between CO_2 fixation and photosynthetic electron transport of *Stevia Rebaudiana bertoni*. *Plant Physiol. Biochem.* **118**, 178–186 (2017).
36. Prasad, T. K. Mechanisms of chilling-induced oxidative stress injury and tolerance in developing maize seedlings: changes in antioxidant system, oxidation of proteins and lipids, and protease activities. *The Plant Journal* **10**(6), 1017–1026 (1996).
37. Wise, R. R. Chilling-enhanced photooxidation: the production, action and study of reactive oxygen species produced during chilling in the light. *Photosynthesis research* **45**(2), 79–97 (1995).
38. Pérez-Romero, J. A. *et al.* Atmospheric CO_2 enrichment effect on the Cu-tolerance of the C4 cordgrass *Spartina densiflora*. *Journal of plant physiology* **220**, 155–166 (2018b).
39. Castroviejo, S. C. In: Castroviejo S, Laínz M, Gonzá lezGL, Montserrat P, Garmendia FM, Paiva J, Villar L(eds) FloraIberica, vol. II. Real Jardín Botánico C.S.I.C., Madrid, pp 476–553 (1990).
40. Labajo, A. L., Egido, M., Martín, Q., Labajo, J. & Labajo, J. L. Definition and temporal evolution of the heat and cold waves over the Spanish Central Plateau from 1961 to 2010. *Atmósfera* **27**(3), 273–286 (2014).
41. Hoagland, D. R. & Arnon, D. I. The water culture method for growing plants without soil. *California Agricultural Experiment Station Circulation* **347**, 32 (1938).
42. Mateos-Naranjo, E. *et al.* Environmental limitations on recruitment from seed in invasive Spartina densiflora on a southern European salt marsh. *Estuarine, Coastal and Shelf Science* **79**(4), 727–732 (2008).
43. Redondo-Gómez, S., Mateos-Naranjo, E., Parra, R. & Figueroa, M. E. Modular response to salinity in the annual halophyte. *Salicornia ramosissima*. *Photosynthetica* **48**(1), 157–160 (2010).
44. Ethier, G. J. & Livingston, N. J. On the need to incorporate sensitivity to CO_2 transfer conductance into the Farquharevon CaemmereBerry leaf photosynthesis model. *Plant Cell Environ.* **27**, 137–153 (2004).
45. Sharkey, T. D., Bernacchi, C. J., Farquhar, G. D. & Singsaas, E. L. Fitting photosynthetic carbon dioxide response curves for C3 leaves. *Plant Cell Environ.* **30**, 1035–1040 (2007).
46. Pons, T. L. *et al.* Estimating mesophyll conductance to CO2, methodology, potential errors, and recommendations. *J. Exp. Bot.* **60**(8), 2217–2234 (2009).
47. Long, S. P. & Bernacchi, C. J. Gas exchange measurements, what can they tell us about the underlying limitations to photosynthesis? Procedures and sources of error. *Journal of experimental botany* **54**(392), 2393–2401 (2003).
48. Flexas, J. *et al.* Diffusional conductances to CO_2 as a target for increasing photosynthesis and photosynthetic water-use efficiency. *Photosynth. Res.* **117**(1–3), 45–59 (2013).
49. Redondo-Gómez, S., Mateos-Naranjo, E., Figueroa, M. E. & Davy, A. J. Salt Stimulation of Growth and Photosynthesis in an Extreme Halophyte. *Arthrocnemum Macrostachyum. Plant Biology* **12**(1), 79–87 (2010).
50. Grassi, G. & Magnani, F. Stomatal, mesophyll conductance and biochemical limitations to photosynthesis as affected by drought and leaf ontogeny in ash and oak trees. *Plant, Cell & Environment* **28**(7), 834–849 (2005).
51. Schreiber, U., Schliwa, W. & Bilger, U. Continuous recording of pho- tochemical and non-photochemical chlorophyll fluorescence quenching with a new type of modulation fluorimeter. *Photosynth. Res.* **10**, 51–62 (1986).
52. Marshall, H. L., Geider, R. J. & Flynn, K. J. A mechanistic model of photoinhibition. *New Phytol.* **145**(2), 347–359 (2000).
53. Küpper, H., Seibert, S. & Parameswaran, A. Fast, sensitive, and inexpensive alternative to analytical pigment HPLC: quantification of chlorophylls and carotenoids in crude extracts by fitting with Gauss peak Spectra. *Anal. Chem.* **79**(20), 7611–7627 (2007).
54. Teranishi, Y., Tanaka, A., Osumi, M. & Fukui, S. Catalase activities of hydrocarbonutilizing Candida yeasts. *Agric. Biol. Chem.* **38**(6), 1213–1220 (1974).
55. Tiryakioglu, M., Eker, S., Ozkutlu, F., Husted, S. & Cakmak, I. Antioxidant defense system and cadmium uptake in barley Genotypes differing in cadmium tolerance. *J. Trace Elem. Med. Biol.* **20**(3), 181–189 (2006).
56. Bergmeyer, H.U. Methods of enzymatic analysis. *Academic Press.* **4** (1974).
57. Bradford, M. M. A rapid and sensitive method for the quantification of micro- gram quantities of protein utilizing the principle of protein–dye binding. *Anal. Biochem.* **72**, 248–254 (1976).

Acknowledgements

This work has been funded by Ministerio de Economía y Competitividad (MINECO Project CGL2016–75550-R cofunded by FEDER). J.A Pérez-Romero thanks Ministerio de Educación, Cultura y Deporte for its financial support (FPU014/03987). We are grateful to Antonio J. Ruiz Rico for revision of the English text of this manuscript and University of Seville Greenhouse General Services (CITIUS) for its collaboration. We also thank the useful comments of two anonymous reviewers who greatly helped to improve the final version of the manuscript.

Author Contributions

S.R.G., E.M.N. and J.A.P.R. conceived and designed research. J.A.P.R., E.M.N. and J.M.B.P. conducted experiments. J.A.P.R. and E.M.N. analyzed data. J.A.P.R. and E.M.N. wrote the manuscript. All authors read and approved the manuscript.

Additional Information

Competing Interests: The authors declare no competing interests.

Publisher's note: Springer Nature remains neutral with regard to jurisdictional claims in published maps and institutional affiliations.

CAPÍTULO 5:

Atmospheric CO_2 enrichment effect on the Cu-tolerance of the C_4 cordgrass Spartina densiflora.

Pérez-Romero et al., 2018, Journal of Plant Physiology

Journal of Plant Physiology 220 (2018) 155–166

Contents lists available at ScienceDirect

Journal of Plant Physiology

journal homepage: www.elsevier.com/locate/jplph

Atmospheric CO_2 enrichment effect on the Cu-tolerance of the C_4 cordgrass *Spartina densiflora*

Jesús Alberto Pérez-Romero[a,1], Yanina Lorena Idaszkin[b,c,1], Bernardo Duarte[d], Alexandra Baeta[e], João Carlos Marques[e], Susana Redondo-Gómez[a], Isabel Caçador[d], Enrique Mateos-Naranjo[a,*]

[a] Departamento de Biología Vegetal y Ecología, Facultad de Biología, Universidad de Sevilla, 1095, 41080, Sevilla, Spain
[b] Instituto Patagónico para el Estudio de los Ecosistemas Continentales (IPEEC-CONICET), Boulevard Brown 2915, U9120ACD Puerto Madryn, Chubut, Argentina
[c] Universidad Nacional de la Patagonia San Juan Bosco, Boulevard Brown 3051, U9120ACD Puerto Madryn, Chubut, Argentina
[d] MARE – Marine and Environmental Sciences Centre, Faculty of Sciences of the University of Lisbon, Campo Grande, 1749-016 Lisbon, Portugal
[e] MARE – Marine and Environmental Sciences Centre, c/o DCV, Faculty of Sciences and Technology, University of Coimbra, Coimbra, Portugal

ARTICLE INFO

Keywords:
CO_2 enrichment
Chlorophyll fluorescence
Cu-stress
Gas exchange
Growth
Spartina densiflora

ABSTRACT

A glasshouse experiment was designed to investigate the effect of the co-occurrence of 400 and 700 ppm CO_2 at 0, 15 and 45 mM Cu on the Cu-tolerance of C_4 cordgrass species *Spartina densiflora*, by measuring growth, gas exchange, efficiency of PSII, pigments profiles, antioxidative enzyme activities and nutritional balance. Our results revealed that the rising atmospheric CO_2 mitigated growth reduction imposed by Cu in plants grown at 45 mM Cu, leading to leaf Cu concentration bellow than 270 mg Kg^{-1} Cu, caused by an evident dilution effect. On the other hand, non-CO_2 enrichment plants showed leaf Cu concentration values up to 737.5 mg Kg^{-1} Cu. Furthermore, improved growth was associated with higher net photosynthetic rate (A_N). The beneficial effect of rising CO_2 on photosynthetic apparatus seems to be associated with a reduction of stomatal limitation imposed by Cu excess, which allowed these plants to maintain greater ¡WUE values. Also, plants grown at 45 mM Cu and 700 ppm CO_2, showed higher ETR values and lower energy dissipation, which could be linked with an induction of Rubisco carboxylation and supported by the recorded amelioration of N imbalance. Furthermore, higher ETR values under CO_2 enrichment could lead to an additional consumption of reducing equivalents. Idea that was reflected in the lower values of ETR_{max}/A_N ratio, malondialdehyde (MDA) and ascorbate peroxidase (APx), guaiacol peroxidase (GPx) and superoxide dismutase (SOD) activities under Cu excess, which could indicate a lower production of ROS species under elevated CO_2 concentration, due to a better use of absorbed energy.

1. Introduction

Climatic change and environmental pollution, due to heavy metal, are two of the major challenges to which humanity will to face for the conservation of ecosystems worldwide (Occhipinti-Ambrogi, 2007). Climate change is likely to alter plants species composition, structure and distribution (Allen et al., 2010). In fact, there is a consensus that atmospheric CO_2 enrichment could stimulate development and growth of hundred plants species (Ghannoum et al., 2000). However, it have been stated that this positive effect is highly dependent on the plant photosynthetic metabolism, being in certain degree less evident in plants species with C_4 photosynthesis metabolic pathway compared with their C_3-conterparts (Ghannoum et al., 2000). Also, this effect it could be influenced by other environmental factors, such as salinity (Lenssen et al., 1993, 1995; Rozema, 1993; Geissler et al., 2009, 2010; Mateos-Naranjo et al., 2010a,b), drought (Calvo et al., 2017), flooding (Setter et al., 1989; Duarte et al., 2014a), etc. Recently there are increasing reports indicating that the co-occurrence of heavy metal contamination in natural soils, due to anthropogenic activity, and rising atmospheric CO_2, due to climate change, may have important consequences for plants development. Thus, few of those studies have indicated that metal stress diminished in non-metal tolerance plants when grown under elevated atmospheric CO_2 concentration (Tian et al., 2014), while other have found that phytoremediation efficiency increased in those which have demonstrated high tolerance and metal uptake capacity (Li et al., 2012). However, despite of these positives evidences, there is not a general consensus, since metal tolerance may vary depending on specific plants species and metals.

Up-to-date, most studies regarding the effect of atmospheric CO_2 fertilization on plant tolerance and biomass production have been

* Corresponding author at: Dpto. Biología Vegetal y Ecología, Facultad de Biología, Universidad de Sevilla, Av Reina Mercedes s/n, 41012 Sevilla, Spain.
E-mail address: emana@us.es (E. Mateos-Naranjo).
[1] Both authors contributed equal to this work.

https://doi.org/10.1016/j.jplph.2017.11.005
Received 20 June 2017; Received in revised form 13 November 2017; Accepted 15 November 2017
Available online 23 November 2017

reported in response to Cd, Cd/Zn and Cd/Pb pollution (Guo et al., 2011, 2015; Jia et al., 2011, 2016; Li et al., 2010, 2012; Song et al., 2013, 2015), being certainly scarce in response to an excess in essential elements for plant, such as Cu. In fact, CO_2 enrichment effect along with Cu pollution has been only reported in some crops species, such as *Brassica juncea*, *Helianthus annus* and *Brassica napus* (Tang et al., 2003; Tian et al., 2014), five forage species (Tian et al., 2014) and few ferns (Zheng et al., 2008). In addition, there is a lack of knowledge about the physiological and biochemical mechanisms involved in these responses, especially in plants with C_4 metabolism photosynthetic pathway and in those which have evolved natural ability to cope with extreme metal polluted environments. Therefore, this experiment was arranged and developed to fill these gaps of knowledge.

The C_4 halophytic cordgrass, *Spartina densiflora* Brongn is a suitable model plant to study in detail the effect of atmospheric CO_2 enrichment on C_4 metal tolerant plant performance in the presence of high Cu amounts in the grown medium, due to its ability to tolerate metal contamination based in several physiological mechanisms which allows it to tolerate wide range of environmental factors (Mateos-Naranjo et al., 2007, 2011), including heavy metal concentrations (Mateos-Naranjo et al., 2008a). Therefore, this study aimed to: (1) assess the growth *S. densiflora* plants in experimental treatments ranging from 0 to 45 Mm Cu at ambient and elevated CO_2 concentrations (400 and 700 ppm CO_2, respectively); (2) determine the extent to which responses could be linked with the photosynthetic apparatus responses, in terms of CO_2 fixation, PSII efficiency, photosynthetic pigments and electron transport energy fluxes; (3) with water balances and nutrient and Cu accumulation patterns; and (4) its relationship with the antioxidant defence abilities consequent of the jointly effect of rising CO_2 and Cu.

2. Material and methods

2.1. Plant material

Seeds of *S. densiflora* were collected during January 2015 at Odiel estuary (37°15′N, 6°58′W; Huelva SW Spain) from 20 different patches randomly chosen, located in a well-drained gently sloping intertidal lagoon (mean sea level +1.70 m relative to SHZ). In the laboratory seeds were dried in a desiccator for 5 days to remove the humidity and stored in the dark for 4 months at 4 °C. In May 2015, seeds placed agar-filled petri dishes and germinated inside a germinator (ASL Aparatos Científicos M-92004, Madrid, Spain), under a photoperiod of 16 h of light (photon flux rate, 400–700 nm, 35 μmol m^{-2} s^{-1}) at 25 °C and 8 h of darkness at 18 °C, for 15 days. The resulting seedlings were then transferred to individual pots filled with pearlite and placed in a glasshouse (during summer 2015) for plant development and biomass increase (minimum-maximum temperatures of 21–25 °C, relative humidity 40–60% and natural daylight of 250 as minimum and 1000 μmol m^{-2} s^{-1} as maximum light flux). During this period pots were irrigated with 20% Hoagland's solution.

2.2. Experimental design description

In October 2015, after four months of seedlings culture, plants were randomly divided in six block and subjected to three Cu concentrations (0, 15 and 45 mM) in shallow trays and in combination with two atmospheric CO_2 concentration (400 ppm and 700 ppm) in controlled-environment chambers (Aralab/Fitoclima 18.000EH, Lisbon, Portugal) for one month (n = 10 pots per treatment). Chambers were programmed with alternating diurnal regime of 16 h of light (maximum photon flux rate, 300 μmol m^{-2} s^{-1}) at 25 ± 0.5 °C and 8 h of darkness at 18 ± 0.5 °C and relative humidity 50 ± 5%. Atmospheric CO_2 concentrations in chambers were continuously recorded by CO_2 sensors (Aralab, Lisbon, Portugal) and maintained by supplying pure CO_2 from a compressed gas cylinder (Air liquide, B50 35 K).

At the beginning of the experiment, 2 L of each Cu treatments, obtained combining 20% Hoagland's solution with adequate amount of $CuSO_4{\cdot}7H_2O$, were placed in each of the trays down to a depth of 1 cm. During the experiment, the levels were controlled to limit the variation of Cu concentration due to water evaporation. In addition, complete solution (including $CuSO_4{\cdot}7H_2O$) was changed weekly. The control treatment, 0 mM Cu, had exactly 0.0005 mM of Cu, derived from Hoagland's solution composition. These Cu concentrations were the same used in our previous experiments with *S. densiflora* (Mateos-Naranjo et al., 2008a, 2015), being evident differences in Cu uptake capacity and symptoms of stress in *S. densiflora* respect to the control treatments.

2.3. Growth analysis

At the end of the experiment (n = 10) plants were collected and divided in shoots and roots and dried at 60 °C for 48 h until constant weight. Leaf elongation rate (LER) was measured in randomly selected young leaves (n = 10, per treatment) according to Mateos-Naranjo et al. (2008b).

2.4. Gas exchange analysis

Instantaneous gas exchange measurements were performed in randomly selected fully expanded leaves 15 and 30 days after treatment initiation (n = 10) using an open infrared gas analyzer system (LI-6400XT, LI-COR Inc., Neb., USA) equipped with a light leaf chamber (Li-6400-02B, Li-Cor Inc.). Net photosynthetic rate (A_N), stomatal conductance (g_s), intrinsic water use efficiency ($_i$WUE) and intercellular CO_2 concentration (C_i) were determined under the following leaf chamber conditions: light photon flux density of 1500 μmol m^{-2} s^{-1}, leaf temperature of 25 °C, 50 ± 2% relative humidity and CO_2 concentration surrounding leaf (C_a) 400 and 700 μmol mol^{-1} air for plants grown at 400 and 700 ppm CO_2, respectively. Before to record each measurement, gas exchange was allowed to equilibrate (300 s). Photosynthetic area was approximated as the area of a trapezium. Intrinsic water use efficiency ($_i$WUE) was calculated as the ratio between A_N and g_s.

2.5. Stable isotope analysis and C and N concentrations in leaves

At the end of the experiment, carbon isotopic composition of the pulverized dry leaf samples randomly collected (n = 3) was determined according to Duarte et al. (2014b), using A Flash EA 112 Series elemental analyzer couple on line via Finningan conflo III interface to a Thermo delta V S mass spectrometer. The carbon isotope ratio was expressed in delta (δ) notation as the parts per thousand (‰) considering its deviation from a standard material (PDB limestone) through the formula: $\delta^{13}C$ or $\delta^{15}N = [(R_{sample}/R_{standard}) - 1] \times 10^3$, where R is $^{13}C/^{12}C$. The analytical precision for the measurement was 0.2‰. Carbon and nitrogen contents (%) were attained during the same analysis (n = 3).

2.6. Gauss peak-spectra pigment analysis

At the end of the experiment period, photosynthetic pigments in leaf samples randomly collected (n = 5), flash-frozen in liquid N_2 and freeze-dried for 48 h in the dark to avoid photodegratation processes (Duarte et al., 2014b). Samples were subsequently grinded in pure acetone and pigments extracted at −20 °C during 24 h in the dark to prevent its degradation, centrifuged at 4000 rpm during 15 min at 4 °C and the resulting supernatant scanned in a dual beam spectrophotometer (Hitachi Ltd., Japan) from 350 to 750 nm at 0.5 nm step. The resulting absorbance spectrum was use to the determination of all the target pigments, after application of the using Gauss-Peak Spectra (GPS) algorithm according to Küpper et al. (2007). For this Sigma Plot

Software with a GPS fitting library was employed. From the resulting pigment concentrations was also possible to calculate the De-Epoxidation State (DES) as follow (Duarte et al., 2014b):

DES = [Antheraxantin] + [Zeaxanhin]/[Violaxanthin] + [Antheraxantin] + [Zeaxanthin]

2.7. Chlorophyll fluorescence analysis

Modulated chlorophyll fluorescence measurements were made on the same leaves of gas exchange on the day of maximum stress, 30 days after treatment initiation (n = 10), using a FluorPen FP100 PAM (Photo System Instruments, Czech Republic) on light and 30 min dark-adapted leaves. Light energy yields of the Photosystem II (PSII) reaction centres were determined with a saturation pulse method as described by Schreiber et al. (1986), using a 0.8 s saturating light pulse with an intensity of 8000 µmol $m^{-2} s^{-1}$. Furthermore, maximum electron transport rate (ETR_{max}) was also obtained using the pre-programmed Rapid Light Curve protocol, by exposing dark-adapted leaves to increasing light levels and recording the quantum yield after exposure to each light intensity level. Additionally the chlorophyll a fast kinetics, or JIP-test (or Kautsky curves), which depicts the rate of reduction kinetics of various components of PSII, were also measured in dark-adapted leaves (n = 5 for each one) according to Duarte et al. (2015), using the pre-programmed OJIP protocols of the FluorPen. All derived parameters for both RLC and OJIP were calculated according to Marshall et al. (2000) and Strasser et al. (2004), respectively (Table 1).

Table 1
Summary of fluorometric analysis parameters and their description (Strasser and Stribet, 2001).

Photosystem II Efficiency	
Fv/Fm	Maximum quantum efficiency of PSII photochemistry
PS II Operational and Maximum Quantum Yield (ΦPSII)	Light and dark-adapted quantum yield of primary photochemistry, equal to the efficiency by which a PS II trapped photon will reduce Q_A to Q_A^-
Rapid Light Curves (RLCs)	
rETR	Relative electron transport rate at each light intensity (rETR = ΦPSII x PAR x 0.5)
ETR_{max}	Maximum ETR after which photo-inhibition can be observed
E_k	The onset of light saturation
α	Photosynthetic efficiency, obtained from the initial slope of the RLC
Energy Fluxes (Kautsky curves)	
Area	Corresponds to the oxidized quinone pool size available for reduction and is a function of the area above the Kautsky plot
φP0	Maximum yield of primary photochemistry
φE0	Probability that an absorbed photon will move an electron into the electronic transport chain
φD0	Quantum yield of the non-photochemical reactions
Ψ0	Probability of a PS II trapped electron to be transported from Q_A to Q_B
N	Reaction centre turnover rate
Sm	Net rate of PS II RC closure
M○	Net rate of PS II RC closure
δR0	Efficiency with which an electron can move from the reduced intersystem electron acceptors to the PS I end electron acceptors
ABS/CS	Absorbed energy flux per leaf cross-section.
TR/CS	Trapped energy flux per leaf cross-section
ET/CS	Electron transport energy flux per leaf cross-section
DI/CS	Dissipated energy flux per leaf cross-section.
RC/CS	Number of available reaction centres per leaf cross section
PI Total	Performance index
Grouping Probability (P_G)	The grouping probability is a direct measure of the connectivity between the two PS II units

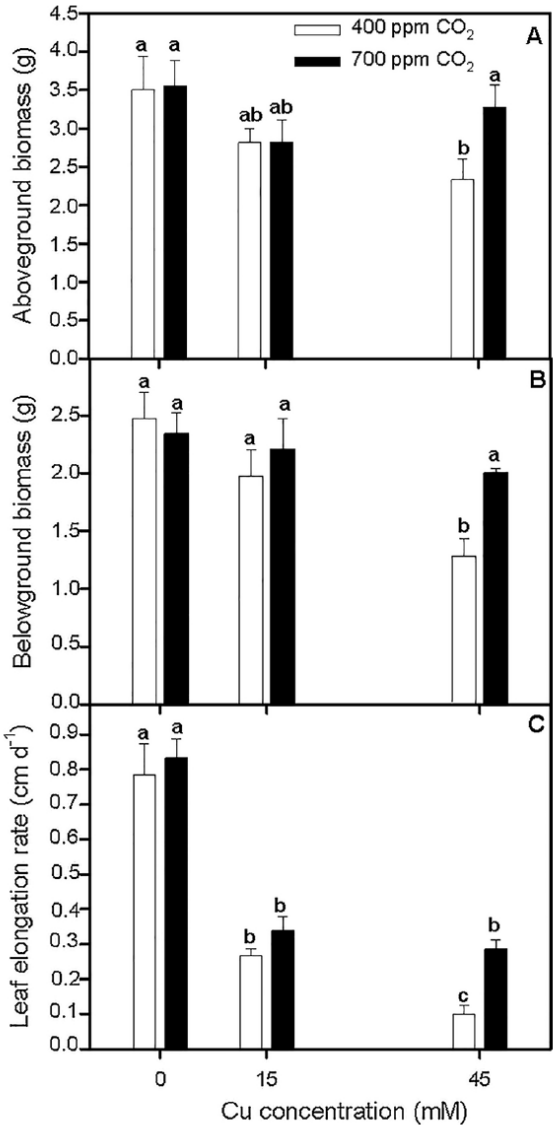

Fig. 1. Growth of *Spartina densiflora* in response to treatment with a range of Cu concentrations at 400 and 700 ppm CO_2 for 30d. Aboveground biomass (A), belowground biomass (B) and leaf elongation rate (C). Values represent mean ± SE, n = 10. Different letters indicate means that are significantly different from each other (LSD test, P < 0.05).

2.8. Antioxidant enzymes analysis

At the end of experiment, 500 mg of fresh leaves tissues were powdered in liquid nitrogen then homogenized under cold conditions in 8.0 mL of extraction buffer containing 50 mM phosphate buffer (pH 7.6) with 0.1 mM EDTA. After centrifugation at 8923 rpm for 20 min at 4 °C, the supernatant was used in enzymatic analysis, and the specific enzyme activities were expressed as units per mg of protein (n = 3). Total protein content analysis was carried out according to Bradford (1976), using bovine serum albumin as a standard.

Ascorbate peroxidase (APx) was assayed according to Tiryakioglu et al. (2006). Shortly, the reaction mixture contained 50 mM of sodium phosphate buffer (pH 7.0), 12 mM of H_2O_2, 0.25 mM L-arcorbate. The enzymatic reaction was started with the addition of 100 µL of plant extract and its activity recorded at 290 nm and the amount of ascorbate oxidized calculated from the molar extinction coefficient of 2.8 mM^{-1} cm^{-1}. Catalase (CAT; EC1.11.1.6) was assayed according to

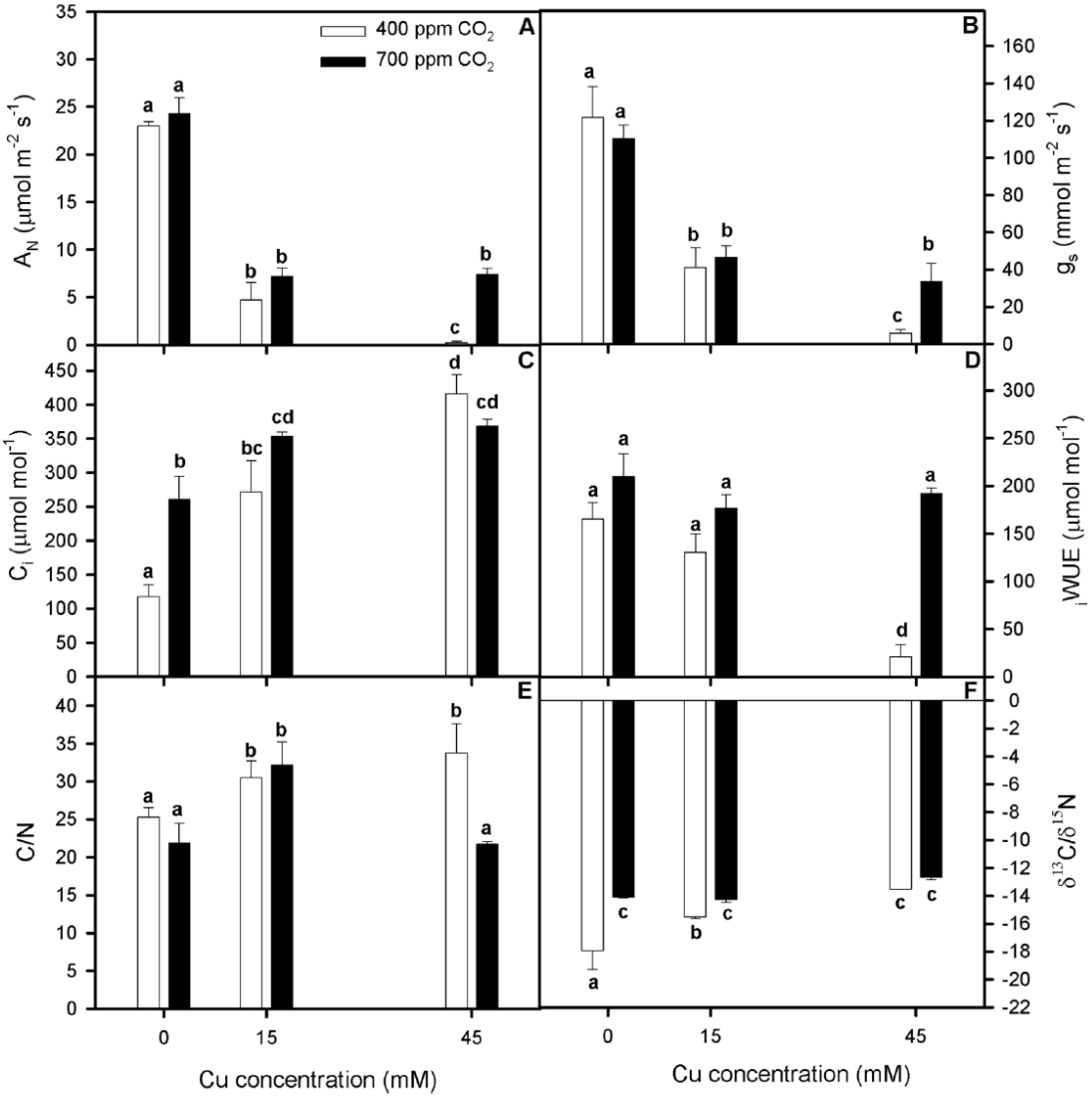

Fig. 2. Net photosynthetic rate, A_N (A), stomatal conductance, g_s (B), intercellular CO_2 concentration, C_i (C), and intrinsic water use efficiency, $_iWUE$ (D), Carbon an nitrogen concentrations ratio, C/N (E) and stable carbon isotope signature $\delta^{13}C/\delta^{15}$ N ratio in randomly selected, fully expanded penultimate leaves of *Spartina densiflora* in response to treatment with a range of Cu concentrations at 400 and 700 ppm CO_2 after 15 and 30d of treatment. Values represent mean ± SE, n = 10 for gas exchange parameter and n = 3 for C/N and $\delta^{13}C/\delta^{15}$ ratios. Different letters indicate means that are significantly different from each other (LSD, $P < 0.05$).

Table 2
Photosynthetic pigments concentrations (µg/g) and DES state in randomly selected, fully expanded penultimate leaves of *Spartina densiflora* in response to treatment with a range of Cu concentrations at 400 and 700 ppm CO_2 after 30 d of treatment. Values represent mean ± SE, n = 5. Different letters indicate means that are significantly different from each other (LSD, $P < 0.05$).

[Cu] (mM)	[CO_2] (ppm)	Chl *a*	Chl *b*	Phe *a*	b-carotene	Lutein	Neoxanthin	Violaxanthin	Zeaxanthin	DES
0	400	242.5 ± 19.2^a	91.5 ± 6.7^a	14.1 ± 2.3^a	5.8 ± 0.5^a	20.1 ± 4.1^a	8.9 ± 1.4^a	3.8 ± 1.1^a	6.4 ± 0.9^a	0.60 ± 0.05^a
	700	200.4 ± 17.4^a	82.6 ± 5.1^a	15.5 ± 2.5^a	5.6 ± 0.4^a	17.8 ± 2.4^a	7.1 ± 1.2^a	4.5 ± 0.9^a	5.9 ± 1.1^a	0.52 ± 0.04^a
15	400	162.6 ± 6.5^b	51.4 ± 1.9^b	5.7 ± 0.2^b	4.5 ± 0.2^a	15.3 ± 0.8^a	7.1 ± 0.4^a	3.6 ± 0.2^a	4.7 ± 0.3^a	0.42 ± 0.01^a
	700	174.2 ± 11.5^b	44.4 ± 1.6^b	8.8 ± 2.4^b	5.9 ± 1.4^a	15.4 ± 2.9^a	5.5 ± 1.1^a	6.7 ± 2.2^a	5.9 ± 1.2^a	0.49 ± 0.06^a
45	400	167.3 ± 8.7^b	54.0 ± 3.1^b	4.9 ± 0.5^b	5.1 ± 0.3^a	15.9 ± 0.9^a	6.8 ± 0.6^a	3.6 ± 1.2^a	5.1 ± 0.3^a	0.41 ± 0.07^a
	700	166.5 ± 7.4^b	58.3 ± 4.5^b	7.8 ± 1.2^b	5.1 ± 0.4^a	15.3 ± 1.8^a	6.6 ± 0.2^a	5.4 ± 1.3^a	5.5 ± 0.4^a	0.51 ± 0.04^a

the protocol of Teranishi et al. (1974) in a mixture of 890 mL of sodium phosphate buffer (50 mM, pH 7.0), 100 mL of plant extract and 10 mL H_2O_2 (15%). Enzyme activity was recorded at 240 nm and calculated using the molar extinction coefficient for H_2O_2 (39.4 mM^{-1} cm^{-1}). Guaiacol peroxidase (GPx; EC1.11.1.7) activity was determined according to Zhou et al. (1997) in 1 mL of reaction mixture containing 590 mL of sodium phosphate buffer (50 mM, pH 7.0), 200 mL of H_2O_2 (50 mM) and 10 mL of plant extract. After guaiacol addition (20 mM) the reaction absorbance is monitored for 2 min at 470 nm (guaiacol molar extinction coefficient = 26.6 mM^{-1} cm^{-1}). Superoxide dismutase (SOD; EC1.15.1.1) was assayed according to Marklund and Marklund (1974) by calculating the inhibition of pyrogallol

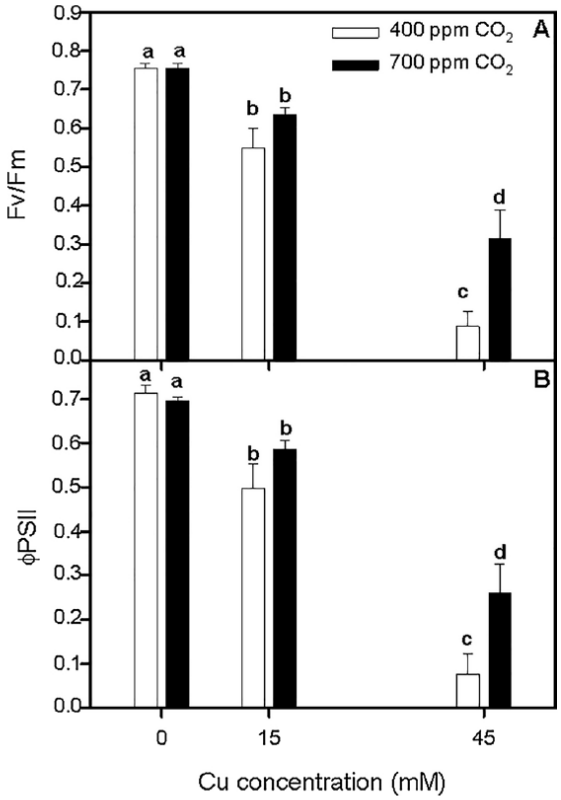

Fig. 3. Maximum quantum efficiency of PSII photochemistry, F_v/F_m (A) and quantum efficiency of PSII, Φ_{PSII} (B) in randomly selected, fully expanded penultimate leaves of *Spartina densiflora* in response to treatment with a range of Cu concentrations at 400 and 700 ppm CO_2 after 30d of treatment. Values represent mean ± SE, n = 10. Different letters indicate means that are significantly different from each other (LSD, P < 0.05).

autooxidation by SOD at 325 nm for 2 min in a reaction vase containing 550 mL sodium phosphate buffer (50 mM, pH 7.6), 360 mL Milli-Q water and 10 mL of plant extract. The reaction was started with the addition of 80 mL Pyrogallol (3 mM). One enzyme activity is defined as the amount of enzyme capable of inhibiting 50% of the autooxidation of pyrogallol.

2.9. Membrane lipid peroxidation

According to Heath and Packer (1968), leaf samples were homogenized in 20% Trichloroacetic acid (TCA), containing 0.5% Tiobarbituric acid (TBA) at a ratio of 100:1 (m/v) leaf fresh weight to acid. The homogenate was extracted at 95 °C for 30 min, and the reaction was immediately stopped in ice and centrifuged at 15,000 rpm for 5 min at 4 °C. Absorbance at 532 nm and 600 nm was detected in a Shimadzu UV-1603 spectrophotometer. The concentration of malondialdehyde (MDA) was calculated using the molar extinction coefficient, 155 mM^{-1} cm^{-1} (n = 3).

2.10. Ions concentration of plant tissues analysis

At the end of the experiment, 30 days after treatments initiation, leaves and roots were successively and meticulously washed with distilled water in order to remove ions from the free spaces and from its surface prior to analysis and then dried at 60 °C for 48 h. After that subsamples (0.5 g) from leaves or roots compounded from the 10 replicate plants were digested in triplicates with 6 mL HNO_3, 2 mL NaOH and 1 mL H_2O_2. Ttotal Cu, Ca, K, Mg and P concentrations were measured by inductively coupled plasma (ICP) spectroscopy (Mateos-Naranjo et al., 2011).

2.11. Statistical analysis

All the statistic tests were performed by a statistical software package Statistica v. 6.0 (Statsoft Inc.). The differential effect of copper and atmospheric CO_2 concentrations treatments were determined by Two-way analysis of variance. Multiple comparisons were analyzed by a LSD test. Before statistical analysis Kolmogorov-Smirnov and Levene tests were used to verify the assumptions of normality and homogeneity of variances, respectively.

3. Results

3.1. Growth analysis

Total dry mass (above- and belowground) was considerably reduced at the highest Cu concentration in plants grown at 400 ppm CO_2, while it was not significantly affected in those grown at 700 ppm CO_2 (Two-way ANOVA: CO_2 × Cu, $p < 0.05$; Fig. 1A and B). Furthermore, leaf elongation rate decreased in presence of Cu concentration in similar degree in both atmospheric CO_2 concentrations, but this effect was more acute in plants grown at 45 mM Cu under ambient atmospheric CO_2 concentration, (Two-way ANOVA: CO_2 × Cu, $p < 0.05$; Fig. 1C).

3.2. Gas exchange analysis

There was significant effect of CO_2 and Cu concentrations in several gas exchange variables, and overall our results showed similar trend at each of the two sampling time for each specific parameter. Also there is to note that our statistical analyses indicated that Cu had a more significant effect than CO_2 concentration on gas exchange characteristics especially in plants grown at the highest Cu concentration treatment. Thus, A_N showed a similar sharp decreased in presence of Cu in growth medium for both atmospheric CO_2 levels after 15 d of treatment (Two-way ANOVA: Cu, $p < 0.05$; data non presented); however, after 30 day of treatment, plants grown at 400 ppm CO_2 with 45 mM Cu showed lower values than those at high CO_2 concentration (Two-way ANOVA: CO_2 × Cu, $p < 0.05$; Fig. 2A). g_s showed a highly similar trend to that of A_N, recording the lowest values for *S. densiflora* plants grown at 45 mM Cu and 400 ppm CO_2 after 30 d of treatment (Fig. 2B). Contrarily, C_i values increased with Cu concentration for both atmospheric CO_2 levels in each specific sampling time, and overall those values were higher in plants grown at 700 ppm CO_2 at 0 and 15 mM Cu (Two-way ANOVA: CO_2 × Cu, $p < 0.05$; Fig. 2C). Finally, $_i$WUE decreased in presence Cu in plants grown at 400 ppm CO_2, while it did not vary respect to the control in those expose to high atmospheric CO_2 concentration after 15 d (Two-way ANOVA: CO_2 × Cu, $p < 0.05$; data non presented). Similar trend was recorded after 30 d, although this was only statistically different between CO_2 treatments in plants grown at 45 mM Cu (Fig. 2D).

3.3. Stable isotope analysis and C and N concentrations in leaves

Leaves C/N ratio increased in presence of Cu in growth medium at both atmospheric CO_2 concentrations treatments, except in plants exposed to 45 mM Cu and 700 ppm CO_2 which did not vary respect to control treatment (Two-way ANOVA: CO_2 × Cu, $p < 0.05$; Fig. 2E). This response was linked with the maintaining of N content compared with their non-supplied CO_2 counterparts. On the other hand, leaves stable isotope composition showed that $\delta^{13}C/\delta^{15}N$ ratio signature decreased with Cu concentration in *S. densiflora* plants at ambient CO_2 concentration (Two-way ANOVA: CO_2 × Cu $p < 0.05$; Fig. 2F), whereas those grown at 700 ppm CO_2 maintained its isotopic signature almost unaffected.

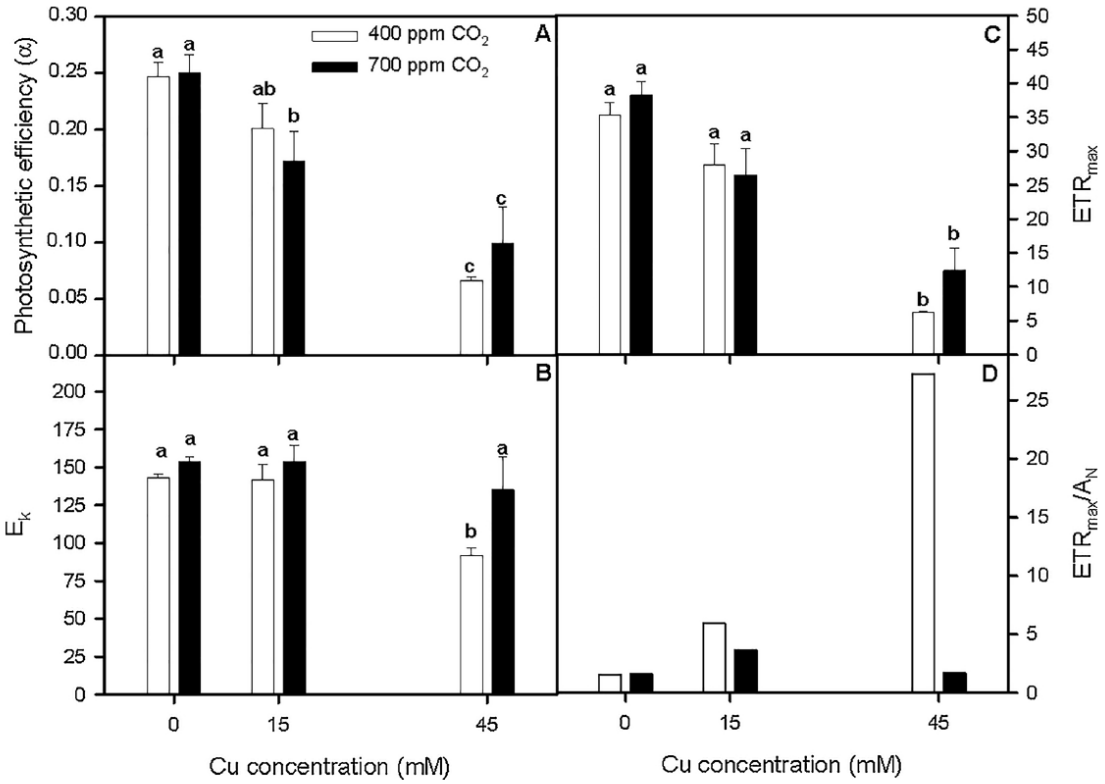

Fig. 4. Photosynthetic efficiency, α, (A), the onset of light saturation, E_k (B), maximun ETR, ETR_{max} (C) in dark adapted randomly selected and ETR_{max}/A_N ratio (D), fully expanded penultimate leaves of *Spartina densiflora* in response to treatment with a range of Cu concentrations at 400 ppm CO_2 (A) and 700 ppm CO_2 (B) after 30d of treatment. Values represent mean ± SE, n = 5. Different letters indicate means that are significantly different from each other (LSD, $P < 0.05$).

3.4. Leaves pigments analysis

Chl *a*, Chl *b* and Phe *a* concentrations decreased in presence of Cu in similar degree in both atmospheric CO_2 concentrations treatment (Two-way ANOVA: Cu, $p < 0.05$), but without statistical differences between Cu treatments (Table 2). Contrarily the concentrations of each specific carotenoids and DES state did not vary with Cu and CO_2 concentrations treatments (Table 2).

3.5. Chlorophyll fluorescence analysis

F_v/F_m and Φ_{PSII} values decreased with the increased of Cu concentration in both atmospheric CO_2 concentrations, but this reduction was more acute in plants grown at 45 mM Cu and 400 ppm CO_2 compared with the CO_2 enrichment treated plants (Two-way ANOVA: $CO_2 \times$ Cu, $p < 0.05$; Fig. 3A and B).

On the other hand the increment of Cu concentration induced a marked decrease in the ETR values at all tested light levels at both atmospheric CO_2 concentrations, being this deleterious effect mitigated in a certain degree in plants grown at 700 ppm CO_2 at the highest Cu concentration treatment (data non-presented). This response was evident for the specific RLC-derived parameters. Thus α and ETR_{max} values were lower in plants grown at 45 mM Cu compared with the rest of treatments, without any statistical differences between both CO_2 treatments (Two-way ANOVA: Cu, $p < 0.05$; Fig. 4A and C). Similar trend showed E_k in plants grown at ambient CO_2, while at 700 ppm CO_2 it didn't show any significant difference upon the application of Cu (Fig. 4B). As a consequence of previous described trends, ETR_{max}/A_N ratio increased considerably mainly in plants grown at 45 mM Cu and ambient atmospheric CO2 concentration, reaching values up to 27 (Fig. 4D).

Focusing on derived-parameters from the Kautsky curves, there is to notice that overall there was significant effect of Cu and CO_2 concentrations in several variables. Thus, the *Area* above the Kautsky plot was lower in plants grown at low and middle Cu concentrations under rising atmospheric CO_2 concentration compared with those grown at 400 ppm (Two-way ANOVA: $CO_2 \times$ Cu, $p < 0.05$; Fig. 5A). This parameter also decreased at the highest Cu concentration in similar degree for both CO_2 levels. Furthermore, in general the presence of Cu increased PG, N, Sm, Mo and δR0 values, being these increments considerably greater in plants grown at 45 mM Cu compared with the rest of Cu treatments (Two-way ANOVA: Cu, $p < 0.05$; Fig. 5B–F) and without significant differences between both CO_2 level. On the other hand, φ_{P0}, φ_{E0} and φ_0 decreased gradually with the increment of Cu concentration, showing the lower values in plants grown at 45 mM Cu (Two-way ANOVA: Cu, $p < 0.05$; Fig. 6A–C). However these reductions were in certain degree mitigated in plants grown at elevated CO_2 concentration, which did not show significant differences respect those exposed to 15 mM at both CO_2 concentrations. Contrary φ_{D0} increased gradually with Cu concentration, being this increment greater in plants grown at 400 ppm CO_2 but without significant differences respect to those exposed to 700 ppm CO_2 (Two-way ANOVA: Cu, $p < 0.05$; Fig. 6D).

Finally regarding the energetic fluxes on a leaf cross-section basis (phenomological fluxes) showed that RC/CS, TR/CS and ET/CS decreased mainly in plants growth at 45 mM Cu compared with the rest of treatment (Two-way ANOVA: $CO_2 \times$ Cu, $p < 0.05$; Fig. 7A–C), although these reductions were in certain degree mitigation at 700 ppm CO_2, being this positive effect only statistically significant for ET/CS (Fig. 7C). Furthermore the presence of Cu in growth medium promoted a sharp decrease on PI for all plants and without any statistical differences between both Cu or CO_2 concentrations treatments (Fig. 7F). Contrary DI/CS and ABS/CS values increased considerably in plants grown at 45 mM compared with the other treatments for both CO_2

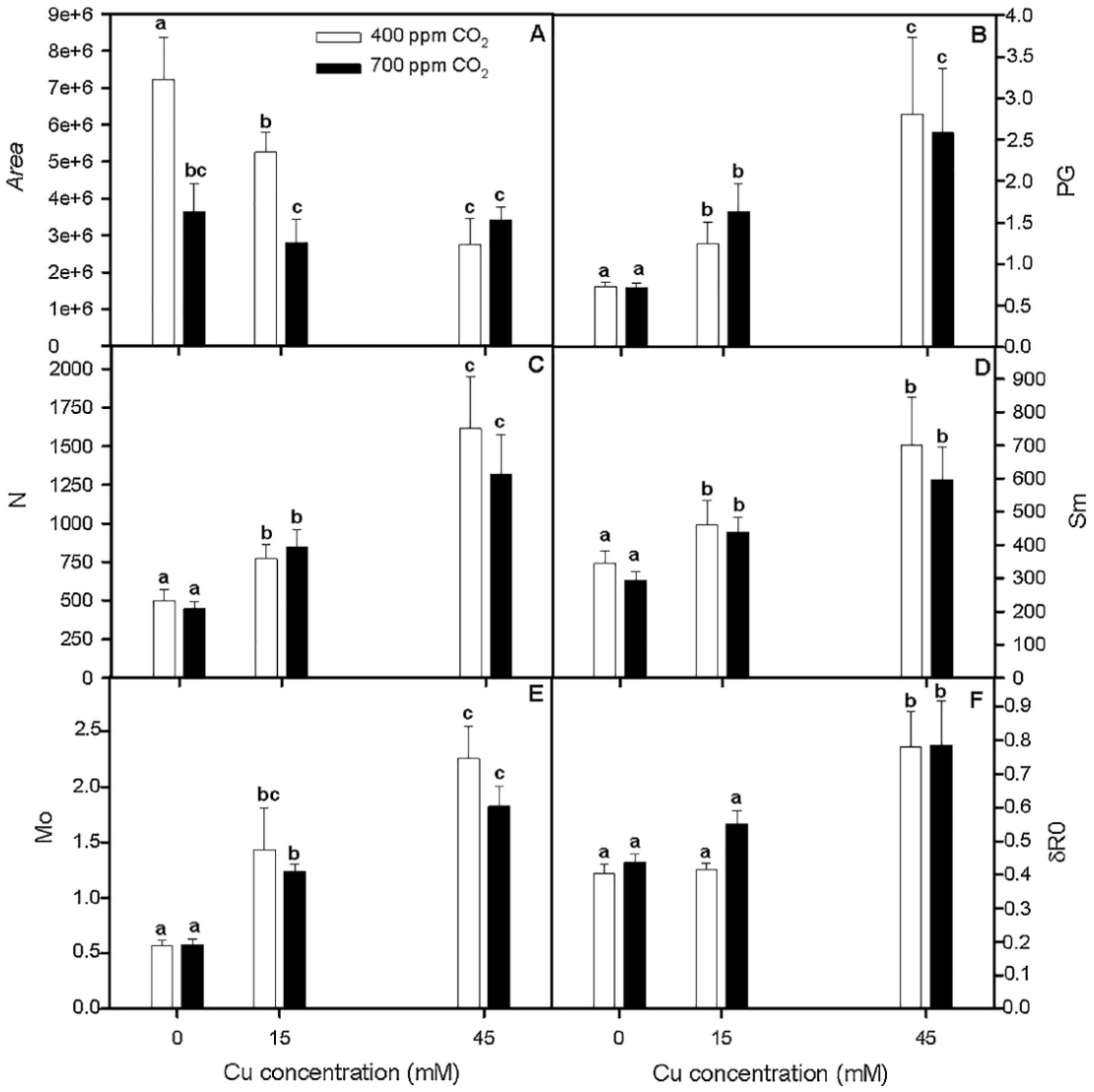

Fig. 5. *Area* (A), grouping probability PG, (B), reaction centre turnover rate, N (C), Sm (D), net rate of PS II RC closure, M_0 (E) and δR_0 (F) in dark adapted randomly selected, fully expanded penultimate leaves of *Spartina densiflora* in response to treatment with a range of Cu concentrations at 400 ppm CO_2 (A) and 700 ppm CO_2 (B) after 30d of treatment. Values represent mean ± SE, n = 10. Different letters indicate means that are significantly different from each other (LSD, $P < 0.05$).

concentration treatments, with the exception of the DI/CS values in plants grown at 700 ppm CO_2, which did not show significant differences respect to the control treatment (Fig. 7D and E).

3.6. Oxidative damage biomarkers

CAT activity did not vary with Cu and CO_2 concentrations treatments, showing mean values around 0.12 U μg^{-1} protein (Fig. 8A). Contrary in certain degree APx and GPx activities increased in plants grown at 45 mM Cu and 400 ppm CO_2, compared with their CO_2-enrichment counteracts (Two-way ANOVA: $CO_2 \times Cu$, $p < 0.05$; Fig. 8B and C). Finally SOD activity showed a sharp increment in plants grown at 15 mM Cu and then decreased to similar values than control, being this increment greater in plants grown at 400 ppm CO_2 (Two-way ANOVA: $CO_2 \times Cu$, $p < 0.05$; Fig. 8D). As for membrane damage, there was an evident augmentation in the accumulation of MDA in plants grown at 45 mM, which showed values of 0.026 and 0.021 mM g^{-1} FW for plant grown at 400 and 700 ppm CO_2, compared with the other treatments with mean values c. 0.010 mM g^{-1} FW.

3.7. Ions concentration analysis

There were significant effects of Cu and CO_2 concentration treatments on the tissues ions concentrations (Two-way ANOVA: $CO_2 \times Cu$, $p < 0.05$; Table 3). Copper concentration within the tissues showed an increase along the external Cu exposure, but the trajectory of Cu concentration in leaves and roots was different in relation with atmospheric CO_2 concentration. Thus, in plants grown at 400 ppm CO_2, leaves Cu concentration increased markedly with external Cu concentration, ranging between 4.9 and 737.5 mg kg^{-1} Cu, while at 700 ppm CO_2 it showed mean values c. 270 mg kg^{-1} Cu in presence of Cu. Contrary roots Cu concentrations did not showed any statistical relationship with atmospheric CO_2 concentration treatment, showing values which varied between 581.3 mg kg^{-1} Cu and 715.8 mg kg^{-1} Cu of plants grown at 15 mM Cu and 700 ppm CO_2 and those exposed to 15 mM Cu and 400 ppm CO_2, respectively. Concentrations of Ca, Mg in leaves and Mg and P in roots did not vary with Cu or CO_2 concentration treatments. In contrast, overall decreases in K and P concentrations in leaves and in Ca and K concentrations in roots were recorded in presence of Cu. However, few differences were noted between both CO_2

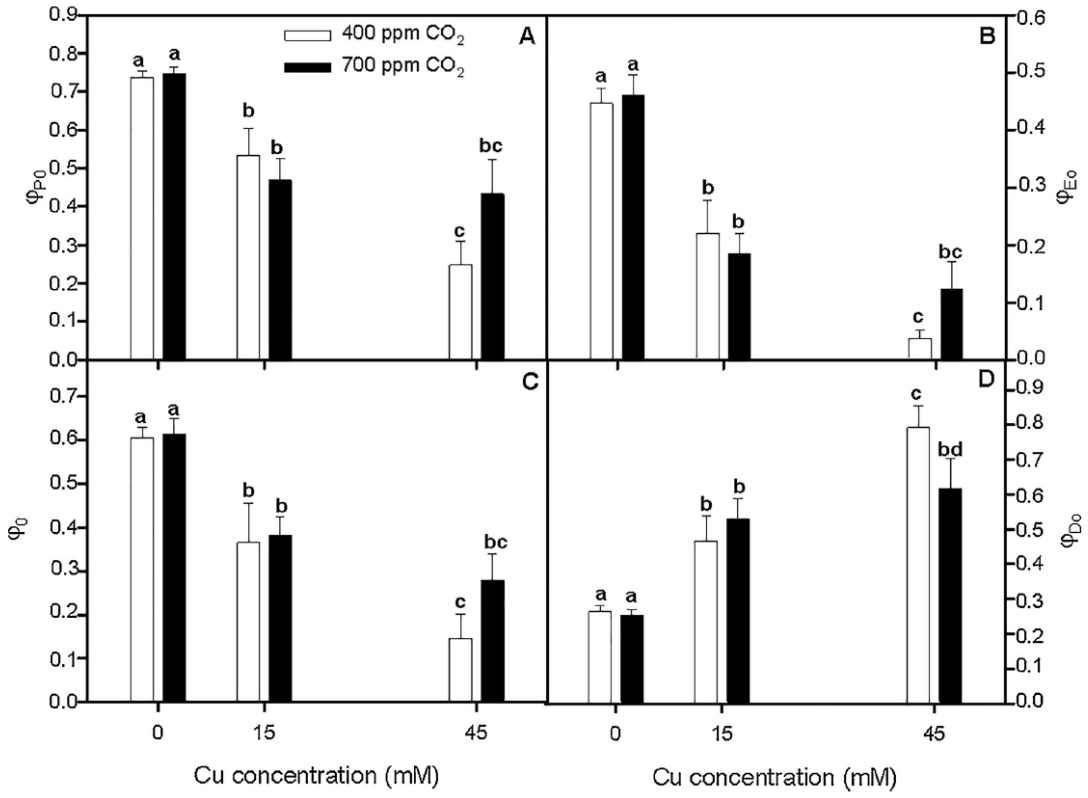

Fig. 6. Maximum yield of primary photochemistry, φ_{P0}, (A), the probability that an absorbed photon will move an electron into the ETC, φ_{E0} (B), the probability of a PS II trapped electron to be transported from QA to QB, φ_0 (C) and the quantum yield of the non-photochemical reactions, φ_{D0} (D) in dark adapted randomly selected, fully expanded penultimate leaves of *Spartina densiflora* in response to treatment with a range of Cu concentrations at 400 ppm CO_2 (A) and 700 ppm CO_2 (B) after 30d of treatment. Values represent mean ± SE, n = 10. Different letters indicate means that are significantly different from each other (LSD, $P < 0.05$).

treatments.

4. Discussion

4.1. Effect of atmospheric CO_2 enrichment and cu excess on S. densiflora tolerance and Cu accumulation

Our study indicated that although *Spartina densiflora* has denoted a great tolerance to copper exposure and even a high capacity for accumulating it in its tissues (Mateos-Naranjo et al., 2008a, 2015), at high metal concentration (45 mM Cu) its growth was clearly impaired, with total above- and belowground dry mass reduction of 33% and 48% respectively compared with the control treatment. Crossing this trend with Cu concentration in plants tissues, we found that Cu concentration in *S. densiflora* tissues increased significantly with metal addition, reaching values up to 737.5 mg kg^{-1} Cu for leaves in plants grown at 45 mM and ambient CO_2 concentration. These values are much higher than those suggested as normal in plants tissues and thus could be toxic for *S. densiflora* plants (Kabata-Pendias and Pendias, 2001), explaining the reported growth reduction. However, the rising atmospheric CO_2 concentration, in a certain extent, mitigated growth reduction, being this positive effect more evident in aboveground and belowground dry mass for plants grown at 45 mM Cu. This positive impact on carbon assimilation would contribute to explain the recorded differences in isotope composition signature, which could have been also affected by the surrounding CO_2 concentration, since stable isotopes are a reflection of the source and fixation of carbon (Guy et al., 1986).

On the other hand, the higher biomass accumulation in plants grown at elevated CO_2 concentration could explain the reduction in Cu leaves concentration recorded due to dilution effect, which made that Cu concentration did not exceed values greater than 270 mg kg^{-1} Cu. Contrary, roots Cu concentration did not vary between CO_2 concentration treatments, showing in both cases concentrations as higher as previously recorded in other studies (Mateos-Naranjo et al., 2008a, 2015). This result indicates that atmospheric CO_2 enrichment would increase the Cu toxicity threshold previously reported for *S. densiflora*, maintaining at the same time its high phytostabilization potential by the accumulation of great amount of Cu in its roots (Mateos-Naranjo et al., 2008a).

4.2. Effect of atmospheric CO_2 enrichment and Cu excess on S. densiflora photosynthetic gas exchange characteristics

Although Cu is an essential nutrient for plant development, its excess can lead to several phytotoxicity effects on plant performance and metabolic process, and these effects are often the results of mineral nutrition and water imbalances (Kabata-Pendias and Pendias, 2001), as well as photosynthetic metabolism alterations (Nalewajko and Olaveson 1995; Mallick and Mohn, 2003). In fact, our results revealed deficiencies in mineral nutrition in the plants grown in presence of Cu. Furthermore, according to Mateos-Naranjo et al. (2008a, 2015), we found that A_N sharply declined in presence of Cu in growth medium. However, these effects were in certain modulated by atmospheric CO_2 enrichment. Thus although the different CO_2 exposure levels didn't affect *S. densiflora* nutrient balances, we found that plants grown at 45 mM Cu and elevated atmospheric CO_2 concentration were able to maintain higher A_N values than their non-supplied CO_2 counterparts. These results are in agreement with previously recorded by Wang et al. (2012) and Guo et al. (2015), who found that atmospheric CO_2 enrichment stimulated leaf photosynthesis in *Populus* and *Salix* species at

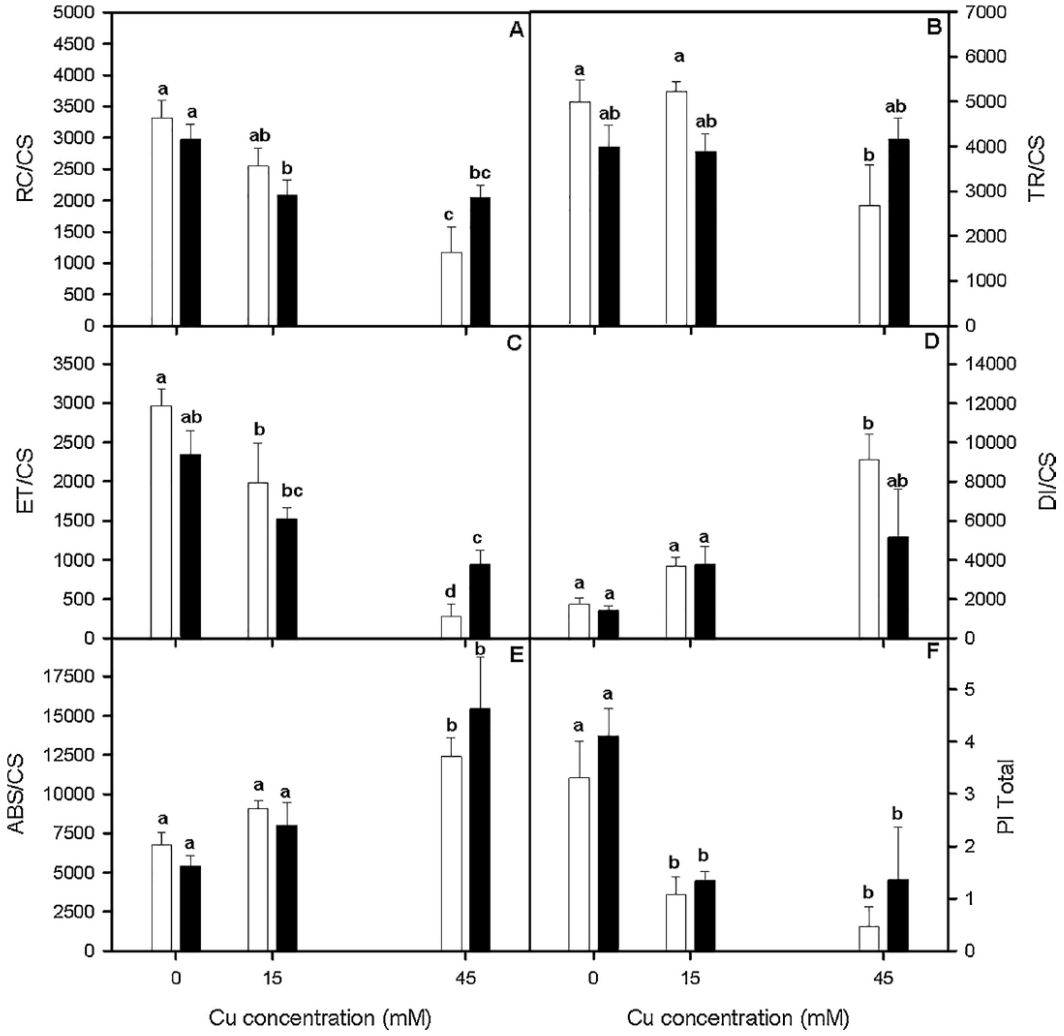

Fig. 7. Number of available reaction centres, RC/CS (A), trapped energy flux, TR/CS (B) electron transport energy flux ET/CS (C), dissipated energy fluxes, DI/CS (D) and absorbed, ABS/CS (E) energy fluxes per leaf cross section and the performance index on absorption basis, PI (F) in dark adapted randomly selected, fully expanded penultimate leaves of *Spartina densiflora* in response to treatment with a range of Cu concentrations at 400 ppm CO_2 (A) and 700 ppm CO_2 (B) after 30d of treatment. Values represent mean ± SE, n = 5. Different letters indicate means that are significantly different from each other (LSD, $P < 0.05$).

elevate Cd concentrations. However, our experiment is the first complete report which downscaling to the possible mechanisms involved with positive effect of rising CO_2 concentration on photosynthetic response of a C_4 metabolic photosynthetic pathway species, which apparently would not be so favoured in similar degree compared with their C_3-conterparts (Duarte et al., 2014b), under Cu excess.

CO_2 enrichment-mediated alleviation of Cu toxicity on the photosynthetic apparatus of *S. densiflora* could be attributed to several reasons (e.g. CO_2 fixation, enzyme activities and electron transport), since many or even most steps in photosynthetic pathway may be favoured under metal excess and synergy atmospheric CO_2 enrichment. Our results indicated that the most obvious effect of CO_2 enrichment on the photosynthesis response of *S. densiflora* grown at the highest Cu concentration was ascribed to the reduction of stomatal limitation imposed to CO_2 transport imposed by Cu excess (Mateos-Naranjo et al., 2008a, 2015). In sum, plants exposed to 700 ppm CO_2 were able to maintain higher g_s values than their non-supplied CO_2 counterparts. However, this positive effect on g_s was less pronounced than the previously highlighted in A_N, leading to a higher ability of these plants to maintain a better water balance, as indicated its greater ¡WUE values. The positive effect of atmospheric CO_2 enrichment on water relationships on others C_4 plants species and also in *S. densiflora* in response to environmental stress, such as drought (Wall et al., 2001) and salinity (Mateos-Naranjo et al., 2010a,b), has been reported previously.

4.3. Effect of atmospheric CO_2 enrichment and Cu excess on S. densiflora light energy use efficiency

Our results revealed that Cu excess injured *S. densiflora* photosystems functionality, as has been previously described in *S. densiflora* (Mateos-Naranjo et al., 2008a, 2015), indicating that Cu excess enhances photoinhibition induced by light excess. However, these effects were in certain mitigated by atmospheric CO_2 enrichment. Thus, although the different CO_2 exposure levels didn't affect *S. densiflora* light energy efficiency at level of photosynthetic pigment, we found beneficial effects in terms of improvement of PSII efficiency, electron transport rate energy fluxes and the reduction of the over-reduction of the reaction centres of PSII under light excess. Thus at 45 mM Cu and 700 ppm CO_2 plants were able to maintain greater values of F_v/F_m, Φ_{PSII} φ_{P0}, φ_{E0} and φ_0 than non-treated CO_2 enrichment plants. This reported enhanced of PSII efficiency under elevated CO_2 is consistent with the results of Wall et al. (2001) and Cousins et al. (2002), who

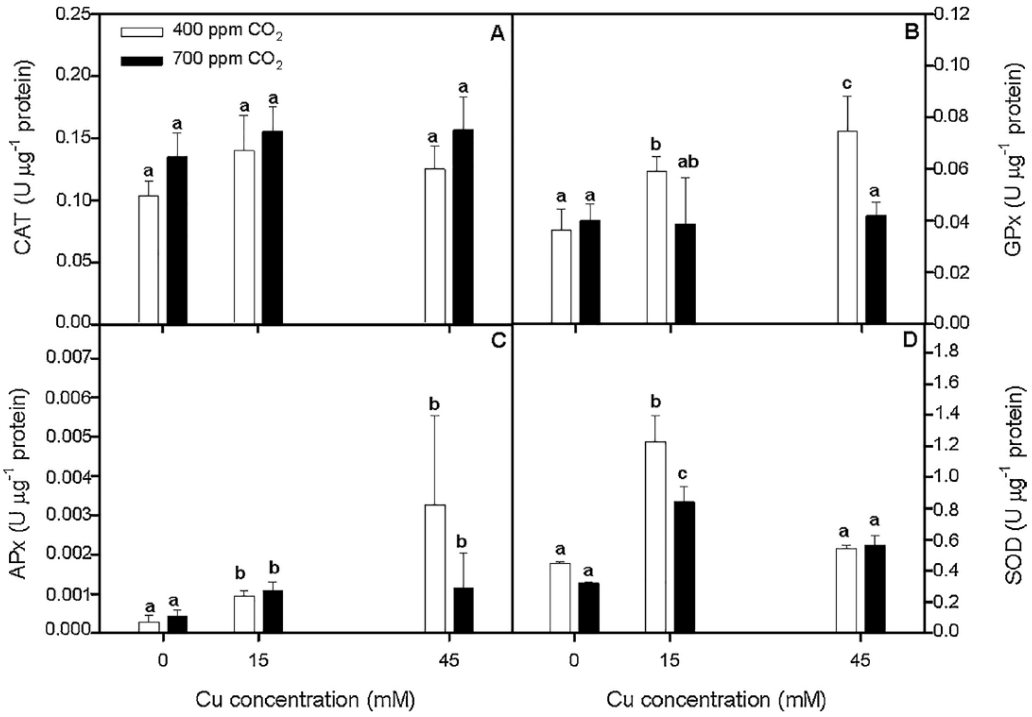

Fig. 8. Catalase, CAT (A), guaiacol peroxidase, GPx (B), ascorbate peroxidase, APx (C) and superoxide dismutase, SOD (D) enzymatic activities in randomly selected, fully expanded penultimate leaves of *Spartina densiflora* in response to treatment with a range of Cu concentrations at 400 ppm CO_2 (A) and 700 ppm CO_2 (B) after 30d of treatment. Values represent mean ± SE, n = 5. Different letters indicate means that are significantly different from each other (LSD, $P < 0.05$).

Table 3
Total Cu, Ca, K, Mg and P concentrations for leaves and roots of *Spartina densiflora* in response to treatment with a range of Cu concentrations at 400 and 700 ppm CO_2 for 30d.

Tissue	[Cu] (mM)	[CO_2] (ppm)	Cu (mg Kg^{-1})	Ca (mg g^{-1})	K (mg g^{-1})	Mg (mg g^{-1})	P (mg g^{-1})
Leaves	0	400	4.9 ± 1.0^{a}	3.4 ± 0.3^{a}	25.4 ± 0.2^{a}	3.3 ± 0.2^{a}	2.6 ± 0.1^{a}
		700	5.4 ± 0.2^{a}	3.1 ± 0.2^{a}	24.3 ± 0.3^{a}	2.9 ± 0.1^{a}	2.9 ± 0.1^{a}
	15	400	179.6 ± 2.0^{b}	3.1 ± 0.2^{a}	17.8 ± 0.4^{b}	2.9 ± 0.1^{a}	1.6 ± 0.2^{b}
		700	248.9 ± 6.3^{bc}	3.1 ± 0.2^{a}	19.2 ± 0.4^{b}	2.7 ± 0.1^{a}	1.9 ± 0.2^{b}
	45	400	737.5 ± 4.0^{d}	3.6 ± 0.1^{a}	22.1 ± 0.6^{ab}	3.4 ± 0.4^{a}	2.6 ± 0.2^{a}
		700	291.4 ± 4.9^{c}	2.9 ± 0.4^{a}	19.6 ± 1.1^{b}	3.0 ± 0.2^{a}	2.1 ± 0.1^{ab}
Roots	0	400	7.6 ± 0.5^{a}	2.4 ± 0.1^{a}	10.5 ± 0.3^{a}	1.4 ± 0.1^{a}	1.9 ± 0.2^{a}
		700	8.2 ± 1.4^{a}	2.2 ± 0.1^{a}	15.3 ± 1.0^{a}	1.7 ± 0.3^{a}	2.7 ± 0.1^{b}
	15	400	715.8 ± 11.0^{b}	1.9 ± 0.1^{b}	7.8 ± 0.5^{b}	1.1 ± 0.2^{a}	1.3 ± 0.2^{a}
		700	581.3 ± 9.0^{c}	1.6 ± 0.2^{b}	6.0 ± 0.3^{b}	1.0 ± 0.2^{a}	1.0 ± 0.5^{a}
	45	400	588.5 ± 3.0^{c}	1.5 ± 0.2^{b}	7.3 ± 0.4^{b}	1.2 ± 0.2^{a}	1.5 ± 0.2^{a}
		700	627.7 ± 12.0^{c}	1.5 ± 0.3^{b}	8.6 ± 0.5^{a}	1.1 ± 0.2^{a}	1.8 ± 0.4^{a}

Values represent mean ± SE, n = 6. Different values indicate means that are significantly different from each other (Two-way ANOVA, $p < 0.05$).

found also that CO_2 fertilization stimulated photosynthetic rates of the C_4 species *Sorghum bicolor* under drought stress. These authors indicated that the enhancement of PSII efficiency was related to an increase in ETR rate. According to this study, plants grown at 45 mM Cu and 700 ppm CO_2, presented greater values of ETR. In addition, an enhancement of ETR under elevated CO_2 concentration has been related with an induction of Rubisco carboxylation capacity which allow plants to maintain its photosynthetic capacity in response to metal stress (Guo et al., 2015) or other environmental stresses (Mateos-Naranjo et al., 2010a). Down-regulation of Rubisco enzymes has also been previously observed in response to Cu stress in *S. densiflora* (Mateos-Naranjo et al., 2008a, 2015). Rubisco enzyme activity is highly related with the photosynthetic potential as well as with N economy, since great amounts of N are invested in Rubisco protein (Evans 1989; Makino et al., 1992). Thus, our results indicated that in a certain degree, the beneficial effect of CO_2 enrichment on *S. densiflora* photosynthetic apparatus could be ascribed to the maintenance of Rubisco activity, through the amelioration of leaves N imbalance in plants grown under Cu excess, together with the documented enhancement of ETR. Furthermore, CO_2 positive effect on ETR was linked with the higher availability of electron acceptors as well as with the greater efficiency in transporting absorbed energy from the light-harvesting complexes to the PSII reaction centres, as was observed by the overall higher values of RC/CS, TR/CS, ET/CS and ABS/CS. Additionally these plants showed lower energy dissipation values, which would indicate an enhancement in photochemical light use efficiency at elevated CO_2 levels (Duarte et al., 2014b). This fact indicates that CO_2 enrichment plants through the maintenance of a greater efficiency in the electron transport rate would able to cope with the over-reduction of the reaction centres of PSII, which could derive from inadequate performance of its photosystems (Cousins et al., 2002; Duarte et al., 2014b).

4.4. Effect of atmospheric CO_2 enrichment and Cu excess on S. densiflora ability to cope with the excess of energy absorbed by its photosystems

Plants undergo light stress when they absorbed more light than they could employ in photosynthesis activity. Under stress conditions this situation can be exacerbated, since the already stress photosystems cannot withstand the same light energy levels than healthy photosynthetic apparatus (Duarte et al., 2013). Our study indicates that the modifications in the photosynthetic rates observed under Cu excess in plants grown at ambient CO_2, would contribute to the accumulation of excessive reducing power. This excessive redox energy stored within the stroma has to be dissipated through activation of protection mechanism, such as the xanthophyll cycle in order to avoid the damage on the thylakoid membrane system due to ROS production and D1 protein destruction, with inevitable decoupling of the PSII subunits (Duarte et al., 2013, 2014b). In fact, the increase in energy dissipation mechanisms was clearly observed in *S. densiflora* plants grown ambient CO_2, as indicated by the higher DI/CS and φ_{D0} values, which in certain degree contribute to cope with the excess energy absorbed, but reducing the efficiency of PSII through photoinhibition, as it was previously described for other halophytes (Redondo-Gómez et al., 2010). This depletion in the photosynthetic productivity has its higher expression if the lower development of *S. densiflora* plants grown under Cu excess and at ambient atmospheric CO_2 is considered (Melis, 1999). Thus the maintenance of cyclic electron transport under CO_2 enrichment could be a mechanism to protect *S. densiflora* against excess of radiation under Cu excess, which could lead to an additional consumption of reducing equivalents and can thus function as sinks for excessive excitation energy (Asada, 1996). This idea is supported by the antioxidants defence enzymes response modulation under elevated CO_2. The overall lower values of APx and GPx activities at both Cu concentration treatments and lower SOD activity for plants grown at 15 mM Cu indicates a lower ROS production under elevated CO_2 concentration, which is supported by the abovementioned thesis, where the enhanced use of reducing power for assimilation in photosynthesis would reduce the ROS generation. According Guo et al. (2015), the conservation of high levels of photosynthetic activity in *Populus* and *Salix* species under Cd stress under CO_2 enrichment was related with the decreasing of reactive oxygen species accumulation. In addition the lower risk of ROS production was supported by the lower MDA concentration and ETR_{max}/A_N ratio recorded mainly in plants grown at 45 mM Cu and 700 ppm CO_2 compared with their non-CO_2 treated counteracts, since this ration has been considered an indicator of ROS production in plants in response to several stress (Hussin et al., 2017).

5. Conclusion

This study indicates that atmospheric CO_2 enrichment would increase Cu toxicity threshold previously reported for *S. densiflora*, maintaining at the same time its high phytostabilization potential. This mitigation effect of atmospheric CO_2 enrichment on *S. densiflora* growth under Cu excess appears to be linked with the protection of several steps in its photosynthetic pathway, such us CO_2 fixation due to reduction stomatal limitation, which also contribute to improve *S. densiflora* water balance. Furthermore the positive impact of rising CO_2 was ascribed to a better use of absorbed energy, which could lead to an additional consumption of reducing equivalents reducing the risk of ROS species production, as indicated the greater ETR values and the non enhanced ETR_{max}/A_N ratio and MDA concentration, lower dissipation energy rate and the modulation antioxidant enzymes activities under elevated CO_2.

Acknowledgements

This work has been co-funded by Oficina de Cooperación Universidad de Sevilla (Conv. Ay. Act. y Proy. Coop. Des. Mod. 2, 2014/15-2015/2016) and Ministerio de Economía y Competitividad (MINECO Project CGL2016-75550-R cofunded by FEDER). J.A Pérez-Romero thanks Ministerio de Educación, Cultura y Deporte for its personal financial support (FPU014/03987). We are grateful University of Seville Greenhouse General Services (CITIUS) for its collaboration. The authors would also like to thank to the "Fundação para a Ciência e Tecnologia (FCT)" for funding the research in the Marine and Environmental Sciences Centre (MARE) throughout the project UID/MAR/04292/2013. B. Duarte investigation was supported by FCT throughout a Posdoctoral grant (SFRH/BPD/115162/2016). We also appreciate the valuable feedback from reviewers insofar as it has helped us improve and enrich our work.

References

Allen, C.D., Macalady, A.K., Chenchouni, H., Bachelet, D., McDowell, N., Vennetier, M., Kitzberger, T., Rigling, A., Breshears, D.D., Hogg, E.H., Gonzalez, P., Fensham, R., Zhang, Z., Castro, J., Demidova, N., Lim, J.-H., Allard, G., Running, S.W., Semerci, A., Cobb, N., 2010. A global overview of drought and heat induced tree mortality reveals emerging climate change risk for forests. For. Ecol. Manage. 259, 660–684.

Asada, K., 1996. Radical production and scavenging in the chloroplasts. In: Baker, N.R. (Ed.), Photosynthesis and the Environment. Kluwer Academic publishers, Dordrecht, pp. 123–150.

Bradford, M., 1976. A rapid and sensitive method for the quantification of microgram quantities of protein utilizing the principle of protein-dye-binding. Anal. Biochem. 72, 248–254.

Calvo, O.C., Franzaring, J., Schmid, I., Muller, M., Brohon, N., Fangmeier, A., 2017. Atmospheric CO_2 enrichment and drought stress modify root exudation of barley. Glob. Change Biol. 23, 1292–1304.

Cousins, A., Adam, N., Wall, G., Kimball, B., Pinter, P., Ottman, M., Leavitt, S., Webber, A., 2002. Photosystem II energy use, non-photochemical quenching and the xanthophyll cycle in Sorghum bicolor grown under drought and free-air CO_2 enrichment (FACE) conditions. Plant Cell Environ. 25, 1551–1559.

Duarte, B., Santos, D., Marques, J.C., Caçador, I., 2013. Ecophysiological adaptations of two halophytes to salt stress: photosynthesis, PS II photochemistry and anti-oxidant feedback – Implications for resilience in climate change. Plant Physiol. Biochem. 67, 178–188.

Duarte, B., Silva, H., Marques, J.C., Caçador, I., Sleimi, N., 2014a. Light-dark O_2 dynamics in submerged leaves of C_3 and C_4 halophytes under increased dissolved CO_2: clues for saltmarsh response to climate change. Ann. Bot. Plants 6, plu067.

Duarte, B., Santos, D., Silva, H., Marques, J.C., Caçador, I., 2014b. Photochemical and biophysical feedbacks of C_3 and C_4 mediterranean halophytes to atmospheric CO_2 enrichment confirmed by their stable isotope signatures. Plant Physiol. Biochem. 80, 10–22.

Duarte, B., Marques, J.C., Caçador, I., 2015. Impact of extreme heat and cold events on the energetic metabolism of the C_3 halophyte *Halimione portulacoides*. Estuar. Coast. Shelf Sci. 167, 166–177.

Evans, J.R., 1989. Photosynthesis and nitrogen relationships in leaves of C_3 plants. Oecologia 78, 9–19.

Geissler, N., Hussin, S., Koyro, H.W., 2009. Elevated atmospheric CO_2 concentration ameliorates effects of NaCl salinity on photosynthesis and leaf structure of *Aster tripolium* L. J. Exp. Bot. 60, 137–151.

Geissler, N., Hussin, S., Koyro, H.W., 2010. Elevated atmospheric CO_2 concentration enhances salinity tolerance in *Aster tripolium* L. Planta 231, 583–594.

Ghannoum, O., von Caemmerer, S., Ziska, L.H., Conroy, J.P., 2000. The growth response of C_4 partial pressure: a reassessment. Plant Cell Environ. 23, 931–942.

Guo, H.Y., Zhu, J.K., Zhou, H., Sun, Y.Y., Yin, Y., Pei, D.P., Ji, R., Wu, J.C., Wang, X.R., 2011. Elevated CO_2 levels affects the concentrations of copper and cadmium in crops grown in soil contaminated with heavy metals under fully open-air field conditions. Environ. Sci. Technol. 45, 6997–7003.

Guo, B., Dai, S., Wang, R., Gua, J., Ding, Y., 2015. Combined effect of elevated CO_2 and Cd-contaminated soil on the growth gas exchange, antioxidant defense, and Cd accumulation of poplars and willows. Environ. Exp. Bot. 115, 1–10.

Guy, R.D., Reid, D.M., Krouse, H.R., 1986. Factors affecting 13C/12C ratios of inland halophytes: I. Controlled studies on growth and isotopic composition *of Puccinellia nuttalliana*. Can. J. Bot. 64, 2693–2699.

Heath, R.L., Packer, L., 1968. Photoperoxidation in isolated chloroplasts I. Kinetics and stoichiometry of fatty acid peroxidation. Arch. Biochem. Biophys. 125, 189–198.

Hussin, S., Geissler, N., El-Far, M.M.M., Koyro, H.W., 2017. Effects of salinity and short-term elevated atmospheric CO_2 on the chemical equilibrium between CO_2 fixation and photosynthetic electron transport of *Stevia rebaudiana* Bertoni. Plant Physiol. Biochem. http://dx.doi.org/10.1016/j.plaphy.2017.06.017.

Jia, Y., Tang, S., Ju, X., Shu, L., Tu, S., Feng, R., Giusti, L., 2011. Effects of elevated CO_2 level on root morphological traits and Cd uptakes of two Lolium species under Cd stress. J. Zhejiang Univ.–Sci. B (Biomed. Biotechnol.) 12, 313–325.

Jia, X., Liu, T., Zhao, Y.H., He, Y.H., Yang, M.Y., 2016. Elevated atmospheric CO_2 affected photosynthetic products in wheat seedlings and biological activity in rhizosphere soil under cadmium. Environ. Sci. Pollut. Res. 23, 514–526.

Küpper, H., Seibert, S., Aravind, P., 2007. A fast, sensitive and inexpensive alternative to analytical pigment HPLC: quantification of chlorophylls and carotenoids in crude extracts by fitting with Gauss-peak-spectra. Anal. Biochem. 79, 7611–7627.

Kabata-Pendias, A., Pendias, H., 2001. Trace Elements in Soils and Plants. CRC Press, Boca Ratón, Florida.
Lenssen, G.M., Lamers, J., Stroetenga, M., Rozema, J., 1993. Interactive effects of atmospheric CO_2 enrichment, salinity and flooding on growth of C_3 (Elymus athericus) and C_4 (Spartina anglica) salt species. Vegetatio 104/105, 379–388.
Lenssen, G.M., van Duin, W.E., Jak, P., Rozema, J., 1995. The response of *Aster tripolium* and *Puccinellia maritima* to atmospheic carbon dioxide enrichment and their interactions with flooding and salinity. Aquat. Bot. 50, 181–192.
Li, Z.Y., Tang, S.R., Deng, X.F., Wang, R.G., Song, Z.G., 2010. Contrasting effects of elevated CO_2 on Cu and Cd uptake by different rice varieties grown on contaminated soil with two levels of metals: implication for phytoextraction and food safety. J. Hazard. Mater. 177, 352–361.
Li, T.Q., Di, Z.Z., Han, X., Yang, X.E., 2012. Elevated CO_2 improves root growth and cadmium accumulation in the hyperaccumulator *Sedum alfredii*. Plant Soil 354, 325–334.
Makino, A., Sakashita, H., Hidema, J., Mae, T., Ojima, K., Osmond, B., 1992. Distinctive responses of ribulose-1, 5-bisphosphate carboxylase and carbonic anhydrase in wheat leaves to nitrogen nutrition and their possible relationships to CO_2 transfer resistance. Plant Physiol. 100, 1737–1743.
Mallick, N., Mohn, F.H., 2003. Use of chlorophyll fluorescence in metal-stress research: a case of study with the green microalga Scenedesmus. Ecotoxicol. Environ. Saf. 55, 64–69.
Marklund, S., Marklund, G., 1974. Involvement of superoxide anion radical in the autoxidation of pyrogallol and a convenient assay for superoxide dismutase. Eur. J. Biochem. 47, 464–469.
Marshall, H.J., Geider, R.J., Flynn, K.J., 2000. A mechanistic model of photoinhibition. New Phytol. 145, 347–359.
Mateos-Naranjo, E., Redondo-Gómez, S., Silva, J., Santos, R., Figueroa, M.E., 2007. Effect of prolonged flooding on the invader *Spartina densiflora* Brong. J. Aquat. Plant Manage. 45, 121–123.
Mateos-Naranjo, E., Redondo-Gómez, S., Cambrollé, J., Figueroa, M.E., 2008a. Growth and photosynthetic responses to copper stress of an invasive cordgrass, *Spartina densiflora*. Mar. Environ. Res. 66, 459–465.
Mateos-Naranjo, E., Redondo-Gómez, S., Cambrollé, J., Luque, T., Figueroa, M.E., 2008b. Growth and photosynthetic responses to zinc stress of an invasive cordgrass, *Spartina densiflora*. Plant Biol. 10, 754–762.
Mateos-Naranjo, E., Redondo-Gómez, S., Álvarez, A., Cambrollé, J., Bandullo, J., Figueroa, M.E., 2010a. Synergic effect of salinity and CO_2 enrichment on growth and photosynthetic responses of the invasive cordgrass *Spartina densiflora*. J. Exp. Bot. 61, 1643–1654.
Mateos-Naranjo, E., Redondo-Gómez, S., Andrades-Moreno, L., Davy, A.J., 2010b. Growth and photosynthetic responses of the cordgrass *Spartina maritima* to CO_2 enrichment and salinity. Chemosphere 81, 725–731.
Mateos-Naranjo, E., Andrades-Moreno, L., Redondo-Gómez, S., 2011. Comparison of germination, growth, photosynthetic responses and metal uptake between three populations of *Spartina densiflora* under different soil pollutions conditions. Ecotoxicol. Environ. Saf. 74, 2040–2049.
Mateos-Naranjo, E., Gallé, A., Florez-Sarasa, I., Perdomo, J.A., Galmés, J., Ribas-Carbó, M., Flexas, J., 2015. Assessment of the role of silicon in the Cu-tolerance of the C_4 grass *Spartina densiflora*. J. Plant Physiol. 178, 74–83.
Melis, A., 1999. Photosystem-II damage and repair cycle in chloroplasts: what modulates the rate of photodamage in vivo? Trends Plant Sci. 4, 130–135.
Nalewajko, C., Olaveson, M.M., 1995. Differential responses of growth, photosynthetic, respiration and phosphate uptake to copper in copper-tolerant and copper-intolerant strains of *Scenedesmus acutus* (Chlorophyceae). Can. J. Bot. 73, 1295–1303.
Occhipinti-Ambrogi, A., 2007. Global change and marine communities: alien species and climatic change. Mar. Pollut. Bull. 55, 342–352.
Redondo-Gómez, S., Mateos-Naranjo, E., Figueroa, M.E., Davy, A.J., 2010. Salt stimulation of growth and photosynthesis in an extreme halophyte, *Arthrocnemum macrostachyum*. Plant Biol. 12, 79–87.
Rozema, J., 1993. Plant responses to atmospheric carbon dioxide enrichment: interactions with some soil and atmospheric condictions. Vegetatio 104/105, 173–190.
Schreiber, U., Schliwa, W., Bilger, U., 1986. Continuous recording of photochemical and non-photochemical chlorophyll fluorescence quenching with a new type of modulation fluorometer. Photosynth. Res. 10, 51–62.
Setter, T.L., Waters, I., Wallace, I., Bhekasut, P., Greenway, H., 1989. Submergence of rice I: growth and photosynthetic response to CO_2 enrichment of floodwater. Aust. J. Plant Physiol. 16, 251–263.
Song, N.N., Wang, F.L., Zhang, C.B., Tang, S.R., Guo, J.K., Ju, X.H., Smith, D.L., 2013. Fungal inoculation and elevated CO_2 mediate growth of *Lolium mutiforum* and *Phytolacca americana* metal uptake, and metal bioavailability in metalcontaminated soil: evidence from DGT measurement. Int. J. Phytoremediat. 15, 268–282.
Song, N., Ma, Y., Zhao, Y., Tang, S., 2015. Elevated ambient carbon dioxide and *Trichoderma inoculums* could enhance cadmium uptake of *Lolium perenne* explained by changes of soil pH, cadmium availability and microbrial biomass. Appl. Soil Ecol. 85, 56–64.
Strasser, R.J., Tsimilli-Michael, M., Srisvastava, A., 2004. Analysis of the chlorophyll-a fluorescence transient. In: Papageorgiou, G.C., Govindjee (Eds.), Advances in Photosynthesis and Respiration. Springer, Berlin, pp. 321–362.
Tang, S., Xi, L., Zheng, J., Li, H., 2003. Responses to elevated CO_2 of indian mustard and sunflower growing on copper contaminated soil. Bull. Environ. Contam. Toxicol. 71, 988–997.
Teranishi, Y., Tanaka, A., Osumi, M., Fukui, S., 1974. Catalase activities of hydrocarbon-utilizing Candida yeast. Agri. Biol. Chem. 38, 1213–1220.
Tian, S., Jia, Y., Ding, Y., Wang, R., Feng, R., Song, Z., Guo, J., Zhou, L., 2014. Eleavated atmospheric CO_2 enhances copper uptake in crops and pasture species grown in copper-contaminated soils in a micro-plot study. Clean–Soil Air Water 42, 347–354.
Tiryakioglu, M., Eker, S., Ozkutlu, F., Husted, S., Cakmak, I., 2006. Antioxidant defense system and cadmium uptake in barley genotypes differing in cadmium tolerance. J. Trace Elem. Med. Biol. 20, 181–189.
Wall, G.W., Brooks, T.J., Adam, N.R., Cousings, B.A., Kimball, B.A., Pinter, P.J., LaMorte, R.L., Triggs, J., Ottman, M.J., Leavitt, S.W., Matthias, A.D., Williams, D.G., Webber, A.N., 2001. Elevated atmospheric CO_2 improved sorghum plant water status by ameliorating the adverse effects of drought. New Phytol. 152, 231–248.
Wang, R.G., Dai, S.X., Tang, S.R., Tian, S., Song, Z.G., Deng, X.F., Ding, Y.Z., Zou, X.J., Zhao, Y.J., Smith, D.L., 2012. Growth gas exchange, root morphology and cadmium uptake responses of poplars and willows grown on cadmium contaminated soil to elevated CO_2. Environ. Earth Sci. 67, 1–13.
Zheng, J.M., Wang, H.Y., Li, Z.Q., Tang, S.R., Chen, Z.Y., 2008. Using elevated carbon dioxide to enhance copper accumulation in *Pteridium revolutum*, a copper-tolerant plant, under experimental conditions. Int. J. Phytopharm. 10, 161–172.
Zhou, W., Zhao, D., Lin, X., 1997. Effects of waterlogging on nitrogen accumulation and alleviation of waterlogging damage by application of nitrogen fertilizer and Mixtalol in winter rape (*Brassica napus L.*). J. Plant Growth Regul. 16, 47–53.

CAPÍTULO 6:

Salinity alleviates zinc toxicity in the saltmarsh zinc-accumulator *Juncus acutus*

Mateos-Naranjo et al., 2018, Ecotoxicology and Environmental Safety

Ecotoxicology and Environmental Safety 163 (2018) 478–485

Contents lists available at ScienceDirect

Ecotoxicology and Environmental Safety

journal homepage: www.elsevier.com/locate/ecoenv

Salinity alleviates zinc toxicity in the saltmarsh zinc-accumulator *Juncus acutus*

Enrique Mateos-Naranjo[a,*], Jesús Alberto Pérez-Romero[a], Susana Redondo-Gómez[a], Jennifer Mesa-Marín[a], Eloy Manuel Castellanos[b], Anthony John Davy[c]

[a] Departamento de Biología Vegetal y Ecología, Facultad de Biología, Universidad de Sevilla, 1095, 41080 Sevilla, Spain
[b] Departamento de Biología Ambiental y Salud Pública, Facultad de Ciencias Experimentales, Universidad de Huelva, 21071 Huelva, Spain
[c] Centre for Ecology, Evolution and Conservation, School of Biological Sciences, University of East Anglia, Norwich Research Park, Norwich NR4 7TJ, UK

ARTICLE INFO

Keywords:
Chlorophyll fluorescence
Gas exchange
Halophyte
Photoinhibition
Salinity
Zn-stress

ABSTRACT

The potential importance of *Juncus acutus* for remediation of Zn-contaminated lands has been recognized, because of its Zn tolerance and capacity to accumulate Zn. Since it is also a halophyte, the extent to which salinity influences its Zn tolerance requires investigation. A factorial greenhouse experiment was designed to assess the effect of NaCl supply (0 and 85 mM NaCl) on the growth, photosynthetic physiology and tissue ions concentrations of plants exposed to 0, 30 and 100 mM Zn. Our results indicated that NaCl supplementation alleviated the effects of Zn toxicity on growth, as Zn at 100 mM reduced relative growth rate (RGR) by 60% in the absence of NaCl but by only 34% in plants treated also with NaCl. This effect was linked to a reduction in Zn tissue concentrations, as well as to overall protective effects on various stages in the photosynthetic pathway. Thus, at 85 mM NaCl plants were able to maintain higher net photosynthesis (A_N) than in the absence of added NaCl, although there were no differences in stomatal conductance (g_s). This contributed to preserving the trade-off between CO_2 acquisition and water loss, as indicated by higher intrinsic water use efficiency ($_i$WUE). Hence, A_N differences were ascribed to limitation in the RuBisCO carboxylation, manifested as higher intercellular CO_2 concentration (C_i), together with dysfunction of PSII photochemistry (in term of light harvest and energy excess dissipation), as indicated by higher chronic photoinhibition percentages and variations in the photosynthetic pigment profiles in presence of Zn under non-saline conditions.

1. Introduction

Juncus acutus L., is a caespitose, halophytic rush, with a sub-cosmopolitan distribution, that inhabits coastal marshes and dune slacks encompassing a wide range of salinity (Fernández-Carvajal, 1982). Together with various other *Juncus* species, it has been proposed as a bio-tool for wetland restoration projects around the world (Sparks et al., 2013; Marques et al., 2011). In particular, it has potential for the remediation of metal pollution, since it shows great tolerance to excess metals and the capacity to accumulate large amounts of them in its tissues without serious symptoms of toxicity (Mateos-Naranjo et al., 2014; Santos et al., 2014; Christofilopoulos et al., 2016). Medas et al. (2017) have recently suggested that *J. acutus* is able to optimize its response to metal pollution by tuning different biomineralization mechanisms with the minerals and geochemical conditions of the site. Previous studies of metal accumulation and its effects on the performance *J. acutus* have focused on zinc (Mateos-Naranjo et al., 2014; Santos et al., 2014; Christofilopoulos et al., 2016; Medas et al., 2017), although recently interactions of Zn with Cr, Ni and Cd have also been assessed (Christofilopoulos et al., 2016).

Zinc is an essential element for plant metabolism (Kabata-Pendias and Pendias, 2001). However, its excess can lead to various phytotoxicity effects on plant metabolism (Chaney, 1993), including on that of halophytic species (Liu et al., 2016). The photosynthetic apparatus (i.e. Calvin cycle and photosystem functionality) is especially sensitive to this ion excess (Van Assche and Clijsters, 1986). Despite such potentially deleterious effects, *J. acutus* is regarded as Zn-hypertolerant, a feature attributable to a series of physiological and biochemical adaptations. In particular, Mateos-Naranjo et al. (2014) showed that carbon assimilation and the efficiency of PSII were not affected by high concentrations of Zn in the culture solution. Furthermore, Santos et al. (2014) found that maintenance of the functionality of its photosynthetic apparatus was linked with its ability to overcome oxidative damage produced by excess Zn uptake, through the modulation of its

* Correspondence to: Dpto. Biología Vegetal y Ecología, Facultad de Biología, Universidad de Sevilla, Av Reina Mercedes s/n, 41012 Sevilla, Spain.
E-mail address: emana@us.es (E. Mateos-Naranjo).

https://doi.org/10.1016/j.ecoenv.2018.07.092
Received 31 January 2018; Received in revised form 21 July 2018; Accepted 23 July 2018
Available online 31 July 2018

antioxidant enzymatic machinery and efficient dissipation of the cellular redox potential consequent on Zn incorporation into chlorophyll molecules. These studies however, did not take account of the potential interaction of Zn with other important factors characteristic of marshes ecosystems, particularly salinity. It has been demonstrated that the accumulation of sodium in another halophyte, *Spartina densiflora*, can mitigate its responses to Zn-induced stress (Redondo-Gómez et al., 2011). Hence knowledge of the extent to which salinity might modulate the physiological responses of *J. acutus* to excess Zn is necessary for a realistic assessment of its metal toxicity thresholds and its potential for the remediation of zinc-polluted saltmarshes.

This study employed a factorial experiment which aimed to: (1) investigate the influence of NaCl on the growth responses of *J. acutus* plants exposed to different Zn concentrations; (2) determine the extent to which this influence could be accounted for by impacts on its photosynthetic apparatus, both in terms of carbon assimilation and efficiency of light-energy use, and (3) assess the nutrient and Zn accumulation patterns consequent on the joint effects of treatment with elevated NaCl and Zn.

2. Material and methods

2.1. Plant material

Seeds of *Juncus acutus* were collected in December 2013 from different individuals (n = 20) randomly selected from a well-established population in Doñana National Park (Huelva, SW Spain). The seeds were transported to the laboratory for germination in a germination chamber (ASL Aparatos Científicos M-92004, Madrid, Spain) under the following conditions: photoperiod, 16/8 h light/darkness; temperature, 24/15 °C; photon flux rat (400–700 nm), 35 μmol m^{-2} s^{-1}. Germinated seedlings were immediately transferred to individual plastic pots (12 cm in depth, 0.5 L total volume) filled with perlite and placed in a glasshouse (University of Seville, Greenhouse Service) at controlled temperature of 25 ± 3 °C, and a relative humidity of 40–60%, with natural day light (maximum quantum flux rate of 1000 μmol m^{-2} s^{-1}). Pots were irrigated with nutrient solution (Hoagland and Arnon, 1938) before the onset of the experimental treatments.

2.2. Zn and NaCl experimental stress treatments

In June 2014, pots containing the *J. acutus* plants were randomly assigned to three Zn treatments (concentrations of 0, 30 and 100 mM) in factorial combination with two NaCl concentrations (0 and 85 mM) for 40 days. Zn and NaCl concentrations were established by combining Hoagland´s solution with appropriate amounts of $ZnSO_4{\cdot}7H_2O$ and NaCl, respectively. Thus, at the beginning of the experiment, the pots were placed in plastic trays containing appropriate solutions to a depth of 1 cm (10 replicate pots per stress treatment combination). In order to avoid changes of Zn and NaCl concentration caused by water evaporation from the nutrient solution, levels in the trays were monitored continuously throughout the experimental and topped up to the marked level with Hoagland's solution (without additional $ZnSO_4{\cdot}7H_2O$ or NaCl). Furthermore, pH of the solution was monitored and adjusted to 6.5–7.0. The entire solution (including $ZnSO_4{\cdot}7H_2O$ and NaCl) in the trays was renewed weekly and their positions were changed randomly every 2 days to avoid effects of environmental heterogeneity inside the glasshouse.

After 40 days of exposure to the stress-inducing treatments, measurements of growth, gas exchange, chlorophyll fluorescence, photosynthetic pigment concentrations and tissue ion concentrations were made.

2.3. Growth measurements

Four plants from each treatment were harvested at the beginning of the experiment and a further ten at the end. Plants were divided in roots and shoots and these biomass fractions were oven dried (60 °C for 48 h) and then weighed. In addition, the number of dead tillers was recorded at the end of the experiment.

The relative growth rate (RGR) of whole plants was calculated using the formula:

$$RGR = (\ln B_f - \ln B_i)\cdot D^{-1} (g\ g^{-1}\ day^{-1})$$

where B_f = final dry mass, B_i = initial dry mass (the mean of the four plants from each treatment sampled at the beginning of the experiment) and D = duration of experiment (days).

2.4. Photosynthetic physiology

Gas exchange and chlorophyll fluorescence parameters were measured on the same sections of randomly selected, fully developed photosynthetic tillers (n = 10) using an infrared gas analyzer (LI-6400-XT, Li-COR Inc., NE., USA) and a modulated fluorimeter (FMS-2; Hansatech Instruments Ltd., UK), respectively. The following gas exchange parameters were recorded at a light flux density of 1500 μmol photons m^{-2} s^{-1}, ambient CO_2 concentration (C_a) 400 μmol mol^{-1} air, leaf temperature of 25 °C and 50 ± 5% relative humidity: net photosynthetic rate (A_N), stomatal conductance (g_s), intercellular CO_2 concentration (C_i), and intrinsic water use efficiency ($_i$WUE). The saturation pulse method was used to determine the energy yields of the Photosystem II (PSII) reaction centers: maximum quantum efficiency of PSII photochemistry (F_v/F_m), quantum efficiency of PSII (Φ_{PSII}; Genty et al., 1989) and non-photochemical quenching (NPQ). As described by Schreiber et al. (1986), a 0.8 s saturating actinic light pulse of 15000 μmol m^{-2} s^{-1} was given, at dawn (stable, 50 μmol m^{-2} s^{-1} ambient light) and midday (1700 μmol photons m^{-2} s^{-1}), to photosynthetic tillers previously dark-adapted or exposed to light for 30 min.

Finally, the total chlorophyll a (Chl *a*), chlorophyll b (Chl *b*) and carotenoid (C*x* + *c*) contents of extracts obtained from randomly selected fully developed photosynthetic tillers (n = 5), were determined with a Hitachi U-2001 spectrophotometer (Hitachi Ltd., Japan), using three wavelengths (663.2, 646.8 and 470.0 nm). For more details, see Mateos-Naranjo et al. (2008). Concentrations of pigments (μg g^{-1} fw) were calculated according to Lichtenthaler (1987).

2.5. Tissues ion concentrations

Tiller and root samples taken from ten plants per treatment were dried at 80 °C for 48 h and ground, according to the protocols of Mateos-Naranjo et al. (2011). Then, triplicate 0.5 g samples from each specific tissue were digested in 6 ml HNO3, 0.5 ml HF and 1 ml H_2O_2. Ca, Mg, K, P, Na and Zn concentrations in the digests were measured by inductively coupled plasma (ICP) spectroscopy (ARL-Fison 3410, USA).

2.6. Statistical analysis

Statistical tests were performed in the software package Statistica v. 6.0 (Statsoft Inc.). Generalized linear models (GLM) were used to analyze the interactive effects of Zn and NaCl concentrations (as categorical factors) on the growth and physiological parameters (as dependent variables) of *J. acutus* plants. Multiple comparisons were analyzed by a LSD (post hoc) test. Before statistical analysis Kolmogorov-Smirnov and Brown-Forsythe tests were used to verify the assumptions of normality and homogeneity of variances, respectively. Differences between tiller and root ion concentrations were compared by the Student test (*t*-test).

Table 1
Generalized linear model (GLM) results for the growth, physiological characteristics and tissue-ion concentrations of *J. acutus* plants in response to Zn and NaCl concentration (as categorical variables) and their interaction. * Significance level 95% and ** Significance level 99%. Md (mid-day), Pd (predawn), T (tiller) and R (root).

Parameter	*Na*	*Zn*	*Na × Zn*
RGR	0.03*	0.00**	0.06
Dead tillers (%)	0.07	0.00**	0.19
A_N	0.02*	0.00**	0.01*
g_s	0.30	0.00**	0.06
C_i	0.04*	0.05	0.22
$_i$WUE	0.02*	0.00**	0.03*
$F_v/F_{m,\ Md}$	0.00*	0.00**	0.02*
$F_v/F_{m,\ Pd}$	0.00**	0.00**	0.02*
$\Phi_{PSII,\ Md}$	0.09	0.00**	0.02*
$\Phi_{PSII,\ Pd}$	0.01**	0.00**	0.06
$NPQ_{,\ Md}$	0.01**	0.00**	0.10
$NPQ_{,\ Pd}$	0.63	0.51	0.62
Chl *a*	0.00**	0.88	0.00**
Chl *b*	0.06	0.57	0.04*
Cx + *c*	0.02*	0.22	0.04*
$[Zn]_T$	0.00**	0.00**	0.00**
$[Zn]_R$	0.00**	0.00**	0.00**
$[Na]_T$	0.00**	0.00**	0.00**
$[Na]_R$	0.00**	0.00**	0.00**
$[K]_T$	0.95	0.58	0.47
$[K]_R$	0.00**	0.00**	0.00**
$[Mg]_T$	0.00**	0.00**	0.00**
$[Mg]_R$	0.00**	0.00**	0.00**
$[Ca]_T$	0.00**	0.00**	0.00**
$[Ca]_R$	0.00**	0.00**	0.00**
$[P]_T$	0.02*	0.00**	0.04*
$[P]_R$	0.00**	0.00**	0.01**
$[Mn]_T$	0.78	0.00**	0.88
$[Mn]_R$	0.00**	0.00**	0.00**

3. Results

3.1. Effects of Zn and NaCl on growth

There were significant effects of both zinc and salinity on the RGR of *Juncus acutus* but no significant interactions (Table 1, GLM: salinity, $p < 0.05$; Zn, $p < 0.01$). Thus, in non-saline conditions RGR decreased 25% and 60% in plants grown at 30 and 100 mM Zn, respectively, compared to control; however, growth was much less affected by Zn in plants exposed to 85 mM NaCl (i.e. 11% and 34% for 30 and 100 mM Zn, respectively; Fig. 1A). Similarly, the percentage of dead tillers increased sharply with Zn concentration (GLM: Zn, $p < 0.01$), but this increase was less acute in plants grown in saline conditions (GLM: salinity, $p = 0.07$; Fig. 1B).

3.2. Effects of Zn and NaCl on photosynthetic physiology

There were significant effects of salinity and Zn treatments on net photosynthetic rate (A_N) after 40 d of treatment (Table 1, GLM: salinity, $p < 0.05$; Zn, $p < 0.01$ and salinity × Zn, $p < 0.01$). Thus A_N decreased progressively with increasing Zn concentration in plants grown at both NaCl concentrations. However, plants exposed to saline conditions maintained higher CO_2 assimilation rates at both increased concentrations of Zn than their non-saline counterparts (Fig. 2A). Very similar trends were recorded for stomatal conductance (g_s) but salinity did not significantly affect the responses to Zn (GLM: salinity × Zn, $p = 0.06$; Fig. 2B). In contrast, salinity significantly reduced the intercellular CO_2 concentration (C_i) (GLM: salinity, $p < 0.05$), whereas Zn concentration per se did not. However, C_i values were reduced at the high salinity only in the presence of excess (30 or 100 mM) Zn (Fig. 2C). Salinity and Zn had synergistic effects on intrinsic water use efficiency ($_i$WUE; GLM: salinity × Zn, $p < 0.05$). Thus, plants grown under saline conditions had consistently higher $_i$WUE but the difference was only significant at 30 mM Zn (Fig. 2D).

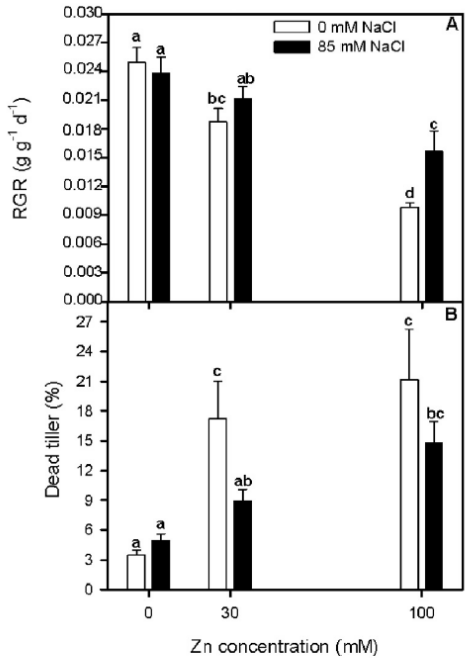

Fig. 1. Relative growth rate, RGR (A) and percentage of dead tillers (B) in *Juncus acutus* plants in response to a treatment with a range of Zn concentration with (•) and without (○) NaCl addition, after 40 days. Values represent mean ± SE, n = 10. Different letters indicate means that are significantly different from each other (LSD test, $P < 0.05$).

Chlorophyll fluorescence parameters were also affected by the combination of Zn and salinity treatments. F_v/F_m values, both at dawn and midday, tended to decrease with increasing Zn concentration in plants grown in non-saline conditions. However, in plants exposed to salinity, this effect was less marked and only evident at the highest Zn concentration treatment (Table 1, $GLM_{Md\ and\ Pd}$: salinity × Zn, $p < 0.05$; Fig. 3A, B). Φ_{PSII} values at dawn and at midday followed a similar pattern to those of F_v/F_m (GLM_{Md}: salinity × Zn, $p < 0.05$; Fig. 3C, D), except that the differences in predawn values were minimal. NPQ values at midday increased markedly with Zn concentration, both in the absence and presence of salinity, but this effect was substantially stronger in the absence of salinity (Table 1, GLM_{Md}: salinity, $p < 0.01$ and Zn, $p < 0.001$; Fig. 3E). Predawn NPQ did not show any response to Zn or salinity, with values c. 0.15 in all cases (Fig. 3F).

The percentage of chronic photoinhibition increased progressively with increasing Zn concentration at both NaCl concentrations (Fig. 4A, B). However, this increment was more acute in plants grown under non-saline conditions. The percentage of dynamic photoinhition did not vary with salinity or Zn treatments, except in plants grown at the highest Zn concentration and 85 mM NaCl, which showed a greater percentage inhibition than in the other treatments (Fig. 4A, B).

The concentration of chlorophyll a (Chl *a*) was decreased by excess Zn in the growth medium, although this reduction was entirely mitigated by salinity (Table 1, GLM: salinity × Zn, $p < 0.01$; Fig. 5A). Chlorophyll b (Chl *b*) and carotenoid (C*x* + *c*) concentrations did not show any response to excess Zn in plants grown in the absence of salinity, but they increased in those exposed to both Zn and salinity ($GLM_{Chl\ b\ and\ Cx+c}$: salinity × Zn, $p < 0.01$; Fig. 5B, C).

3.3. Effects of Zn and NaCl on tissue ion concentrations

Tissue ion concentrations were greater in roots than in tillers, except

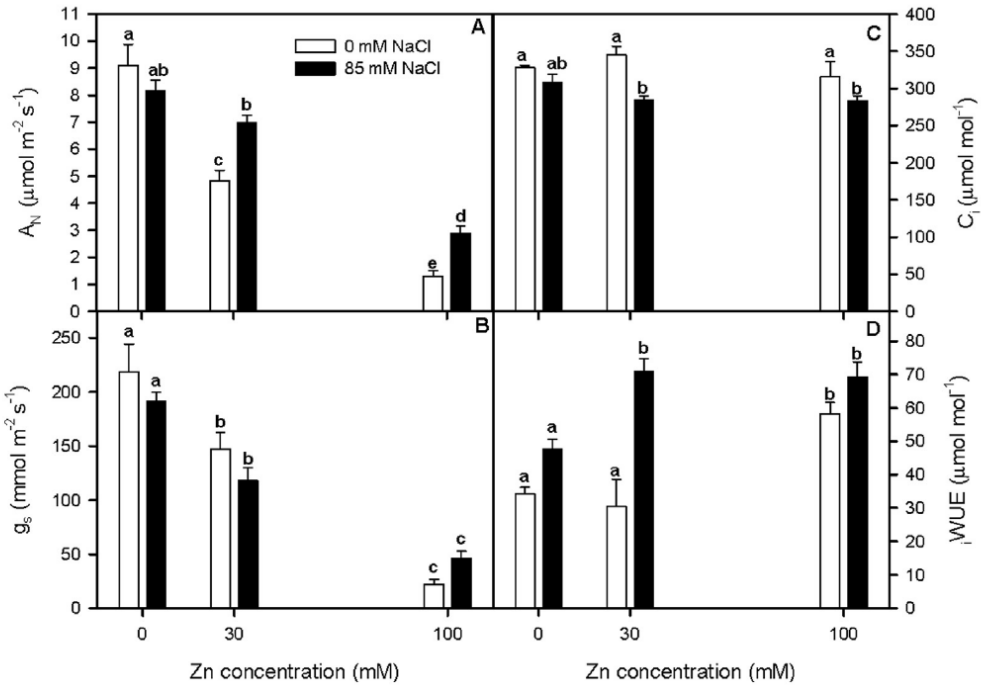

Fig. 2. Net photosynthetic rate, A_N (A), stomatal conductance, g_s (B), intercellular CO_2 concentration, C_i (C), and intrinsic water use efficiency, $_i$WUE (D) in randomly selected, fully developed photosynthetic tillers of *Juncus acutus* treated with a range of Zn concentration with (•) and without (○) NaCl addition, after 40 days. Values represent mean ± SE, n = 10. Different letters indicate means that are significantly different from each other (LSD test, $P < 0.05$).

for K in all specific treatments and for P in plants grown at 100 mM Zn + 0 mM NaCl, 0 mM Zn + 85 mM NaCl and 30 mM Zn + 85 mM NaCl, (*t*-test, $p < 0.05$; Table 2). In addition, there were significant effects of salinity and Zn treatments on tissue ion concentrations except for K and Mn tiller concentrations (Table 1). Thus Zn concentrations increased markedly with the concentration of Zn in the growth medium in both roots and tillers, but this increment was more acute in the absence of NaCl addition (GLM: salinity × Zn, $p < 0.01$; Table 2). Furthermore, tissue Na concentrations were considerably greater under saline conditions and tended to increase with the Zn concentration. Except for roots in presence of NaCl, where Na concentration showed a reduction with Zn augmentation (GLM: salinity × Zn, $p < 0.01$; Table 2). On the other hand, overall the concentrations of Mg, Ca, P and Mn in tillers and roots, and K in roots decreased with the increase of the concentration of Zn in the growth medium at both saline levels (Table 2). In general, the concentrations of these elements were significantly lower in plants grown with NaCl supplementation (Table 2).

4. Discussion

Understanding the effects of high metal concentrations on tolerant species and the thresholds for phytotoxicity is essential for the design and development of effective methodologies for environmental remediation. Similarly important is knowledge of possible interactions between metals, and between metals and other important environmental factors that may limit species distribution; in estuarine ecosystems interactions with salinity are relevant to the future use of halophytes that can cope with the growing problem of metal pollution of salinized lands (Kholodova et al., 2010).

This experiment confirmed previous work that had demonstrated hypertolerance to Zn stress in *Juncus acutus* (Mateos-Naranjo et al., 2014). Thus, the concentration of Zn required to kill 50% of its tillers after 40 days of exposure (LC_{50}; Paschke et al., 2000) was greater than our most severe treatment of 100 mM. However, elevated concentrations of Zn in the culture solution progressively affected plant development, and this was particularly reflected in a clear reduction of RGR and an increase in the percentage of dead tillers. These deleterious effects are consistent with previously described general responses of vascular plants to excess Zn (Vaillant et al., 2005; Mateos-Naranjo et al., 2008; Santos et al., 2014). Nevertheless, we found that Zn toxicity was partially counterbalanced by addition of NaCl to the growth medium, such that salinity-treated plants were able to maintain a higher RGR than their non-salinity treated counterparts. In addition, they reduced toxicity, as indicated by lower percentages of dead tillers at both 30 and 100 mM Zn. Therefore, the results suggest that salinity increases the tolerance of *J. acutus* to the toxic effects of high concentrations of Zn. This interaction is consistent with results for species not recognized as hypertolerant to Zn: Redondo-Gómez et al. (2011) demonstrated that the addition 170 mM NaCl to a growth medium with 1 mM Zn diminished the damage caused by metal excess in *Spartina densiflora*, and Han et al. (2013) reported similar amelioration of the effects of 100 µM Zn by the addition of 50 mM NaCl to the growth medium with in *Kosteletzkya virginica*.

The mechanisms by which NaCl supplementation could enhance plant tolerance to elevated metal concentrations are not clear. Effects on metal uptake and translocation, and the resulting nutrient uptake balance have been described in certain estuarine species (Fitzgerald et al., 2003; Kadukova and Kalogerakis, 2007; Han et al., 2013). Redondo-Gómez et al. (2011) found that NaCl supplementation increased Zn accumulation in *S. densiflora* tissues compared with non-salinized plants, but this was accompanied by an overall improvement in nutrient uptake. Similar modifications in mineral content were recorded in *Kosteletzkya virginica* tissues in response to salinity and Zn (Han et al., 2013), but in that case NaCl addition acted through a modification of Zn distribution rather than a decrease in plant Zn uptake capacity. In contrast, we found that although tissues Zn concentrations in *J. acutus* increased markedly with the external concentration in accordance with previous studies, this increase was progressively lower as tissue Na concentration increased in response to NaCl supplementation. Furthermore, salinity hindered the uptake of most nutrients in the highest Zn concentration. These discrepancies may be ascribed to the severity of stress imposed, since a maximum concentration of 100 mM Zn was used in the present study whereas Redondo-Gómez et al. (2011) and Han et al. (2013) used only 1 mM and 100 µM, respectively. Reduced nutrient concentrations with the progressive accumulation of Na in roots and shoots have been found

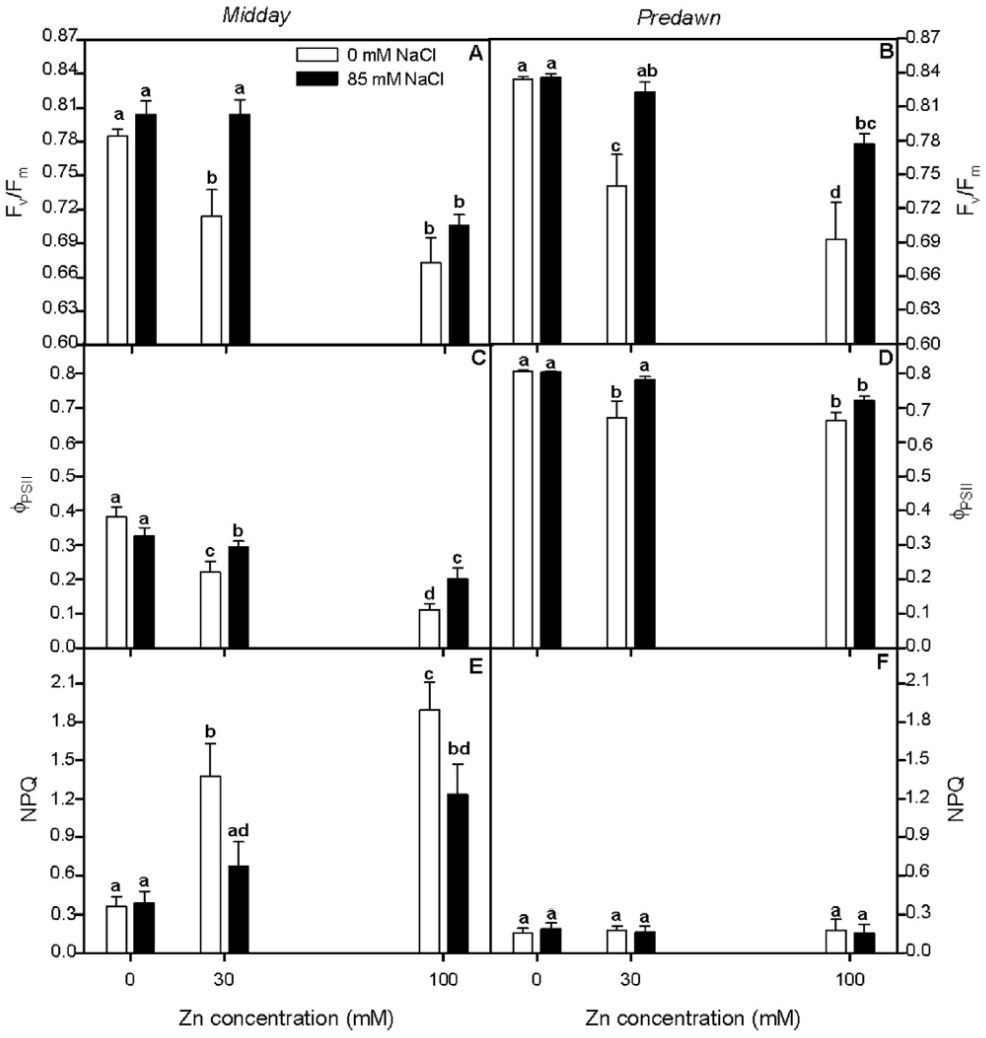

Fig. 3. Maximum quantum efficiency of PSII photochemistry, F_v/F_m (A, B), quantum efficiency of PSII, ΦPSII (B, C), and non-photochemical quenching, NPQ (D, E), at midday and predawn in randomly selected, fully developed photosynthetic tillers of *Juncus acutus* treated with a range of Zn concentration with (•) and without (○) NaCl addition, after 40 days. Values represent mean ± SE, n = 10. Different letters indicate means that are significantly different from each other (LSD test, $P < 0.05$).

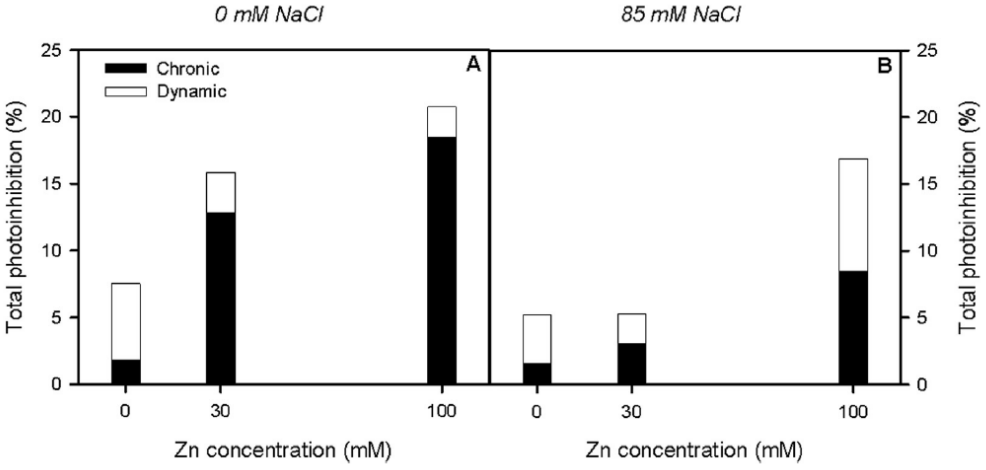

Fig. 4. Total chronic and (•) and dynamic (○) photoinhibition percentage in randomly selected, fully developed photosynthetic tillers of *Juncus acutus* treated with a range of Zn concentration at 0 mM (A) and 85 mM (B) NaCl concentration, after 40 days. Values represent absolute percentage per each treatment.

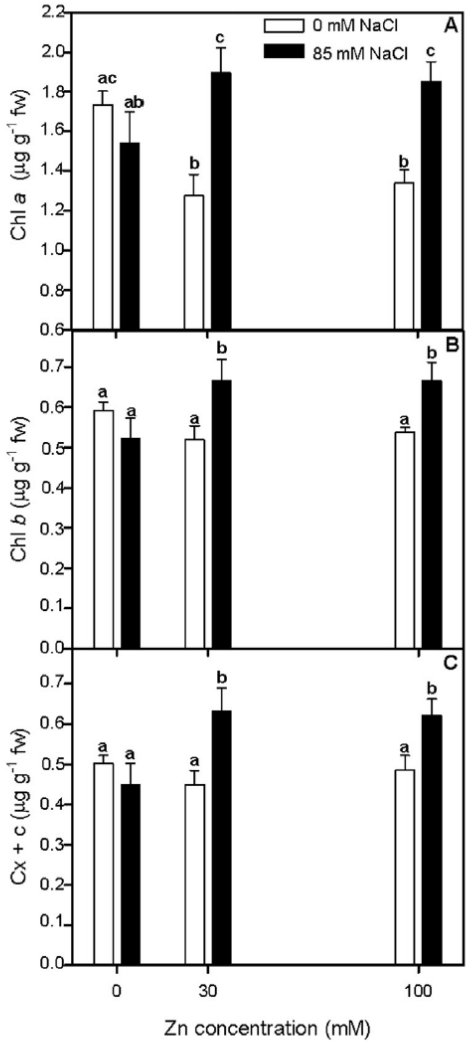

Fig. 5. Chlorophyll a, Chl *a* (A), chlorophyll b, Chl *b* (B) and carotenoids, C*x* + *c* (C) concentrations in randomly selected, fully developed photosynthetic tillers of *Juncus acutus* treated with a range of Zn concentration with (•) and without (○) NaCl addition, after 40 days. Values represent mean ± SE, n = 5. Different letters indicate means that are significantly different from each other (LSD test, P < 0.05).

previously in other halophytes (Redondo-Gómez et al., 2007, 2010).

Notwithstanding the nutritional imbalance induced by Na accumulation, the lower concentrations of Zn in the tissues of plants grown in the presence of NaCl could help to explain their higher tolerance. Excess Zn accumulated in the tissues is likely to be toxic, affecting a variety of physiological and biochemical processes (Kabata-Pendias and Pendias, 2001). However, despite such reductions in tissue Zn concentration in *J. acutus*, it must be acknowledged that concentrations were still greater than the toxicity threshold for plants generally (Kabata-Pendias and Pendias, 2001). Consequently, other mechanisms must be involved in the ameliorative effect of NaCl on Zn toxicity in *J. acutus*.

Metal hypertolerance has been associated with various ecophysiological adaptations to metalliferous environments (Evangelou et al., 2004; Mateos-Naranjo et al., 2014; Santos et al., 2014). In particular, Mateos-Naranjo et al. (2014) indicated that Zn hypertolerance in *J. acutus* was linked with its capacity to maintain carbon assimilation and the efficiency of PSII even at Zn concentration of 100 mM. In contrast we found a clear deleterious effect of Zn at this concentration on the photosynthetic apparatus in the present experiment; this discrepancy may be attributable to different experimental and measurement conditions. Although A_N (along with g_s) decreased considerably with increasing Zn concentration, plants grown at 85 mM NaCl were able to maintain higher A_N values than their non-saline counterparts. However, this positive effect cannot be attributed to alleviation of stomatal limitation, since g_s values did not vary between salinity levels in either Zn treatment. Therefore, differences in A_N value between NaCl levels et each specific Zn concentration treatment could be explained by non-stomatal limitations (Flexas and Medrano, 2002). In this regard, Pérez-Romero et al. (2016) found that photosynthesis activity was more limited by mesophyll conductance (g_m) than g_s in *Salicornia ramosissima* in response to Cd. Moreover, g_m has been widely implicated in photosynthetic responses patterns to salinity (Flexas et al., 2012). Hence, it is possible that A_N differences between salinity levels in *J. acutus* plants at the same Zn concentration could be linked with g_m variations; however this area requires further research. Another possibility relates to impairment of major carbon-assimilation enzyme activities, such as RuBisCO that may degrade the photosynthetic pathway under metal stress (Perfus-Barbeoch et al., 2002; Khan and Khan, 2014). A degree of metal tolerance has been demonstrated in the maintenance such enzyme functions (Ying et al., 2010; Pérez-Romero et al., 2016). Taking into account these issues, the higher C_i in *J. acutus* plants grown without NaCl addition suggests that differences in carbon assimilation between salinity treatments could have been linked to limitation in RuBisCO carboxylation capacity (Mateos-Naranjo et al., 2008, 2014).

Table 2
Ion concentration in tillers and roots of *Juncus acutus* treated with a range of Zn concentration in combination with 0 mM and 85 mM NaCl, after 40 days. Values represent mean ± SE, n = 5.

Treatments								
Zn (mM)	NaCl (mM)	Zn (mg kg^{-1})	Na (mg g^{-1})	K (mg g^{-1})	Mg (mg g^{-1})	Ca (mg g^{-1})	P (mg g^{-1})	Mn (mg kg^{-1})
		Ion concentration						
0	0	32.3 ± 0.5^{a}	0.97 ± 0.1^{a}	29.9 ± 0.1^{a}	3.54 ± 0.3^{a}	5.89 ± 0.1^{a}	2.95 ± 0.2^{a}	35.5 ± 0.6^{a}
30	0	304.6 ± 1.4^{b}	1.84 ± 0.2^{b}	29.4 ± 0.3^{a}	3.19 ± 0.2^{a}	4.97 ± 0.2^{b}	2.39 ± 0.1^{b}	27.3 ± 0.3^{b}
100	0	611.7 ± 0.8^{c}	3.65 ± 0.2^{c}	30.2 ± 0.1^{a}	3.04 ± 0.1^{a}	4.09 ± 0.2^{c}	2.50 ± 0.2^{b}	23.9 ± 0.4^{c}
0	85	36.9 ± 0.6^{a}	7.75 ± 0.5^{d}	28.9 ± 0.5^{a}	3.31 ± 0.3^{a}	4.20 ± 0.2^{c}	2.89 ± 0.5^{a}	32.7 ± 0.2^{a}
30	85	248.5 ± 0.5^{d}	6.96 ± 0.1^{e}	29.7 ± 0.2^{a}	3.06 ± 0.2^{a}	3.85 ± 0.4^{c}	2.82 ± 0.2^{a}	27.3 ± 0.4^{b}
100	85	412.3 ± 1.1^{e}	8.41 ± 0.3^{d}	30.9 ± 0.3^{a}	2.83 ± 0.1^{b}	3.71 ± 0.3^{c}	2.52 ± 0.3^{b}	22.9 ± 0.1^{c}
		Root concentration						
0	0	87.3 ± 0.7^{a}	1.48 ± 0.1^{a}	28.9 ± 0.2^{a}	5.48 ± 0.2^{a}	15.84 ± 0.5^{a}	3.36 ± 0.5^{ab}	39.3 ± 0.2^{a}
30	0	2122.6 ± 1.3^{b}	2.92 ± 0.2^{b}	24.5 ± 0.3^{b}	4.60 ± 0.2^{a}	17.36 ± 0.2^{a}	4.25 ± 0.5^{a}	39.9 ± 0.4^{a}
100	0	2479.0 ± 0.3^{c}	5.78 ± 0.4^{c}	16.8 ± 0.4^{c}	4.07 ± 0.1^{b}	8.54 ± 0.2^{b}	2.39 ± 0.2^{b}	33.5 ± 0.1^{b}
0	85	58.4 ± 1.2^{d}	21.17 ± 0.2^{d}	20.2 ± 0.4^{b}	4.87 ± 0.2^{a}	13.27 ± 0.6^{a}	2.63 ± 0.1^{b}	33.5 ± 0.1^{b}
30	85	1455.4 ± 2.2^{e}	16.14 ± 0.3^{e}	20.5 ± 0.2^{b}	3.62 ± 0.1^{b}	8.67 ± 0.2^{b}	2.71 ± 0.1^{b}	27.5 ± 0.2^{c}
100	85	1969.2 ± 1.1^{f}	13.95 ± 0.4^{f}	17.3 ± 0.3^{c}	3.41 ± 0.2^{c}	4.89 ± 0.1^{c}	2.67 ± 0.1^{b}	26.4 ± 0.2^{c}

Different letters indicate means that are significantly different from each other. (LSD test, P < 0.05).

On the other hand, the greatest photosynthetic tolerance to Zn-induced stress under saline conditions was associated with the highest integrity and functionality of the photochemical apparatus of *J. acutus*. It is known that Zn is concentrated in chloroplasts and interacts with the PSII donor, inhibiting the photosynthetic fixation of CO_2 and the Hill reaction (Prasad and Strzalka, 1999). In addition, Monnet et al. (2001) indicated that the destruction of antenna pigments would affect the efficiency of PSII. Our results revealed that F_v/F_m and Φ_{PSII} values were affected by elevated Zn and this effect was more acute in plants grown in absence of NaCl, suggesting that NaCl alleviates Zn-induced, excess-light photoinhibition. Furthermore, under non-saline conditions and in presence of Zn, NPQ values were higher, which indicates that more of the absorbed energy would have been dissipated as heat and would not taken the photochemical pathway (Flexas et al., 2012). In line with our results, Padinha et al. (2000) and Mateos-Naranjo et al. (2008) also found that Zn stress affected the PSII photochemistry of the halophytes *Spartina maritima* and *S. densiflora*, respectively. Damage to photosynthetic components may lead to an increase of photoinhibition (Werner et al., 2002), a phenomenon that affects photosynthetic productivity and, consequently, plant growth (Melis, 1999). This fact could contribute to explaining our growth data, since chronic photoinhibition percentage increased in presence of Zn under non-saline conditions, whereas this increased photoinhibition was ameliorated under saline conditions, although less so in plants exposed to 100 mM Zn. However, these plants showed a greater dynamic photoinhition percentage compared to other treatments, which would indicate an overcompensation effect of the excess of energy fixed, through thermal dissipation mechanisms, thereby protecting the leaf from light-induced damage (Maxwell and Johnson, 2000). In addition, the benefit of NaCl supplementation to photosynthetic-pigment concentration in the presence of Zn could contribute to explaining its positive effects on the photosynthetic apparatus efficiency of *J. acutus*.

Finally the greater tolerance to Zn in plants treated with NaCl was linked with a better water balance, an idea supported by the overall higher $_i$WUE values. Thus, these plants would be able better to preserve the trade-off between CO_2 acquisition for growth and water loss, as indicated by the higher A_N and the invariable g_s values compared with their counterparts not treated with NaCl. Han et al. (2013) also found a positive effect of NaCl supplementation on water relations, in *Kosteletzkya virginica*, under Zn excess. This beneficial effect could be linked with the key role of Na accumulation in plant osmotic adjustment (Shabala et al., 2009). Hence, it is possible that the higher Na concentration in tissues of *J. acutus* under saline conditions and the reduction in g_s in the presence of Zn might help to alleviate any water stress ascribed to Zn toxicity.

5. Conclusions

We may conclude that the presence of NaCl in the growth medium, at concentrations representative of estuarine environments, considerably reduces the deleterious effects of elevated Zn concentrations on the growth and development of *J. acutus*. This beneficial effect was largely mediated by the reduction of Zn levels in *J. acutus* tissues, together with an overall protective effect on its photosynthetic apparatus, manifested as improved carbon harvesting, functionality of the photochemical apparatus (PSII) and photosynthetic pigment concentrations. Furthermore, amelioration by NaCl was linked with the maintenance of a more advantageous water balance. These ecophysiological characteristics would enhance the fitness and competitive ability of *J. acutus* in zinc-polluted estuaries and saltmarshes, providing a tolerant bio-tool for the management and restoration metal pollution in salinized lands.

Acknowledgements

This work has been supported by Ministerio de Economía y Competitividad (MINECO Project CGL2016-75550-R cofunded by FEDER). J.A Pérez-Romero thanks Ministerio de Educación, Cultura y Deporte for its personal financial support (FPU014/03987). We are grateful University of Seville Greenhouse General Services (CITIUS) for its collaboration and Antonio León for his technical assistance.

References

Chaney, R.L., 1993. Zinc phytotoxicity. In: Robson, A.D. (Ed.), Zinc in Soils and Plants. Kluwer Academic Press, New York, pp. 131–150.
Christofilopoulos, S., Syranidou, E., Gkavrou, G., Manousaki, E., Kalogerakis, N., 2016. The role of halophyte *Juncus acutus* L. in the remediation of mixed contamination in a hydroponic greenhouse experiment. J. Chem. Technol. Biotechnol. 91 (6), 1665–1674.
Evangelou, M.W., Daghan, H., Schaeffer, A., 2004. The influence of humic acids on the phytoextraction of cadmium from soil. Chemosphere 57, 207–213.
Fernández-Carvajal, M.C., 1982. Revisión del género *Juncus* L. en la Península Ibérica. An. Jardín Botánico Madr. 38, 417–467.
Fitzgerald, F.J., Caffrey, J.M., Nesaratnam, S.T., McLoughlin, P., 2003. Copper and lead concentrations in salt marsh plants on the Suir Estuary, Ireland. Environ. Pollut. 123, 67–74.
Flexas, J., Medrano, H., 2002. Drought-inhibition of photosynthesis in C3 plants: stomatal and non-stomatal limitations revised. Ann. Bot.-Lond. 89, 183–189.
Flexas, J., Loreto, F., Medrano, H., 2012. Terrestrial Photosynthesis in a Changing Environment. A Molecular, Physiological and Ecological Approach. Cambridge University Press, Cambridge, pp. 723.
Genty, B., Briantais, J.M., Baker, N.R., 1989. The relationship between the quantum yield of photosynthetic electron transport and quenching of chlorophyll fluorescence. Biochem. Biophys. Acta 990, 87–92.
Han, R., Quinet, M., André, E., Teun van Elteren, J., Destrebecq, F., Vogel-Mikus, K., Cui, G., Debeljak, M., Lefevre, I., Lutts, S., 2013. Accumulation and distribution of Zn in the shoots and reproductive structures of the halophyte plant species Kosteletzkya virginica as a function of salinity. Planta 238, 441–457.
Hoagland, D., Arnon, D.I., 1938. The water culture method for growing plants without soil. Calif. Agric. Exp. Stn. Bull. 347, 1–39.
Kabata-Pendias, A., Pendias, H., 2001. Trace Elements in Soils and Plants. CRC Press, Boca Raton, Florida, pp. 131–142.
Kadukova, J., Kalogerakis, N., 2007. Lead accumulation from non-saline and saline environments by *Tamarix smyrnensis* Bunge. Eur. J. Soil Biol. 43, 216–223.
Khan, M.I.R., Khan, N.A., 2014. Ethylene reverses photosynthetic inhibition by nickel and zinc in mustard through changes in PS II activity, photosynthetic nitrogen use efficiency, and antioxidant metabolism. Protoplasma 251, 1007–1019.
Kholodova, V.P., Volkov, K., Kuznetsov, V., 2010. Plants under heavy metal stress in saline environments. In: Sherameti, I., Varma, A. (Eds.), Soil Heavy Metals, Soil Biology 19. Springer-Verlag, Heidelberg, Germany, pp. 163–183.
Lichtenthaler, H.K., 1987. Chlorophylls and carotenoids: pigments of photosynthetic biomembranes. Method. Enzymol. 148, 350–382.
Liu, X., Shen, X., Lai, Y., Ji, K., Sun, H., Wang, Y., Hou, C., Zou, N., Wan, J., Yu, J., 2016. Toxicology proteomic responses of halophyte *Suaeda salsa* to lead and zinc. Ecotoxiol. Environ. Saf. 134, 163–171.
Marques, B., Lillebo, A.L., Pereira, E., Duarte, A.C., 2011. Mercury cycling and sequestration in salt marshes sediments: an ecosystem service provided by *Juncus maritimus* and *Scirpus maritimus*. Environ. Pollut. 159, 1869–1876.
Mateos-Naranjo, E., Redondo-Gómez, S., Cambrollé, J., Luque, T., Figueroa, M.E., 2008. Growth and photosynthetic responses to zinc stress of an invasive cordgrass, Spartina densiflora. Plant Biol. 10, 754–762.
Mateos-Naranjo, E., Andrades-Moreno, L., Redondo-Gómez, S., 2011. Comparison of germination, growth, photosynthetic responses and metal uptake between three populations of Spartina densiflora under different soil pollution conditions. Ecotoxiol. Environ. Saf. 74, 2040–2049.
Mateos-Naranjo, E., Castellanos, E.M., Pérez-Martin, A., 2014. Zinc tolerance and accumulation in the halophytic species *Juncus acutus*. Environ. Exp. Bot. 100, 114–121.
Maxwell, K., Johnson, G.N., 2000. Chorophyll fluorescence a practical guide. J. Exp. Bot. 51, 659–668.
Medas, D., De Giudici, G., Pusceddu, C., Casu, M.A., Birarda, G., Vaccari, L., Gianoncelli, A., Meneghini, C., 2017. Impact of Zn excess on biomineralization processes in *Juncus acutus* grown in mine polluted sites. J. Hazard. Mater. https://doi.org/10.1016/j.jhazmat.2017.08.031.
Melis, A., 1999. Photosystem-II damage and repair cycle in chloroplasts: what modulates the rate of photodamage in vivo? Trends Plant. Sci. 4, 130–135.
Monnet, F., Vaillant, N., Vernay, P., Coudret, A., Sallanon, H., Hitmi, A., 2001. Relationship between PSII activity, CO_2 fixation, and Zn, Mn and Mg contents of *Lolium perenne* under zinc stress. J. Plant Physiol. 158, 1137–1144.
Padinha, C., Santos, R., Brown, M.T., 2000. Evaluating environmental contamination in Ria Formosa (Portugal) using stress indexes of *Spartina maritima*. Mar. Environ. Res. 49, 67–78.
Paschke, M.W., Redente, E.F., Levy, D.B., 2000. Zinc toxicity thresholds for important reclamation grass species of the western United States. Environ. Toxicol. Chem. 19, 2751–2756.
Pérez-Romero, J.A., Redondo-Gómez, S., Mateos-Naranjo, E., 2016. Growth and photosynthetic limitation analysis of the Cd-accumulator *Salicornia ramosissima* under excessive cadmium concentrations and optimum salinity conditions. Plant Physiol. Biochem. 109, 103–113.
Perfus-Barbeoch, L., Leonhardt, N., Vavasseur, A., Forestier, C., 2002. Heavy metal toxicity: cadmium permeates through calcium channels and disturbs the plant water

status. Plant J. 32, 539–548.
Prasad, M.N.V., Strzalka, K., 1999. Impact of heavy metals on photosynthesis. In: Prasad, M.N.V., Hagemeyer, J. (Eds.), Heavy Metals Stress in Plants: From Molecules to Ecosystems. Springer, Berlin, Germany, pp. 117–138.
Redondo-Gómez, S., Mateos-Naranjo, E., Davy, A.J., Fernández-Muñoz, F., Castellanos, E., Luque, T., Figueroa, M.E., 2007. Growth and photosynthetic responses to salinity of the salt-marsh shrub Atriplex portulacoides. Ann. Bot.-Lond. 100, 555–563.
Redondo-Gómez, S., Mateos-Naranjo, E., Figueroa, M.E., Davy, A.J., 2010. Salt stimulation of growth and photosynthesis in an extreme halophyte, *Arthrocnemum macrostachyum*. Plant Biol. 12, 79–87.
Redondo-Gómez, S., Andrades-Moreno, L., Mateos-Naranjo, E., Parra, R., Valera-Burgos, J., Aroca, R., 2011. Synergic effect of salinity and zinc stress on growth and photosynthetic responses of the cordgrass *Spartina densiflora*. J. Exp. Bot. 62, 5521–5530.
Santos, D., Duarte, B., Caçador, I., 2014. Unveiling Zn hyperaccumulation in *Juncus acutus*: implications on the electronic energy fluxes and on oxidative stress with emphasis on non-functional Zn-chlorophylls. J. Photochem. Photobiol. B 140, 228–239.
Schreiber, U., Schliw, U., Bilger, W., 1986. Continuous recording of photochemical and non-photochemical chlorophyll fluorescence quenching with a new type of modulation fluorimeter. Photosynth. Res. 10, 51–62.
Shabala, L., McMeekin, T., Shabala, S., 2009. Osmotic adjustment and requirement for sodium in marine protist thraustochytrid. Environ. Microbiol. 11, 1835–1843.
Sparks, E.L., Cebrian, J., Bilber, P.D., Sheehan, K.L., Tobias, C.R., 2013. Cost-effectiveness of two small-scale salt marsh restoration designs. Ecol. Eng. 53, 250–256.
Vaillant, N., Monnet, F., Hitmi, A., Sallanon, H., Coudret, A., 2005. Comparative study of responses in four *Datura* species to zinc stress. Chemosphere 59, 1005–1013.
Van Assche, F.V., Clijsters, H., 1986. Inhibition of photosynthesis by treatment of Phaseolus vulgaris with toxic concentration of zinc: effects on electron transport and photophosphorylation. Physiol. Plant. 66, 717–721.
Werner, C., Correia, O., Beyschlag, W., 2002. Characteristic patterns of chronic and dynamic photoinhibition of different functional groups in a Mediterranean ecosystem. Funct. Plant Biol. 29, 999–1011.
Ying, R.R., Qiu, R.L., Tang, Y.T., Hu, P.J., Qiu, H., Chen, H.R., Shi, T.H., Morel, J.L., 2010. Cadmium tolerance of carbon assimilation enzymes and chloroplast in Zn/Cd hyperaccumulator *Picris divaricata*. J. Plant Physiol. 167, 81–87.

CAPÍTULO 7: DISCUSIÓN GENERAL

El aumento de la concentración atmosférica de CO_2, que comenzó con la etapa preindustrial, está provocando un cambio en muchos factores ambientales del planeta, tales como: aumento de la temperatura media y del nivel del mar o una mayor frecuencia de eventos climáticos extremos, circunstancias que llevarán a un incremento de la salinización y degradación de los suelos (IPCC, 2007). Todos estos cambios tendrán consecuencias sobre las respuestas ecofiosiológicas de las especies vegetales (Curtis et al., 1995), lo que podría afectar a la distribución, el ciclo vital y la producción de cientos de especies (Naudts et al., 2014; Orsenigo et al., 2014). Del mismo modo, se ha descrito cómo los cambios inherentes al Cambio Climático podrían alterar ciertos servicios ecosistémicos relacionados con las respuestas vegetales, como podría ser su capacidad fitorremediadora de contaminantes (Li et al., 2012; Tian et al., 2014).

Especialmente vulnerables serán las especies que viven en ecosistemas costeros, como las marismas, que no solo estarán sometidas a los factores ambientales citados, sino también a otros factores de estrés de origen antrópico, como los contaminantes orgánicos e inorgánicos que se acumulan en esta zona de transición entre ecosistemas marítimos y terrestres (Lu et al., 2018). Por ello, en esta Tesis Doctoral se establecieron dos objetivos principales, complementarios, para mejorar el conocimiento sobre la respuesta fisiológica de las halófitas frente a las condiciones climáticas previstas en el escenario de Cambio Climático. El primer objetivo fue comprobar los efectos que diferentes factores derivados del Cambio Climático podrían tener sobre la fisiología de una halófita modelo, *Salicornia ramosissima*. El segundo, analizar el efecto de la interacción de factores derivados del Cambio Climático y factores relacionados con la contaminación en dos halófitas de probada capacidad fitorremediadora, *Spartina densiflora* y *Juncus acutus*. Así, los capítulos 2, 3 y 4 se desarrollaron para la consecución del primer objetivo y los capítulos 5 y 6 para dar respuesta al segundo. A continuación, me referiré a cada uno de estos capítulos.

En el capítulo 2 de esta Tesis Doctoral se comprobó cómo el enriquecimiento atmosférico de CO_2 (700 ppm CO_2) mejoró la respuesta ecofisiológica de la halófita *Salicornia ramosissima* frente a otro factor estresante relacionado con el Cambio Climático, como es el aumento de la salinización de los suelos. Este efecto sinérgico ha sido descrito para otras especies de halófitas previamente (Geissler et al., 2009; 2010;

Mateos-Naranjo 2010a; b). Los resultados de esta Tesis mostraron que las plantas crecidas a una concentración de 700 ppm de CO_2 fueron capaces de mantener valores de tasa de fotosíntesis neta (A_N) similares a los de aquellas crecidas a 171 mM NaCl y 400 ppm CO_2, incluso con 510 mM NaCl en el medio de crecimiento. Las plantas crecidas a alto CO_2 también incrementaron sus valores de eficiencia intrínseca en el uso del agua ($_i$WUE) para las dos salinidades estudiadas y presentaron una mejor respuesta frente a las especies reactivas del oxígeno (ROS) inducidas por el estrés salino.

El efecto sinérgico del incremento de la concentración de CO_2 y la salinidad también se vio en combinación con otro factor de estrés, la inundación prolongada (capítulo 3). En un escenario de Cambio Climático la inundación puede ser más común en zonas donde actualmente no ocurren con tanta frecuencia, como la marisma alta, donde se pueden encontrar muchas especies de halófitas, debido a la subida del nivel del mar (IPCC, 2014). El estudio llevado a cabo en el capítulo 3, sobre la respuesta fisiológica de la halófita modelo *S. ramosissima* frente a la interacción de tres factores ambientales relacionados con el Cambio Climático (elevado CO_2, salinidad e inundación) es algo novedoso, siendo escasos los trabajos que lo hayan realizado (Lenssen et al., 1993; 1995). No obstante, ninguno de esos estudios realizó un análisis detallado del efecto de estas interacciones sobre el aparato fotosintético, tal y como se muestra en el capítulo 3 de esta Tesis, donde se presta especial atención a la eficiencia energética de los fotosistemas y al metabolismo relacionado con la respuesta al estrés oxidativo.

Así, se encontró que el aumento de la concentración de CO_2 en plantas de *S. ramosissima* crecidas con sal (171 y 510 mM NaCl) e inundación mejoró los valores de A_N. Dicha mejora parece estar relacionada con una mayor eficiencia en el uso del agua, a través de una reducción de la conductancia estomática (g_s). Otros autores también han indicado cómo los valores de g_s disminuían en presencia de alta salinidad (Flexas et al., 2004; Fanourakis et al., 2015), aunque este efecto desaparecía en las plantas sometidas a inundación prolongada en su zona radicular, como ya describieron Ullah et al. (2017) para *Vigna angularis* bajo condiciones de encharcamiento. En el caso de la halófita elegida como modelo, los mayores valores de A_N se debieron a que la alta concentración de CO_2 posibilitó mayores valores de C_i que compensaron el descenso de g_s, tal y como ya describieron Robredo et al. (2007) para cebada crecida a 700 ppm de CO_2. En cambio, en ausencia de inundación, se registró una disminución de A_N para las plantas crecidas a 510

mM de NaCl y alto CO_2, que parecía estar relacionada con una bajada de g_m o de la $V_{c,max}$; pues los valores de C_i eran parecidos al resto de plantas crecidas en alto CO_2.

Por otro lado, los resultados del capítulo 2 mostraron que el efecto positivo del incremento atmosférico de CO_2 frente a condiciones de alta salinidad viene medidado por una mejora en la eficiencia energética del fotosistema II (PSII). Los valores obtenidos de la fluorescencia de la clorofila *a* indicaban una mejora para estas plantas en valores relacionados con la absorción (ABS/CS), transformación (TR/CS) y transporte de energía (ET/CS) bajo condiciones de elevada salinidad, aunque esta mejora no se apreciaba bien en estas variables al estudiar la interacción entre la inundación, la alta salinidad y elevado CO_2 (capítulo 3). Además, se observó una mejora en el transporte de electrones (ETR_{max}) en condiciones de alto CO_2, lo que permitió a las plantas sometidas a salinidad alta tener un menor riesgo de estrés por la presencia de especies reactivas del oxígeno; y este efecto fue más evidente en condiciones de inundación. Estudios previos resaltaron los efectos perjudiciales que la inundación (Mateos-Naranjo et al., 2007; Cao et al., 2017; Ullah et al., 2017) y las altas salinidades (Flexas et al., 2004; Mateos-Naranjo y Redondo-Gómez et al., 2016) tienen sobre los fotosistemas y su funcionamiento en halófitas. No obstante, en esta Tesis se pudo constatar la integridad de los fotosistemas, que conservaron su función en los diferentes tratamientos, habiendo pocas diferencias entre ellos cuando se observaban los valores de ABS/CS, ET/CS o TR/CS, así como parámetros derivados del protocolo OJIP.

Por otro lado, aunque se observó una mejora en la respuesta fotosintética de *S. ramosissima* por el aumento del CO_2 bajo condiciones de salinidad elevada e inundación (capítulo 3), este efecto no se reflejó en un aumento sustancial del crecimiento de la planta; a diferencia de lo registrado por Lenssen et al. (1993), quienes encontraron un aumento de la biomasa de la halófita *Elymus athericus* crecida a 720 ppm de CO_2, que fue más patente a alta salinidad (310 mM NaCl). También hay estudios que han obtenido resultados similares, en cuanto a la ausencia de diferencias entre el crecimiento de plantas sometidas a diferentes condiciones de CO_2 (Geissler et al. 2009 a,b; 2010). En nuestro caso, la falta de respuesta a nivel de crecimiento podría estar relacionada con diversos factores, no excluyentes. Así, por un lado, podría deberse al tiempo de los experimentos, que fue de 30 días. La diferencia en A_N entre los diferentes tratamientos, mantenida en el tiempo, podría llegar a generar un mayor crecimiento de las plantas sometidas a elevadas concentraciones de CO_2. Por otro lado, la falta de efecto en la biomasa podría ser debida

a un aumento de la inversión energética en mecanismos de defensa frente al estrés (Geissler et al., 2015). En este sentido, los resultados de esta Tesis Doctoral indicaron que la halófita *S. ramosissima* mostraba un aumento de diferentes mecanismos de defensa frente al estrés ambiental, tales como un aumento de la actividad de las enzimas anti-estrés oxidativo: superóxido dismutasa (SOD) en condiciones de hipersalinidad y ascorbato peroxidasa (APx) bajo condiciones subóptimas de salinidad e inundación prolongada; respuesta que fue potenciada en condiciones de elevado CO_2. Además, se registró en el capítulo 3 un aumento de la producción de betaína en presencia de alta salinidad, independientemente del grado de inundación y más evidente a 700 ppm CO_2. Este compuesto es producido por las especies vegetales para contrarrestar los efectos negativos de la salinidad o la sequía (Moradi et al., 2017). Igualmente, se detectó una mayor disipación de energía en forma de calor (DI/CS). Los valores de DI/CS obtenidos, junto con los datos de concentraciones de pigmentos fotosintéticos, evidenciaron una mayor activación del ciclo de las xantofilas, que se encarga de reducir al PSII y sus proteínas asociadas, cuando están excesivamente protonadas, por medio de la depoxidación de las xantofilas (Duarte et al., 2015b). Finalmente, la ausencia de diferencias en la biomasa podría haber estado ocasionada por la edad de las plantas con las que se llevaron a cabo los ensayos, al tratarse de una especie anual y haber usado plantas de una edad de 3 meses. Aunque esto no parece probable, puesto que las plantas utilizadas tenían una altura inicial media de unos 13 cm y esta especie puede alcanzar un máximo de altura en campo de unos 40 cm (Castroviejo, 1986).

Una de las lagunas de conocimiento, en relación a las respuestas ecofisiológicas de las halófitas frente a factores relacionados con el Cambio Climático, es la respuesta frente a eventos cortos extremos, como las olas de frío y de calor que están aumentando su duración y frecuencia en los últimos años (IPCC, 2014). Por eso, en el Capítulo 4 de esta Tesis Doctoral se estudió la respuesta de *S. ramosissima* frente a estas condiciones extremas, que se registran en el hábitat de esta especie, en interacción con diferentes salinidades. Se observó una respuesta dependiente de las condiciones térmicas del hábitat de procedencia de la especie, caracterizado por una mayor recurrencia de olas de calor (Labajo et al., 2014). Específicamente, este estudio mostró que el aparato fotosintético de *S. ramosissima* está más adaptado para responder a rangos de temperatura altos (40/28 ºC) que a temperaturas bajas (13/5 ºC), incluso bajo condiciones de hipersalinidad. Esta mayor eficacia fotosintética a alta temperatura se reflejó en diversos componentes clave

de la ruta fotosintética, relacionados con las limitaciones de difusión al CO_2, bioquímicas y energéticas. Así, se midieron mayores valores de conductancia estomática y del mesófilo a alta temperatura. El aumento de las limitaciones a baja temperatura, debido a la disminución de las conductancias estomática y del mesófilo, se ha descrito en especies sensibles al frío (Hendrikson et al., 2006). Además, a alta temperatura *S. ramosissima* fue capaz de mantener los valores de actividad de la Rubisco, caracterizada como $V_{c,max}$, a niveles similares a los del tratamiento control (22/15 ºC y 171 mM NaCl), mientras que a bajas temperaturas este valor fue menor que el control, independientemente de la salinidad. Temperaturas por debajo de los 15 ºC ,y especialmente inferiores a 5 ºC, suelen tener un impacto negativo en la función de la Rubisco (Hendrikson et al., 2004). Sin embargo, aunque las temperaturas elevadas también pueden causar daños en esta enzima (Perdomo et al., 2017), Cen y Sage (2005) registraton que no eran suficientes como para limitar la fotosíntesis. Otra muestra de la mayor adaptación del PS II a las altas temperaturas fue que, aunque los valores de F_v/F_m y ETR_{max} descendieron en ambos tratamientos térmicos, presentaron un descenso más acusado para las plantas crecidas a bajas temperaturas. Las temperaturas elevadas suelen degradar algunos componentes de los PS II, pero esto ocurre a partir de los 45 ºC en especies adaptadas a altas temperaturas (Yamane et al., 1998), como parece ser el caso de nuestra halófita modelo.

Una tendencia similar se observó en los parámetros derivados del protocolo OJIP, pues indicaban que a altas temperaturas la conectividad de los fotosistemas (P_G) y el número de los mismos que permanecían abiertos (M_0) era mayor en comparación con aquellas plantas sometidas a olas de frío. Un mayor número de fotosistemas abiertos pueden contribuir a una mayor disipación de la energía en forma de calor, ayudando a proteger al tejido fotosintético de las altas temperaturas (Strasser et al., 2004). Esto se confirmó con los datos de DI/CS a altas temperaturas, que duplicaron o cuatriplicaron sus valores comparado con el control, dependiendo de si las plantas crecían a moderada o alta salinidad (171 o 1050 mM de NaCl), respectivamente; mientras que a bajas temperaturas el incremento fue mucho menor. El incremento de DI/CS, unido a los datos obtenidos del perfil de pigmentos fotosintéticos, parece indicar que a altas temperaturas y alta salinidad las plantas activaron el ciclo de las xantófilas, favoreciéndose la disipación del exceso de energía; a pesar de que se creía que ni las altas ni las bajas temperaturas lo activaban (Saidi et al., 2010; Duarte et al., 2015). La activación de estos mecanismos junto con el mejor funcionamiento de la cadena de transporte de electrones, como indicaron los

mayores valores de ETR, parecen reducir el riesgo de estrés derivado de la acumulación de especies reactivas de oxígeno (ROS) a altas temperaturas respecto a plantas crecidas a bajas temperaturas. Esta diferencia es mayor cuando se comparan los tratamientos de baja salinidad a ambas temperaturas extremas. Los resultados obtenidos para las actividades de las enzimas de estrés oxidativo parecen confirmar esta idea, ya que APx se activó a altas temperaturas pero no a las bajas.

En general, los tres primeros capítulos de esta Tesis Doctoral constataron una gran resistencia del aparato fotosintético de la halófita *S. ramosissima* frente a condiciones ambientales adversas (salinidad, inundación prolongada o eventos de temperaturas extremas), que serán cada vez más frecuentes en el futuro contexto de Cambio Climático (IPCC, 2014). Además, se registró cómo el aumento del CO_2 mejoró la respuesta a estos factores o a su interacción. Dicha respuesta estuvo mediada por la activación de diversos mecanismos frente al estrés, tal y como hemos comentado previamente. La capacidad de respuesta del aparato fotosintético de *S. ramosissima* frente al estrés abiótico contrasta con los resultados obtenidos para otras halófitas, como *Spartina anglica, Aster tripolium* y *Puccinellia maritima* (Lenssen et al., 1993; 1995), por no mencionar a los cultivos tradicionales, mucho más sensibles (IPCC, 2007). Esto unido a su uso en alimentación (Lu et al., 2010; Barreira et al., 2017) y la capacidad de su género de acumular osmolitos de interés económico (Singh et al., 2014), contribuyen a resaltar el potencial de *S. ramosissima* como cultivo alternativo en condiciones de Cambio Climático. No obstante, se debe profundizar en dicha idea bajo escenarios experimentales desarrollados a mayor escala y bajo situación de campo.

Respecto a los Capítulos 5 y 6 de esta Tesis, se estudió el efecto que los factores ambientales asociados al Cambio Climático podrían tener sobre la capacidad fitorremediadora de sendas halófitas, la C_4 *S. densiflora* y la C_3 *J. acutus*. Ambas, gramínea y juncácea, respectivamente, son especies perennes ampliamente distribuidas en el Golfo de Cádiz y han demostrado un gran potencial para la remediación ambiental de lugares contaminados por metales pesados (Mateos-Naranjo et al., 2008; 2014). Sin embargo, antes de esta Tesis no se había analizado cómo la alteración de factores clave, como el nivel de salinidad del medio o el incremento de la concentración de CO_2 ambiental, podrían alterar dicho potencial. En los Capítulos 5 y 6 se pudo constatar que ambas especies mostraron una gran tolerancia al exceso de cobre y zinc, respectivamente, y que el aumento del CO_2 y la salinidad, en interacción con los metales, mejoró la

respuesta fisiológica al estrés. Así, se vio que el aumento de CO_2 contrarrestó el efecto de la contaminación por cobre en *S. densiflora* y la salinidad elevada mejoró la respuesta de *J. acutus* frente al zinc. Redondo-Gómez et al. (2011) ya encontraron una mejora de la respuesta fisiológica de *S. densiflora* frente a la contaminación por Zn en el medio cuando se exponía a concentraciones moderadas de NaCl (171 mM).

En el caso de *S. densiflora*, ya había sido identificada como una especie resistente al Cu, llegando a tolerar una concentración en hojas de hasta 320 mg Cu kg^{-1} (Mateos-Naranjo et al., 2008). No obstante, el incremento de la concentración de este metal en el medio era inversamente proporcional a la biomasa de la halófita. Sin embargo, en el Capítulo 5 de esta Tesis se muestra que las plantas crecidas a 700 ppm de CO_2 no presentaron diferencias de biomasa para las distintas concentraciones de Cu y mostraron una menor acumulación de metal en sus tejidos aéreos. Incluso en el tratamiento de mayor concentración de Cu (45 mM) las plantas crecidas a elevado CO_2 no disminuían su biomasa. Los tejidos aéreos de las plantas crecidas a 400 ppm de CO_2 alcanzaron valores de acumulación de Cu (737,5 mg kg^{-1}) no compatibles con la vida (Kabata-Pendias and Pendias, 2001), mientras que los valores a alto CO_2 fueron casi un 33% menor. Además, al igual que ocurría con *S. ramosissima*, *S. densiflora* presentaba una mejora de A_N y de la eficiencia en el uso del agua a 700 ppm de CO_2, en comparación con las plantas crecidas 400 ppm de CO_2; a pesar de ser una planta de metalobismo C_4 en las que el efecto del CO_2 se pensaba que podía ser menos evidente (Ghannoum et al., 2000).

Las plantas de *S. densiflora* crecidas a altas concentraciones de CO_2 también mostraron una mejora a nivel de transporte de electrones y de la disipación de energía (Capítulo 5). Además, la disminución en los valores de C/N observada a 45 mM Cu y 700 ppm CO_2 parece indicar una mayor inversión de N para aumentar la producción de Rubisco, algo que también se observó en *S. ramosissima* cuando se expuso a ambientes enriquecidos en CO_2 (700 ppm). Por lo tanto, el incremento de CO_2 mejoró la capacidad de la especie para manejar la energía captada. Por otro lado, las plantas crecidas a alto CO_2 presentaron una menor concentración de MDA en presencia de cobre, indicando un menor daño de las especies reactivas del oxígeno en las membranas celulares.

En el caso de *J. acutus* se observó un incremento de la tasa relativa de crecimento (RGR) de las plantas sometidas a altas concentraciones de Zn y concentraciones moderadas de NaCl (85 mM) en el medio (Capítulo 6). Además, las plantas crecidas en presencia de Zn y 85 mM NaCl experimentaron una menor caída de sus valores de A_N en

comparación con las que crecieron solo en presencia del metal. Esta diferencia, junto a la menor concentración de Zn en los tejidos de las plantas crecidas con sal, podría explicar el mayor crecimiento de la juncácea. La presencia de sal en el medio también mejoró la eficiencia en el uso del agua y, por lo tanto, la respuesta frente al Zn. Los fotosistemas de *J. acutus* mostraron una mejora en el uso energético con la interacción de la sal y de las dos concentraciones de Zn (30 y 100 mM); como nos indicaron los valores de la fluorescencia de la clorofila *a*. Se observó el mismo efecto sinérgico en la concentración de los pigmentos fotosintéticos. Las plantas crecidas con NaCl y Zn presentaron valores para las concentraciones de las clorofilas *a* y *b* incluso mayores que los de las plantas control, lo que sin duda tuvo su repercusión en la mejora que experimentó A_N en presencia de sal y Zn. Por otro lado, se observó una disminución de la fotoinhibición crónica generalizada en presencia de sal, además de un aumento de la fotoinhibición dinámica en el tratamiento de mayor concentración de Zn. La fotoinhibición dinámica se conoce como un mecanismo de defensa en el que el exceso de energía se disipa en forma de calor, ayudando a mantener un buen funcionamiento de la hoja (Maxwell and Johnson, 2000). Por ello, su mayor activación, a concentraciones altas de Zn y en presencia de NaCl en el medio, ratifica la mejora que supone una concentración óptima de sal para *J. acutus* en respuesta al estrés.

Los resultados obtenidos en los Capítulos 5 y 6 confirmaron la tolerancia de *S. densiflora* y *J. acuttus* frente a los excesos de Cu y Zn, respectivamente, ya descritos por otros autores (Mateos-Naranjo et al., 2014; Santos et al., 2014; Christofilopoulos et al., 2016) y añaden una información relevante respecto a la respuesta de ambas especies frente a la interacción de factores derivados del Cambio Climático. Se puede concluir que la presencia de sal y el incremento de CO_2 mejoraron las respuestas fisiológicas de ambas halófitas frente a la contaminación por metales pesados. En el caso de *S. densiflora*, mantuvo su capacidad de acumular Cu en las raíces a alto CO_2 (700 ppm), lo cual, unido a la mejora de la respuesta fisiológica, podría mejorar su potencial como especie fitorremediadora. Li et al. (2012) también encontraron una mayor capacidad de fitorremediación en atmósferas enriquecidas con CO_2 y Tian et al. (2014) observaron una disminución de los efectos negativos en plantas no resistentes a metales pesados cuando crecían con alto CO_2. Sin embargo, en el caso de *J. acutus* la presencia de NaCl en el medio redujo la capacidad de la planta para almacenar Zn en sus tejidos, disminuyendo su potencial fitorremediador. Lo que nos lleva a pensar que, a pesar de que las dos

halófitas demostraron un mejor estado fisiológico en presencia de sal o a elevado CO_2, el efecto en el potencial fitorremediador es específico de cada especie y/o se ve afectado de manera diferencial por el factor ambiental analizado. Esto enfatiza la relevancia de estudiar la respuesta de las plantas frente a la interacción de factores, a la hora de evaluar la capacidad fitorremediadora de una especie.

En conclusión, los estudios realizados en esta Tesis Doctoral en relación a las interacciones de factores ambientales, evidencian, en la misma medida, la complejidad de analizar el efecto en las plantas de más de un factor, actuando al mismo tiempo, y la necesidad de llevarlos a cabo. Pues como se ha podido comprobar, se generan efectos sinérgicos que difieren de las respuestas que se registran cuando se analizan los factores por separado, como un aumento de la biomasa o una mejora de la tasa fotosintética, simplemente por una mayor disponibilidad de CO2 atmosférico (Ghannoum et al., 2000). Las plantas crecidas en una atmósfera enriquecida en CO2 en combinación con otros factores ambientales de estrés mostraron mejor respuesta fisiológica que aquellas sometidas solamente a alta salinidad, inundación o al efecto tóxico de un metal pesado. Además, como ya señalaron Saslis-Lagoudakis et al. (2015), nuestros resultados indican que las halófitas tienen una gran tolerancia a diferentes factores ambientales de estrés, relacionados con el Cambio Global y, más concretamente, con el Cambio Climático (IPCC, 2014), lo que las convierte en especies de interés para su uso en alimentación y/o fitorremediación o para la mejora de cultivos tradicionales mediante la biotecnología. Los resultados obtenidos contribuirán en el desarrollo de modelos predictivos que permitan conocer las respuestas de las halófitas bajo una futura realidad climática. No obstante, esta Tesis también evidencia la necesidad de profundizar en los mecanismos que subyacen en las respuestas de las halófitas.

CONCLUSIONES

1. Response to NaCl excess of the model halophyte *S. ramosissima* was improved by atmospheric CO_2 enrichment due to a reduction on mesophyll and biochemical limitations allowing a higher carbon assimilation capacity and intrisic water use efficiency. This did not result in a significant biomass variation due to the investment of part of the energy fixed for salinity stress defense mechanisms, such as pigments productions or anti-oxidative stress enzymes modulation.
2. Elevated CO_2, salinity and root-flooding had a synergistic effect on carbon assimilation and anti-oxidant stress machinery of *S. ramosissima* by an upregulation of its sink capacity of excess energy and a greater improvement on its intrinsic water use efficiency.
3. *Salicornia ramosissima* photosynthetic metabolism would maintain its functionality better under heat waves than under cold waves, even in presence of hypersaline conditions. This was mainly due to an improvement in its energy sink capacity, while keeping its CO_2 assimilation capacity relatively constant by ameliorating the diffusion and biochemical photosynthesis limitations under those extreme conditions.
4. This higher heat waves tolerance of *S. ramosissima* fits well with its thermal niche characteristics in the Southwest of Iberian Peninsula, where there is a prevalence of daily mean high temperatures and a higher occurrence of heat waves. However, the increase in frequency of extreme cold episodes due to Climate Change would compromise the primary productivity of this important multifunctional cash crop species.
5. Atmospheric CO_2 enrichment improved *S. densiflora* tolerance to Cu pollution maintaining at the same way its Cu root phytostabilization capacity. This

mitigation effect appears to be linked with the protection of several steps in its photosynthetic pathway, such as CO_2 fixation due to reduction of the stomatal limitation, with the consequent improvement of *S. densiflora* water balance.

6. Positive effect of rising CO_2 on *S. densiflora* performance was also related to a better use of absorbed energy, reducing the risk of ROS species production.
7. The presence of NaCl in the growth medium, at concentrations representative of estuarine environments, considerably reduces the deleterious effects of elevated Zn concentrations on the growth and development of *J. acutus*. This beneficial effect was largely mediated by the reduction of Zn levels in *J. acutus* tissues, together with an overall protective effect on its photosynthetic apparatus, manifested as improved carbon harvesting, functionality of the photochemical apparatus (PSII) and photosynthetic pigment concentrations.
8. Overall, studied halophytes shown a better response to abiotic stressors when they were combined, demonstrating the importance of consider the interaction between factors due to the synergetic effects between them when Climate Change is being studied.
9. The positive effect displayed by the halophytes exposed the potential that these species would have as alternative crops or phytoremediation tools in a Climate Change scenario.

REFERENCIAS

Adams, D.A. (1963). Factors influencing vascular plant zonations in North Carolina salt marshes. *Ecology*, **44**: 445-456.

Barbier, E.B., Hacker, S D., Kennedy, C., Koch, E.W., Stier, A.C., y Silliman, B.R. (2011). The value of estuarine and coastal ecosystem services. *Ecological monographs*, **81** (2): 169-193.

Barreira, L., Resek, E., Rodrigues, M. J., Rocha, M. I., Pereira, H., Bandarra, N., ... y Custódio, L. (2017). Halophytes: Gourmet food with nutritional health benefits? *Journal of Food Composition and Analysis*, **59**: 35-42.

Bonometto, A., Feola, A., Rampazzo, F., Gion, C., Berto, D., Ponis, E., y Brusà, R.B. (2019). Factors controlling sediment and nutrient fluxes in a small microtidal salt marsh within the Venice Lagoon. *Science of The Total Environment*, **650**: 1832-1845.

Brady, J.P., Ayoko, G.A., Martens, W.N., Goonetilleke, A., (2014). Temporal trends and bioavailability assessment of heavy metals in the sediments of Deception Bay, Queensland, Australia. *Marine pollution bulletin* **89** (1): 464-472.

Cao, Y., Ma, C., Chen, G., Zhang, J., y Xing, B. (2017). Physiological and biochemical responses of *Salix integra* Thunb. under copper stress as affected by soil flooding. *Environmental Pollution*, **225**: 644-653.

Castellanos, E.M., Figueroa, M.E., Nieva, F.J.J., Luque, C.J. y Castillo, J.M. (2004). Evolución de la vegetación en salinas abandonadas. En: *Salinas de Andalucía*. (eds Junta de Andalucía), Consejería de Medio Ambiente, Junta de Andalucía, Sevilla, España. pp. 196-197.

Castillo, J.M. (2001). Ecología y fisiología comparadas de *Spartina marítima* y *Spartina densiflora* en las marismas mareales mediterráneas. Aplicaciones al control y la prevención de la erosión. Tesis doctoral. Departamento de Biología Vegetal y Ecología, Universidad de Sevilla, España.

Castroviejo, S. (Ed.). (1986). *Flora ibérica: Plantaginaceae-Scrophulariaceae* (Vol. 13). Editorial CSIC-CSIC Press.

Cen, Y. P., y Sage, R. F. (2005). The regulation of Rubisco activity in response to variation in temperature and atmospheric CO_2 partial pressure in sweet potato. *Plant physiology*, **139** (2): 979-990.

Chae, J. S., Choi, M. S., Song, Y. H., Um, I. K., y Kim, J. G. (2014). Source identification of heavy metal contamination using metal association and Pb isotopes in Ulsan Bay sediments, East Sea, Korea. *Marine pollution bulletin*, **88** (1-2) : 373-382.

Chapman, V.J. (1974). Salt Marshes and Salt Deserts of the World. Verlag Von J. Gramer, Lehre, Alemania.

Choi, M. S., Yi, H. I., Yang, S. Y., Lee, C. B., y Cha, H. J. (2007). Identification of Pb sources in Yellow Sea sediments using stable Pb isotope ratios. *Marine Chemistry*, **107** (2): 255-274.

Christofilopoulos, S., Syranidou, E., Gkavrou, G., Manousaki, E., y Kalogerakis, N. (2016). The role of halophyte *Juncus acutus* L. in the remediation of mixed contamination in a hydroponic greenhouse experiment. *Journal of Chemical Technology y Biotechnology*, **91** (6): 1665-1674.

Curtis, P. S., Vogel, C. S., Pregitzer, K. S., Zak, D. R., y Teeri, J. A. (1995). Interacting effects of soil fertility and atmospheric CO_2 on leaf area growth and carbon gain physiology in *Populus× euramericana* (Dode) Guinier. *New Phytologist*, **129**(2): 253-263.

DeLaune, R.D. y Grambell, R.P. (1996). Role of sedimentation in isolating metal contaminants in wetland environments. *Journal of Environmental Science Health*, **31**: 2349-2362.

Dou, Y., Li, J., Zhao, J., Hu, B., y Yang, S. (2013). Distribution, enrichment and source of heavy metals in surface sediments of the eastern Beibu Bay, South China Sea. *Marine pollution bulletin*, **67** (1-2): 137-145.

Duarte, B., Santos, D., Silva, H., Marques, J. C., y Cacador, I. (2014). Photochemical and biophysical feedbacks of C3 and C4 Mediterranean halophytes to atmospheric CO_2 enrichment confirmed by their stable isotope signatures. *Plant physiology and biochemistry*, **80**: 10-22.

Duarte, B., Santos, D., Marques, J. C., y Caçador, I. (2015a). Ecophysiological constraints of two invasive plant species under a saline gradient: halophytes versus glycophytes. *Estuarine, Coastal and Shelf Science*, **167**: 154-165.

Duarte, B., Goessling, J. W., Marques, J. C., y Caçador, I. (2015b). Ecophysiological constraints of *Aster tripolium* under extreme thermal events impacts: Merging biophysical, biochemical and genetic insights. *Plant Physiology and Biochemistry*, **97**: 217-228.

Fagherazzi, S., Wiberg, P.L., Temmerman, S., Struyf, E., Zhao, Y., y Raymond, P.A. (2013). Fluxes of water, sediments, and biogeochemical compounds in salt marshes. *Ecological Processes*, **2** (1): 3.

Fanourakis, D., Giday, H., Milla, R., Pieruschka, R., Kjaer, K. H., Bolger, M., ... y Ottosen, C. O. (2014). Pore size regulates operating stomatal conductance, while stomatal densities drive the partitioning of conductance between leaf sides. *Annals of Botany*, **115** (4): 555-565.

Farhad, S., Gual, M.A. y Ruiz-Ballesteros, E. (2015). Linking governance and ecosystem services: The case of Isla Mayor (Andalusia, Spain). *Land Use Policy*, **46**: 91-102.

Feng, J., Lin, Y., Yang, Y., Shen, Q., Huang, J., Wang, S., ... y Li, Z. (2018). Tolerance and bioaccumulation of combined copper, zinc, and cadmium in *Sesuvium portulacastrum*. *Marine Pollution Bulletin*, **131**: 416-421.

Flexas, J., Bota, J., Loreto, F., Cornic, G., y Sharkey, T. D. (2004). Diffusive and metabolic limitations to photosynthesis under drought and salinity in C3 plants. *Plant biology*, **6** (3): 269-279.

Flowers, T. J., Hajibagheri, M. A., y Clipson, N. J. W. (1986). Halophytes. *The quarterly review of biology*, **61** (3): 313-337.

Flowers, T. J., y Colmer, T. D. (2008). Salinity tolerance in halophytes. *New Phytologist*, **179** (4): 945-963.

Flowers, T. J., y Colmer, T. D. (2015). Plant salt tolerance: adaptations in halophytes. *Annals of botany*, **115** (3): 327-331.

Geissler, N., Hussin, S., y Koyro, H. W. (2009). Elevated atmospheric CO2 concentration ameliorates effects of NaCl salinity on photosynthesis and leaf structure of *Aster tripolium* L. *Journal of Experimental Botany*, **60** (1): 137-151.

Geissler, N., Hussin, S., y Koyro, H. W. (2010). Elevated atmospheric CO2 concentration enhances salinity tolerance in *Aster tripolium* L. *Planta*, **231** (3): 583-594.

Geissler, N., Hussin, S., El-Far, M. M., y Koyro, H. W. (2015). Elevated atmospheric CO_2 concentration leads to different salt resistance mechanisms in a C3 (*Chenopodium quinoa*) and a C4 (*Atriplex nummularia*) halophyte. *Environmental and Experimental Botany*, **118**: 67-77.

Ghannoum, O., Caemmerer, S. V., Ziska, L. H., y Conroy, J. P. (2000). The growth response of C4 plants to rising atmospheric CO_2 partial pressure: a reassessment. *Plant, Cell y Environment*, **23** (9): 931-942.

Hart, C., Gaston, T.F., y Taylor, M.D. (2018). Utilisation of a recovering wetland by a commercially important species of penaeid shrimp. *Wetlands Ecology and Management*, **26**: 665-675.

Hendrickson, L., Chow, W. S., y Furbank, R. T. (2004). Low temperature effects on grapevine photosynthesis: the role of inorganic phosphate. *Functional Plant Biology*, **31** (8): 789-801.

Hendrickson, L., Vlčková, A., Selstam, E., Huner, N., Öquist, G., y Hurry, V. (2006). Cold acclimation of the *Arabidopsis* dgd1 mutant results in recovery from photosystem I-limited photosynthesis. *FEBS letters*, **580** (20): 4959-4968.

Hoornweg, D., Bhada-Tata, P., y Kennedy, C. (2013). Environment: Waste production must peak this century. *Nature News*, **502** (7473): 615.

IPCC (2007) Climate Change 2007: Synthesis Report. Contribution of Working Groups I, II and III to the Fourth Assessment Report of the Intergovernmental Panel on Climate Change [Core Writing Team, Pachauri, R.K and Reisinger, A. (eds.)]. IPCC, Geneva, Switzerland, 104 pp.

IPCC, 2014: Climate Change 2014: Synthesis Report. Contribution of Working Groups I, II and III to the Fifth Assessment Report of the Intergovernmental Panel on Climate Change [Core Writing Team, R.K. Pachauri and L.A. Meyer (eds.)]. IPCC, Geneva, Switzerland, 151 pp.

Kabata-Pendias, A. (2010). *Trace elements in soils and plants*. CRC press.

Keshavarzi, B., Ebrahimi, P., y Moore, F. (2015). A GIS-based approach for detecting pollution sources and bioavailability of metals in coastal and marine sediments of Chabahar Bay, SE Iran. *Chemie der Erde-Geochemistry*, **75** (2): 185-195.

Kessel, G. M., y Phillips, N. E. (2018). Global change scenarios trigger carry-over effects across life stages and generations of the intertidal limpet, *Siphonaria australis*. *PloS one*, **13** (3).

Labajo, A. L., Egido, M., Martín, Q., Labajo, J. y Labajo, J. L. (2014). Definition and temporal evolution of the heat and cold waves over the Spanish Central Plateau from 1961 to 2010. *Atmósfera* **27** (3): 273–286.

Lenssen, G. M., Lamers, J., Stroetenga, M., y Rozema, J. (1993). Interactive effects of atmospheric CO2 enrichment, salinity and flooding on growth of C3 (*Elymus athericus*) and C4 (*Spartina anglica*) salt marsh species. In *CO_2* and *biosphere* (pp. 379-390). Springer, Dordrecht.

Lenssen, G. M., Van Duin, W. E., Jak, P., y Rozema, J. (1995). The response of Aster tripolium and *Puccinellia maritima* to atmospheric carbon dioxide enrichment and their interactions with flooding and salinity. *Aquatic Botany*, **50** (2): 181-192.

Li, Z., Tang, S., Deng, X., Wang, R., y Song, Z. (2010). Contrasting effects of elevated CO2 on Cu and Cd uptake by different rice varieties grown on contaminated soils with two levels of metals: implication for phytoextraction and food safety. *Journal of Hazardous Materials*, **177** (1-3): 352-361.

Liang, L., Liu, W., Sun, Y., Huo, X., Li, S., y Zhou, Q. (2016). Phytoremediation of heavy metal contaminated saline soils using halophytes: current progress and future perspectives. *Environmental Reviews*, **25** (3): 269-281.

Looi, L. J., Aris, A. Z., Yusoff, F. M., y Hashim, Z. (2015). Mercury contamination in the estuaries and coastal sediments of the Strait of Malacca. *Environmental monitoring and assessment*, **187** (1): 4099.

Lu, D., Zhang, M., Wang, S., Cai, J., Zhou, X., y Zhu, C. (2010). Nutritional characterization and changes in quality of *Salicornia bigelovii* Torr. during storage. *LWT-Food Science and Technology*, **43** (3): 519-524.

Lu, Y., Yuan, J., Lu, X., Su, C., Zhang, Y., Wang, C., ... y Garbutt, R. A. (2018). Major threats of pollution and climate change to global coastal ecosystems and enhanced management for sustainability. *Environmental Pollution*, **239**: 670-680.

Luque, C.J., Castellanos, E.M., Castillo, J.M., González, M., González-Vilches, M.C. y Figueroa, M.E. (1999). Metals in halophytes of a contaminated estuary (Odiel Saltmarshes, SW Spain). *Marine Pollution Bulletin*, **38**: 49-51.

Lutts, S., y Lefèvre, I. (2015). How can we take advantage of halophyte properties to cope with heavy metal toxicity in salt-affected areas?. *Annals of Botany*, **115** (3): 509-528.

Mateos-Naranjo, E., Redondo-Gómez, S., Silva, J., Santos, R., y Figueroa, M. E. (2007). Effect of prolonged flooding on the invader *Spartina densiflora* Brong. *Journal of Aquatic Plant Management*, **45**: 121-123.

Mateos-Naranjo, E., Redondo-Gómez, S., Cambrollé, J., y Figueroa, M. E. (2008). Growth and photosynthetic responses to copper stress of an invasive cordgrass, *Spartina densiflora*. *Marine Environmental Research*, **66** (4): 459-465.

Mateos-Naranjo, E., Redondo-Gómez, S., Álvarez, R., Cambrollé, J., Gandullo, J., y Figueroa, M. E. (2010a). Synergic effect of salinity and CO2 enrichment on growth and photosynthetic responses of the invasive cordgrass *Spartina densiflora*. *Journal of experimental botany*, **61** (6): 1643-1654.

Mateos-Naranjo, E., Redondo-Gómez, S., Andrades-Moreno, L., y Davy, A. J. (2010b). Growth and photosynthetic responses of the cordgrass *Spartina maritima* to CO_2 enrichment and salinity. *Chemosphere*, **81** (6): 725-731.

Mateos-Naranjo, E., Castellanos, E. M., y Perez-Martin, A. (2014). Zinc tolerance and accumulation in the halophytic species *Juncus acutus*. *Environmental and Experimental Botany*, **100**: 114-121.

Mateos-Naranjo, E., y Redondo-Gómez, S. (2016). Interpopulation differences in salinity tolerance of the invasive cordgrass *Spartina densiflora*: implications for invasion process. *Estuaries and coasts*, **39** (1): 98-107.

Maxwell, K., y Johnson, G. N. (2000). Chlorophyll fluorescence—a practical guide. *Journal of Experimental Botany*, **51** (345): 659-668.

Moradi, P., Ford-Lloyd, B., y Pritchard, J. (2017). Metabolomic approach reveals the biochemical mechanisms underlying drought stress tolerance in thyme. *Analytical biochemistry*, **527**: 49-62.

Moreno, R., Jover, L., Diez, C., Sanpera, C. (2011). Seabird feathers as monitors of the levels and persistence of heavy metal pollution after the Prestige oil spill. *Environ*mental *Pollution* **159** (10): 2454-2460.

Morzaria-Luna, H.N., Turk-Boyer, P. y Moreno-Baez, M. (2014). Social indicators of vulnerability for fishing communities in the Northern Gulf of California, Mexico: implications for climate change. *Marine Policy*, **45**: 182-193.

Munns, R., y Tester, M. (2008). Mechanisms of salinity tolerance. *Annual Review of Plant Biology*, **59**: 651-681.

Naudts, K., Van den Berge, J., Farfan, E., Rose, P., AbdElgawad, H., Ceulemans, R., ... y Nijs, I. (2014). Future climate alleviates stress impact on grassland productivity through altered antioxidant capacity. *Environmental and Experimental Botany*, **99**: 150-158.

Nieto, J.M., Sarmiento, A.M., Olías, M., Canovas, C.R., Riba, I., Kalman, J., Delvalls, T.A., (2007). Acid mine drainage pollution in the tinto and odiel rivers (Iberian pyrite belt, SW Spain) and bioavailability of the transported metals to the Huelva estuary. *Environmental International* **33** (4): 445-455.

Occhipinti-Ambrogi, A. (2007). Global change and marine communities: alien species and climate change. *Marine pollution bulletin*, **55** (7-9): 342-352.

Orsenigo, S., Mondoni, A., Rossi, G., y Abeli, T. (2014). Some like it hot and some like it cold, but not too much: plant responses to climate extremes. *Plant Ecology*, **215** (7): 677-688.

Osher, L., Leclerc, L., Wiersma, G., Hess, C., Guiseppe, V., (2006). Heavy metal contamination from historic mining in upland soil and estuarine sediments of Egypt Bay, Maine, USA. *Estuarine, Coastal and Shelf Science,* **70** (1): 169-179.

Peng, S., Huang, J., Sheehy, J.E., Laza, R.C., Visperas, R.M., Zhong, X., Centeno, G.S., Khush, G.S., Cassman, K.G., 2004. *Proceedings of the National Academy of Sciences*, **101** (27): 9971–9975

Perdomo, J. A., Capó-Bauçà, S., Carmo-Silva, E., y Galmés, J. (2017). Rubisco and rubisco activase play an important role in the biochemical limitations of photosynthesis in rice, wheat, and maize under high temperature and water deficit. *Frontiers in plant science*, **8**: 490.

Pérez-Romero, J. A., Redondo-Gómez, S., y Mateos-Naranjo, E. (2016). Growth and photosynthetic limitation analysis of the Cd-accumulator Salicornia ramosissima under excessive cadmium concentrations and optimum salinity conditions. *Plant Physiology and Biochemistry*, **109**: 103-113.

Popadic, A., Vidovic, J., Cosovic, V., Medakovic, D., Dolenec, M., Felja, I., (2013). Impact evaluation of the industrial activities in the Bay of Bakar (Adriatic Sea, Croatia): recent benthic foraminifera and heavy metals. *Marine pollution bulletin* **76** (1) : 333-348.

Popescu, A. L., y Luca, O. (2017). Built environment and climate change. *Theoretical and Empirical Researches in Urban Management*, **12** (4): 52-66.

Redondo-Gómez, S., Andrades-Moreno, L., Mateos-Naranjo, E., Parra, R., Valera-Burgos, J., y Aroca, R. (2011). Synergic effect of salinity and zinc stress on growth and photosynthetic responses of the cordgrass, *Spartina densiflora*. *Journal of Experimental Botany*, **62** (15): 5521-5530.

Robredo, A., Pérez-López, U., de la Maza, H. S., González-Moro, B., Lacuesta, M., Mena-Petite, A., y Munoz-Rueda, A. (2007). Elevated CO_2 alleviates the impact of drought on barley improving water status by lowering stomatal conductance and

delaying its effects on photosynthesis. *Environmental and Experimental Botany*, **59** (3): 252-263.

Rockström, J., Steffen, W., Noone, K., Persson, Å., Chapin III, F. S., Lambin, E., ... y Nykvist, B. (2009). Planetary boundaries: exploring the safe operating space for humanity. *Ecology and society*, **14** (2).

Rozema, J. (1993). Plant responses to atmospheric carbon dioxide enrichment: interactions with some soil and atmospheric conditions. In *CO_2 and biosphere* (pp. 173-192). Springer, Dordrecht.

Saidi, Y., Finka, A., y Goloubinoff, P. (2011). Heat perception and signalling in plants: a tortuous path to thermotolerance. *New Phytologist*, **190** (3): 556-565.

Sánchez, M.I., Green, A.J. y Castellanos, E.M. (2006). Internal transport of seeds by migratory waders in the Odiel marshes, south-west Spain: consequences for longdistance dispersal -Research letters. *Journal of avian biology*, **37**: 201-206.

Santos, D., Duarte, B., y Caçador, I. (2014). Unveiling Zn hyperaccumulation in *Juncus acutus*: implications on the electronic energy fluxes and on oxidative stress with emphasis on non-functional Zn-chlorophylls. *Journal of Photochemistry and Photobiology B: Biology*, **140**: 228-239.

Saslis-Lagoudakis, C. H., Hua, X., Bui, E., Moray, C., y Bromham, L. (2014). Predicting species' tolerance to salinity and alkalinity using distribution data and geochemical modelling: a case study using Australian grasses. *Annals of botany*, **115** (3): 343-351.

Singh, D., Buhmann, A. K., Flowers, T. J., Seal, C. E., y Papenbrock, J. (2014). *Salicornia* as a crop plant in temperate regions: selection of genetically characterized ecotypes and optimization of their cultivation conditions. *AoB Plants*, **6**.

Strasser, R. J., Tsimilli-Michael, M., y Srivastava, A. (2004). Analysis of the chlorophyll a fluorescence transient. In *Chlorophyll a fluorescence* (pp. 321-362). Springer, Dordrecht.

Tester, M., y Langridge, P. (2010). Breeding technologies to increase crop production in a changing world. *Science*, **327** (5967): 818-822.

Tian, S., Jia, Y., Ding, Y., Wang, R., Feng, R., Song, Z., ... y Zhou, L. (2014). Elevated Atmospheric CO_2 Enhances Copper Uptake in Crops and Pasture Species Grown in Copper-Contaminated Soils in a Micro-P lot Study. *Clean–Soil, Air, Water*, **42**(3): 347-354.

Ullah, I., Waqas, M., Khan, M. A., Lee, I. J., y Kim, W. C. (2017). Exogenous ascorbic acid mitigates flood stress damages of *Vigna angularis*. *Applied Biological Chemistry*, **60** (6): 603-614.

Van Oosten, M. J., y Maggio, A. (2015). Functional biology of halophytes in the phytoremediation of heavy metal contaminated soils. *Environmental and Experimental Botany*, **111**: 135-146.

Ventura, Y., y Sagi, M. (2013). Halophyte crop cultivation: the case for Salicornia and Sarcocornia. *Environmental and Experimental Botany*, **92**, 144-153.

Ventura, Y., Eshel, A., Pasternak, D., y Sagi, M. (2015). The development of halophyte-based agriculture: past and present. *Annals of botany*, **115** (3): 529-540.

Yamane, Y., Kashino, Y., Koike, H., y Satoh, K. (1998). Effects of high temperatures on the photosynthetic systems in spinach: oxygen-evolving activities, fluorescence characteristics and the denaturation process. *Photosynthesis Research*, **57** (1): 51-59.

Zharikov, Y., Skiller, G.A., Loneragan, N.R., Taranto, T. y Cameron, B.E. (2005). Mapping and characterising suptropical estuarine landscapes using aerial photography and GIS for potential application in wildlife conservation and management. *Biological Conservation*, **125**: 87-100.

Agradecimientos

A mi familia. A mis padres por apoyarme en todo lo que podían y más. Por tener que aguantarme cuando me quejaba y por haber sufrido mis estancias como nadie. Gracias por los periódicos, la ropa de más por si acaso, las tortillas de camarones y los táperes. Gracias por todo. A mis hermanos por estar ahí. A Francisco por acompañarme en mis escapadas frikis para desconectar y a Antonio por ocuparme el piso y cuidarme (sobre todo por los capítulos de The Office). A mi abuelo Paco, que se fue justo antes de empezar esta etapa de mi vida, hasta la vuelta.

A Enrique y a Susana por ser grandes directores y personas. Por ponérmelo todo lo más fácil posible aunque yo no se lo haya puesto tan fácil a la hora de corregir esta tesis. Siempre se podía contar con ellos para lo que fuese, sobre todo para desayunar churros. A Enrique por las visitas al campo, por el negocio de las pelotas de golf, los días de invernadero y los coloquios.

A Jose por ser compañero de largos días en el invernadero con almuerzos del Buen Comer y visitas a la compactadora, pero también por ser compañero y amigo fuera de la facultad incluso en la otra punta del mundo. A Jenni, Salva y Karina, que me ayudaron en todo lo posible cuando tocaba medir mis queridas enzimas o cualquier otra cosa en Farmacia. También mención especial a Jenni por hacer la ratonera algo más habitable y ayudarme con todo el papeleo. A Javi, porque siempre ayuda cuando se le necesita, aunque se quede dormido y no desayune en los coloquios. A Fran por convertirse en el "Demonio del Molinillo" y hacerme la vida más fácil y a Miguel por hacer más llevadero el tramo final de este doctorado con sus partidos de fútbol en Bami.

A Yani, Fede, Agus y Jaz, que nos acogieron en Puerto Madryn como a parte de su familia. A Bernardo, por enseñarme tanto sobre cómo analizar datos, aunque todavía me queda mucho por aprender y ayudarme tanto en la elaboración de esta tesis. A la Profesora Isabel, a la Profesora Ana Rita, a Andreia y a Paloma, por hacer la estancia en Lisboa más llevadera. A Daniela, Marco, Analie, Eduardo y Miguel por ser grandes compañeros dentro y fuera del laboratorio. A Margarida, Alex y Paola por esas cenas internacionales en el piso de Lisboa. A Hervé, Têté, Cedric y todos los de INRA por ayudarme en todo lo posible en Clermont-Ferrand dentro y fuera del trabajo. A Torres por enseñarme tantas cosas nuevas, aunque más de la mitad no funcionasen en mis

plantas, y por ser un gran científico de Sanlúcar de Barrameda y una mejor persona. A Paulo y Fernanda porque son unos grandes profesionales y un encanto ¡Coca Cola para todos! A Bill por enseñarme que lo importante es ser feliz con lo que haces y que nunca es tarde. A Diana por alegrar las curvas de presión volumen con música buena (quitando a Andy y Lucas) y por convertir el último mes en una aventura. A Analie otra vez por acompañarme desde Lisboa a Clermont-Ferrand pasando por Sevilla y Granada y haber sobrevivido para contarlo.

A Roberto, porque ha estado ahí siempre desde sexto de primaria, seguramente porque no tenía otra opción, pero eso es otro tema. He echado de menos los tarareos mientras intentaba concentrarme en esta época y el atún. A Juan, por estar ahí siempre también, aunque estés en Polonia, por ser un loco de la cabeza con una baqueta muy bonita. A los dos, porque habéis sufrido todas mis quejas de estos años y aún así me seguís dirigiendo la palabra.

A Gabriel y Galán por los casi dos años que compartimos en Carlos Brujes, intentando ver la tele por las noches mientras Gabriel hablaba casi solo. Gracias por esos concursos aleatorios, por el maratón de Star Wars, por las cenas en el salón, por las limpiezas del piso con banda sonora y por las charlas interminables. Por hacer de ese piso nuestra casa. A Laura también, que estuvo poco tiempo, pero igualmente ayudó a que todo fuese mejor en ese piso. A Juanmi, Blanca y Toni por todos esos viajes Sanlúcar-Sevilla y Sevilla-Sanlúcar que hemos sufrido. A todos los locos de Sanlúcar.

A Pilar por la compañía en el camino de vuelta, por ese gran examen de inglés que hicimos. A mis compañeros de carrera, sobre todo a Pedro, Chris y Jose, que aunque estábamos ya dispersos siempre hemos encontrado algún hueco para visitar el hiperoriente.

Y a mí “currículum de mierda” por permitirme tener esta oportunidad.